ROCKETDYNE • A DIVISION OF NORTH AMERICAN AVIATION INC

NASA CONTRACT: NAS 7-124
FINAL REPORT FEBRUARY 1963

In Extraterrestrial Landing Environments

VOLUME II B

ROCKETDYNE, Canoga Park, Calif.
A DIVISION OF NORTH AMERICAN AVIATION INC

(NASA CR-55088;) R-5061 OTS: $16.00 ph, $7.43 mf

Propulsion Requirements for Soft Landing in Extraterrestrial Environments,

Final Report

February 1963

(NASA Contract NAS 7-124)

Volume 2 B

Serial Report

Prepared for

National Aeronautics and Space Administration

NASA Headquarters

Mr. H. Burlage

Ames Research Center

Mr. H. Hornby

Prepared by

Advanced Systems Section

Mart S. Bensky

M. S. Bensky Feb. 1963 246 p

Responsible Engineer

Approved by

S. F. Iacobellis

S. F. Iacobellis
Section Chief
Advanced Systems

FOREWORD

This document was prepared in compliance with the requirement for the final report for National Aeronautics and Space Administration contract NAS 7-124, "Propulsion Requirements for Soft Landing in Extraterrestrial Environments."

ABSTRACT

13375

Volumes IIA and IIB, "Propulsion Requirements for Soft Landing in Extraterrestrial Environments," present the analyses conducted under NASA Contract NAS 7-124. Landing trajectory concepts applicable to landings on the moon, Mars, Venus, Mercury and the Earth were analyzed to define the required propulsive maneuvers and to determine the optimum characteristics of propulsion systems for performance of these maneuvers. Related investigations presented herein were conducted to determine appropriate interplanetary trajectories upon which to base landing analyses and to evaluate takeoff propulsion requirements.

AUTHOR

TABLE OF CONTENTS - VOLUME IIA

TABLE OF CONTENTS - VOLUME IIB

INTRODUCTION

Presented in this volume are the analyses conducted and results obtained in the study, "Propulsion Requirements for Soft Landing in Extraterrestrial Environments." The study was performed (1) to define the most suitable landing concepts for landings on Mars, Venus, Mercury, Earth and the moon, in order to specify the required propulsive phases, and (2) to determine the optimum characteristics of propulsion systems for these propulsive phases.

Analysis of landings on these bodies entailed initially the selection of appropriate transfer trajectories and consequent planetary arrival conditions; these results provided the applicable initial conditions upon which to base subsequent studies of landing maneuvers. The sequence of maneuvers comprising an extraterrestrial landing operation was dependent primarily on the presence or absence of an atmosphere about the destination body. As a result, the landing maneuver profiles were qualitatively, though not quantitatively, similar for the all-propulsive lunar and Mercury landings, and for the Earth, Mars and Venus landings, which utilized the atmospheres of those bodies for a major part of the required vehicle deceleration.

For a landing mission as defined in this study, the first in the chronological sequence of propulsive and aerodynamic maneuvers considered for terrestrial and extraterrestrial landing phase analyses was the propulsive terminal correction utilized to establish the initial conditions required for safe entry into a planetary atmosphere or deceleration into a prescribed planetocentric circular orbit. This maneuver, in preference to earlier (e.g., midcourse correction) or later (e.g., deceleration into orbit) maneuvers was chosen, first, because it is essential to satisfactory performance of any subsequent maneuvers, and second, because it is the earliest maneuver primarily influenced by the gravitational field of the destination planet.

Subsequent to the terminal correction, the maneuvers considered for planets having atmospheres were: orbit-establishment, with or without aerodynamic drag providing a portion of the required deceleration; direct atmospheric entry; and near-surface deceleration and maneuvering by means of parachute/retrorocket systems. For Mercury and the moon, neither of which has an atmosphere, the maneuvers of interest were direct landing, or alternatively, orbit-establishment and landing-from-orbit, and propulsive near-surface translation and descent.

The basic results of the study were the definition of the propulsive maneuvers associated with landings on each of the destination bodies, and specification of the velocity requirements and optimum propulsion system parameters for these maneuvers.

LUNAR MISSIONS

INITIAL AND MIDPHASE MANEUVERS

The basic lunar landing mission is comprised of three primary phases: 1) powered flight in the vicinity of Earth to accelerate the vehicle into an Earth-moon coast trajectory, 2) coast to the vicinity of the moon, and 3) propulsive deceleration to the surface of the moon. The mission is illustrated in Figure 1 . The use of separate propulsion systems for Earth-vicinity and lunar-vicinity maneuvers appears to be best suited to the requirements of the mission; as a result, propulsion systems for the landing phase can be evaluated separately. However, the Earth phase and the resultant coast phase affect lunar arrival conditions and therefore must be analyzed as part of a lunar landing investigation.

Effect of Earth Phase on Lunar Arrival

During the Earth powered-flight phase, the vehicle is accelerated to the energy level necessary to enter the selected Earth-moon coast trajectory. Either direct or Earth-orbital departure can be employed; the lunar arrival is not affected by the type of Earth departure. The lunar vicinity trajectory and landing maneuvers are determined only by the position and velocity of the vehicle as it approaches the moon.

The velocity generated during the Earth-departure phase governs the duration of the coast phase and the vehicle velocity at lunar arrival. Transit time can be substantially reduced (from the approximate 5-day duration corresponding to a near minimum-energy transfer) by the addition of a rather modest velocity increment during the Earth-vicinity powered phase; the resulting arrival velocity, however, increases as transit time is reduced and thereby increases landing maneuver propulsion requirements.

To analyze the launch conditions that will enable the vehicle to intercept the moon, it is necessary to examine the Earth-moon orientation. The plane of the moon's path around the bary center (the common center of mass of the Earth-moon system) is inclined 5.15 degrees to the ecliptic; the axis has a 19-year precession period. The plane of the axial rotation of the Earth (equatorial plane) in inclined 23.45 degrees to the ecliptic.

Although the axis of the Earth precesses, the rate is so small that the equatorial plane orientation can be assumed to be fixed in space. Thus,

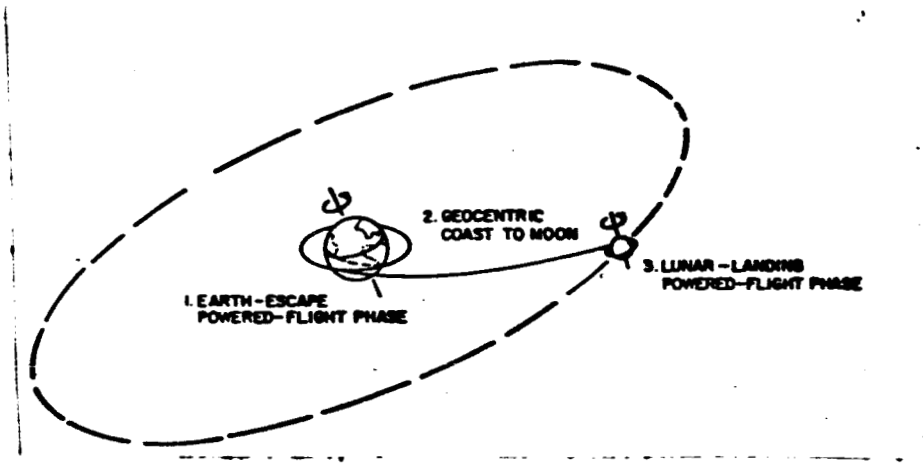

Figure 1 . Division of the Earth-to-Moon Trajectory

the relative angle between the equatorial plane and the lunar plane varies from approximately 28.6 to 18.3 degrees in a 9.5-year period.

To accomplish a direct (i.e., no Earth-orbit) Earth-to-moon transfer, the vehicle is injected from the launch point into a plane (geocentric) that intersects the lunar plane. For an eastward Cape Canaveral launch, illustrated by point L in Figure 2 , the vehicle is in a plane inclined 28.5 degrees to the equatorial plane. With the moon at M at vehicle arrival, the central flight angle is (Ψ_c), which is the total geocentric angle traversed during Earth powered-flight and Earth-to-moon coast. (As the vehicle approaches the moon, it will be perturbed from the geocentric coast ellipse assumed in the study. However, for propulsion analysis, this effect is not significant.)

Caused by Earth rotation, the line of intersection between a potential geocentric transfer plane (inclined 28.5 degrees to the equatorial plane) and the lunar orbital plane rotates through 360 degrees daily. As a result,

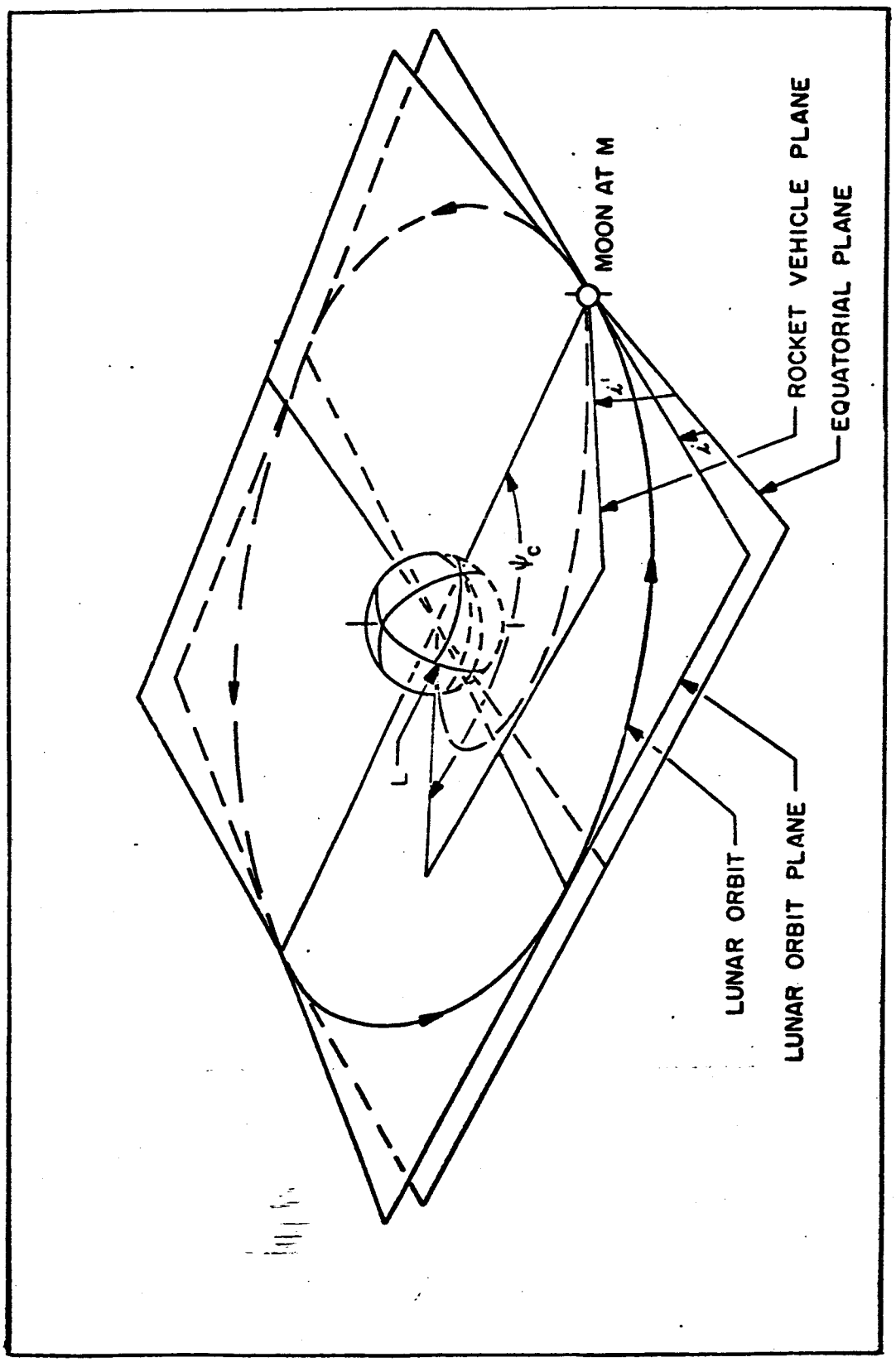

Figure 2 . Lunar and Rocket-Vehicle Planes Shown at Time of 90-Degree (ψ) Central Angle

once a day the transfer plane includes the moon regardless of the moon's orbital position. However, as the moon traverses its 27-day orbit around the Earth, the central angle at intersection changes, and since central angle strongly affects departure and arrival velocities, during each month a minimum-propulsion transfer trajectory exists.

A vehicle which enters Earth orbit prior to injecting into a lunar transfer trajectory gains an advantage of central angle flexibility not available to a direct-flight vehicle. As a result, a minimum propulsion trip can be initiated once daily, as compared to once monthly for direct missions. For example, the vehicle depicted in Figure 2 could reduce propulsion requirements (and extend trip duration) by coasting 270 degrees in Earth orbit before propelling itself into its transfer trajectory. The trajectory would then approximate a Hohmann transfer instead of the 90 degree central-angle trajectory shown.

Coast Phase

Analysis of Earth-moon coast phase trajectories based on geocentric conic sections (ellipse, parabola, hyperbola) indicate the variations of departure and arrival velocities with transit time. A near minimum-energy, maximum-duration trajectory has a transfer time of approximately 5 days. As Earth-departure velocity increases, trip time decreases; for a geocentric escape trajectory, lunar intercept occurs at approximately 2.1 days. Trip times less than 2.1 days are along geocentric hyperbolic paths (Figure 3).

Figure 3 tends to indicate that a conic-section velocity error introduced at the Earth would not necessarily prevent a lunar intercept. If excessive velocity were added in the Earth propulsion phase, a shorter trip time would result, and intercept with the moon would be made at an earlier point in the orbit of the moon (and vice versa). However, as Figure 2 shows, the geometry of the Earth-moon system is such that the transfer orbit plane is inclined to the orbit plane of the moon, so the vehicle orbit and the orbit of the moon are not coplanar. Thus a faster or slower trip could pass above or below the moon so that the self-focusing effect is diminished.

Different Earth-lunar trajectories, resulting from variations in launch date, trip time and injection velocity vector, can result in different selenocentric planes at lunar arrival. By selection of the lunar transfer destination position, a desired lunar plane can be achieved. This selection (i.e., the appropriate correction) can be made in the Earth phase trajectory,

or a midcourse correction as shown in Figure 4 can be used. The assumption that the task of directing the vehicle to the proper lunar orbital plane will be relegated to an Earth-vicinity or midphase propulsion system removes the requirement for plane-change capability in the lunar landing propulsion system; as a result, plane-change was not considered in landing analyses. A final plane change can be made after a lunar orbit is established. The velocity requirements, shown in Figure 5 , for such a maneuver are substantially higher than for earlier corrections; however, the accuracy of the lunar trajectory should preclude a plane-change requirement for most cases.

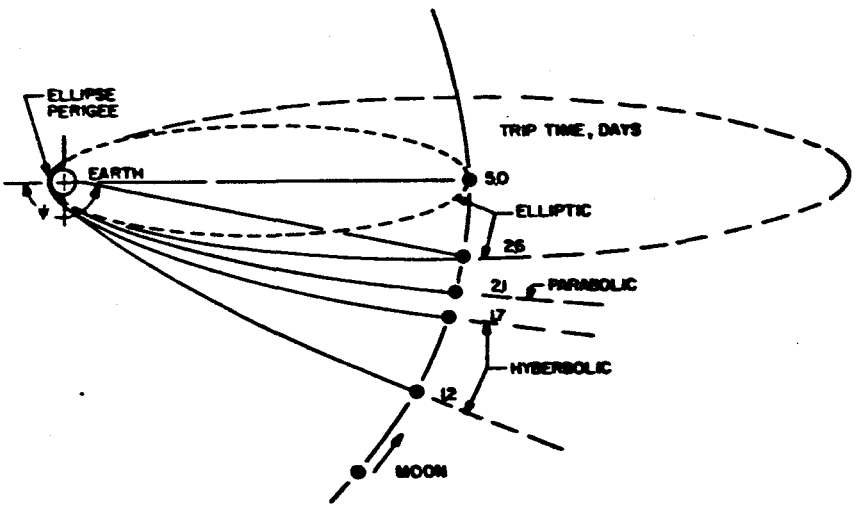

Figure 3 . Earth-to-Moon Geocentric Conic-Section Trajectories

Lunar Midcourse Corrections

The lunar mission differs from other space missions in that the transit time is approximately three days contrasting to transit times of a hundred days or more for other space missions. Since the dynamics of

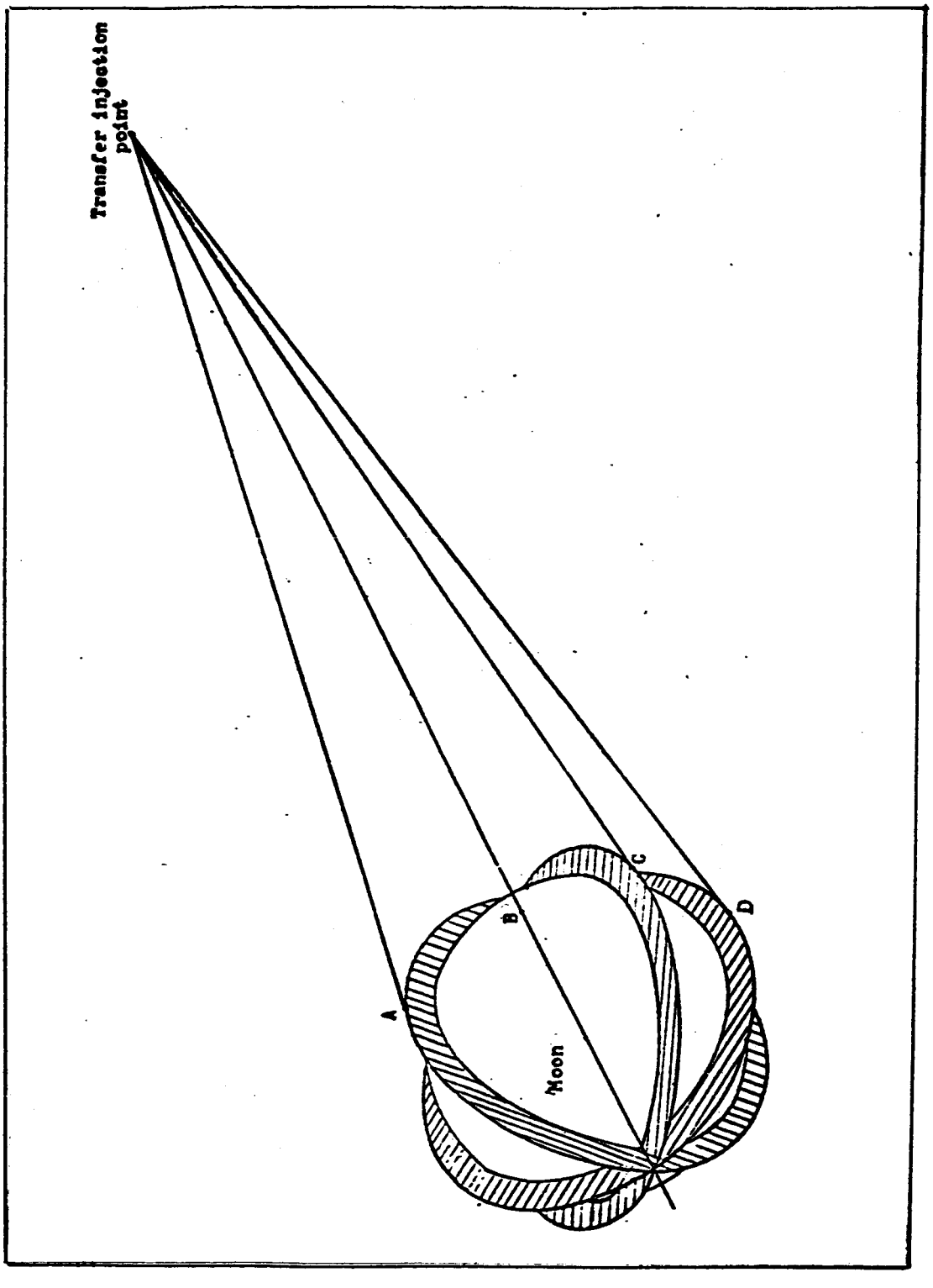

Figure 4 - Possible Lunar Orbit Inclinations

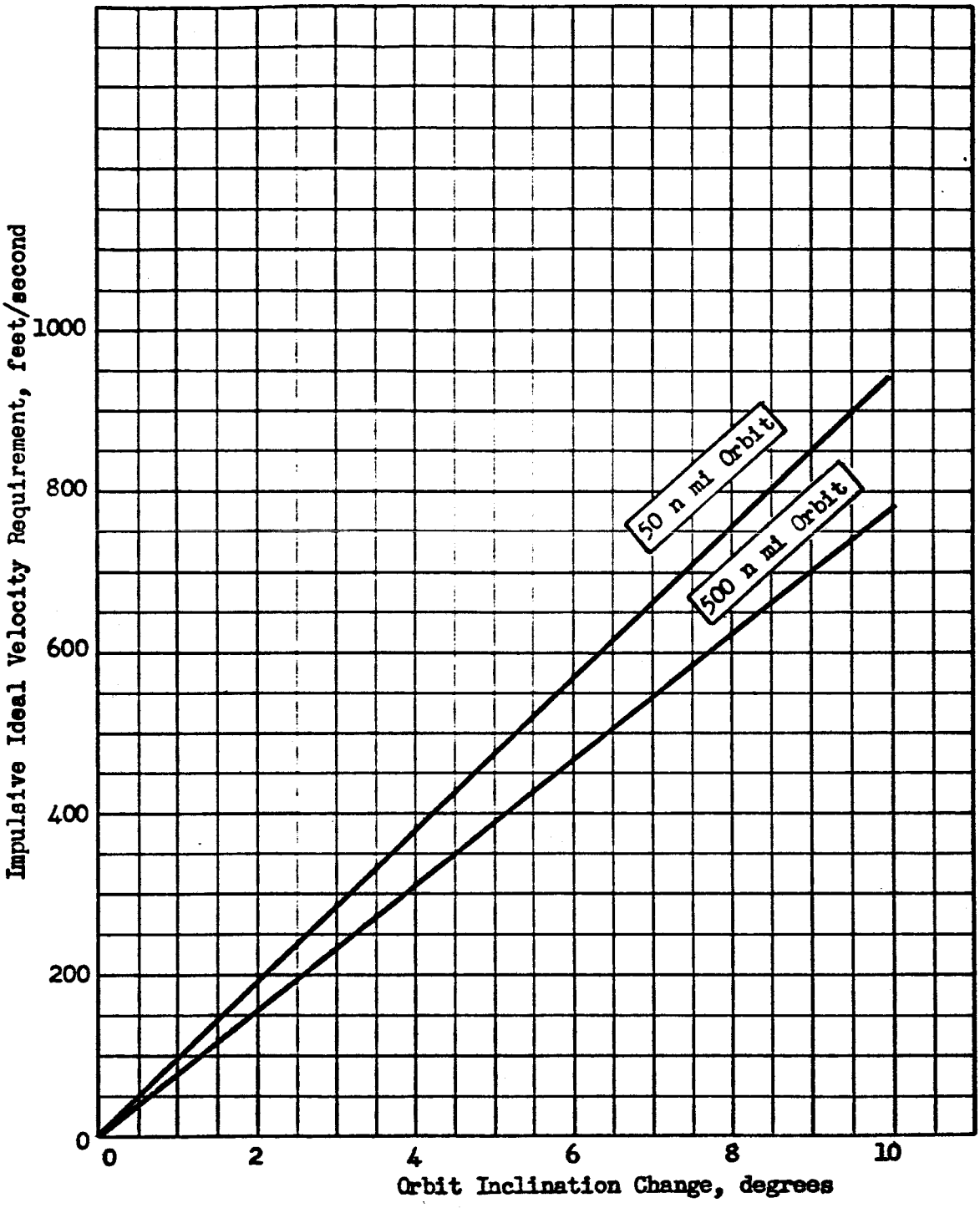

Figure 5 . Ideal Velocity Requirement for Orbit Inclination Change

Earth-moon space are well defined and the distance involved is an order of magnitude less than that of interplanetary missions, the trajectory can be controlled with considerable accuracy.

The need for midcourse corrections emanates from the inherent errors existing in the booster guidance and propulsion systems. If left uncorrected, these errors could cause the vehicle to miss its rendezvous point at the moon by several thousand miles. Numerous analyses have been performed by various members of the aerospace industry in connection with programs such as Apollo, Surveyor and Ranger to determine the midcourse correction requirements for various lunar missions. Similar analyses, conducted at Rocketdyne under NASA contract NAS 7-88, "Space Transfer Phase Propulsion Systems," are described in Reference 1 . These analyses have primarily employed linear perturbation techniques with a fixed-time-of-arrival at the moon. The objective of the midcourse corrections is to return the vehicle to its intended trajectory prior to arriving at the moon.

These analyses have yielded the result that sufficient accuracy can be obtained with a midcourse correction scheme employing three maneuvers (See Figure 6). The first correction is applied as soon as the trajectory can be accurately determined from tracking data; the second is applied sometime before arriving at the aim point to cancel the propulsion and tracking errors of the first correction; the third correction is applied at the aim point to alter the velocity of the vehicle to match that of the intended trajectory. Results of these analyses (based on typical injection errors of 1 n mi in position and 10 ft/sec in velocity and including errors in midcourse position, guidance and execution accuracy) have shown that the total midcourse velocity requirements for a 0.99 probability of success are less than 200 ft/sec while the RMS error existing at the aim point is less than 5 n mi in position and 0.5 fps in velocity. For a mission which includes a propulsive phase to establish a lunar orbit, this accuracy is sufficient; however, for missions that involve circumnavigating the moon, further corrections will most likely be required to improve the trajectory accuracy. Results presented in Reference 1 indicate that these terminal corrections are approximately a few feet per second.

Lunar Mission Selection

The approximate magnitude of the propulsion requirements for a trip from the Earth to the moon is shown in Figure 7 . The ideal velocity requirement is divided into three parts. The first is the Earth-propulsion phase requirement, and the ideal velocities indicated are typical of conventional chemical systems. The vertical distance to the next curve represents the

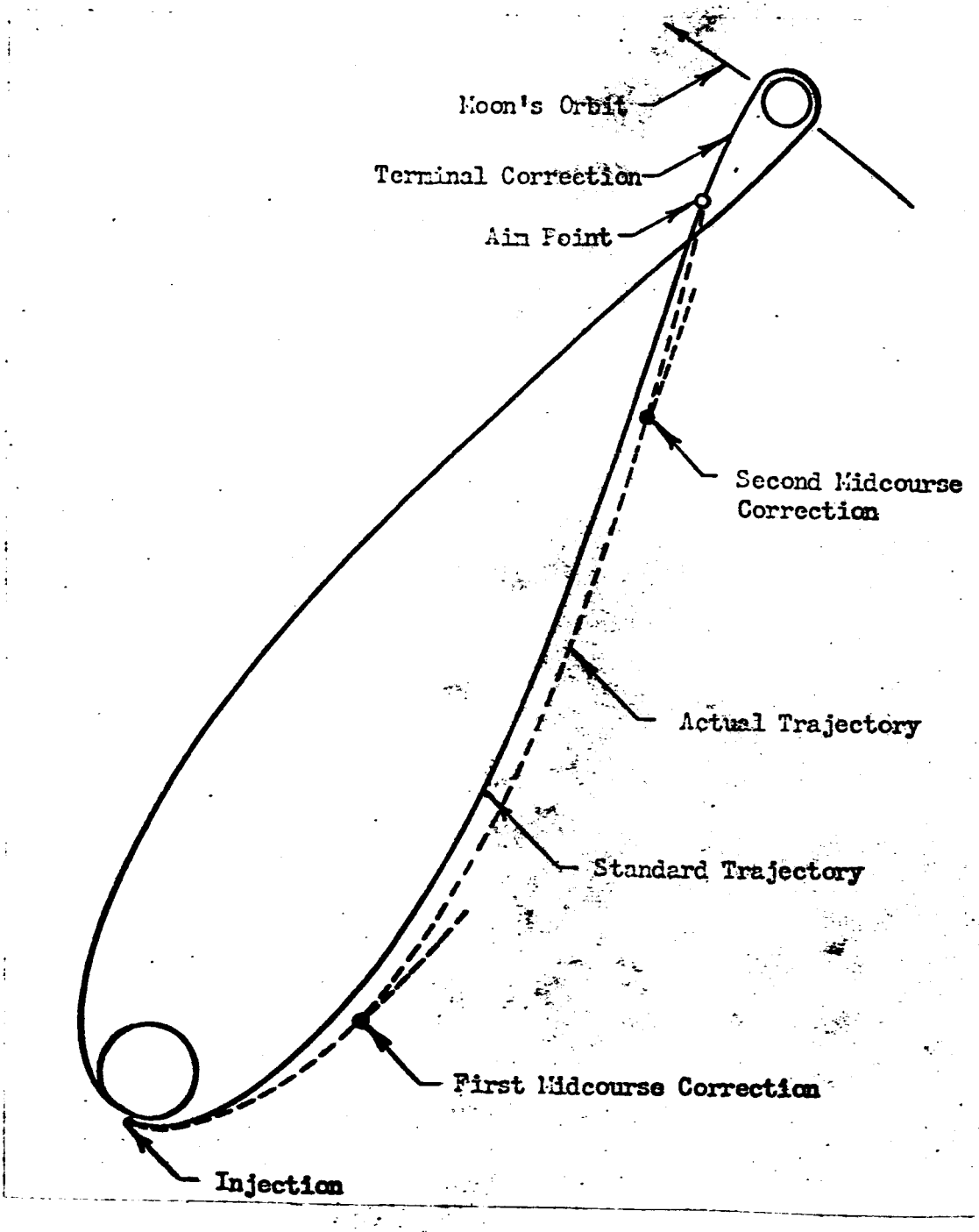

Figure 6 . Midcourse Correction Scheme

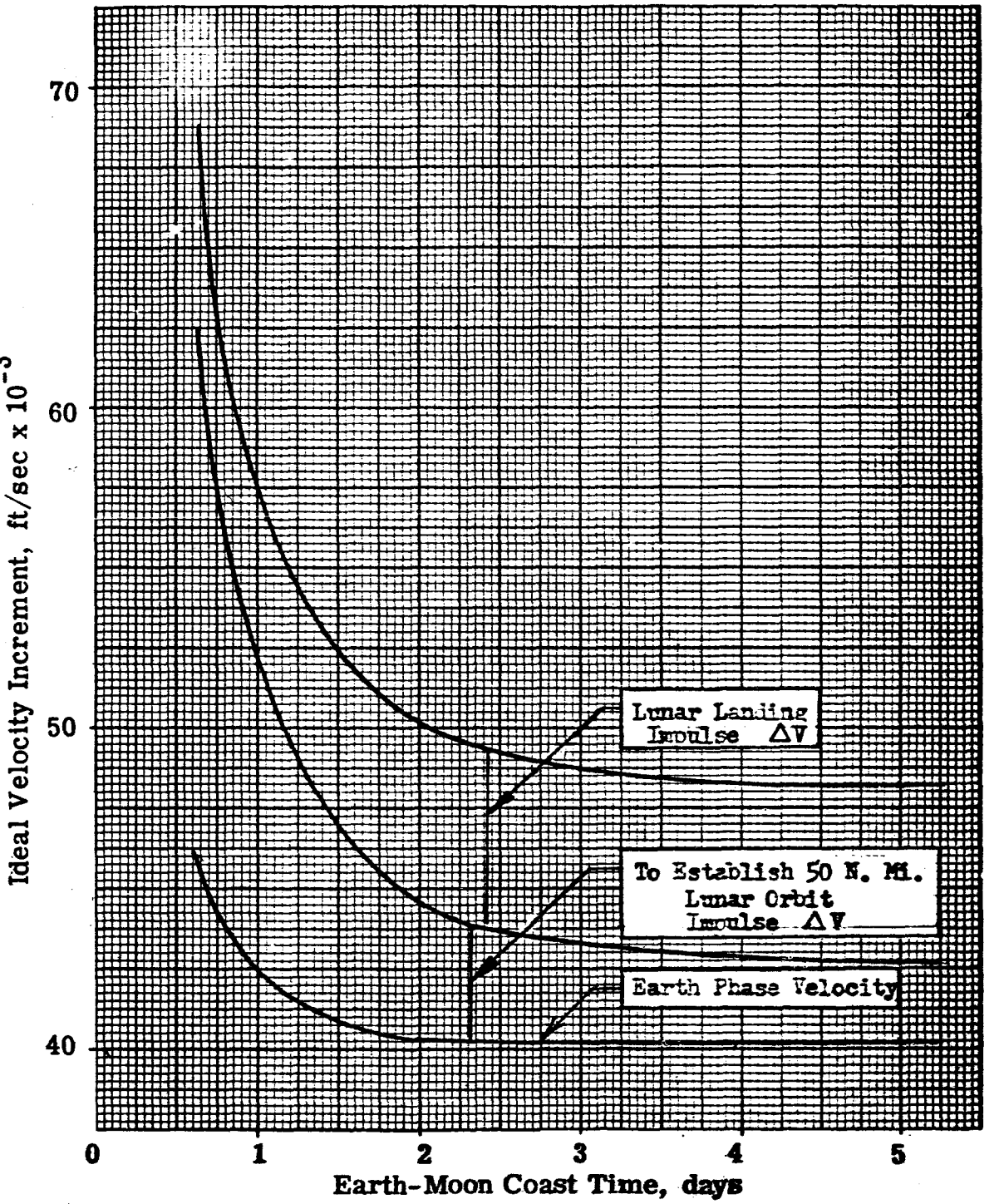

Fig. 7. Lunar Mission Velocity Requirements

lunar orbit-establishment velocity requirement, and the third curve adds a constant velocity for landing from lunar orbit. The latter two velocity requirements shown are predicated on impulsive (instantaneous) velocity changes. (In propulsion system studies presented later, the variation of velocity requirements with thrust-to-weight ratio is considered).

For transfer times shorter than 2.0 days, the Earth-phase velocity increases rapidly (Figure 7), while for times longer than 2.0 days, the Earth-phase velocity is practically constant. The velocity of the vehicle, and therefore the lunar-phase velocity requirement as it enters the lunar gravity field, increases rapidly with the shorter transfer-time trajectories.

For lunar missions, the longer trip is beneficial to the gross payload capabilities of the vehicle because the lower velocity requirements result in less propellant consumption. However, consideration must be given to the effects of trip time on other parameters. For example, life support system weights increase approximately linearly with trip time for durations encountered in typical lunar missions.

Another factor causing reduction of the net payload is the radiation shield requirement for manned, and other radiation-sensitive, payloads. More shielding may be required as the trip time is increased. First, the confidence level of solar flare predictability decreases as the trip duration increases. Second, the probability of encountering a larger flare during flight increases as the flight time is extended. Preliminary analysis was conducted to examine the trip time with respect to shielding and life support equipment, and the results indicate that shield requirements cannot be defined with sufficient clarity to provide a precise value of optimum trip time. Review of available shield and life support information (see, for example, Reference 2), together with the propulsion requirements, indicates trips in the 2- to 3-day range are suitable for lunar missions.

LANDING AND TAKEOFF TRAJECTORIES

Various trajectory concepts exist for soft landing a vehicle from an Earth-moon coast trajectory. Three of these, the direct vertical, direct nonvertical, and the intermediate-orbit type, are illustrated in Figure 8. Other landing trajectory concepts exist; those presented, however, provide sufficient basis for evaluation of propulsion requirements and illustrate the effect of landing method on propulsion parameters and vehicle capabilities.

The direct vertical landing trajectory (Type A) incurs larger gravity losses than do the direct nonvertical (Types B and C) or intermediate orbit (Type D) trajectories. This effect is demonstrated in Figure 9 by a comparison of ideal velocities for landings from a 2.0-day Earth-moon transfer. The effect of trip time on velocity requirements is illustrated in Figure 10.

Because of improved site selection and abort capability, the intermediate orbit landing trajectory is far more flexible than a direct landing for either a manned or unmanned soft-lunar landing mission. The velocity requirements are only very slightly greater than for the minimum-velocity direct landing trajectory (Type C). As a result, the intermediate orbit landing mode is utilized in the major portion of lunar landing analysis.

Orbit Establishment

In the intermediate orbit landing concept, a propulsion maneuver is first used to establish a lunar orbit. Thrust is aligned antiparallel to velocity to provide a near-optimum maneuver.

The velocity requirements for lunar orbit establishment are determined by trip time, orbit height, propulsion-system specific impulse, and thrust-to-weight ratio. These effects are shown in Figures 11, 12, and 13.

For the two-day lunar transfer selected as an example, it is evident that the orbit establishment velocity requirement is relatively constant when initial thrust-to-Earth weight ratio exceeds 0.3.

Landing from Orbit

Two methods of landing from lunar orbit are described below. The first technique (PAW) employs a single, continuous propulsive phase while the second type (ICP) utilizes two powered phases separated by a coast interval.

——— Power
- - - Coast

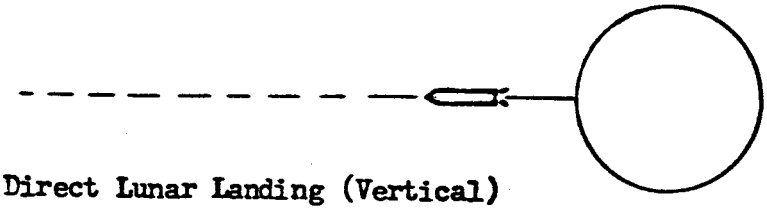

Type A: Direct Lunar Landing (Vertical)

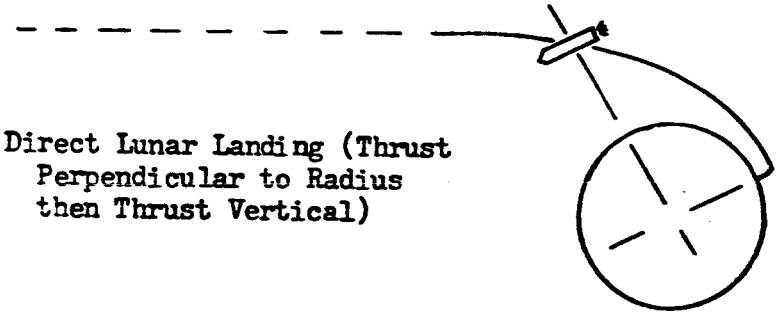

Type B: Direct Lunar Landing (Thrust Perpendicular to Radius then Thrust Vertical)

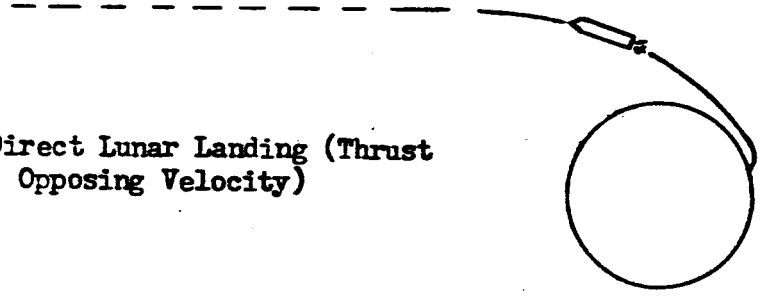

Type C: Direct Lunar Landing (Thrust Opposing Velocity)

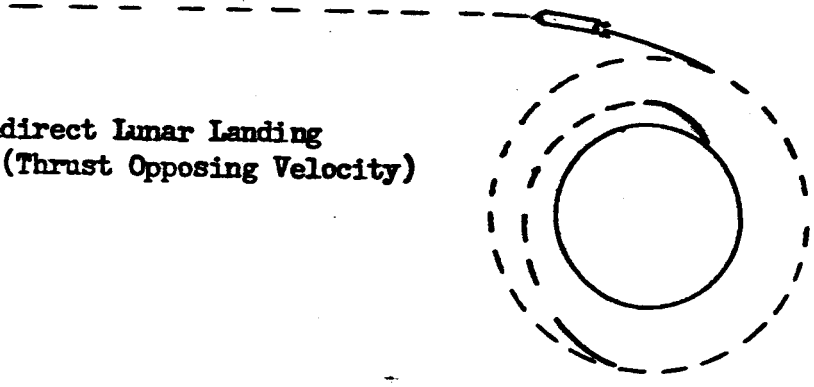

Type D: Indirect Lunar Landing (Thrust Opposing Velocity)

Figure 8. Lunar Landing Trajectories

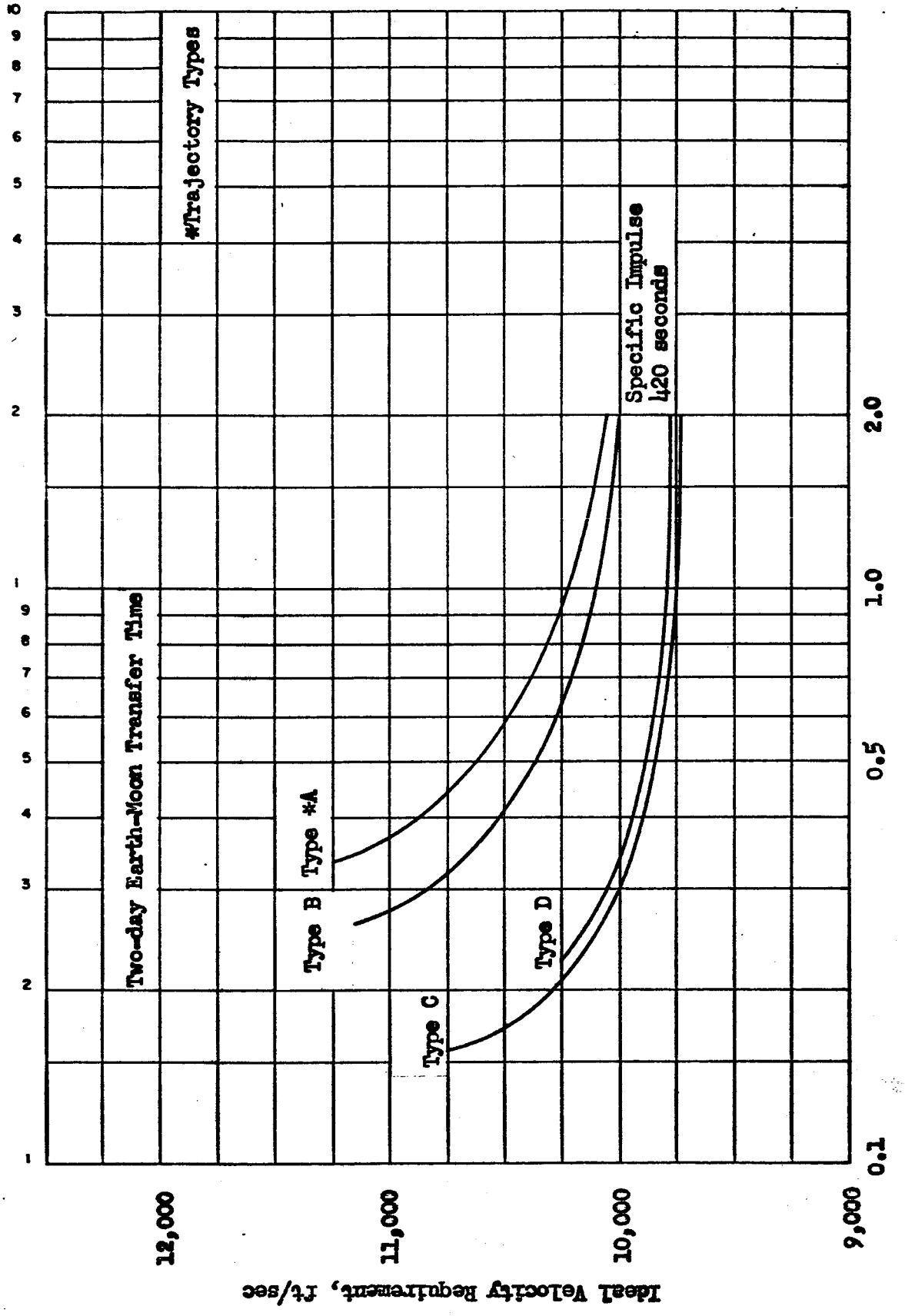

Figure 9 . Ideal Velocity Requirement for Lunar Landing from Earth-Moon Coast Trajectory

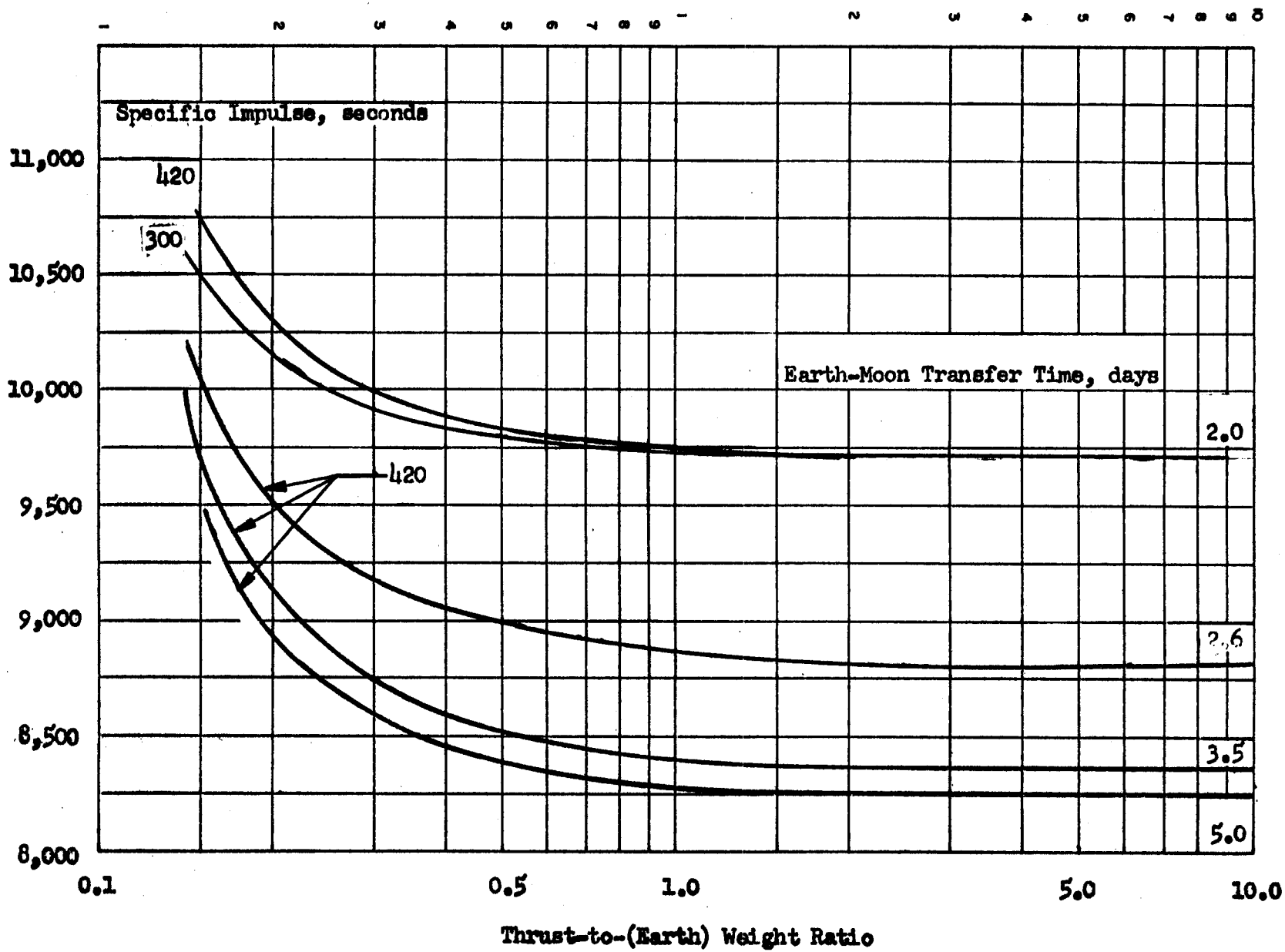

Figure 10 . Ideal Velocity Requirement for Direct Lunar Landing From Earth-Moon Coast Trajectory; Trajectory Type C.

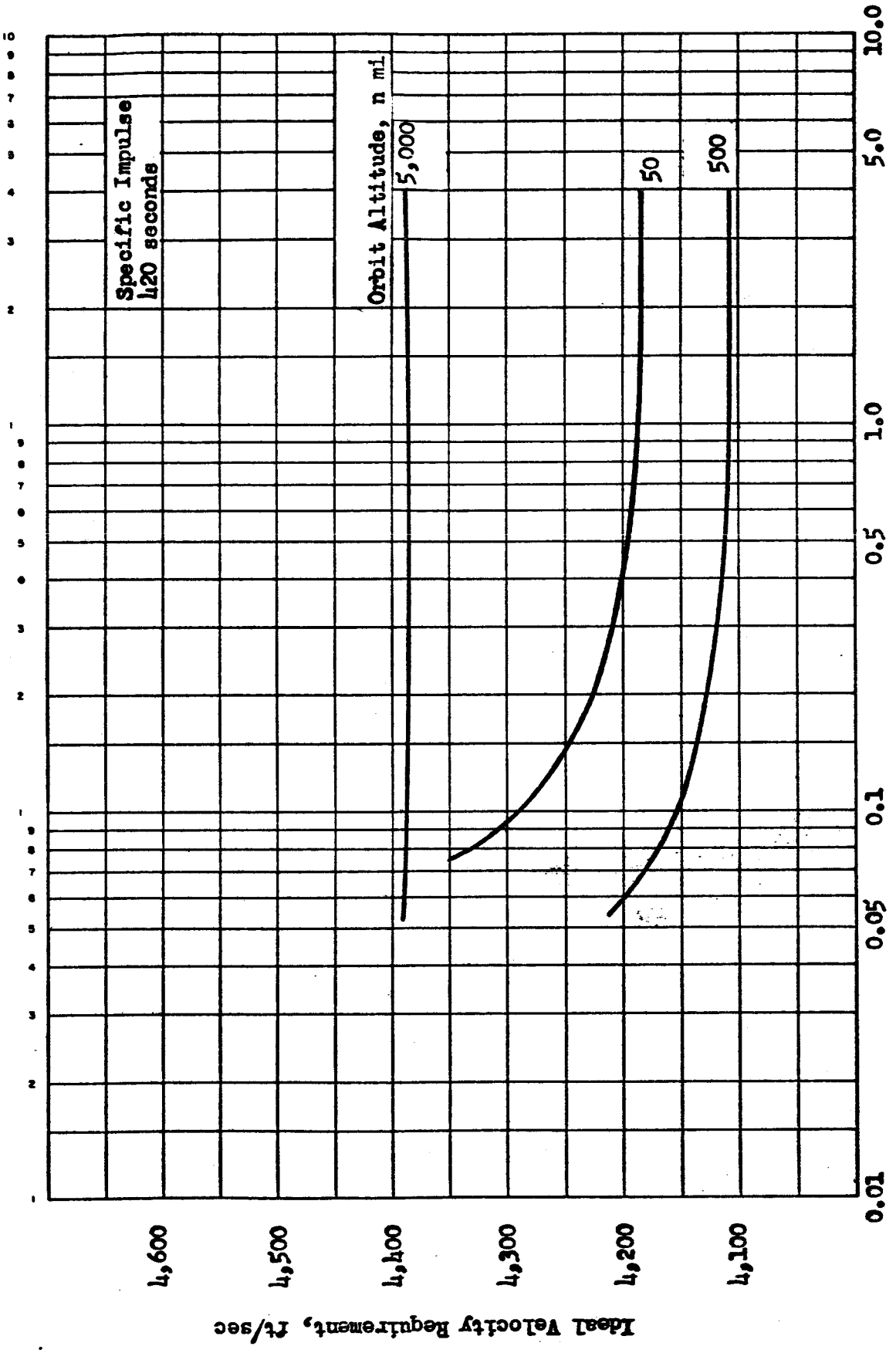

Figure 11. Ideal Velocity Requirement for Establishment of Circular Lunar Orbit from Two-Day Earth-Moon Coast Trajectory

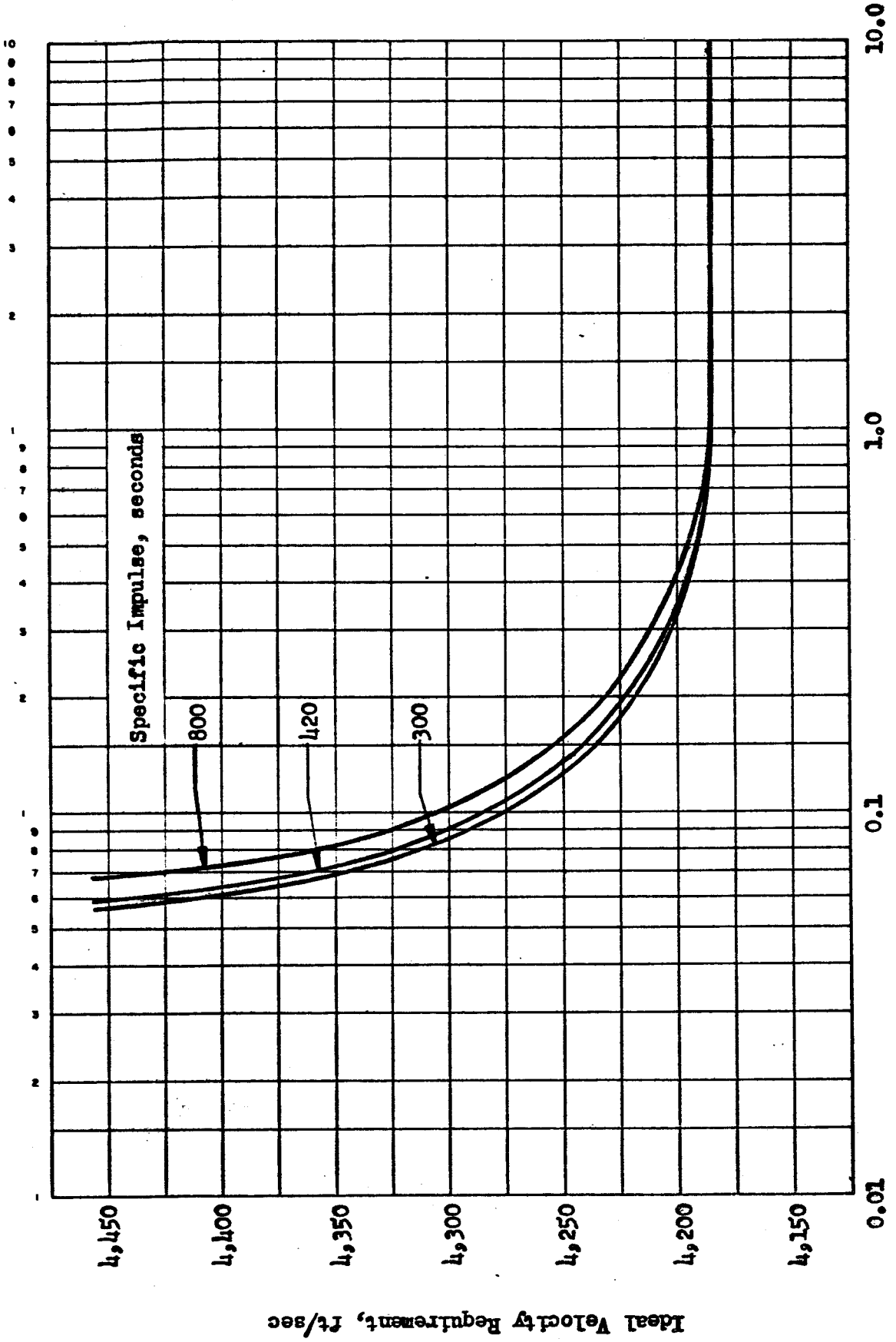

Figure 12. Ideal Velocity Requirements for Establishment of Lunar Orbit (50 n mi) From Earth-Moon Coast Trajectory (with Two Days Transfer Time)

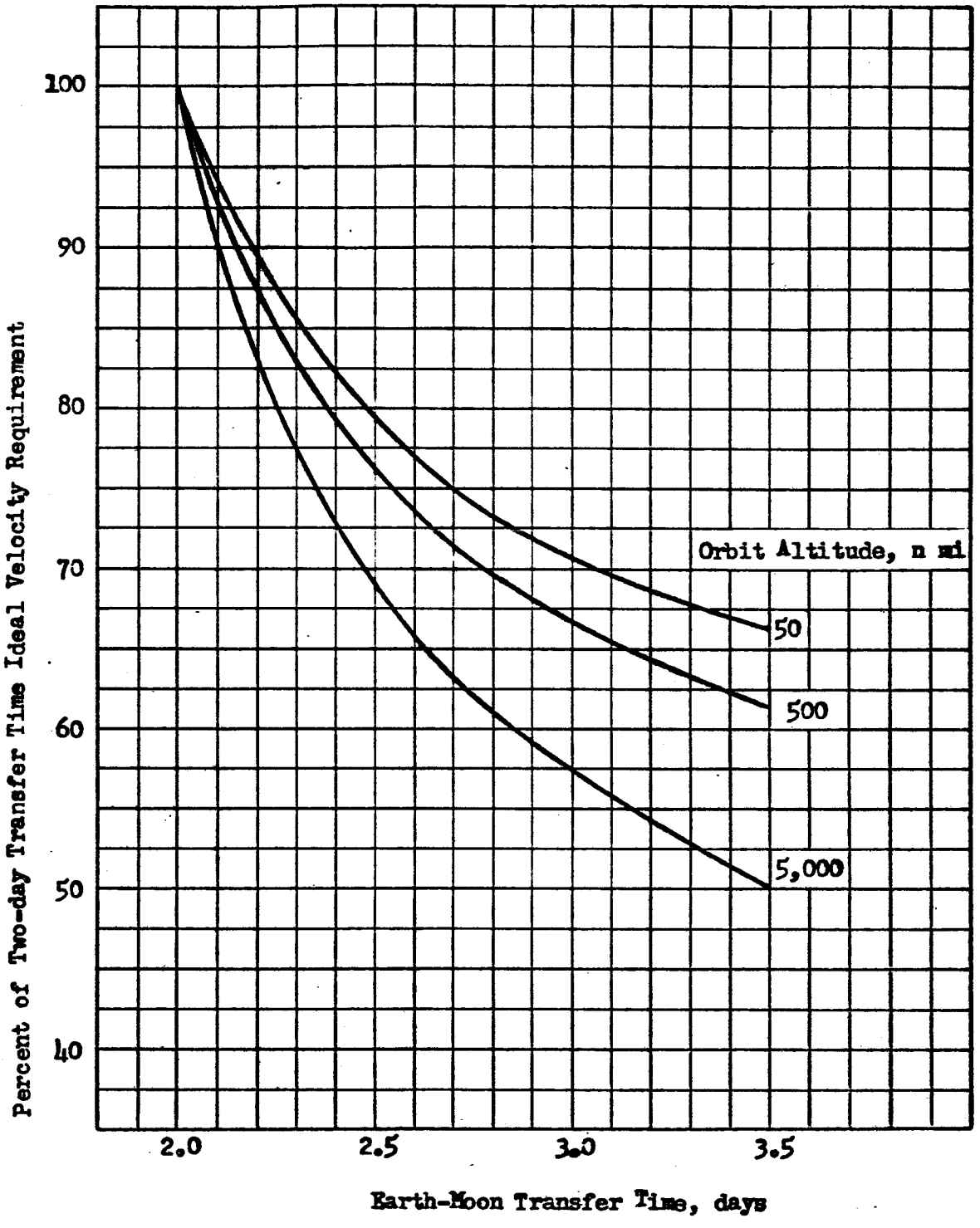

Figure 13. Ideal Velocity Requirements for Establishment of Lunar Orbit From Earth-Moon Coast Versus Earth-Moon Transfer Time

Continuous Powered (PAW). For descent by this technique, retrothrust is initiated in the intermediate lunar orbit and continues until the vehicle reaches zero velocity at the lunar surface. The thrust and thrust attitude during descent must be compatible with the orbit height, or the constraints that altitude and velocity reach zero simultaneously cannot be satisfied by a constant-thrust propulsion system.

For PAW trajectories, results indicate that only a narrow band of initial thrust-to-weight ratios can be used effectively for deceleration from a particular orbit altitude. Thrust-to-weight ratios which are too high result in the vehicle reaching zero velocity before the lunar surface is reached. Thrust-to-weight ratios which are too low allow the vehicle to descend to the surface before the retrothrust can reduce the velocity to zero. Two points are indicated on Figure 14 for continuous-powered landings from a 50-n mi orbit. The restriction to low values of thrust-to-weight ratio (imposed by the high orbit altitude) results in high ideal velocity requirements. PAW trajectories other than the thrust-antiparallel-to-velocity maneuver considered here might be used to increase the applicable range of thrust-to-weight ratios; however, these trajectories further increase ideal velocity requirements. The propulsion requirements for the low-thrust PAW trajectories and equivalent low thrust Intermediate Coast Phase trajectories (described below) are very similar, as indicated by the fact that the selected points lie on the ICP trajectory velocity requirement curves.

Intermediate Coast Phase (ICP). The Intermediate Coast Phase trajectory is characterized by two propulsive applications separated by a coast interval. For optimum execution of this type of descent, a short propulsion phase (small velocity increment) is used to transform the initial circular orbit to a low-periapsis ellipse. The coast phase follows until the vehicle has descended to the trajectory periapsis (i.e., 180 degrees coast). The propulsion system is then reignited and reduces the velocity to zero at the lunar surface. During the final propulsion phase, numerous thrust orientations can be used; thrust antiparallel to velocity is near optimum and is therefore employed in the analysis presented.

A coast interval of approximately 180 degrees yields the minimum propulsion requirement for orbital descent, and was therefore selected as a characteristic of the preferred ICP landing trajectory. ICP trajectories utilizing lesser angular travels are described in detail in Reference 3 ; A significant result obtained is that for thrust-to-weight ratios of interest; there is little change in propulsion requirements for angular travels between 30 and 180 degrees.

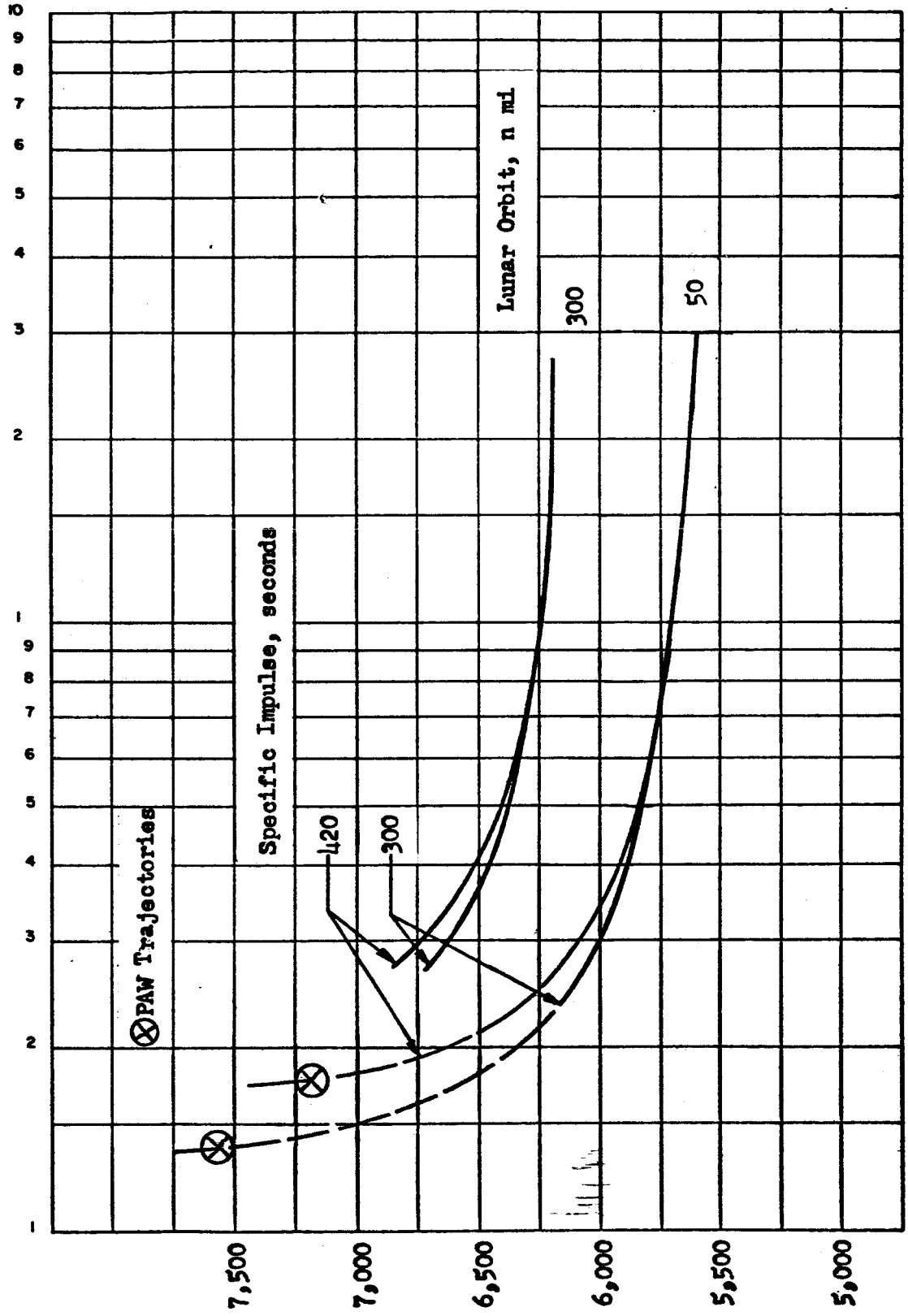

Figure 14 Landing From Lunar Orbit

Lunar landing-from-orbit velocity requirements are shown in Figure 14 for two orbit heights (50 n mi and 300 n mi). For ICP trajectories, use of thrust-to-(Earth) weight ratios greater than 1.0 causes little decrease in ideal velocity requirement; however, for thrust-to-(Earth) weight ratios below 0.4, ideal velocity requirements increase rapidly as thrust-to-weight ratio is decreased. In Figure 14, the velocity requirements are lower for the low specific impulse system because, for a given initial thrust-to-weight ratio (F/W), the average F/W during the landing is higher due to more rapid propellant consumption. The reduction of velocity requirements with increasing F/W results from reduction of gravity losses which in turn is due to the shorter powered flight times at the higher F/W values.

To achieve touchdown at a particular location, the pericynthion should be located a few degrees before the selected landing site. At the pericythion, the landing vehicle applies retrothrust antiparallel to the velocity vector. This descent trajectory is followed until the vehicle is a few thousand feet above the lunar surface and descending almost vertically with a small velocity. Then the final translation/ descent is accomplished.

In a thrust opposing and parallel-to-velocity descent, the F/W ratio and the pericynthion altitude are related to the landing trajectory shape. The pericynthion altitude (PCA) must be increased as F/W is reduced; this is caused by the longer powered flight time required to reduce the vehicle energy at low thrust levels. The increase in ideal velocity increments for descent-from-pericynthion maneuvers as the F/W decreases is caused by additional gravity losses.

The variation in PCA with F/W at the start of descent from circular orbit is shown in Figure 15. Lunar topography limits the PCA to values greater than approximately 30,000 feet, corresponding to a F/W (Earth) of 0.65 or less at the beginning of the descent-from-pericynthion phase. For a well-reconnoitered landing area, the permissable PCA may be less than 30,000 feet but other considerations do not make the lower altitudes attractive. However, since performance optima generally occur in the 0.5 F/W range, the above criteria are satisfied by pericynthion altitude of approximately 50,000 feet.

As PCA (h_o) decreases with increasing F/W, the angular distance from pericynthion to the horizon (θ_n) decreases; but the central angle (θ) subtended by the descent trajectory also decreases with increasing F/W. The difference between these two angles indicates how far below the horizon (angularly) the landing site is at the initiation of the descent maneuver. These values, plotted in Figure 16, indicate that the landing

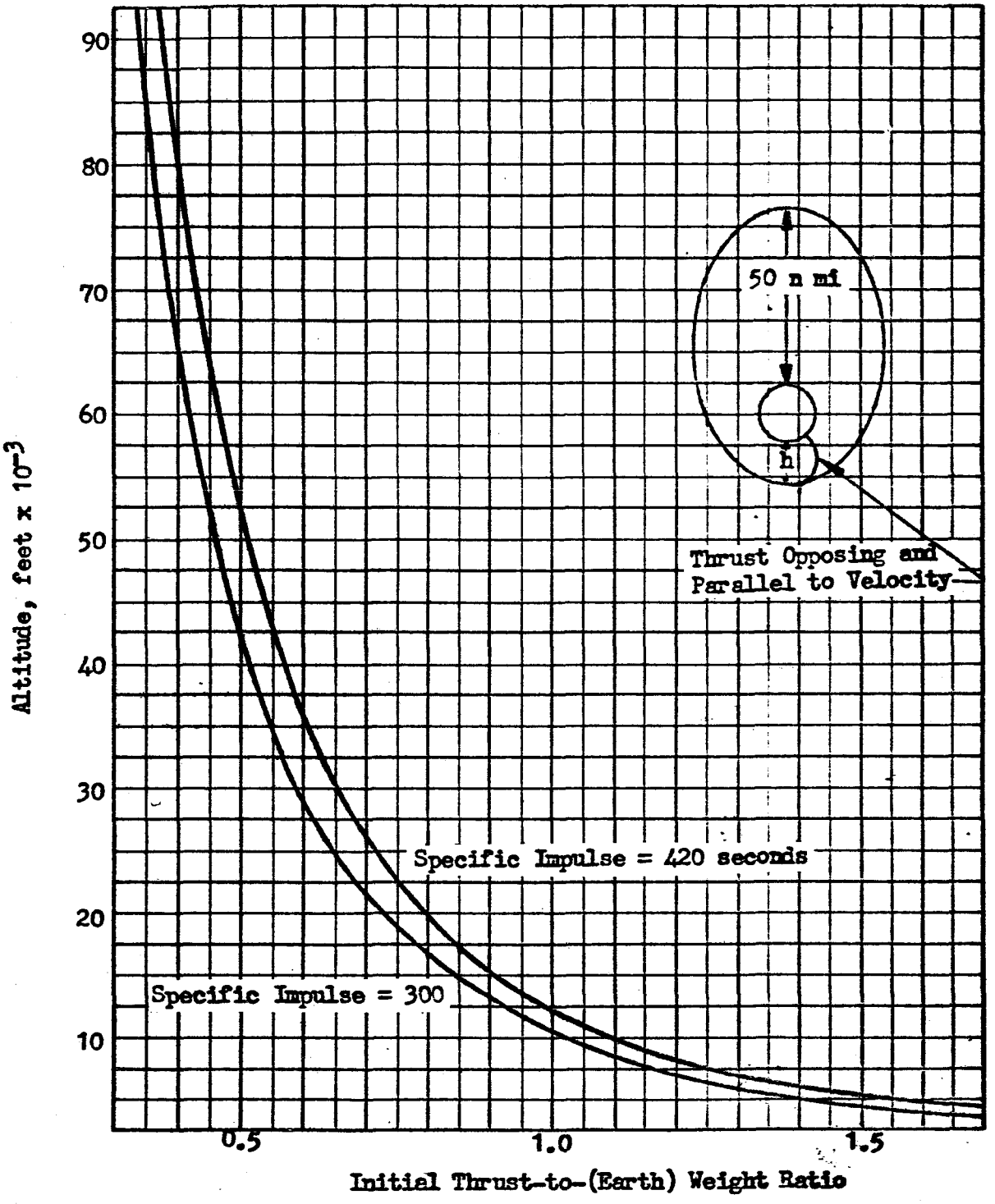

Figure 15. Descent from Pericynthion. Variation of Pericynthion Altitude with Thrust-to-(Earth) Weight Ratio

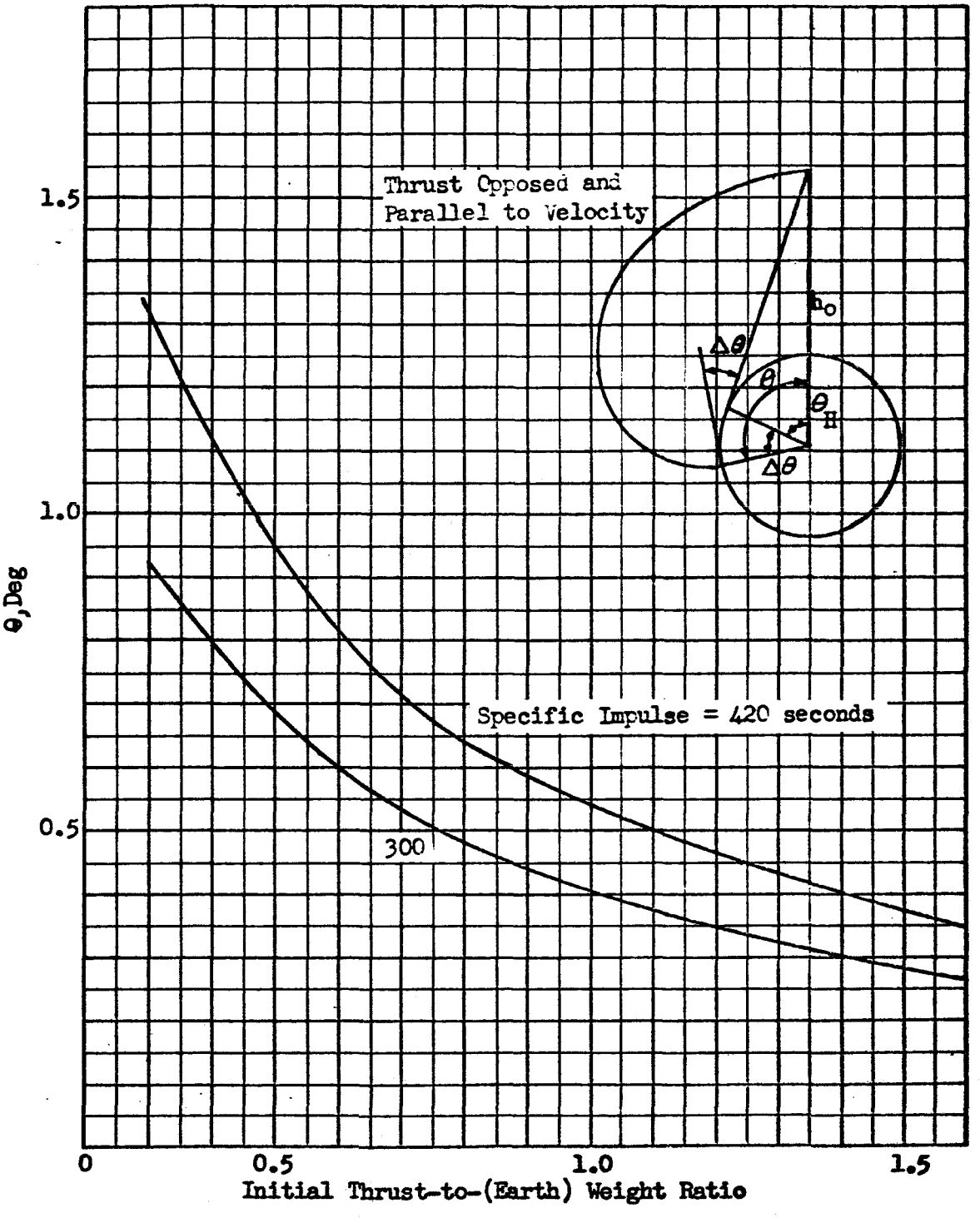

Figure 16 . Descent from Pericynthion Angular Distance from pericynthion to Landing Site Horizon.

site is always below the horizon from the pericynthion point. This may present some problems if it were desired to make optical or radar contact with the site prior to initiating the descent maneuver. However, the shape of the descent trajectory is such that the landing site comes into view in less than 30 seconds after thrust initiation (the entire descent to the hover point takes roughly five minutes).

The thrust opposing-and-parallel-to-velocity method, and two alternative means of thrust vector programming for the descent-from-pericynthion maneuver are shown in Figure 17. To simplify guidance requirements, the thrust may be directed parallel to the horizon until the flight path becomes vertical. At this point the thrust vector may be directed straight upward. A vehicle flight with this thrust program was simulated from a pericynthion altitude of 100,000 feet. For a common reference vehicle, the resultant payload was 40,5000 pounds compared to the 72,000 pounds of payload obtained using the thrust antiparallel to velocity maneuver.

Another method of descending from a given pericynthion is to apply a thrust greater than that which would be required to reduce the velocity to zero at the originally specified hover point. This would result in increasing the increment required during the descent/translation phase. Using impulsive thrust at a 50,000-foot pericynthion, the overall velocity increment (including impulsive braking after free fall to the surface) was found to be 6250 ft/sec compared to 5720 ft/sec when a thrust antiparallel to velocity maneuver was used to descend from that same altitude.

Landing Trajectory Review

Because of greater ideal velocity requirements, the direct vertical landing has a lower payload capability than the direct nonvertical landing or the intermediate orbital landing. A more serious disadvantage of the vertical trajectory is the fact that, should the propulsion system fail to ignite at the prescribed time, a collision with the lunar surface is inevitable; this maneuver was therefore disqualified from further consideration for manned missions.

Both the orbital and direct nonvertical maneuvers may be planned so that in the event of failure of the propulsion system to ignite, the vehicle does not impact the lunar surface but instead returns to Earth along a circumlunar trajectory. The choice of landing sites is restricted for the direct landing, while the orbital landing allows touchdown at any point on the lunar surface below the parking orbit. Two further advantages of the orbital approach are that it uses techniques developed by assumed previous nonlanding flights, and that it allows reconnaisance of the landing site. A disadvantage of the selected intermediate orbit trajectory is that it requires two additional propulsion system starts.

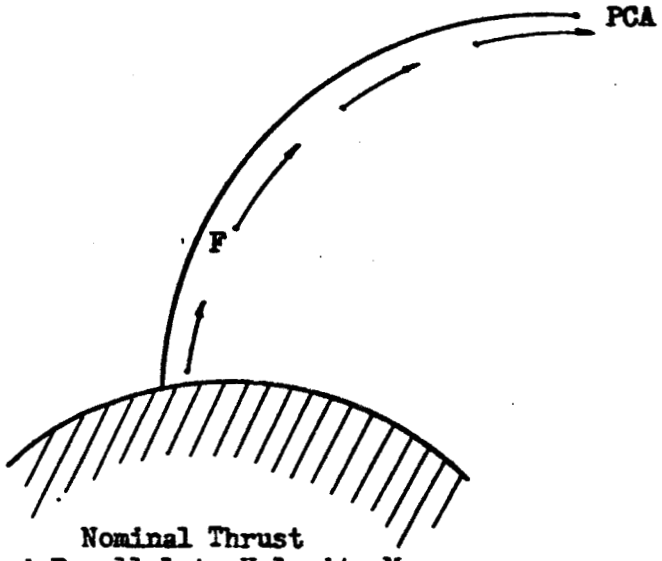

Nominal Thrust
Opposed and Parallel to Velocity Maneuver

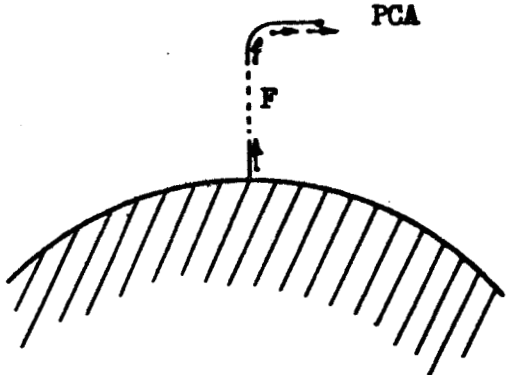

Opposed and Parallel; High Thrust/Weight

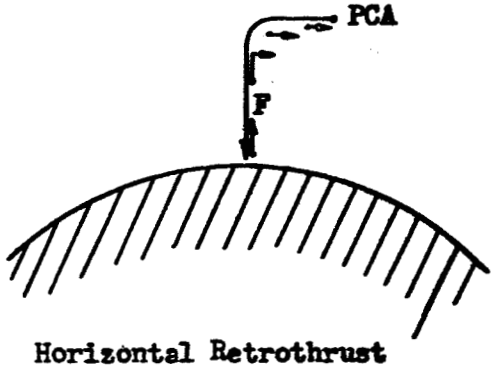

Horizontal Retrothrust

Figure 17 . Alternate Thrust Programs for Descent from Pericynthion

Review of various landing maneuvers (such as those shown) indicates that the use of a lunar parking orbit as an intermediate phase of the landing trajectory is probably the most desirable method for manned (and most unmanned) missions. Because of similar trajectory shapes, a descent-from-orbit trajectory, when combined with an orbit-establishment maneuver (based on the F/W existing at the beginning of each phase) is very similar in velocity requirements and optimum F/W to an optimized direct nonvertical trajectory. Though the analyses of landing-from-orbit maneuvers presented are based on an elliptical descent trajectory in which the ellipse is tangent (at apoapsis) to the original parking orbit, alternatives such as descent via an ellipse whose period matches the parking orbit period are possible; this might be applicable to specific missions such as one in which the descent vehicle has separated from a parent vehicle which remains in the initial circular parking orbit. Variations of this type have only moderate effect on propulsion system velocity requirements and practically no effect on thrust level selection.

Takeoff Maneuvers

Takeoff-to-orbit maneuvers exhibit a velocity requirement vs F/W trend similar to the landing maneuvers. For takeoff using a direct maneuver, where the vehicle leaves the lunar surface and enters a moon-Earth coast trajectory in one propulsion phase, the vehicle first makes a short vertical rise, then turns downrange and enters a thrust-parallel-to-velocity maneuver which continues until vehicle velocity is sufficient for the vehicle to enter the desired moon-Earth coast trajectory. The angle through which the vehicle turns before entering the thrust-parallel-to-velocity maneuver is adjusted such that the vehicle is moving nearly horizontally at the end of the takeoff maneuver. The velocity requirements for the direct maneuver are shown in Figure 18 .

For the indirect takeoff maneuver, the vehicle establishes a lunar parking orbit prior to achieving the velocity necessary for the moon-Earth transfer trajectory. To establish the parking orbit, the vehicle performs a short vertical ascent, then a downrange turn followed by a thrust-parallel-to-velocity maneuver until a coast to the prescribed orbit altitude can be achieved. Restart is required for injection into orbit. Lunar orbit establishment velocity requirements are shown in Figure 19 . After coasting in orbit to the correct position for the return trajectory, a final propulsion phase using a thrust-parallel-to-velocity maneuver accelerates the vehicle from its parking orbit to the velocity necessary to enter the moon-Earth coast trajectory; velocity requirements for this maneuver are shown in Figure 20 and 21 .

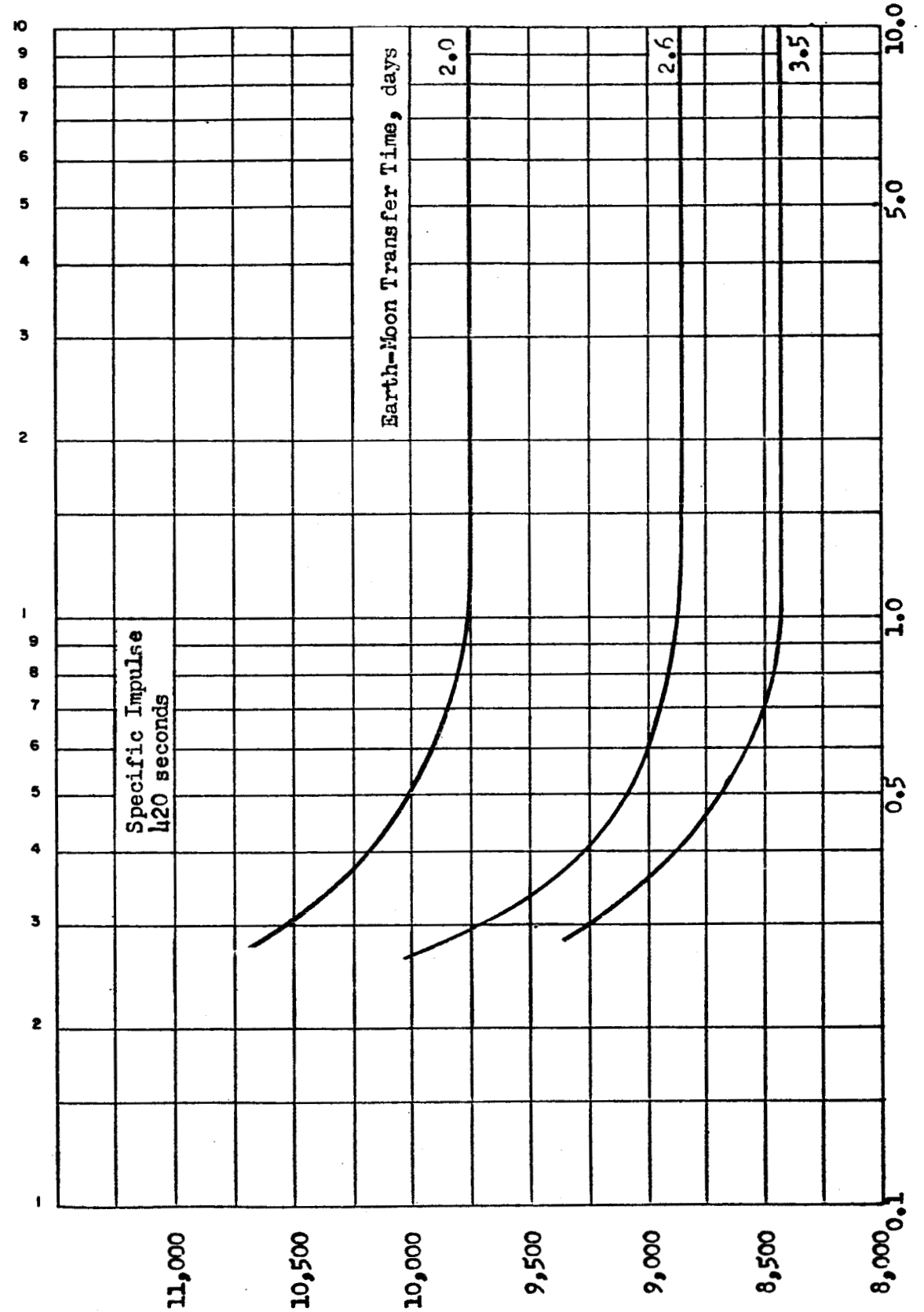

Figure 18. Ideal Velocity Requirement for Direct Lunar Takeoff to Moon-Earth Coast Trajectory

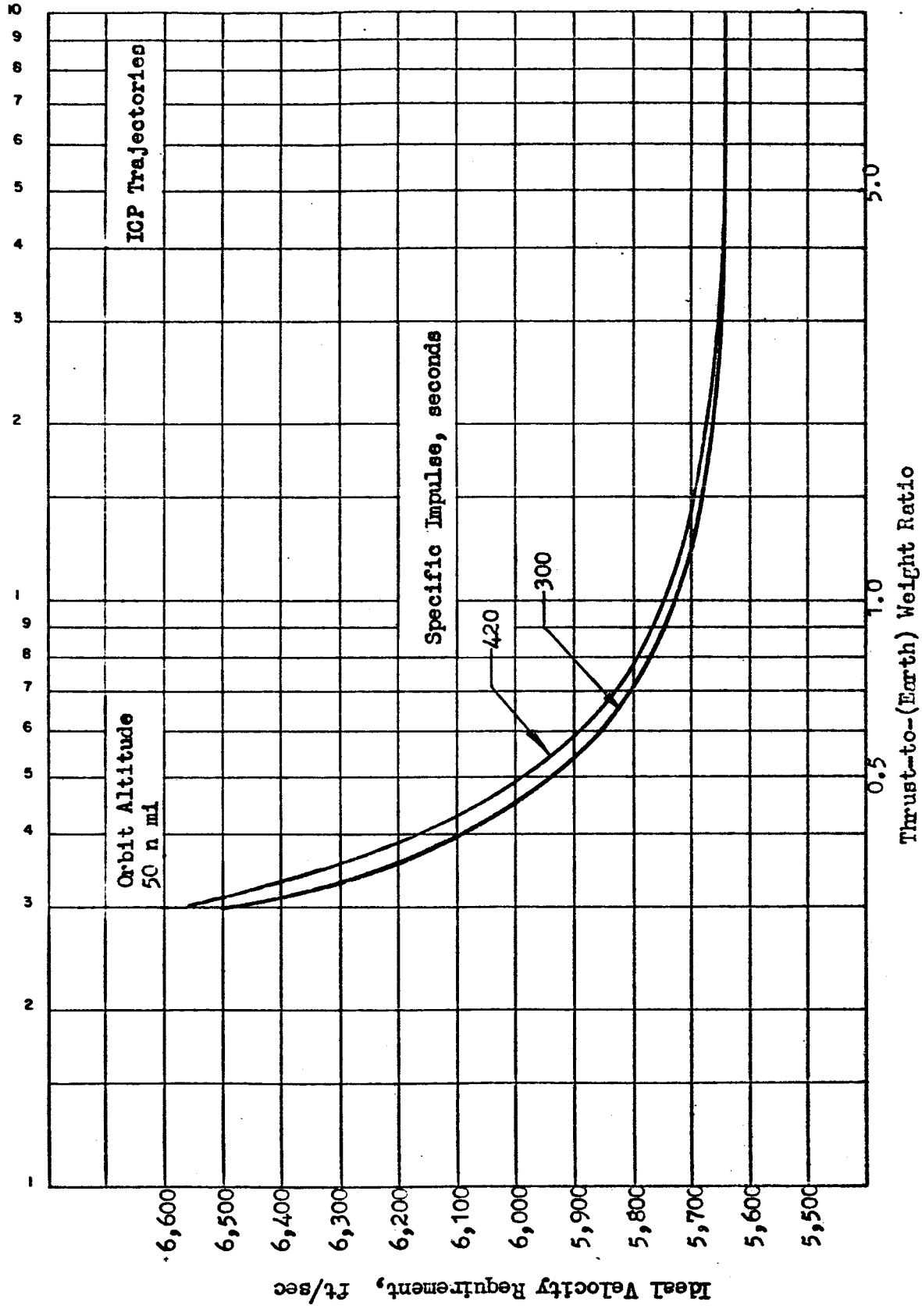

Figure 19. 50 n mi Lunar Orbit Establishment from Lunar Takeoff

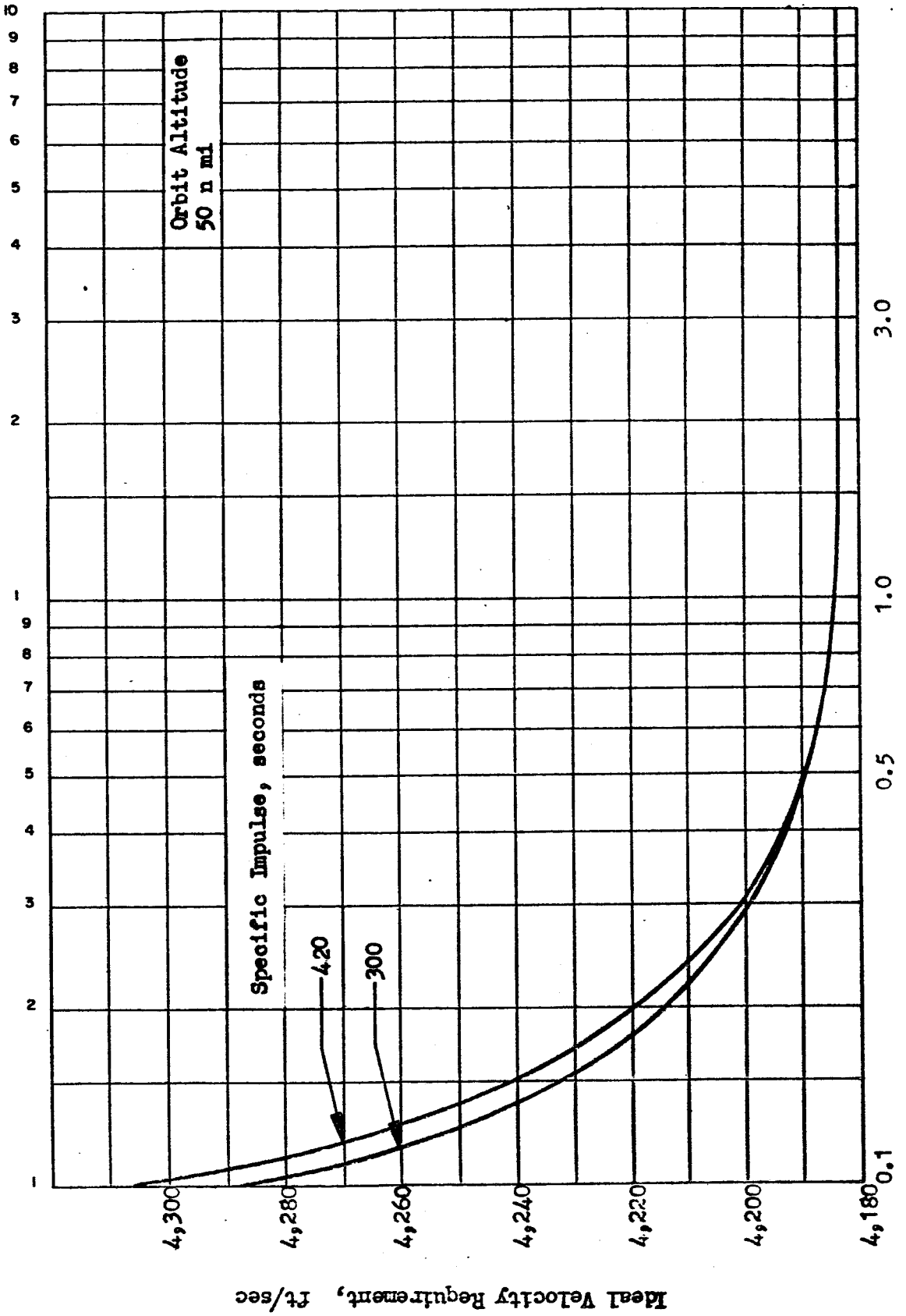

Figure 20. Ideal Velocity Requirement for Departure from Circular Lunar Orbit to Earth-Moon Trajectory (Two-day Moon-Earth Transfer Time)

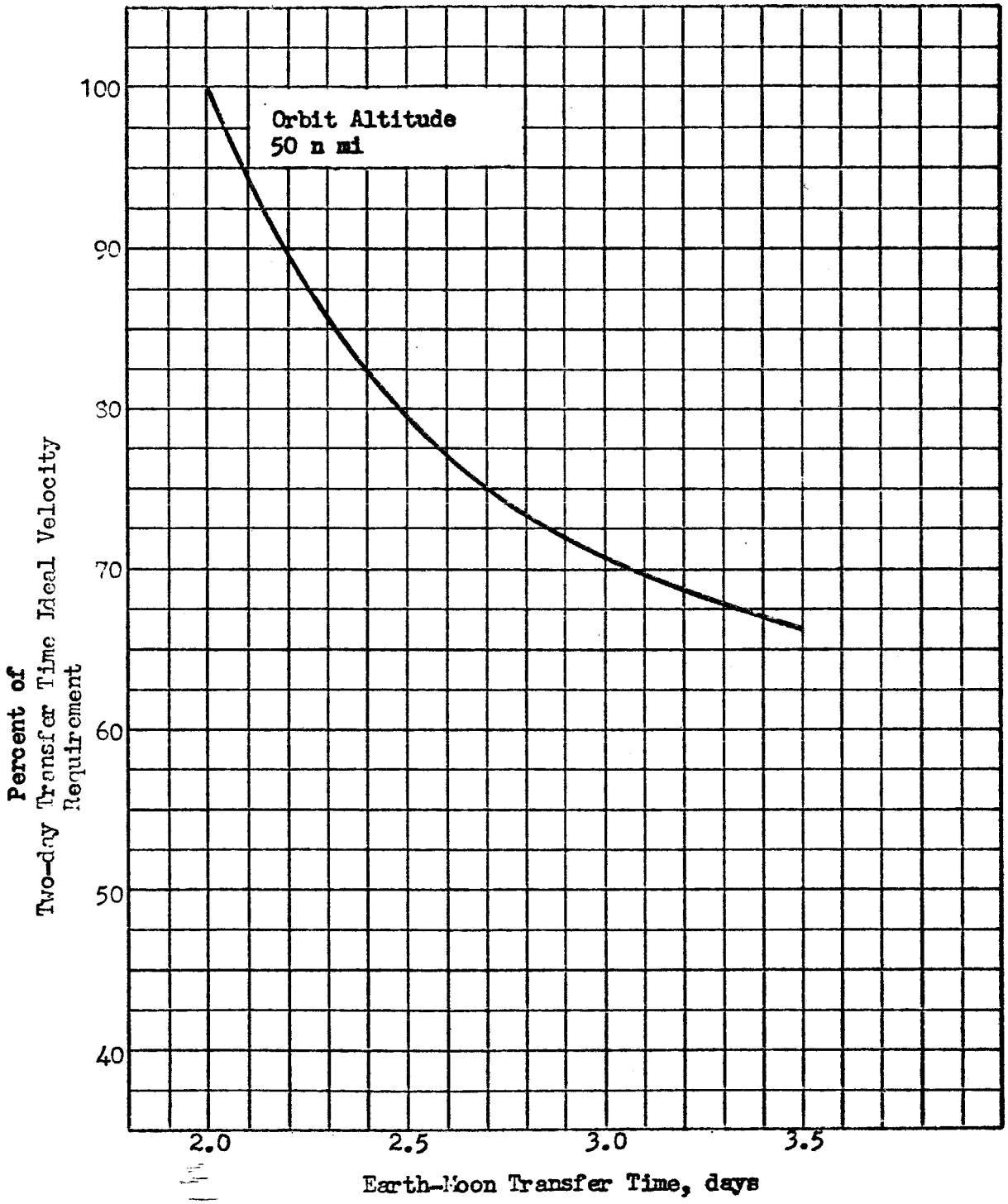

Figure 21. Ideal Velocity Requirement for Departure from Lunar Orbit to Earth-Moon Coast Trajectory versus Earth-Moon Transfer Time.

A comparison of the velocity requirements for the two types of Earth-return maneuvers (direct and intermediate-orbit) are presented in Figure 22 . The curves demonstrate a very similar profile of velocity requirement vs thrust-to-weight ratio. The indirect trajectory requires a slightly greater velocity increment; selection of a lower parking orbit altitude would, however, reduce the indirect mission velocity requirements to values closer to the direct mission values.

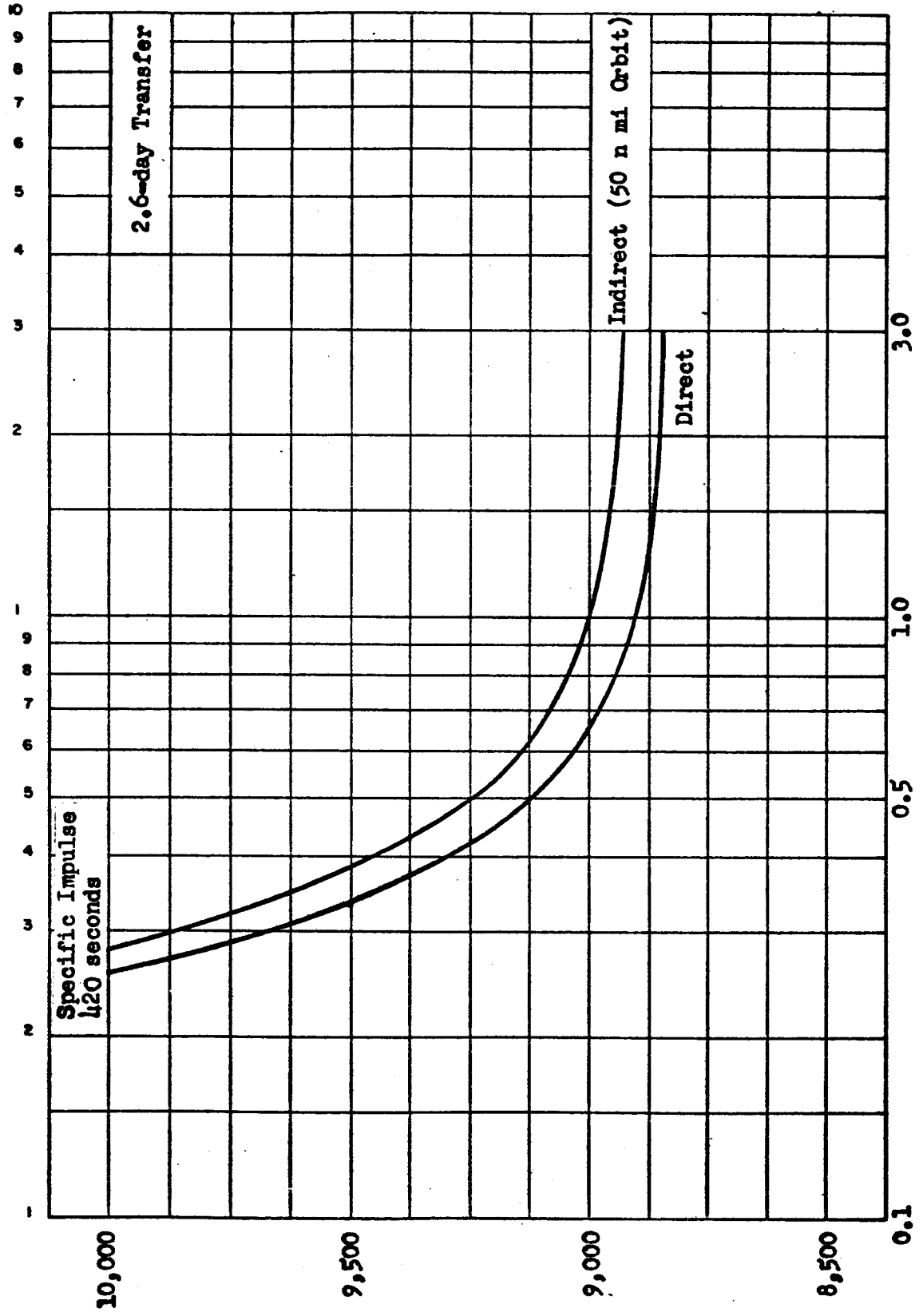

Figure 22. Ideal Velocity Requirement for Lunar Takeoff to Moon-Earth Coast Trajectory

LUNAR LANDING AND TAKE-OFF PROPULSION REQUIREMENTS

Two primary methods of performing a lunar landing mission are the direct mode, in which the entire transfer vehicle (minus propellant expended during the landing maneuver) descends to the lunar surface, and the orbital rendezvous mode, in which the Earth-return propulsion system is left in lunar orbit while only the payload and descent/ascent propulsion systems reach the surface. The propulsion requirements for both the direct and orbital-rendezvous mission propulsive maneuvers were investigated to determine velocity requirements for each of these landing modes and to evaluate the effect on payload of variation of system parameters.

The rendezvous mission technique offers the advantage of greater efficiency (i.e., more payload per unit weight of the transfer vehicle), but this advantage is realized only if the combination of landing site and stay-time is such that significant plane-changes by the ascent vehicle and/or the parent vehicle are avoided.* To obtain complete landing site and stay-time flexibility, with minimum velocity penalties, which is a requirement of later-generation lunar vehicles, the direct landing mode may be superior. The orbital-rendezvous system can avoid plane changes only by utilizing stay-times which are some integral multiple of half lunar cycles; situations may exist in which this restriction might not be feasible.

The analyses of propulsion requirements have in part been based on vehicles of the Apollo size or Saturn C-5 capability; the treatment is parametric and the results presented are applicable to future vehicles of larger sizes.

---

* The extremes of possible situations, neglecting the inclination of the lunar plane, are: (1) an orbit in the lunar plane in conjunction with any lunar-plane landing site and stay-time; in this instance, the orbital plane of the parent vehicle always includes the landing vehicle and the Earth, and no plane changes are required. Or (2) the polar orbit in conjunction with one of the two possible lunar plane landing sites, and approximately a 7-day stay time. For this, the take-off vehicle requires a 90-degree plane-change to return to the parent vehicle, and then the parent vehicle requires a 90-degree plane-change to return to Earth.

Direct Mission

Mission Profile. The mission profile for a (manned) direct lunar mission has the following sequence of maneuvers:

1. Lunar orbit-establishment } Or, Direct landing from
2. Lunar landing-from-orbit } transfer trajectory
3. Lunar takeoff-to-Earth transfer

The total velocity requirement of the landing system analyzed is the sum of velocity additions (chronologically) for midcourse correction ($\sim$150 ft/sec), circular orbit establishment ($\sim$3200 ft/sec), orbit eccentricity change ($\sim$60 ft/sec), velocity cancellation ($\sim$5700 ft/sec), and hovering/translation (from 200 to 1000 ft/sec). In addition, a propellant reserve equivalent to approximately 300 ft/sec ($\sim$3 percent) is included. Thus, the overall velocity requirement is between 9500 ft/sec and 10,500 ft/sec.

Parametric Stage Analysis. The payload capability of a high energy, cryogenic propellant lunar landing stage is presented parametrically in Figure 23, based on a 90,000-pound vehicle gross weight. Propellant fraction is determined by stage design characteristics, and is strongly influenced by the type of feed system chosen for use in the landing stage propulsion system.

For an Earth-return payload of 9000 pounds, results presented in Figures 24 and 25 indicate the takeoff gross weight required as a function of propellant fraction, specific impulse and velocity requirement of cryogenic and noncryogenic systems respectively. The allowable gross weight of the lunar takeoff stage is the landing stage payload. It should be noted that the insulation and shielding associated with the takeoff propulsion system might be jettisoned at the start of the Earth-return phase; this results in a gross takeoff weight smaller than the payload originally landed.

For a reference gross weight of 90,000 pounds (the Saturn C-5 escape payload) and a 9000-pound Earth-return payload, various propulsion systems which could be used for lunar landing and Earth return phase were investigated. For an O_2/H_2 pressure-fed landing system, design studies have indicated that for the stage size considered, a propellant fraction of 0.79 is representative and for a pump-fed system, the approximate value is 0.85. For a pressure-fed, noncryogenic (N_2O_4/50-50) propellant takeoff propulsion system, preliminary designs have yielded propellant fractions of 0.88. For these

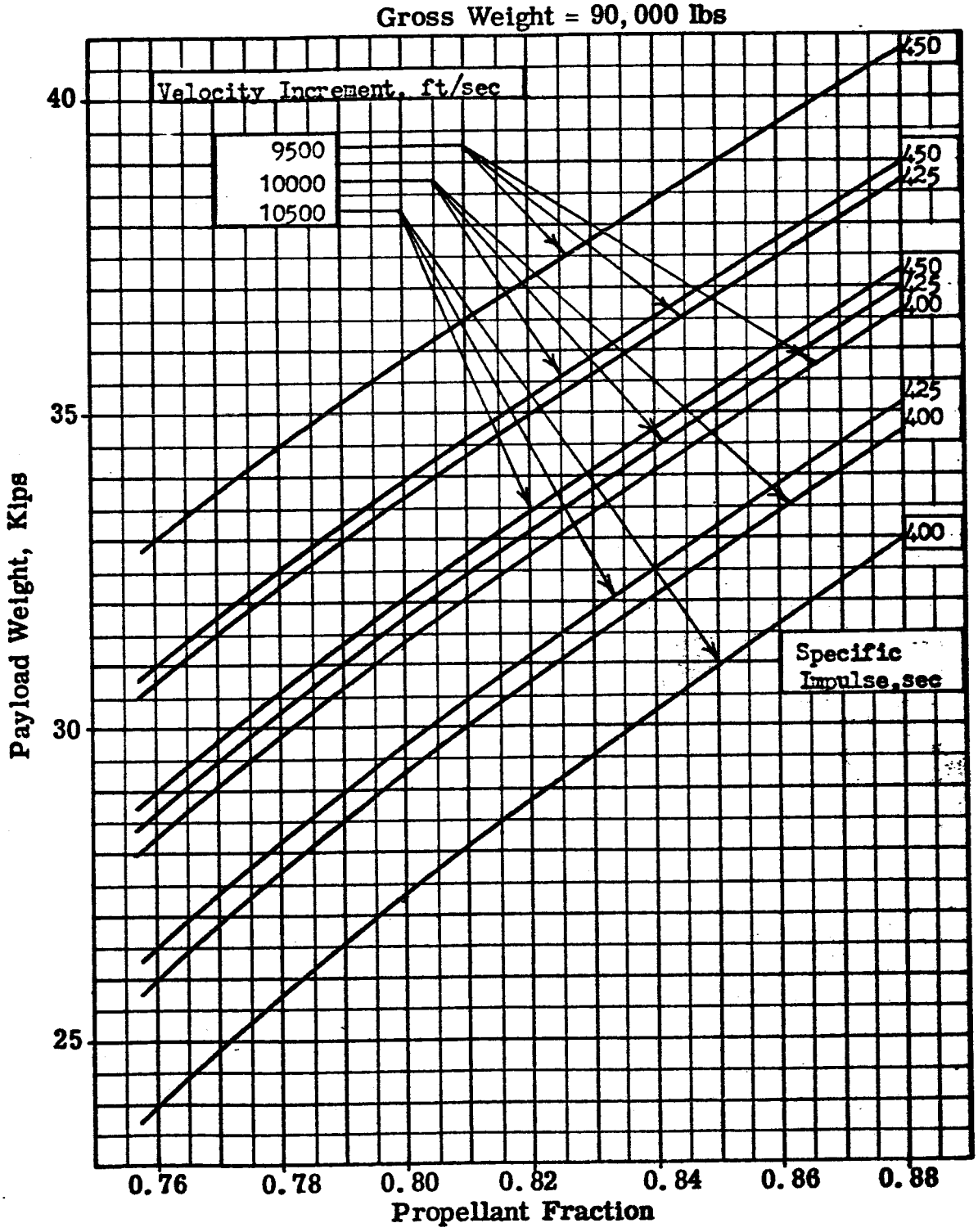

Fig. 23. ..... O_2/H_2 Lunar Landing Vehicles

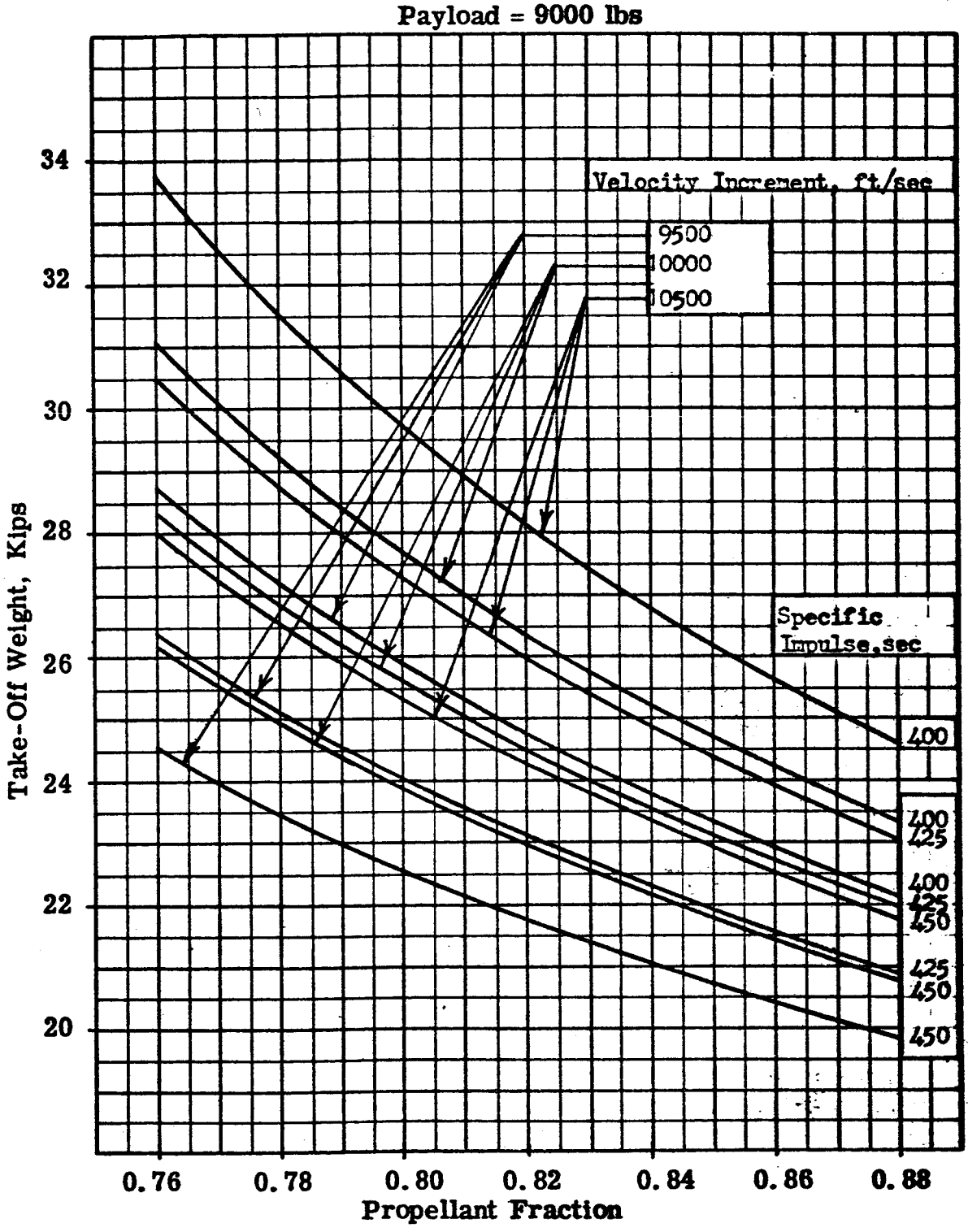

Fig. 24 - O_2/H_2 Lunar Take-Off Vehicles

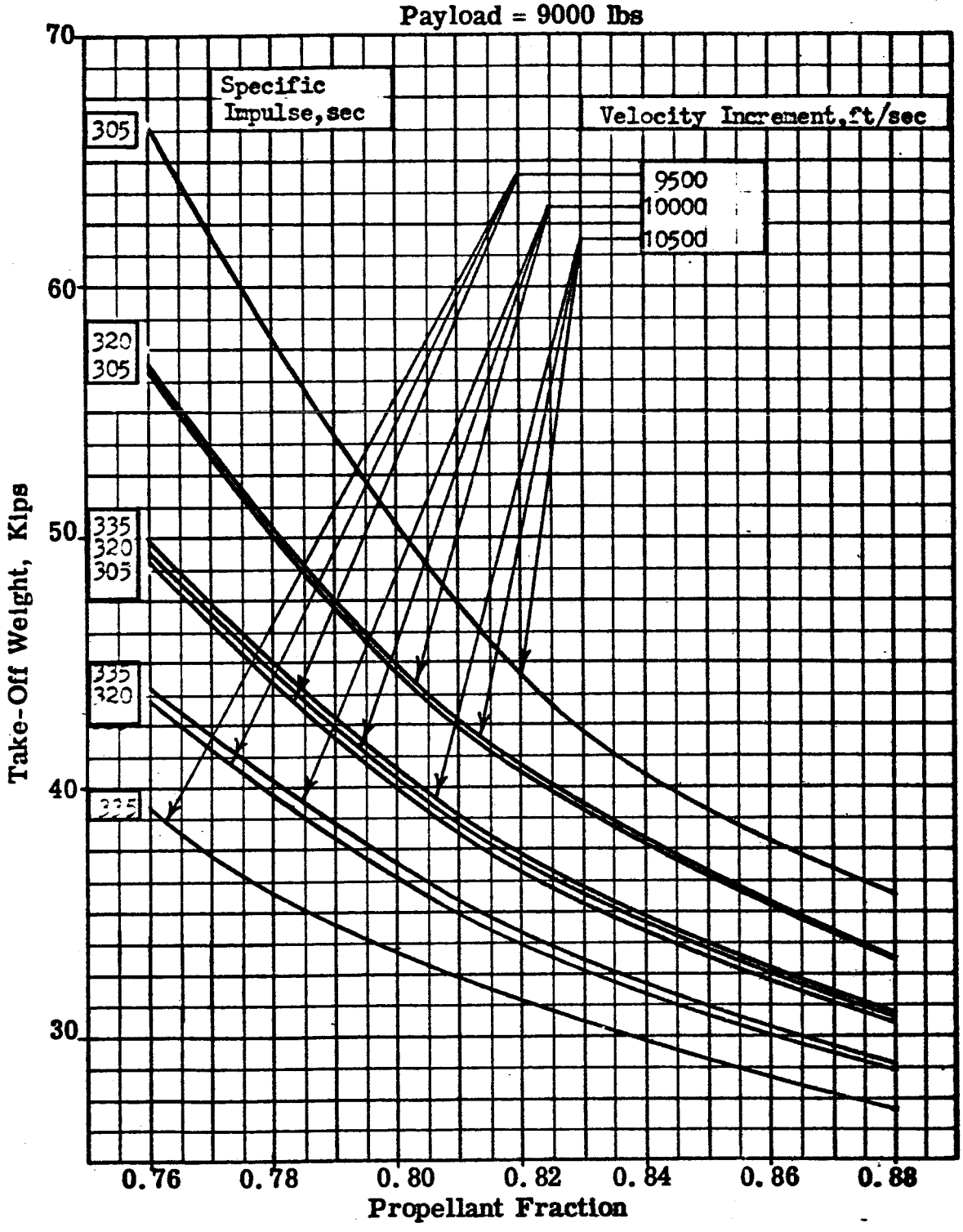

Fig. 25. Nonrygenic Propellant Lunar Take-Off Vehicles

systems, the acceptable combinations of landing and takeoff propulsion systems, within the assumed restrictions, are indicated in Figure 26 .

Thrust Level Selection. The selection of thrust level for lunar landing and takeoff is governed by many factors, including propellant combination, landing trajectory, and vehicle engine and tank weights. Selection of the optimum thrust level for a space vehicle is governed principally by the exchange between velocity requirements and propellant dependent weights (each of which decreases as thrust-to-weight ratio increases) and engine and thrust structure weights (which decrease as thrust-to-weight ratio decreases).

Various trajectory concepts exist for soft landing a vehicle on the lunar surface, as illustrated in Figure 8 . The intermediate orbit landing has velocity requirements very similar to the direct nonvertical landing. From a site selection and abort capability standpoint, the intermediate orbit landing trajectory is more flexible than a direct landing. It was therefore used in the analysis of the effect of various vehicle parameters on thrust level selection. The difference between payload and optimum thrust-to-weight ratios for a vehicle using a direct vertical landing and an intermediate orbital landing vehicle is illustrated in Figure 27 .

For thrust level optimization studies, the propulsion system inert weight can be reasonably characterized by three factors: (1) a fixed weight factor, (2) a thrust dependent weight factor, and (3) a propellant dependent weight factor. The effects of these factors on optimum vehicle thrust-to-weight for a single stage which performs the entire landing maneuver are illustrated in Figures 28 , 29, 30, and 31 , beginning from the lunar approach path resulting from a 2.6-day Earth-moon mission.

Since the duration of the hover-translation phase required near the lunar surface cannot be ascertained precisely, Figure 31 is presented to show, by comparison to Figure 29 , the effect of hovering ΔV on optimum thrust-to-weight ratio. A 1000-ft/sec hovering ΔV is included in Figure 29 while no hovering ΔV is included in Figure 31 . The effects of two other factors which influence optimum thrust-to-weight ratio are illustrated in Figures 32 and 33 . The effect of specific impulse is indicated in Figure 32 . The effect of Earth-moon coast trajectory transfer time is indicated in Figure 33 . Thrust level selection for any mission considered is also affected by the interstage weight changes accompanying thrust level variations.

FIG.26. SATURN C-5 LUNAR LOGISTICS VEHICLE

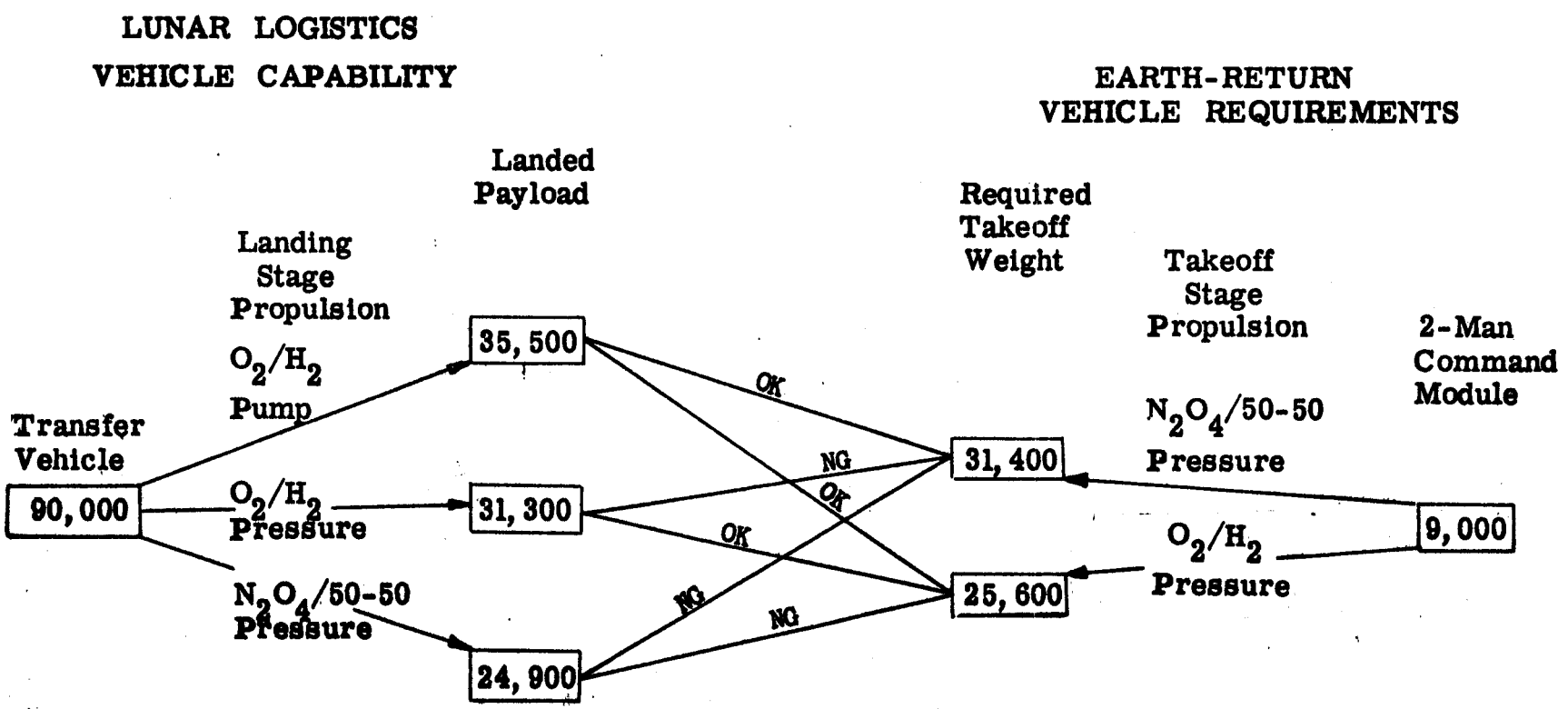

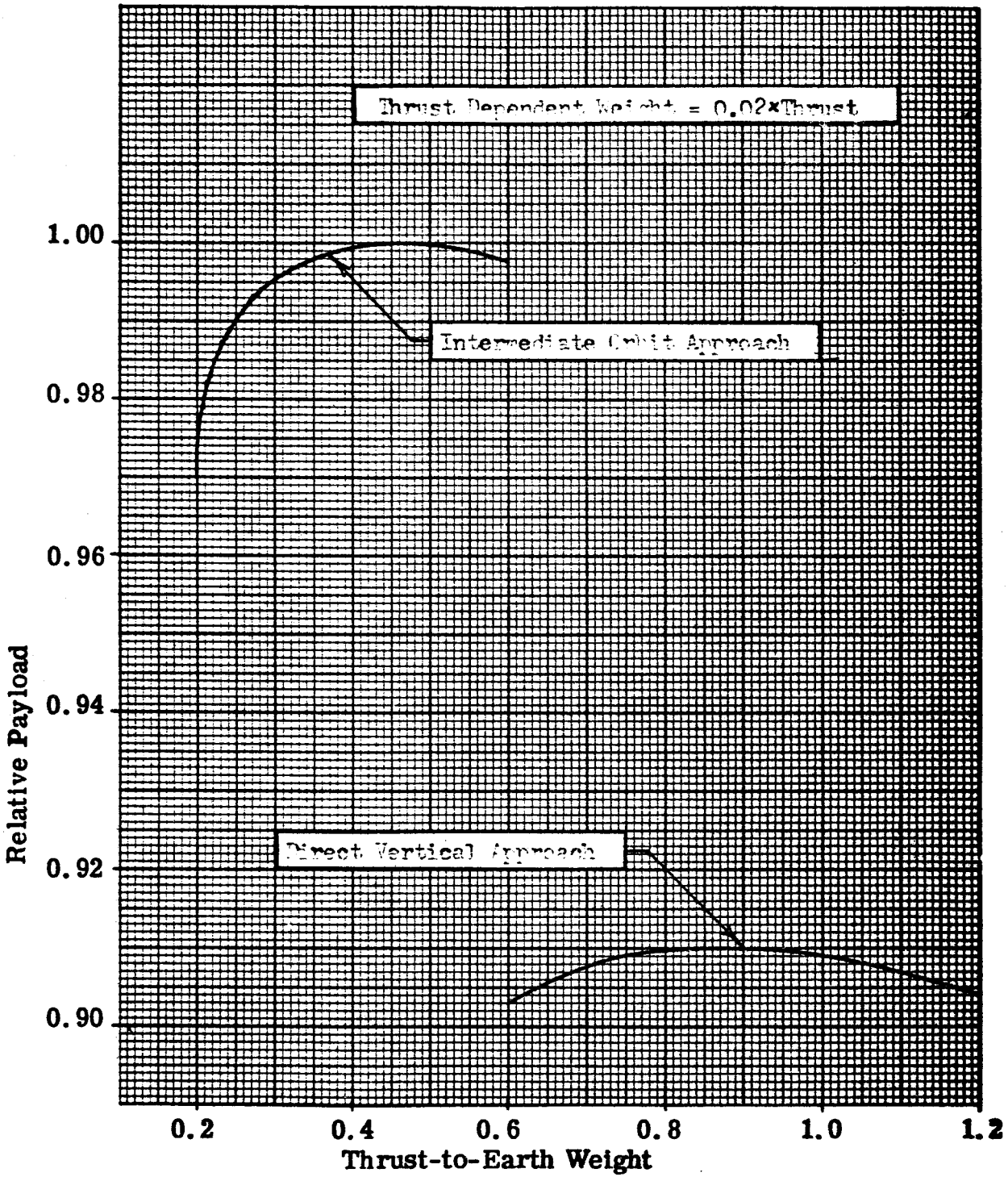

Fig. 27. Effect of Lunar Landing Method on Thrust Level Selection

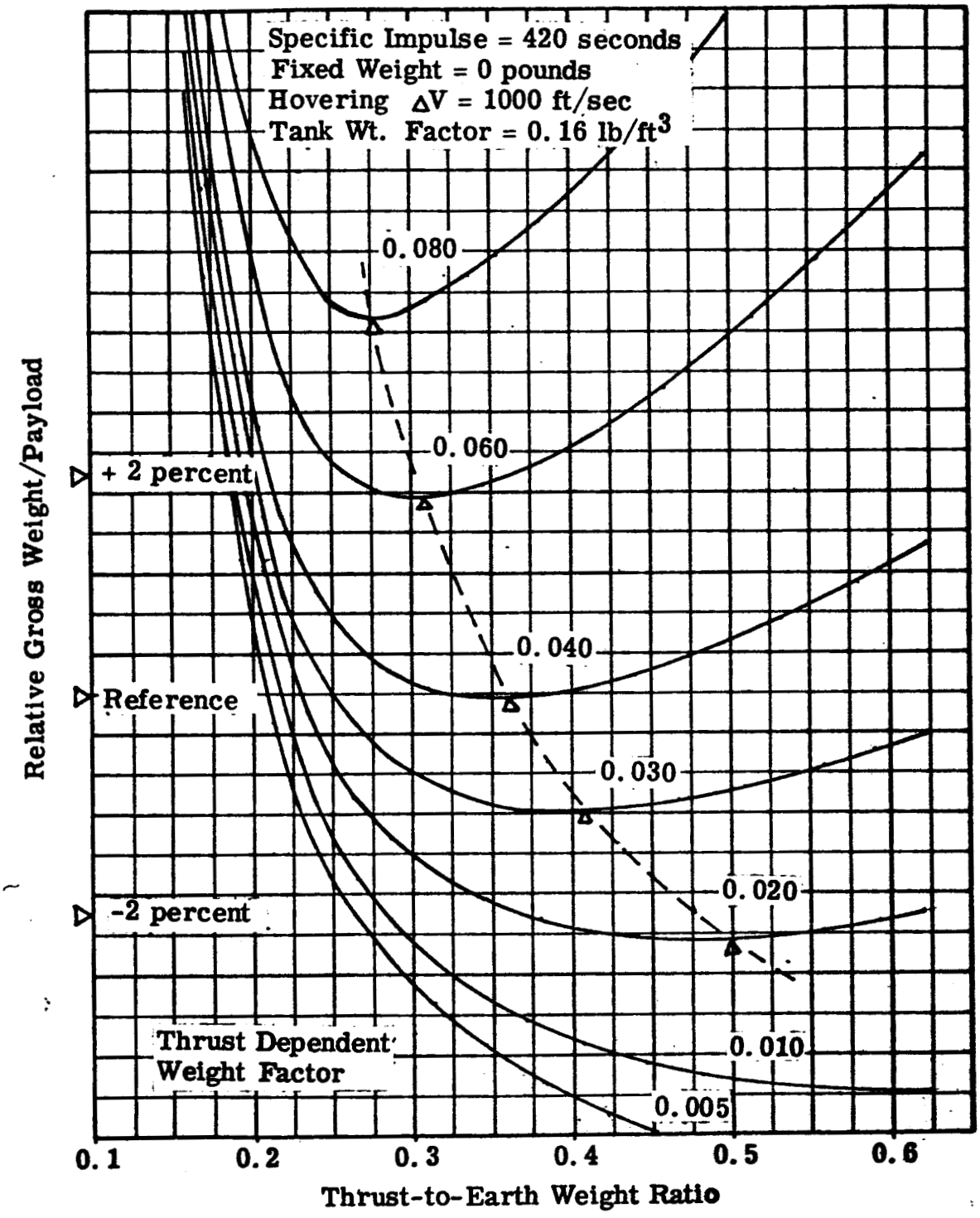

Figure 28 . Thrust Selection for Lunar Landing

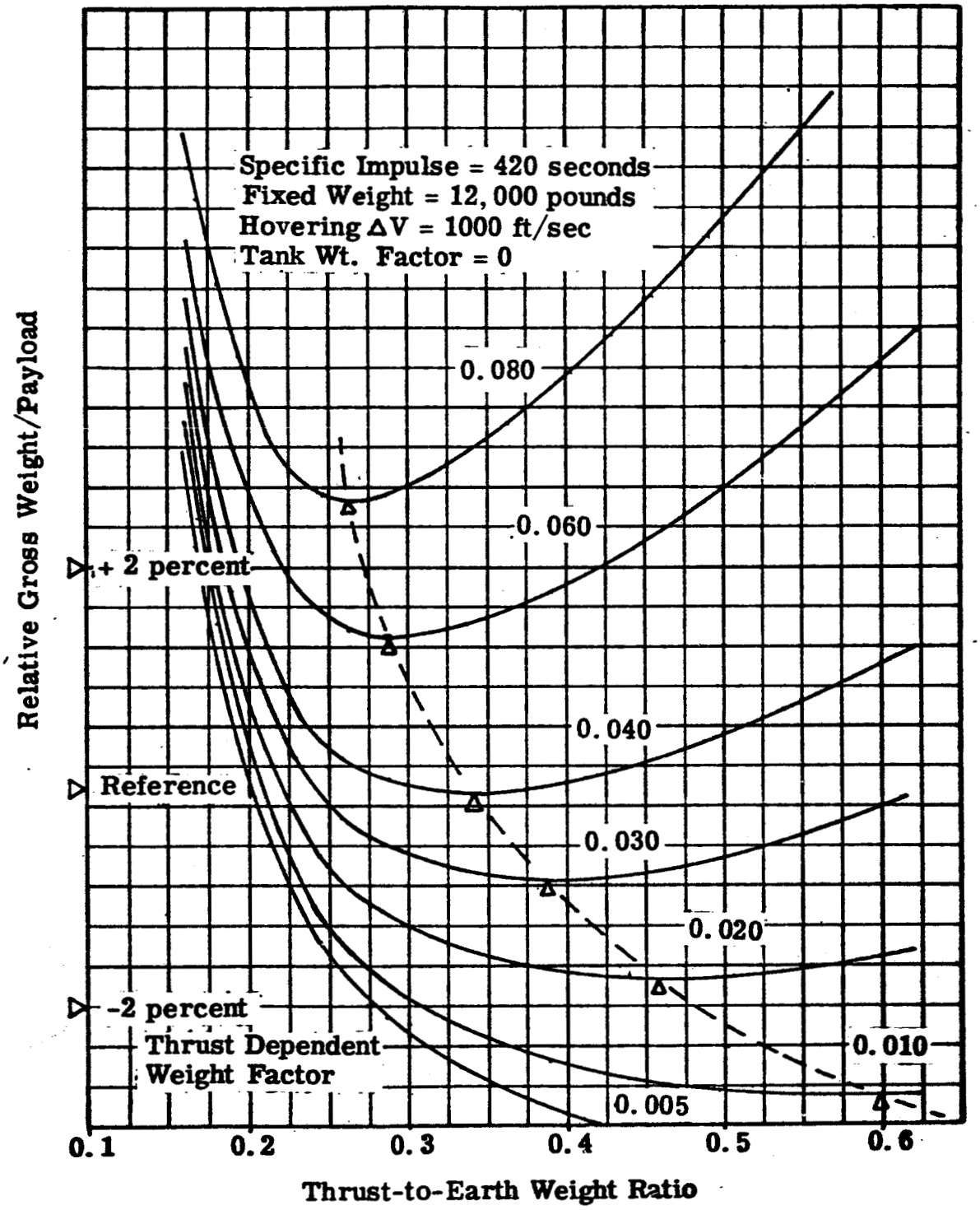

Figure 29. Thrust Selection for Lunar Landing

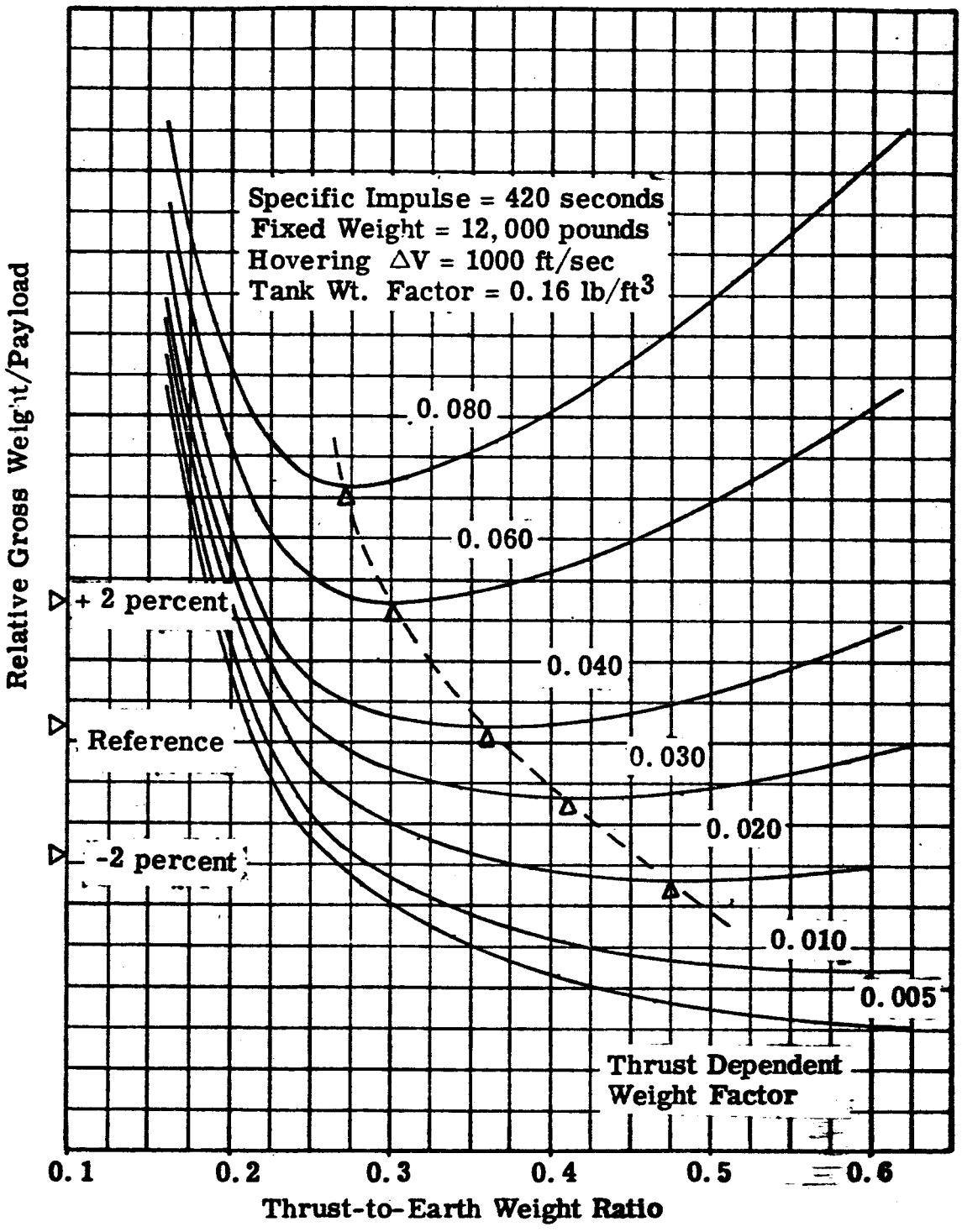

Figure 30. Thrust Selection for Lunar Landing

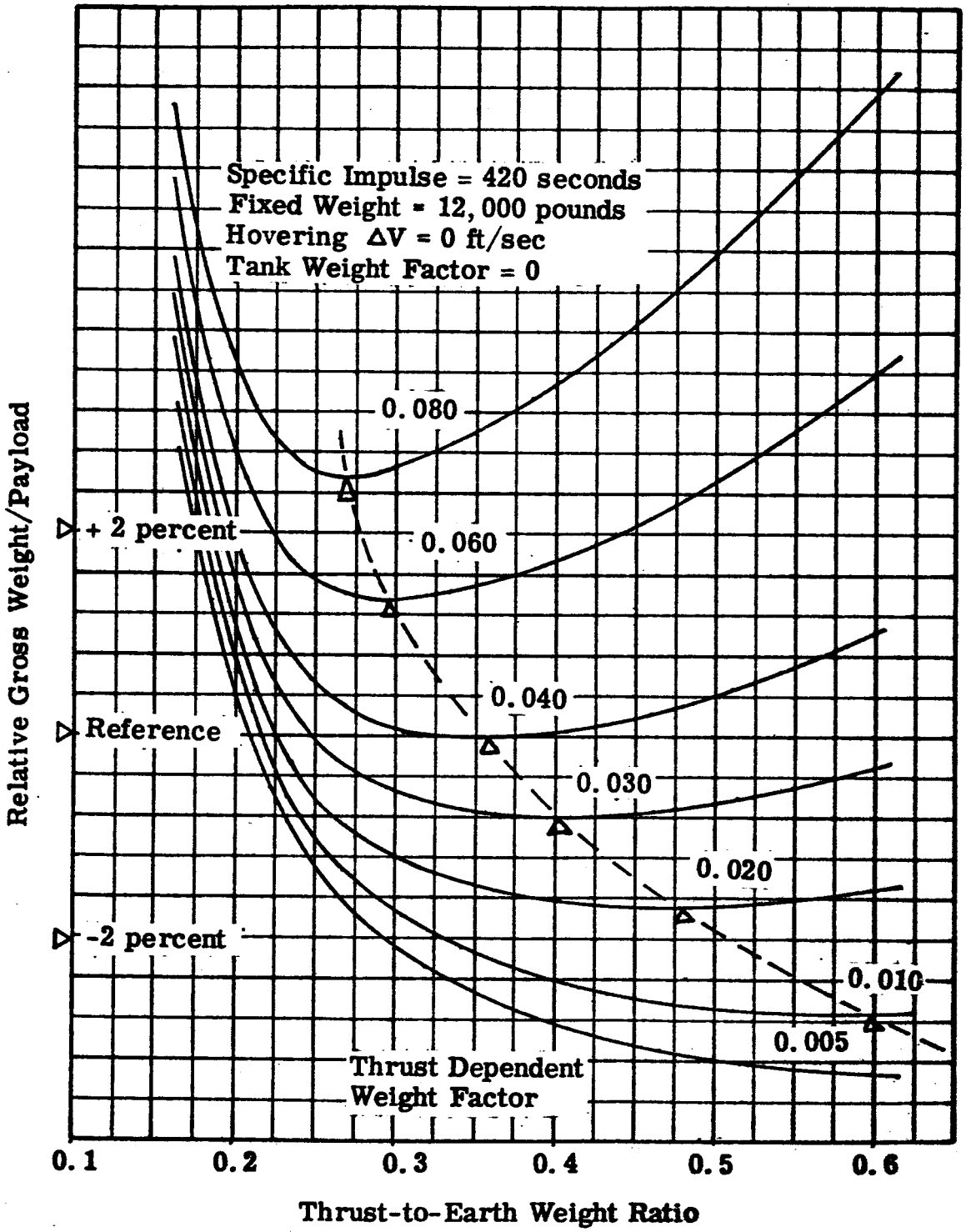

Figure 31. Thrust Selection for Lunar Landing

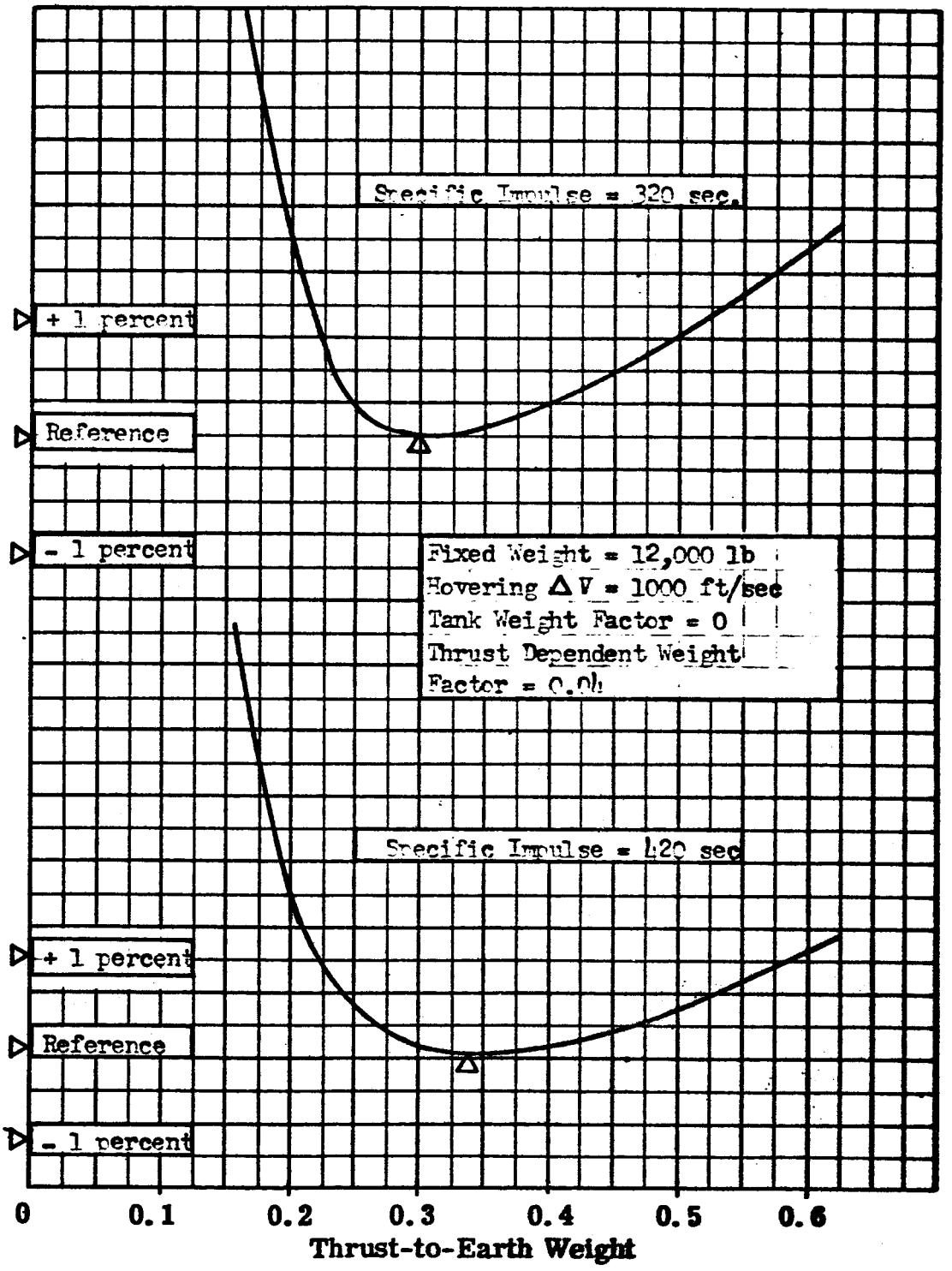

Fig. 32. Thrust Selection for Lunar Landing

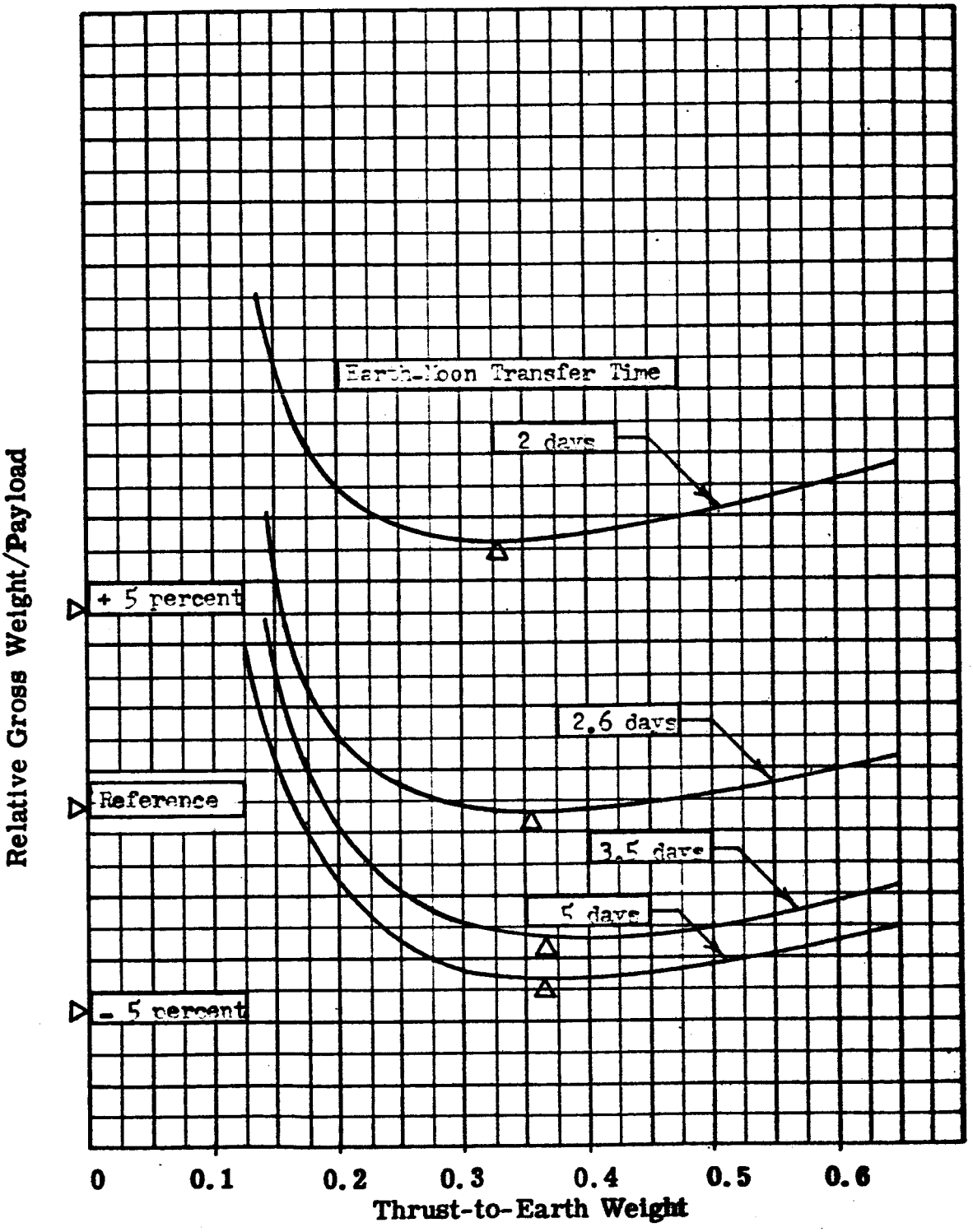

Fig.33. Thrust Selection for Lunar Landing

This effect (somewhat amplified because of a relatively high assumed value of interstage structure weight/inch) is illustrated in Figure 34 for the lunar landing mission.

It is evident from the figures presented that fixed weight, tank weight, hovering ΔV, transfer time, interstage weight, and specific impulse are all factors which do not in general strongly influence thrust level selection. Fixed weight does not affect optimum thrust-to-weight ratio. As the propellant dependent weight factor increases, optimum thrust-to-weight ratio increases. Increase of the hovering ΔV allowance decreases optimum thrust-to-weight ratio slightly. As Earth-moon transfer time increases, the optimum lunar landing thrust-to-weight ratio increases. An increase in the specific weight of interstage structure decreases optimum thrust-to-weight ratio while an increase in specific impulse causes an increase in optimum thrust-to-weight ratio.

The effect of thrust dependent weight factor on optimum thrust-to-weight ratio is shown in Figure 35 as determined from the loci of optimum points of Figures 28 to 31 . Optimum thrust-to-weight ratio decreases from 0.475 when the thrust-dependent weight factor is 0.02 lb/lb thrust to 0.3 when the thrust-dependent weight factor is 0.06. A wide range of thrust-dependent weights must be considered since redundant systems may be employed, and the degree of engine redundancy strongly affects engine weight factor.

Fortunately, since there are so many variables which should be considered, the penalty for operation at an off-optimum thrust level is not severe. For example, from the 420 specific impulse curve of Figure 32 , it is evident that vehicle gross weights within 1 percent of the minimum (which occurs at a thrust-to-weight ratio of 0.34) can be achieved with thrust-to-weight ratios from 0.22 to 0.58.

Maneuver Termination Conditions The thrust-to-weight ratio of the vehicle at the end of the main descent maneuver is of interest since it establishes the initial condition for translation, hovering and final descent maneuvers. The terminal thrust-to-lunar weight ratio is a function of vehicle initial thrust-to-weight ratio and the mass ratio. The variation of terminal thrust-to-weight ratio for a direct landing maneuver is shown in Figure 36 . To achieve a 1:1 vehicle thrust-to-weight ratio (necessary for constant altitude hovering), an engine throttling ratio equal to the terminal thrust-to-lunar weight ratio is required. For satisfactory control during the terminal landing phase, it may be necessary to throttle the landing engine to thrust-to-weight ratios substantially below 1:1, and engine designs must include an allowance for this consideration.

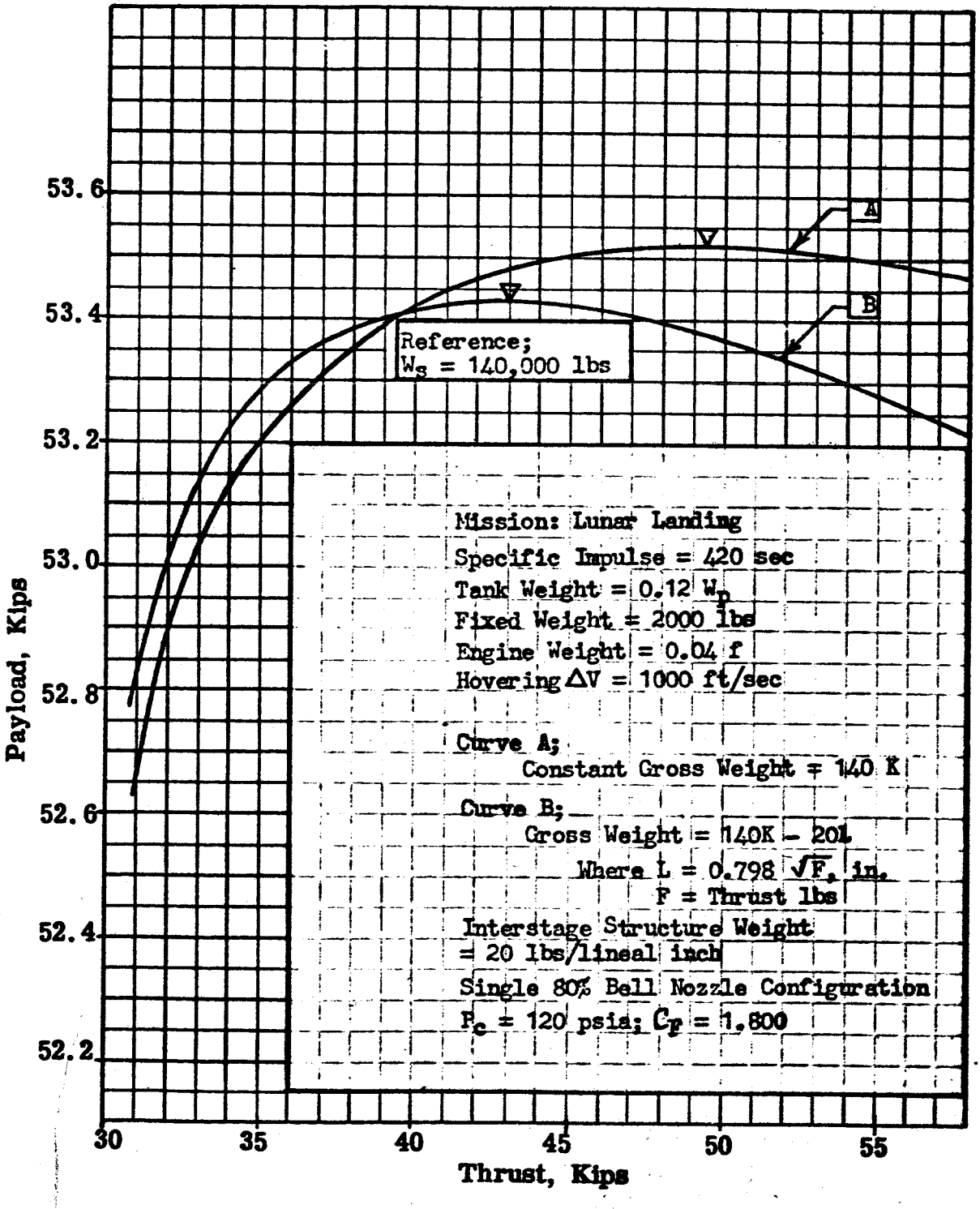

Fig. 34. Effect of Interstage Structure Weight on Thrust Level Selection

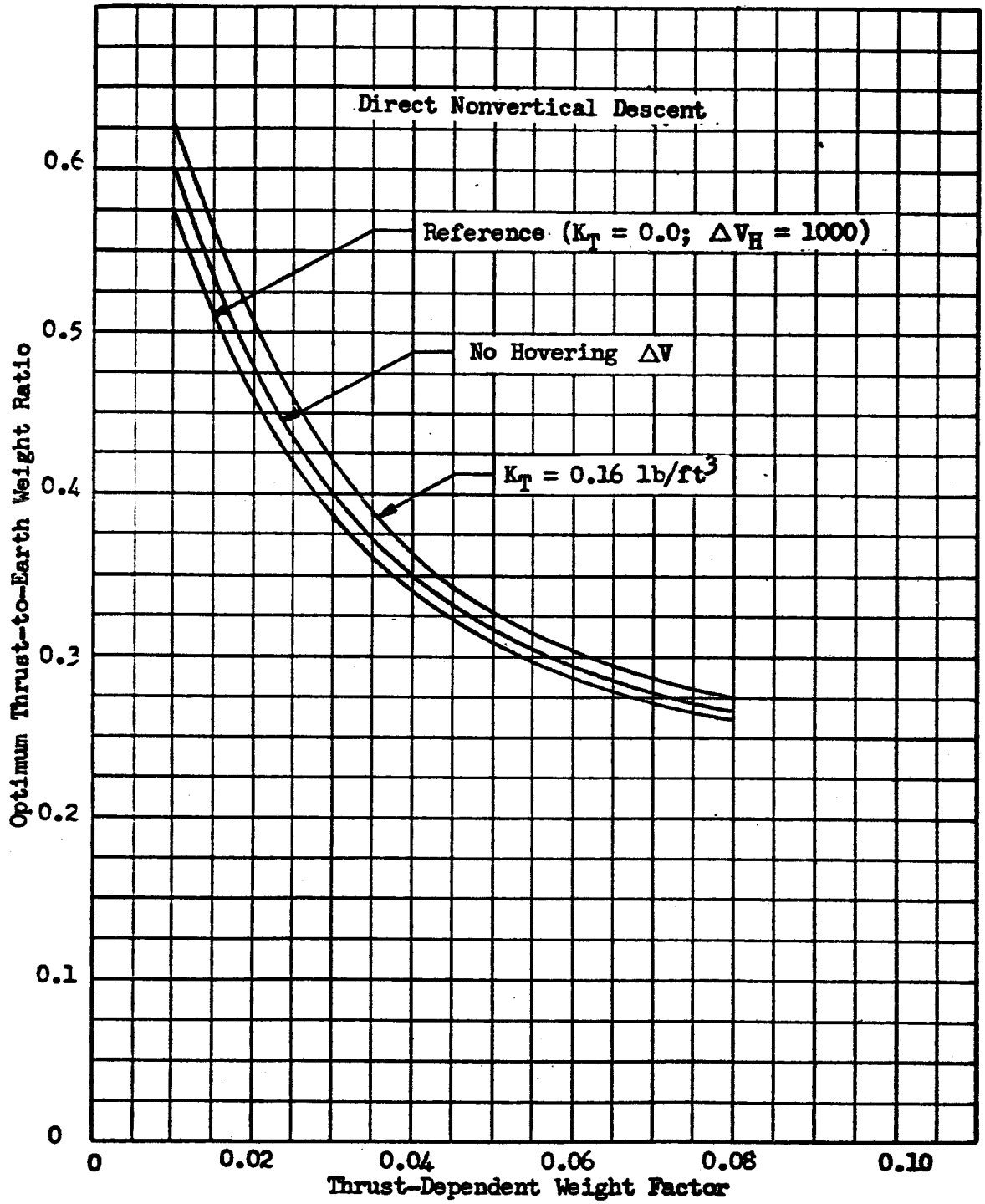

Figure 35. Thrust Selection for Lunar Landing

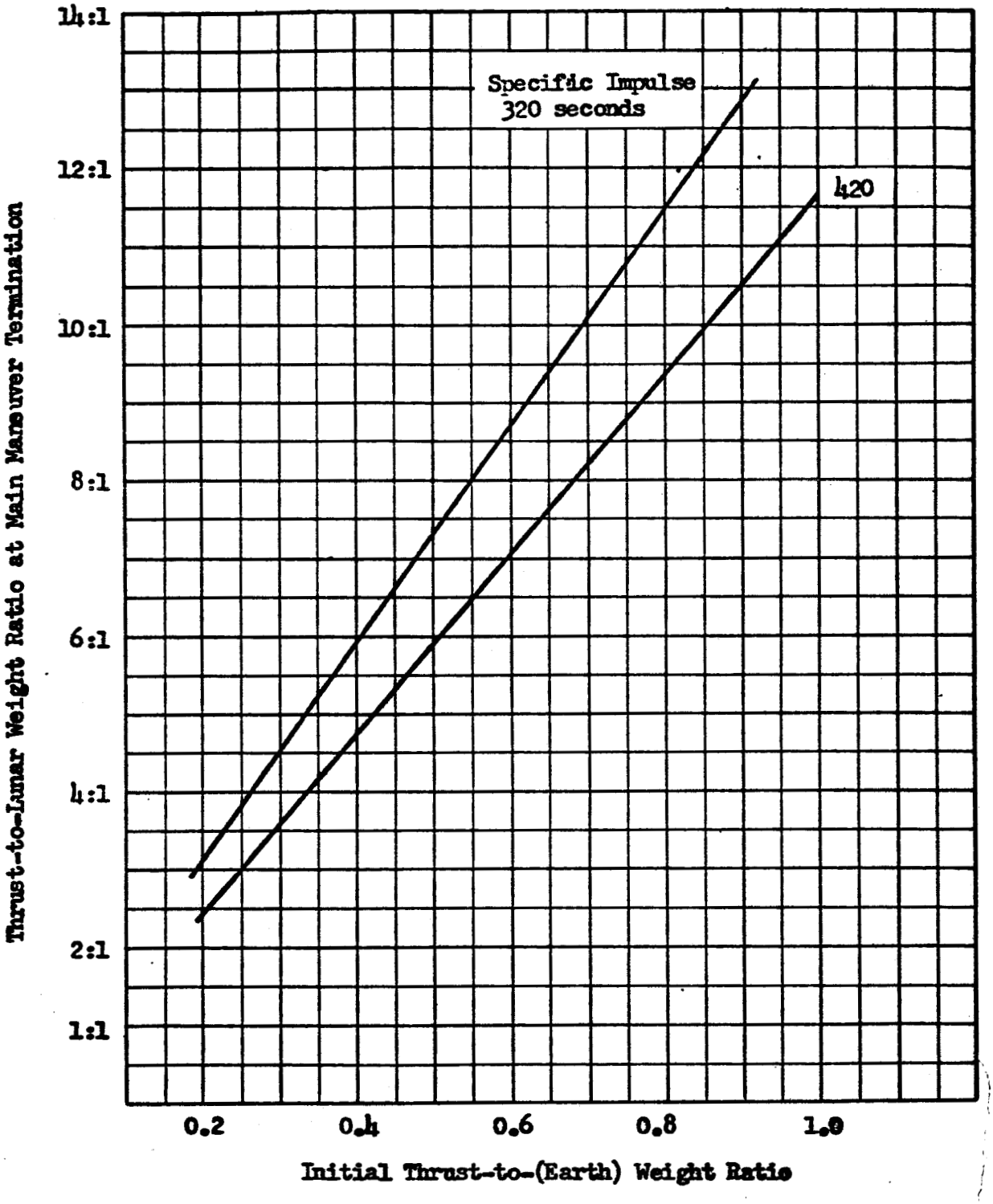

Figure 36. Throttling Ratio Required to Achieve Thrust Equal to Lunar Weight: Direct Lunar Landing

Propulsion Review. The thrust level for the landing engine is determined principally by the type of landing trajectory employed (an intermediate orbit method) and by the relationship between thrust level, engine weight, and the thrust-to-weight versus velocity requirement characteristic for the landing trajectory. For the vehicle and trajectory characteristics considered, a thrust to weight ratio of approximately 0.45 is desirable. An engine throttling capability of 10:1 would provide sufficient thrust control for performance of hovering and translation maneuvers near the lunar surface.

A comparison of the approximate capabilities of various landing vehicle configurations is shown in Figure 37 . The data indicate the advantage of high energy stages over alternative systems, and show the capability of several future launch vehicles.

Lunar Orbit Rendezvous

Vehicle Concept. Landing an entire space vehicle represents a use of propellants during the descent and takeoff maneuvers which may be partially conserved by leaving part of the vehicle in lunar orbit. A propulsion system (single-stage or multi-stage) must then accomplish the descent, translation, takeoff, and rendezvous maneuvers. (Figure 38).

Trajectory analysis for the mission was based on the vehicle being in a 50-n mi circular lunar orbit, and using the intermediate coast trajectory for descent. The landing stage is decelerated into an elliptical orbit with a 50-n mi apocynthion (maximum) altitude and a pericynthion (minimum) altitude determined by the specific impulse and the thrust-to-weight ratio at the beginning of the next maneuver. The vehicle coasts to the pericynthion at which point thrust is applied antiparallel to the velocity vector. At the end of this maneuver, the vehicle is a few thousand feet above the lunar surface and hovering or descending at a relatively slow speed. The hover point is set sufficiently high above the surface to allow for uncertainties during the landing maneuver.

The takeoff maneuver consists of a vertical rise followed by kickover and thrust parallel to velocity sequence. When sufficient velocity has been generated, thrust is terminated and the vehicle coasts to a 50-n mi apocynthion where thrust is again applied to circularize the orbit and rendezvous with the remainder of the spacecraft. The payload is transferred to the spacecraft which provides propulsion for the return transfer.

The ideal velocity requirements for landing from a 50-n mi orbit and takeoff to 50-n mi orbit are shown as a function of initial thrust-to-(Earth) weight ratio (F/W) in Figure 39 . The lower pairs of curves represent

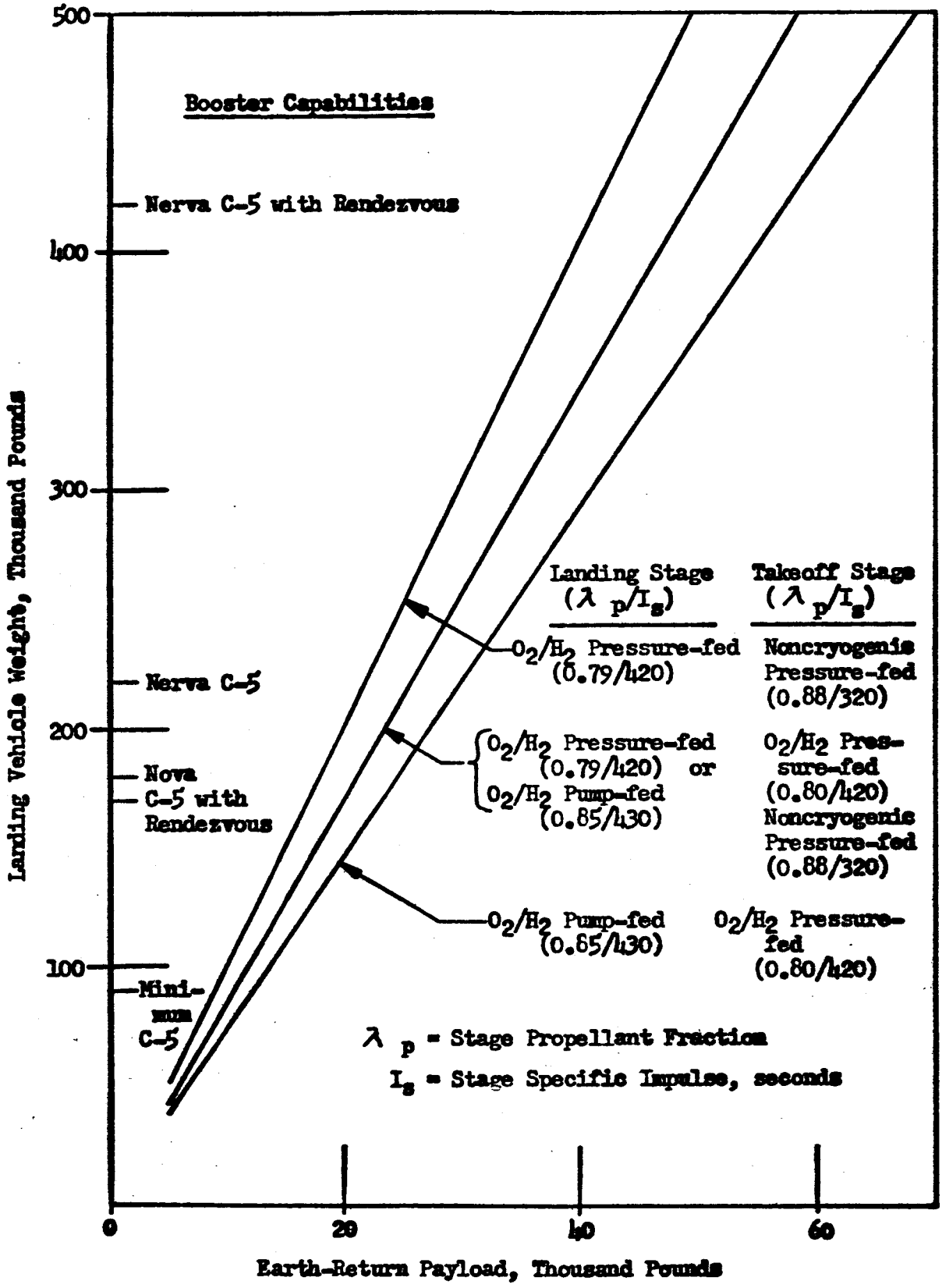

Figure 37 . Lunar Landing and Return Mission-Landing Vehicle Gross Weight vs. Return Payload

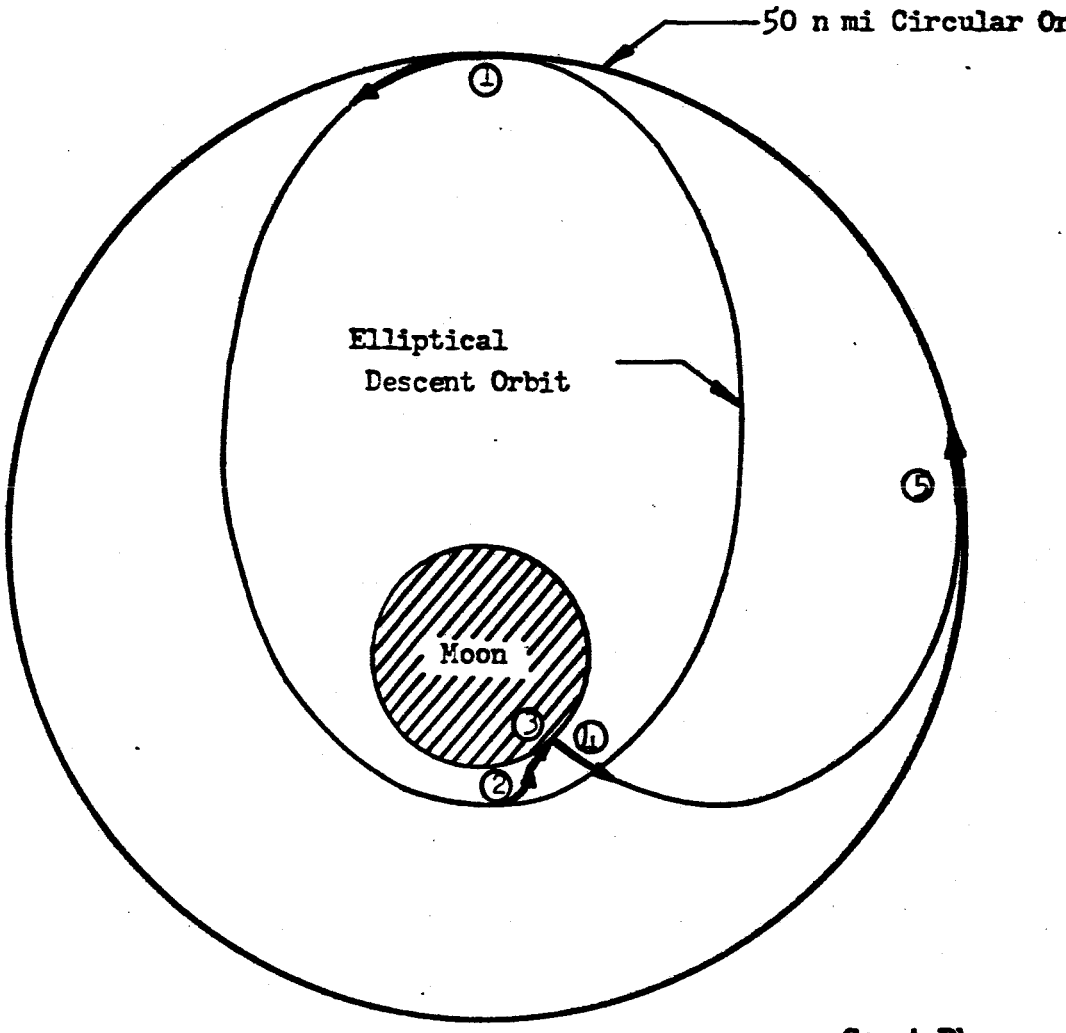

Maneuvers:

1. Orbit Conversion
2. Thrust Opposed and Parallel to Descent
3. Hover-Translate
4. Take-off Ascent
5. Circularization

Fig. 38. Lunar Landing - Take-off Maneuvers

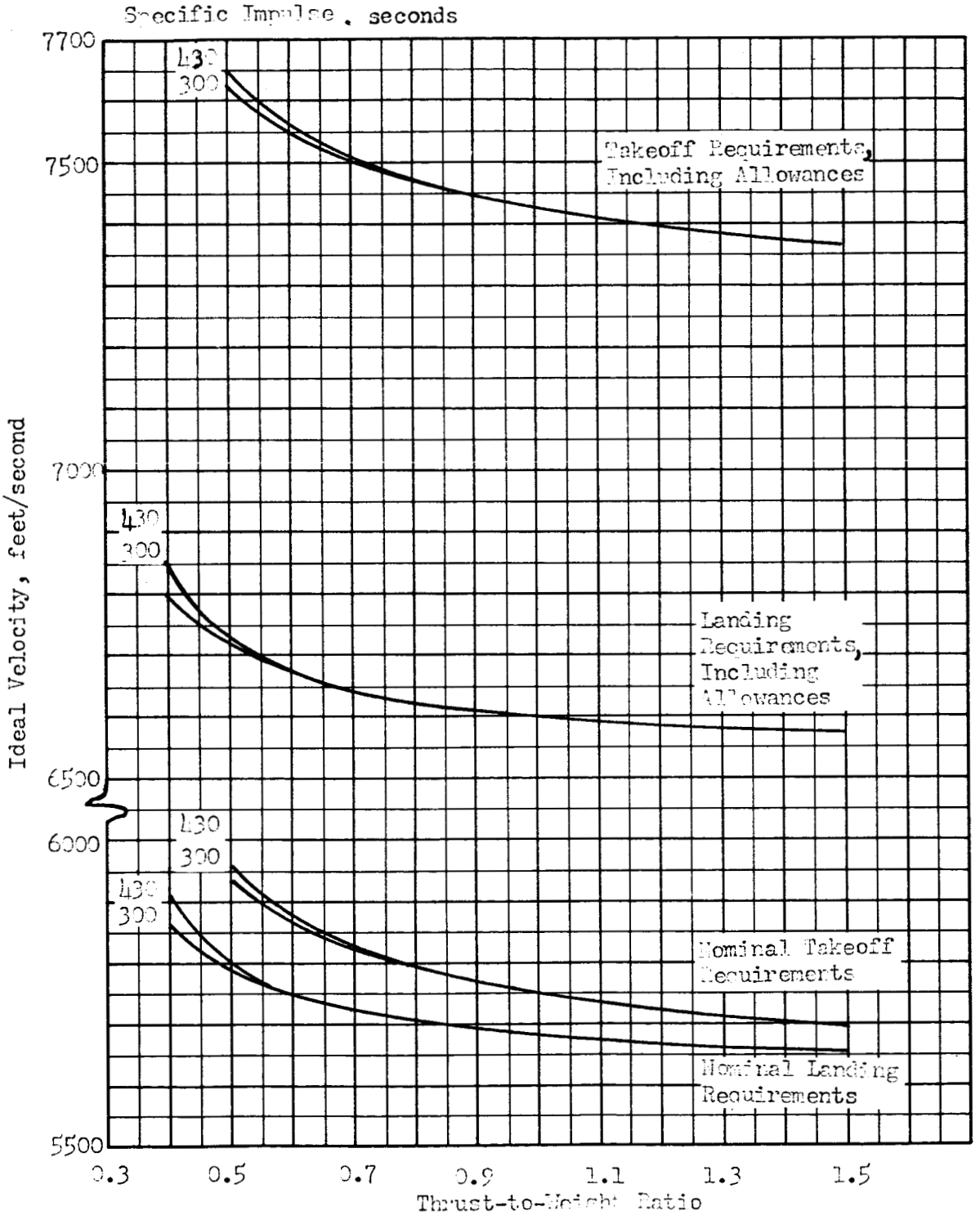

Figure 39. Landing and Takeoff Ideal Velocity Requirements vs Thrust-to-Earth Weight Ratio (50 n mi Orbit)

the nominal values. The upper landing curves include allowances for a 7.5-percent flight performance reserve and a 500-ft/sec hover/translation velocity. The upper takeoff velocity curves include a 1250-ft/sec plane change velocity increment and a 7.5-percent flight performance reserve.

A 35,000-pound landing vehicle was assumed as nominal in some cases, though the parametric analyses and the thrust optimizations were conducted for a range of vehicle weights. The analysis results can therefore be applied to other values of return-to-orbit payload requirements or vehicle gross weight.

Parametric Data. Parametric system weights were formulated for the three vehicle concepts discussed. An ideal velocity requirement of 6,850 ft/sec was used for the landing maneuver, 7450 ft/sec for the takeoff maneuver.

A one-stage vehicle which performs both landing and takeoff is described in Figure 40 and 41 . Figure 40 is for a noncryogenic-propellant vehicle (320 seconds specific impulse) and Figure 41 is for an O_2/H_2 vehicle (420 seconds specific impulse). Payload versus initial vehicle gross weight for various stage propellant fractions are presented in these two curves. For this vehicle, 850 pounds of landing gear is left on the lunar surface when the vehicle gross weight is 35,000 pounds. For other gross weights, landing gear left on the moon was assumed directly proportional to vehicle gross weight. Propellant fraction (λ_p) was defined in this study as the propellant weight divided by the sum of the propellant weight and all inert weights except the landing gear left on the lunar surface.

The effects on payload of changes in various stage parameters for the single stage, landing/takeoff vehicle are illustrated in Figures 42 and 43 . Figure 42 is for a noncryogenic propellant stage, and Figure 43 for an O_2/H_2 vehicle.

For each figure, a reference vehicle was selected and, as various stage parameters were varied, the resulting payloads were expressed as a percent of the reference vehicle payload. On each curve, the variation of payload with specific impulse is presented, assuming propellant fraction remains constant; and the variation of payload with propellant fraction is presented, assuming specific impulse remains constant. Another curve shows the effect of total stage inert weight on payload. Total inert weight here includes the 850 pounds of landing gear which is left on the lunar surface. The effect on payload of the weight of the landing gear jettisoned on the lunar surface is shown in the final curve. For this curve, total stage inert weight and specific impulse are kept equal to those of the reference vehicle. Comparison of Figures 42 and 43 indicates that the payload variation, on a percentage basis, is more sensitive for the storable propellant system.

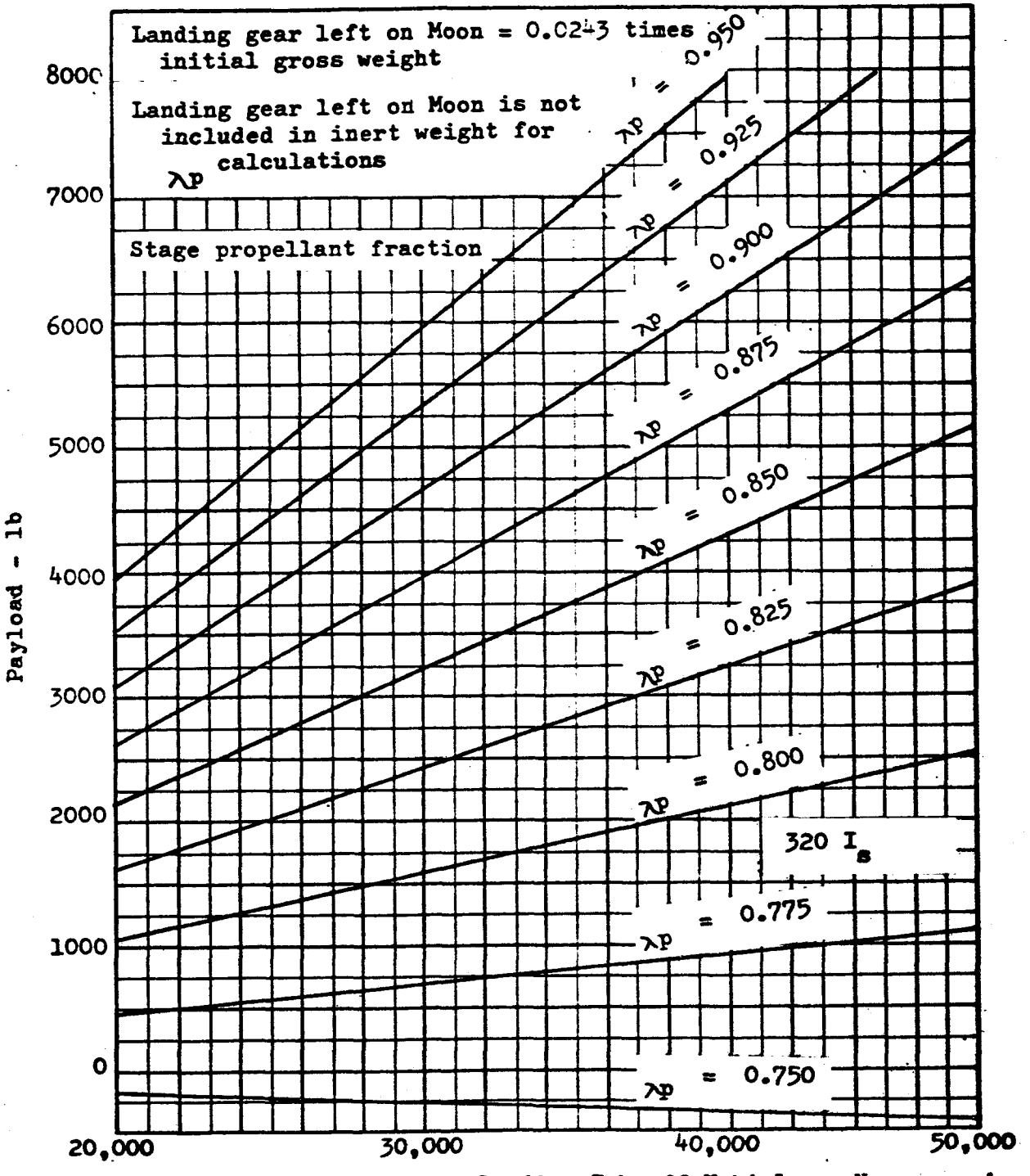

Figure 40. One Stage Landing Takeoff Vehicle - Noncryogenic Propellants; Effect of Gross Weight and Propellant Fraction on Payload

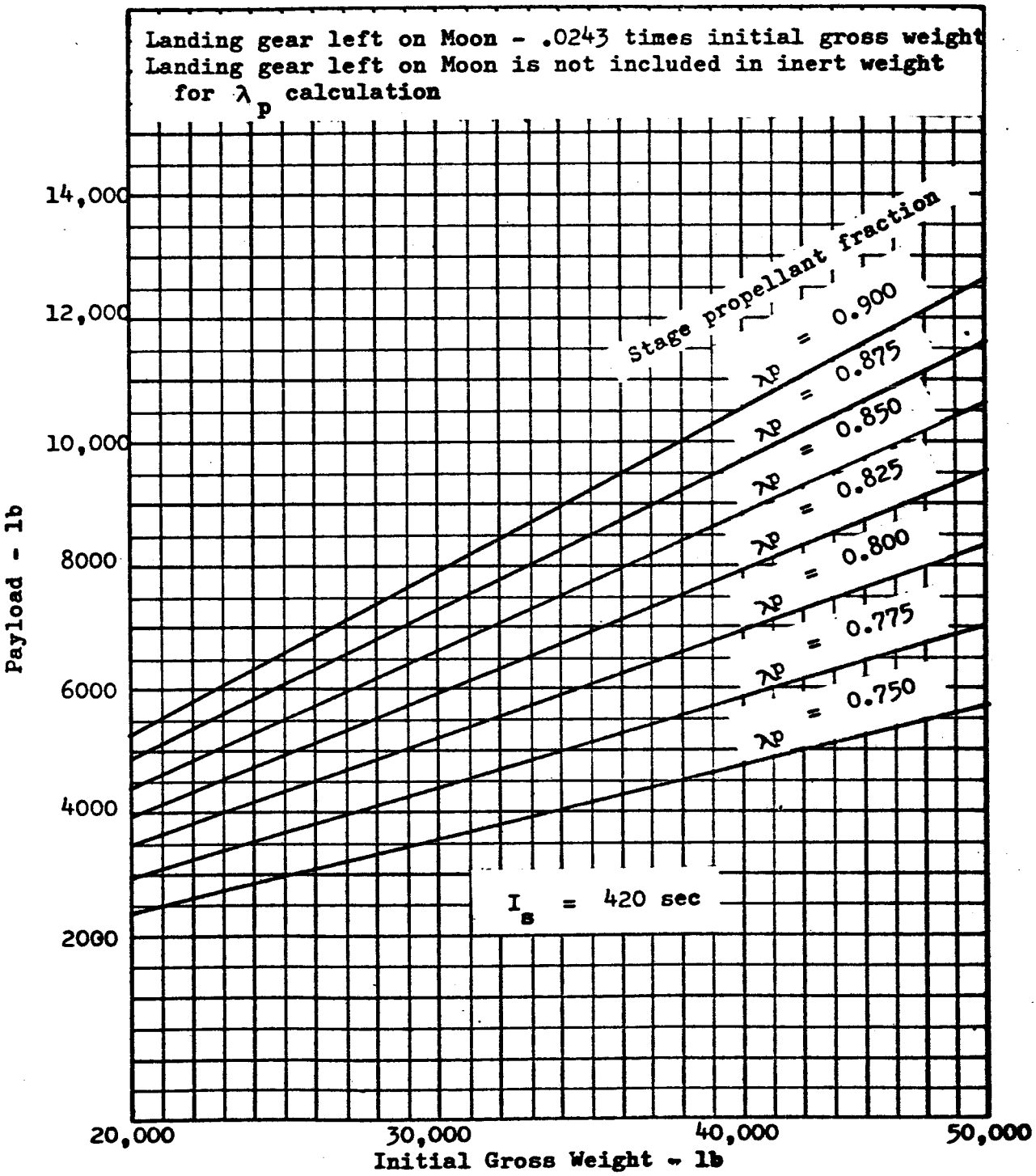

Figure 41 . One Stage Landing Takeoff Vehicle - O_2/H_2 Propellants; Effects of Gross Weight and Propellant Fraction on Payload

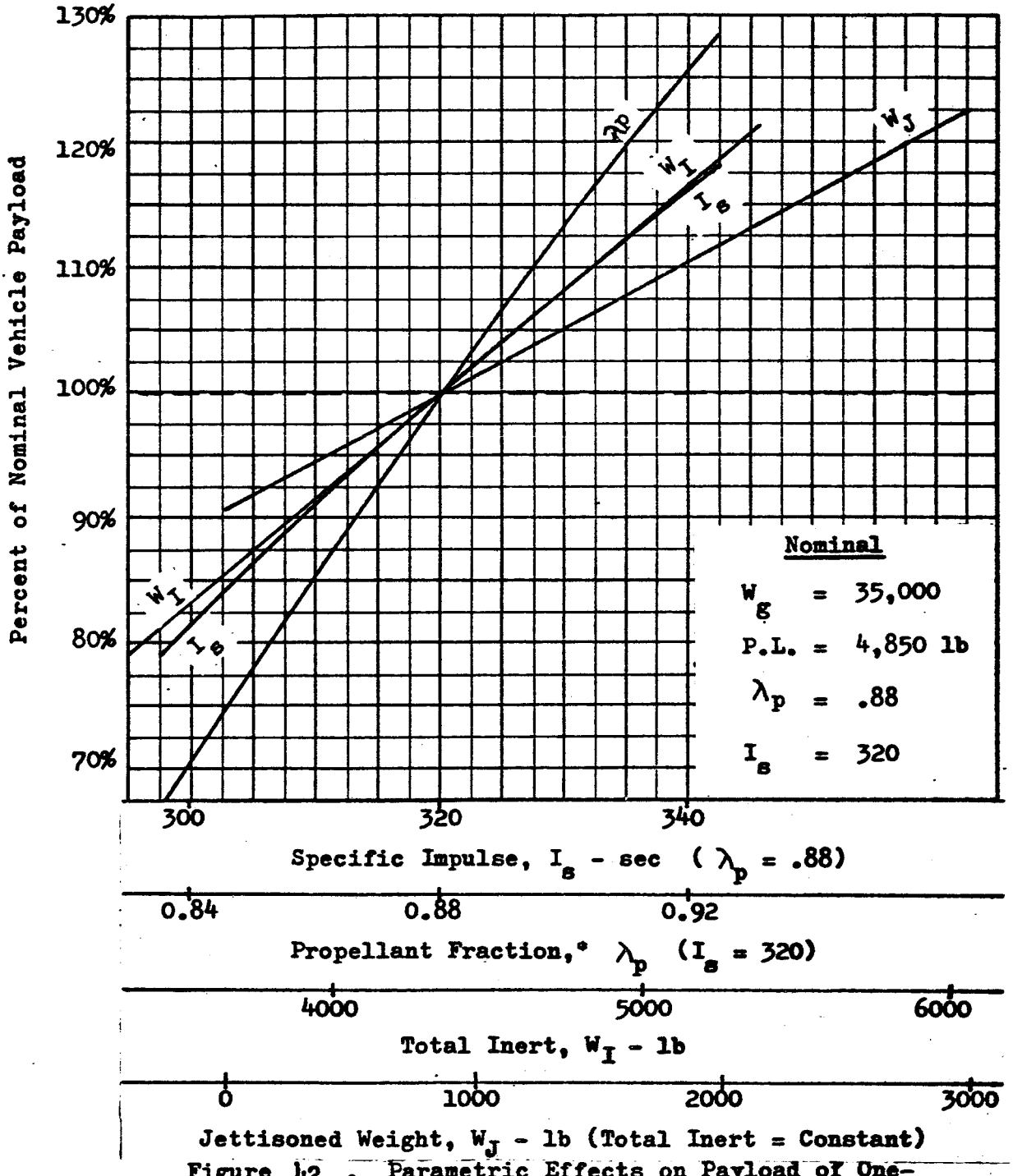

Figure 42 . Parametric Effects on Payload of One-Stage Noncryogenic-Propellant Vehicle

*Does not include jettisoned weight (850 lb)

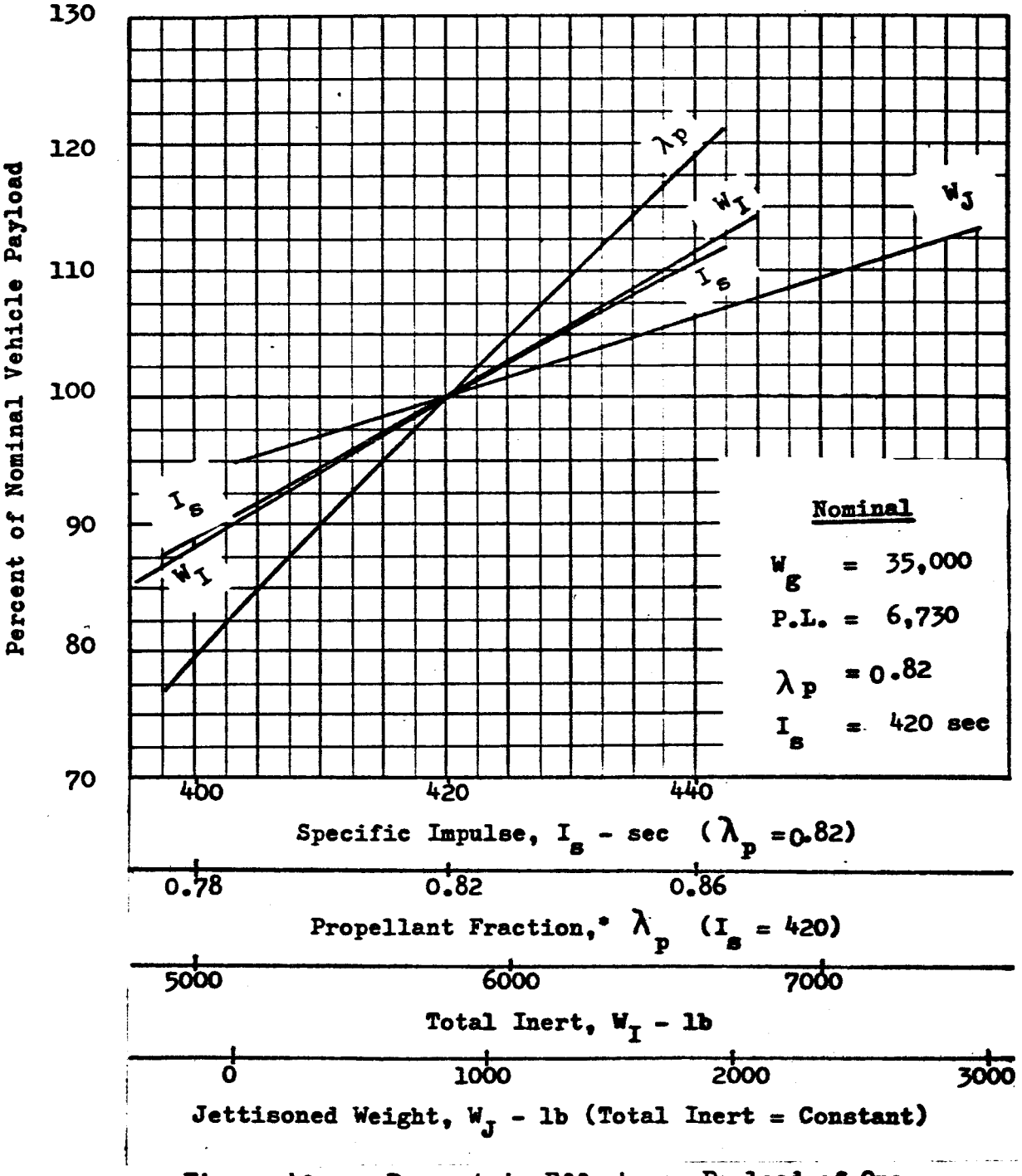

Figure 43 . Parametric Effects on Payload of One-Stage O_2/H_2 Propellant Vehicle

*Does not include 850 lb jettisoned weight

For the two-stage vehicle concept, (one for the landing and another for the takeoff) three sets of curves, each containing three figures, are presented. The first set of curves (Figure 44 , 45 , and 46 are for a vehicle which uses noncryogenic propellants in both the landing and takeoff stage. The second set, Figure 47 , 48 , and 49 are for a vehicle with an O_2/H_2 landing stage and a noncrycgenic takeoff stage. The final set, Figure 50 , 51 , and 52 are for an all-O_2/H_2 vehicle. The variations in payload with the initial vehicle gross weight in lunar orbit is shown in the first curve of each set. Payload as a function of landing and takeoff stage propellant fractions for a vehicle of 35,000 lb gross weight is presented in the second curve of the set. For the first two curves in each set a 320-second specific impulse was used for noncryogenic propellant stages and a 420-second specific impulse was used for the O_2/H_2-propellant stages. The effect on payload of these specific impulses is shown in the last curve of each set. While specific impulse is varied, stage propellant fractions are held constant at 0.85 for the noncryogenic and 0.80 for the O_2/H_2 systems.

It is possible to design a one-stage vehicle so that the tanks containing the landing maneuver propellant could be left on the lunar surface. The effects of jettisoning part of the propellant-dependent weights after landing are illustrated in Figures 53 to 56 . Noncryogenic and O_2/H_2 propellants as well as pump- and pressurized-gas feed systems are considered in these figures. For each vehicle 850 pounds of landing gear is also jettisoned on the surface. For all curves, an initial vehicle gross weight in orbit of 35,000 pounds was used with an engine system of 14,000 pounds thrust. Tank and engine inert weights were determined using estimated nominal values for weight factors as presented in Table 1 . K_T is defined as the weight of propellant dependent structure divided by the propellant weight. K_E is the ratio of the weight of thrust dependent structure to thrust level.

In each figure of the Figure 53 to 56 group are curves of payload plus stage fixed weight* plotted versus the tank weight factor (K_T) for the tanks jettisoned on the lunar surface. Each curve presented is for a different K_T for all the tanks. The "K_T All Tanks" is the effective tank-weight factor which the vehicle has initially, i.e., sum of all propellant dependent weights/total propellant weight. The points where

* From burnout weight, only the inert weights determined using the appropriate tank and engine weight factors are subtracted, leaving a payload plus stage fixed weight number.

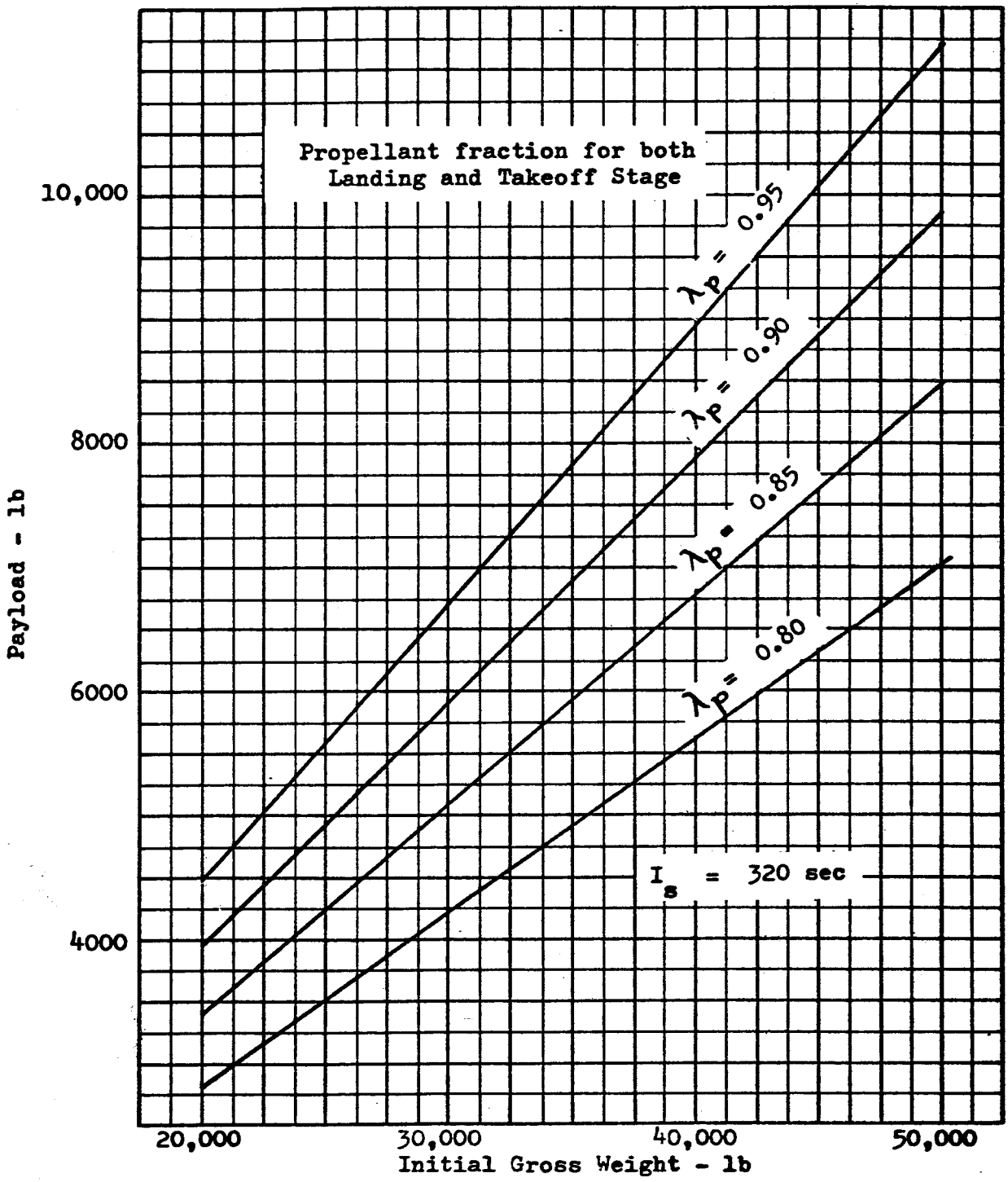

Figure 44. Two-Stage Landing/Takeoff Vehicle - Noncryogenic Propellants; Variation of Payload with Gross Weight and Propellant Fraction

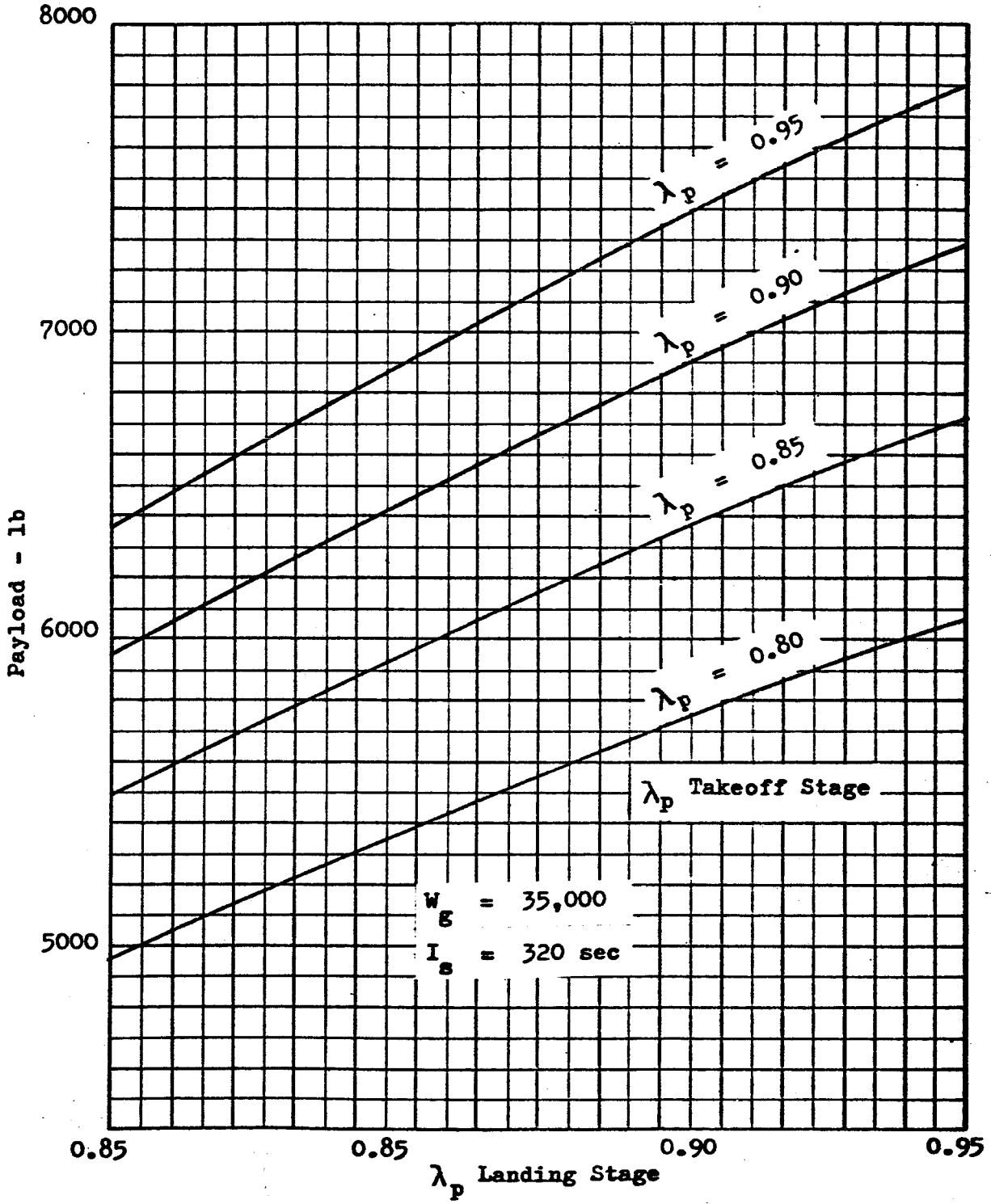

Figure 45. Two-Stage Vehicle, Noncryogenic Propellants; Variation of Payload with Propellant Fraction of Landing and Takeoff Stages

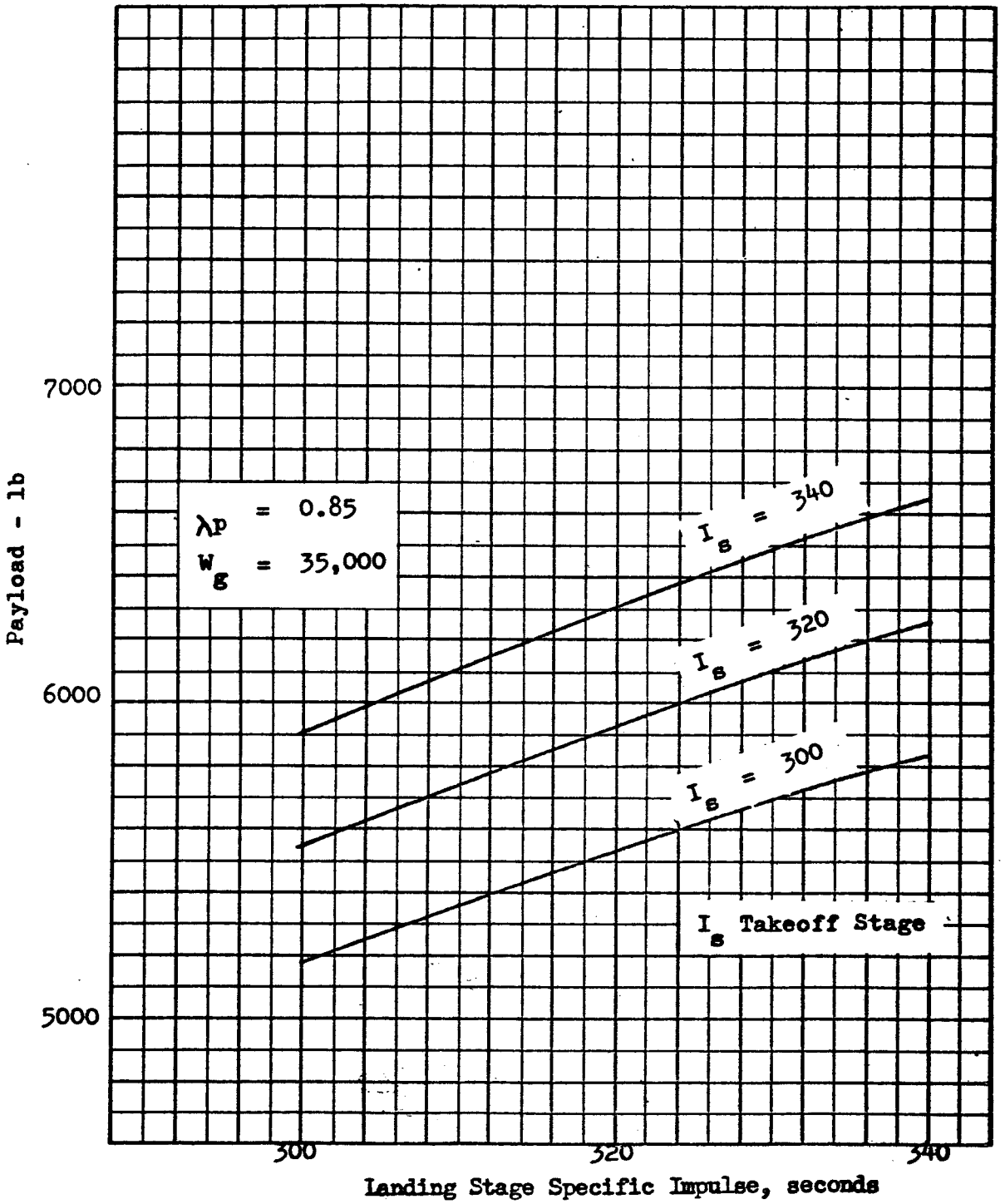

Figure 46 . Two-Stage Vehicle, Noncryogenic Propellants; Variation of Payload with Specific Impulse of Landing and Takeoff Stages

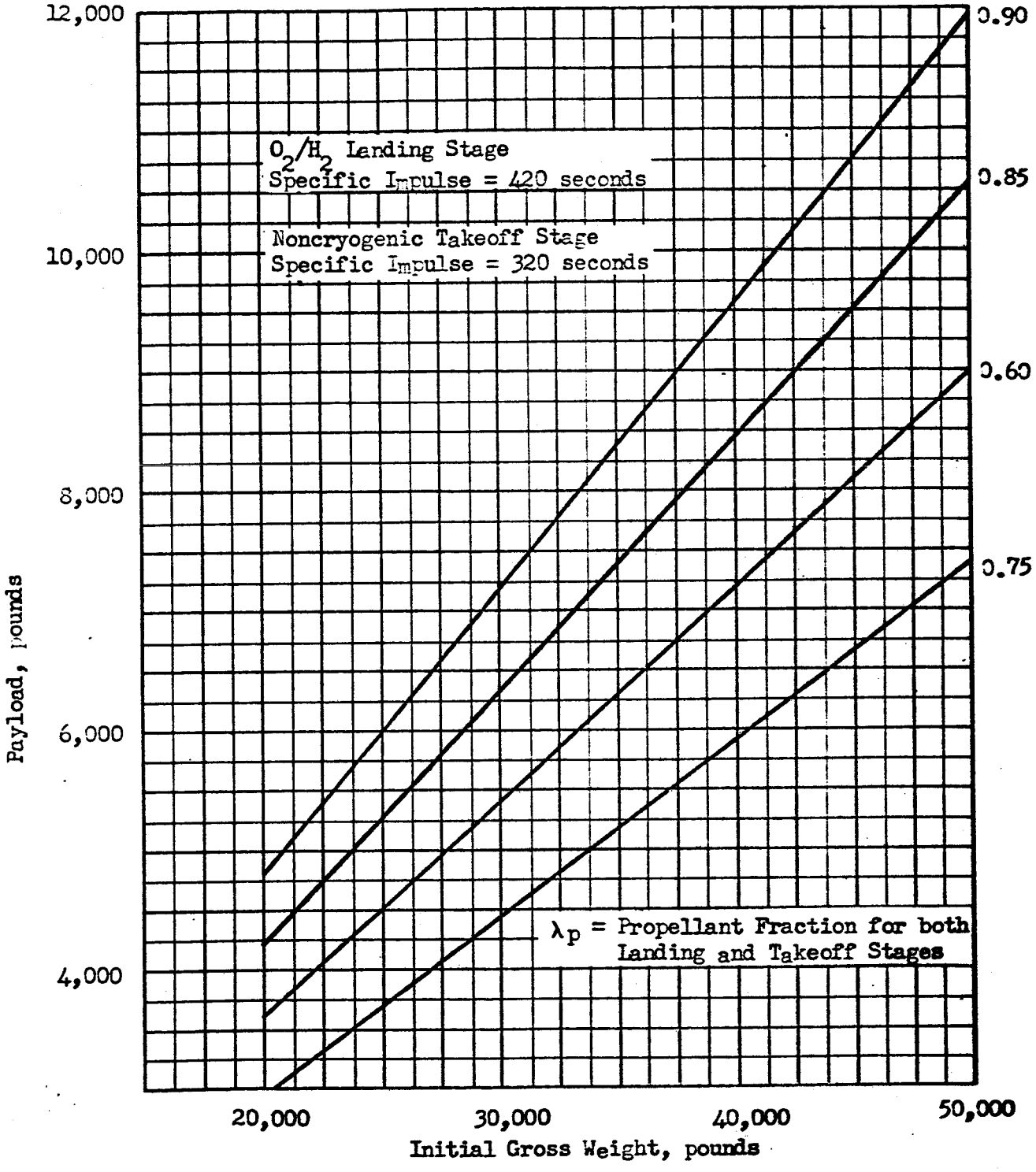

Figure 47. Variation of Payload with Gross Weight for a Two-Stage Landing-Takeoff Vehicle

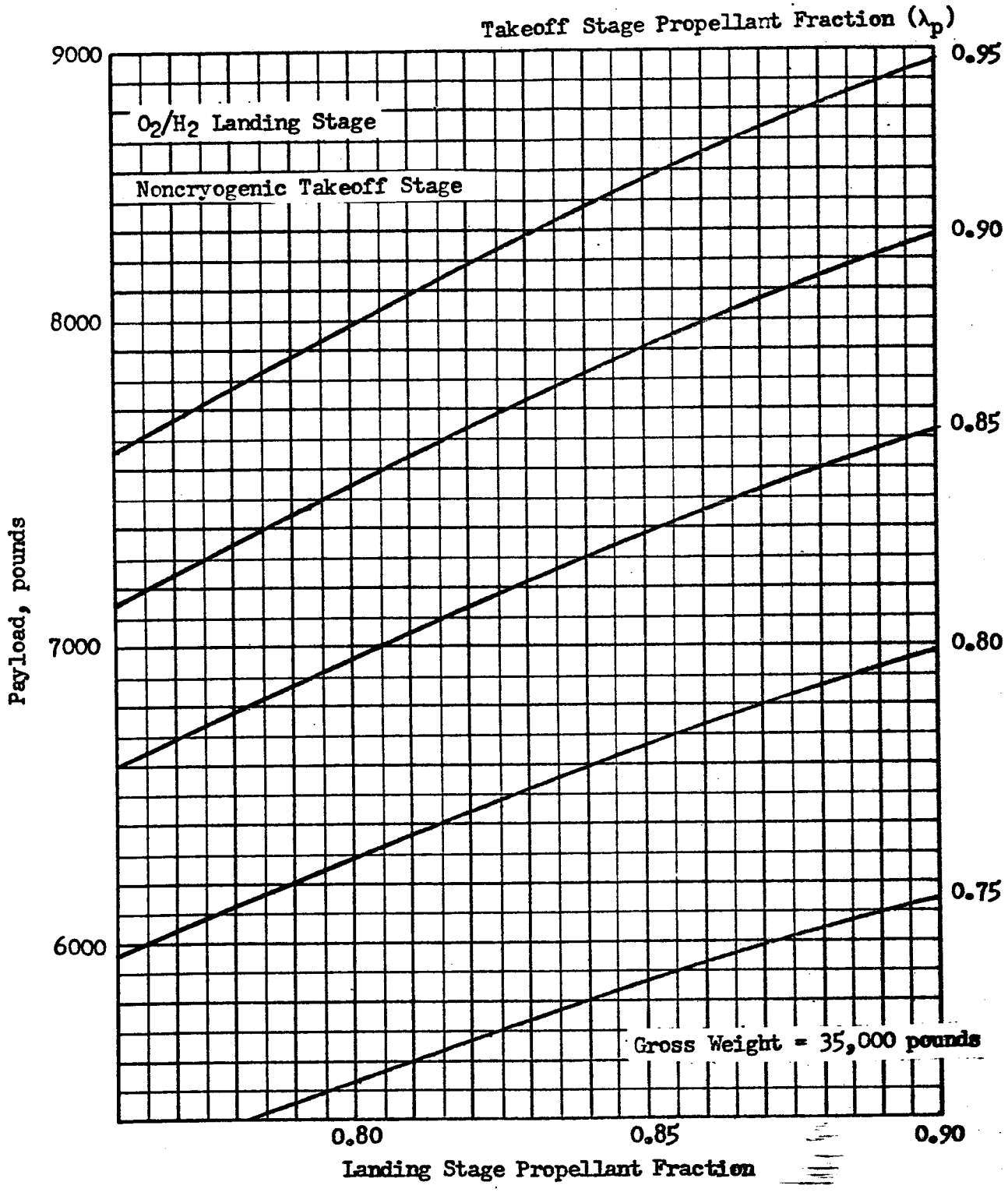

Figure 48. Variation of Payload with Propellant Fraction for a Two-Stage Landing-Takeoff Vehicle

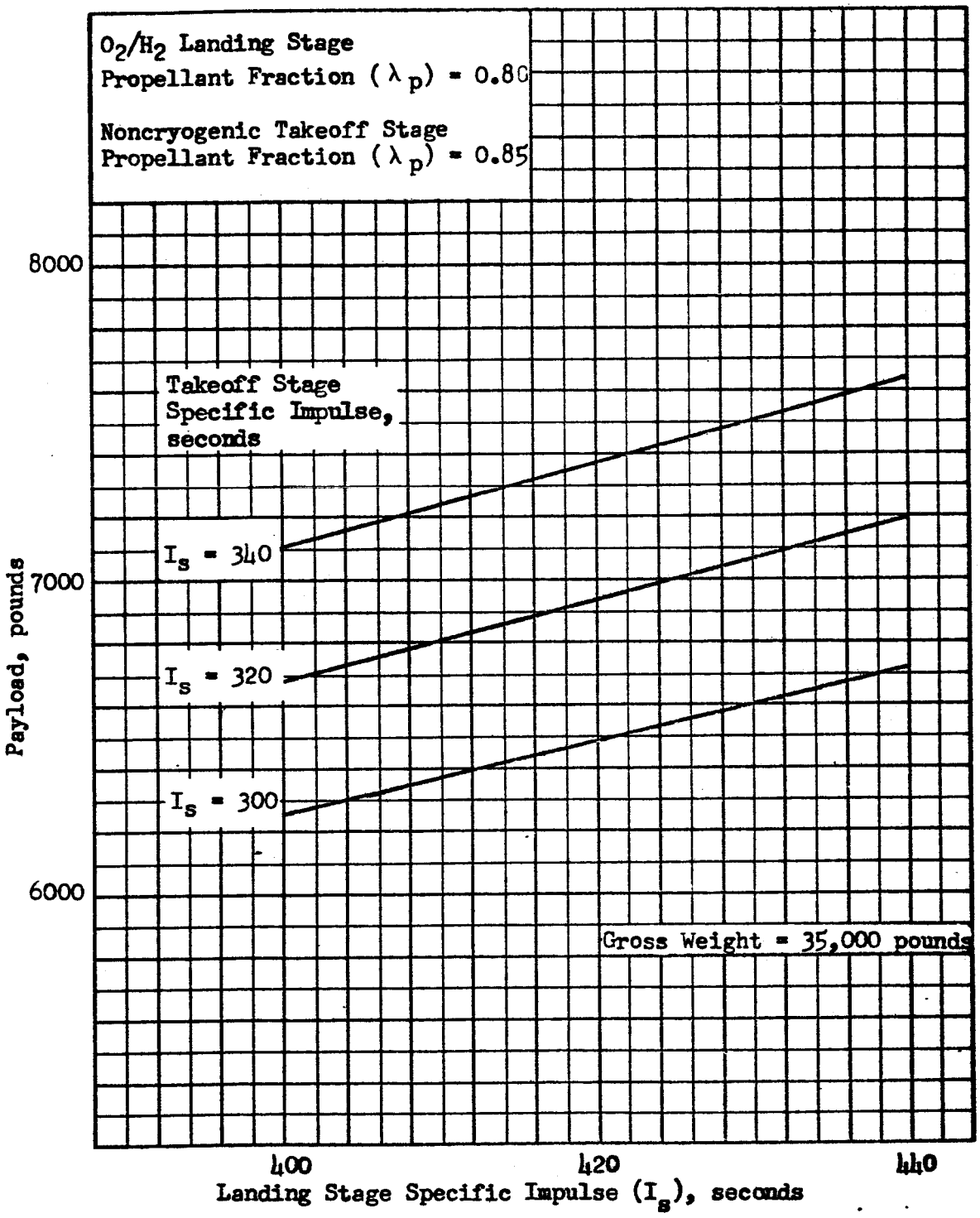

Figure 49. Variation of Payload with Specific Impulse for a Two-Stage Landing-Takeoff Vehicle

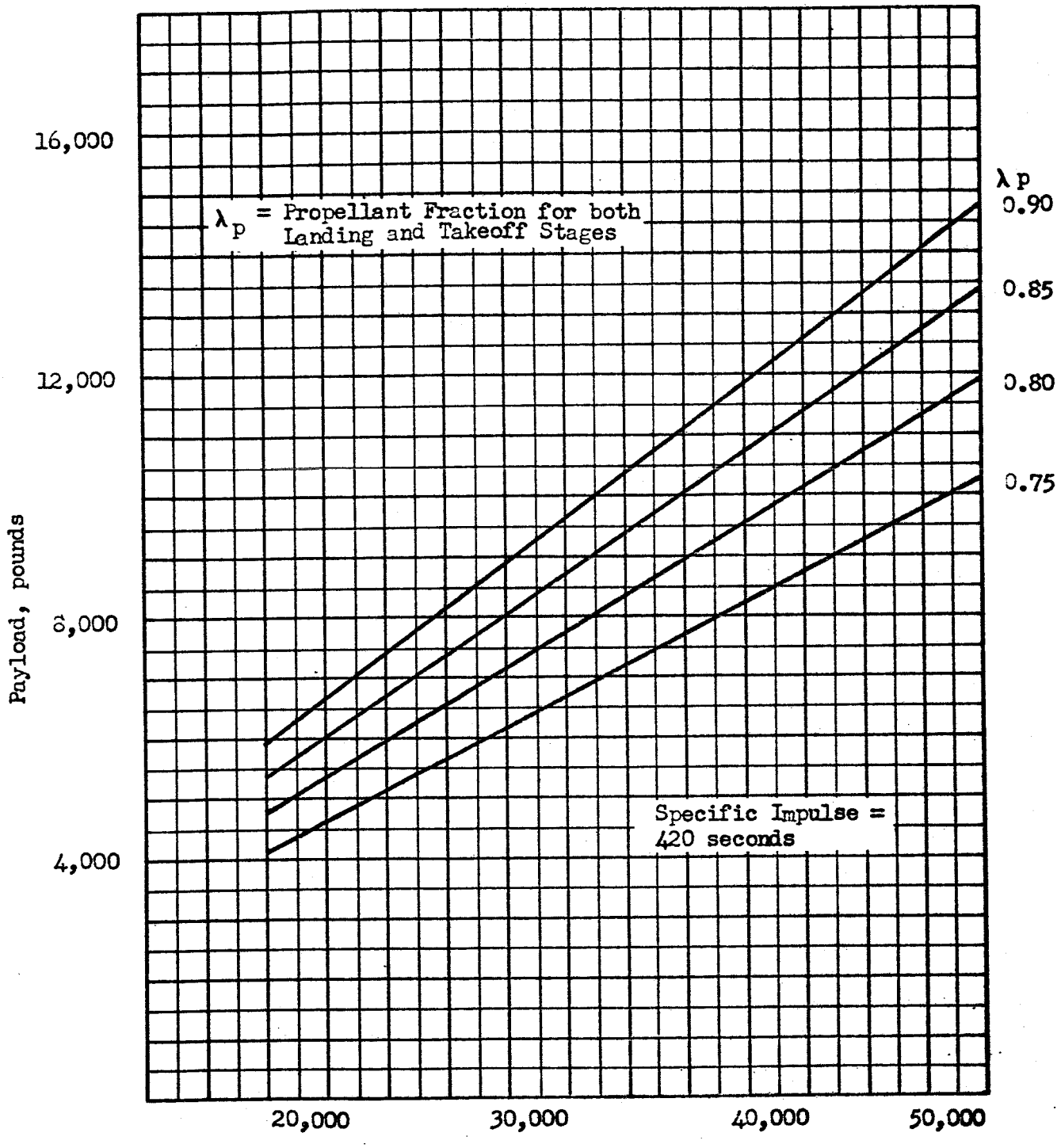

Figure 50. Variation of Payload with Gross Weight for a Two-Stage Vehicle with O_2/H_2 Propellants

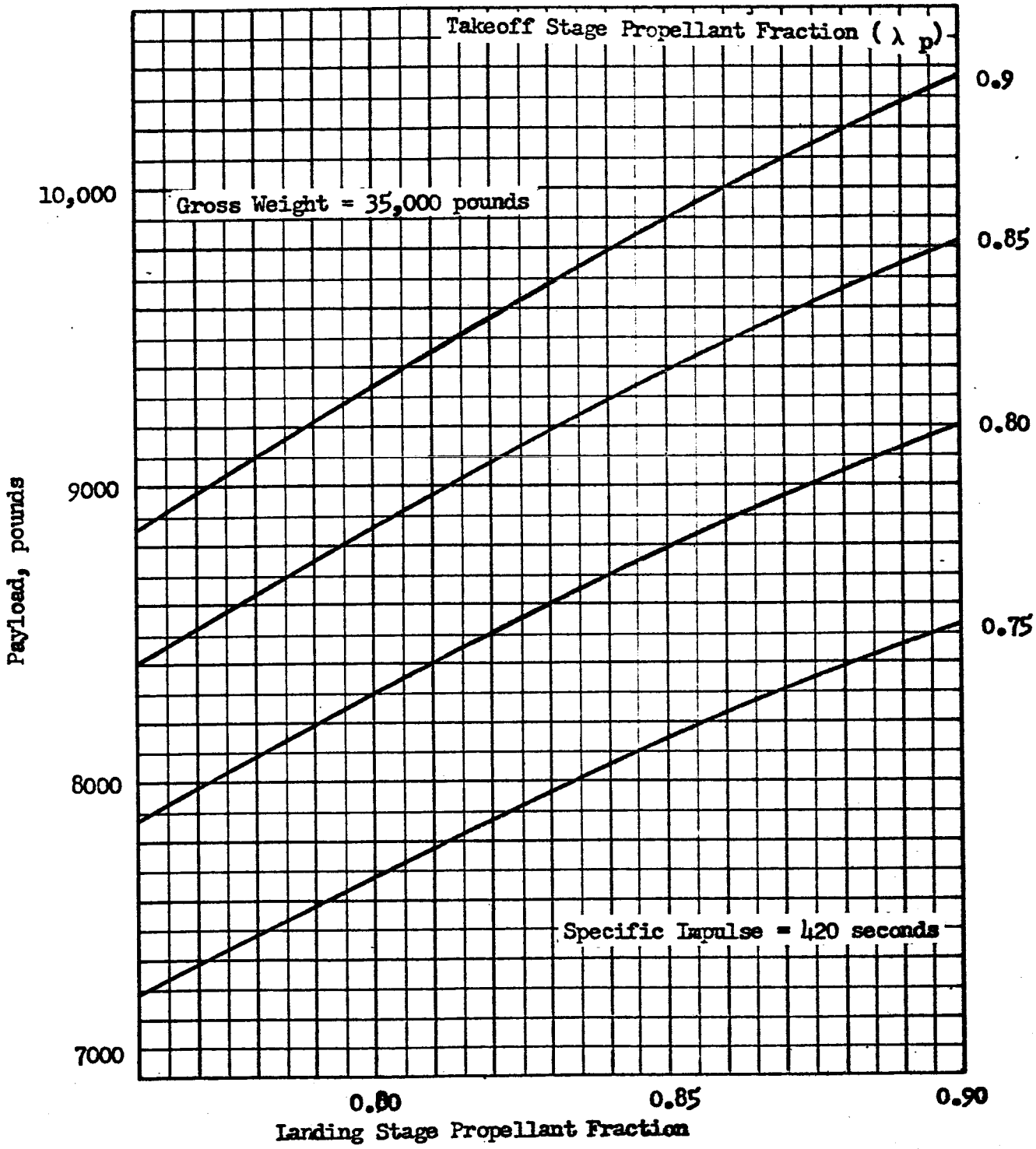

Figure 51. Variation of Payload with Propellant Fraction for a Two-Stage Vehicle with O_2/H_2 Propellants

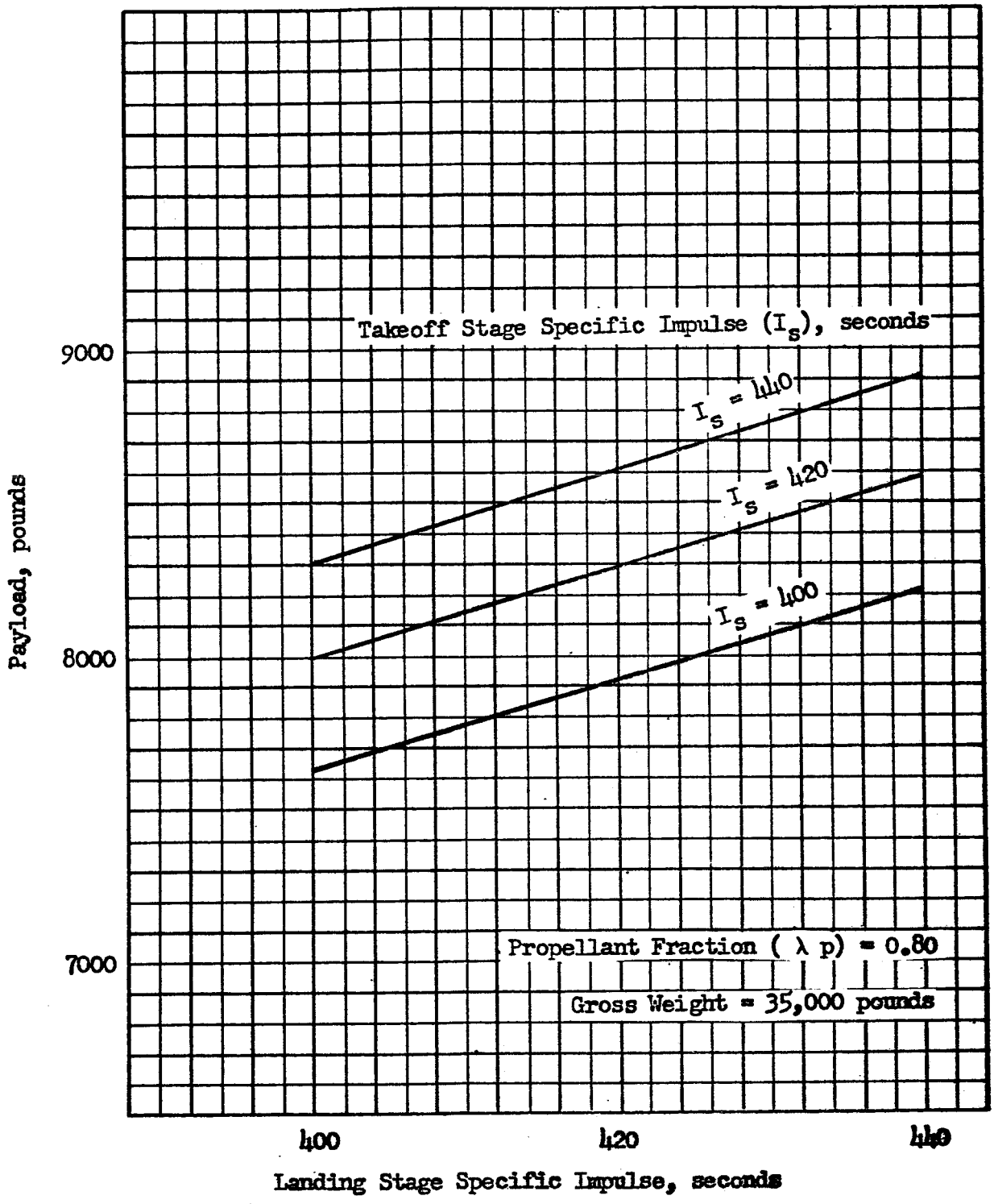

Figure 52. Variation of Payload with Specific Impulse for a Two-Stage Vehicle with O_2/H_2 Propellants.

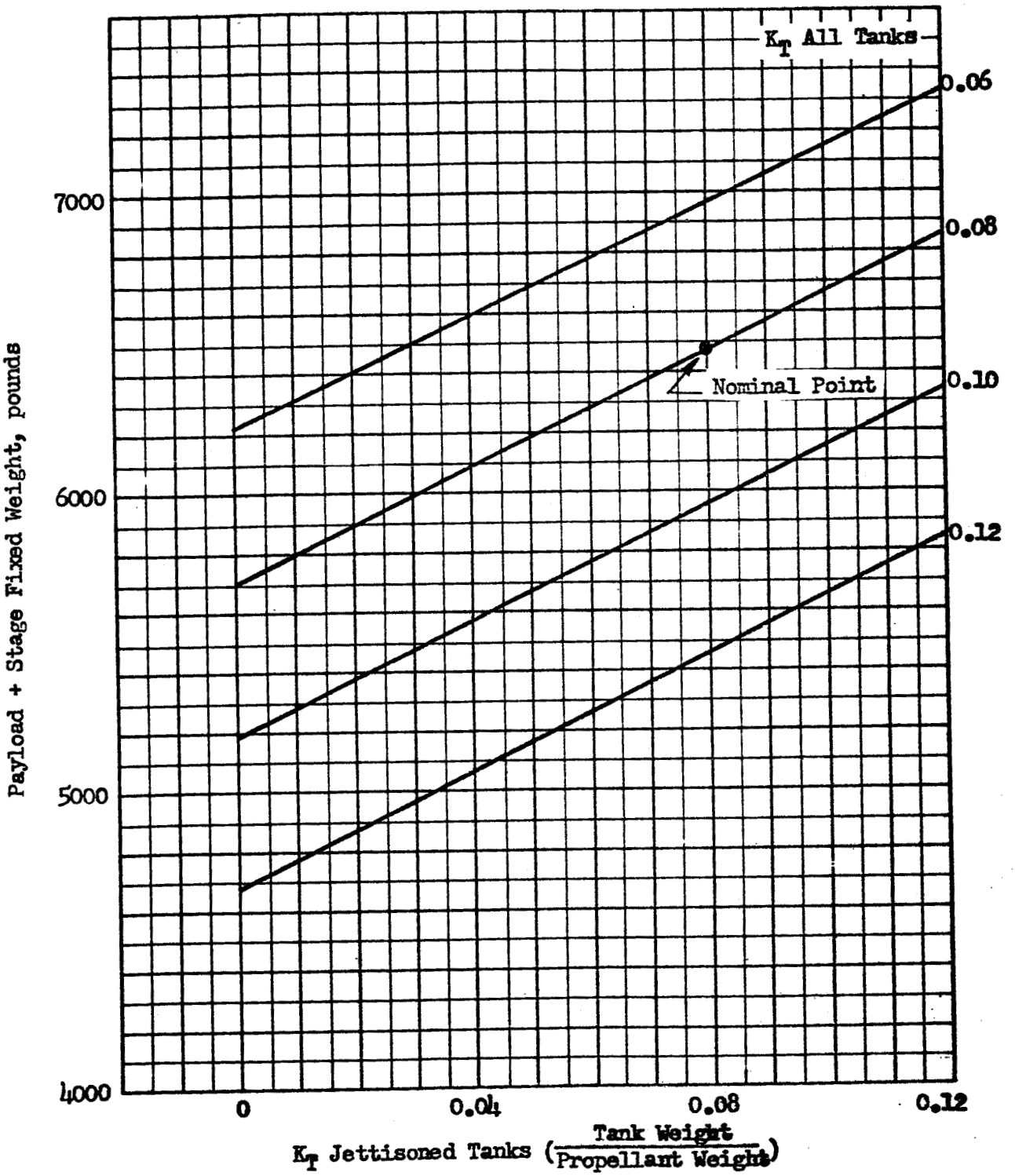

Figure 53. One-Stage Vehicle with Jettisoned Tanks, Pressure-Fed Propellants.

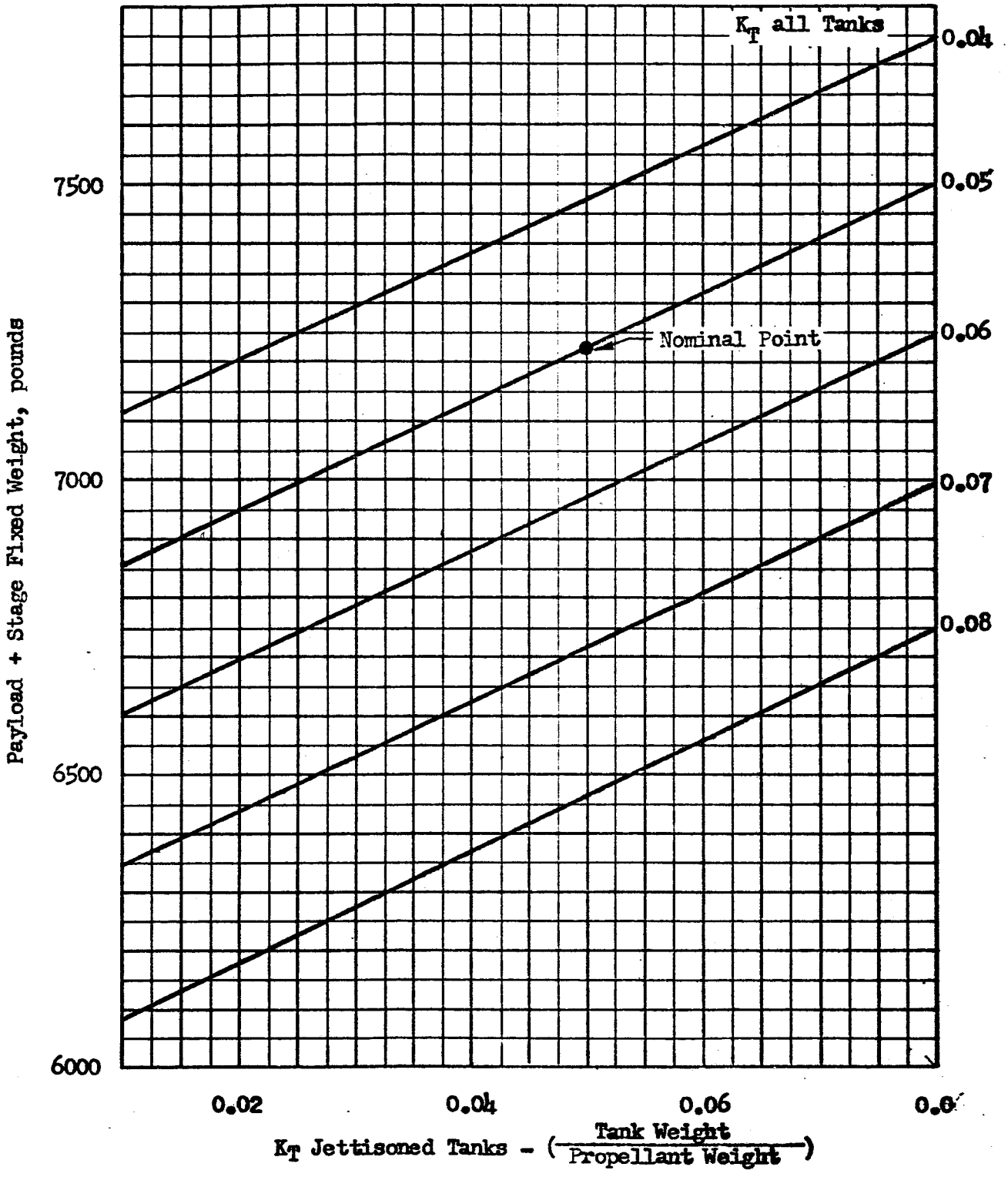

Figure 54. One-Stage Vehicle with Jettisoned Tanks, Pump-Fed Propellants

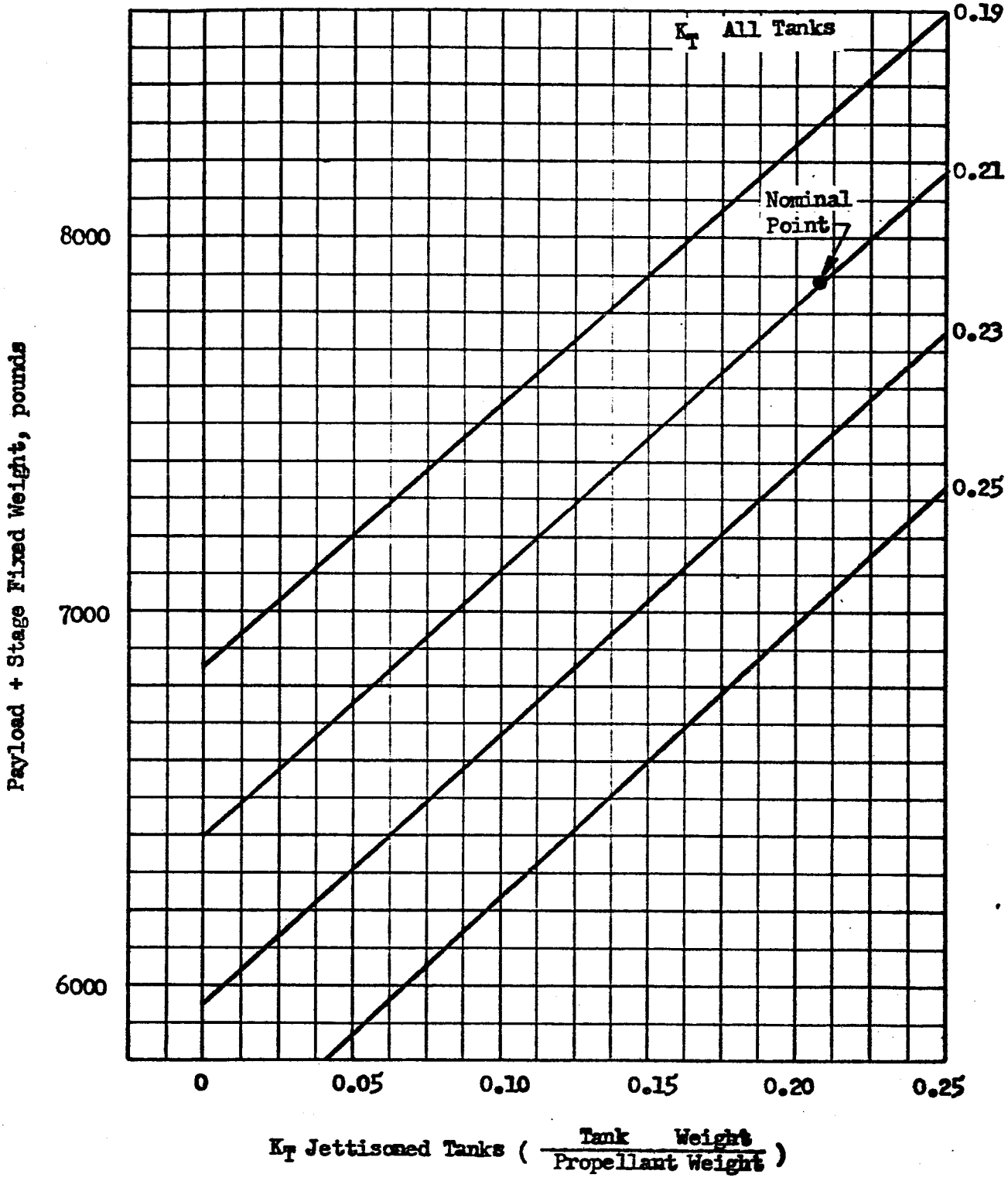

Figure 55. One-Stage Vehicle with Jettisoned Tanks, Pressure-Fed O_2/H_2 Propellants.

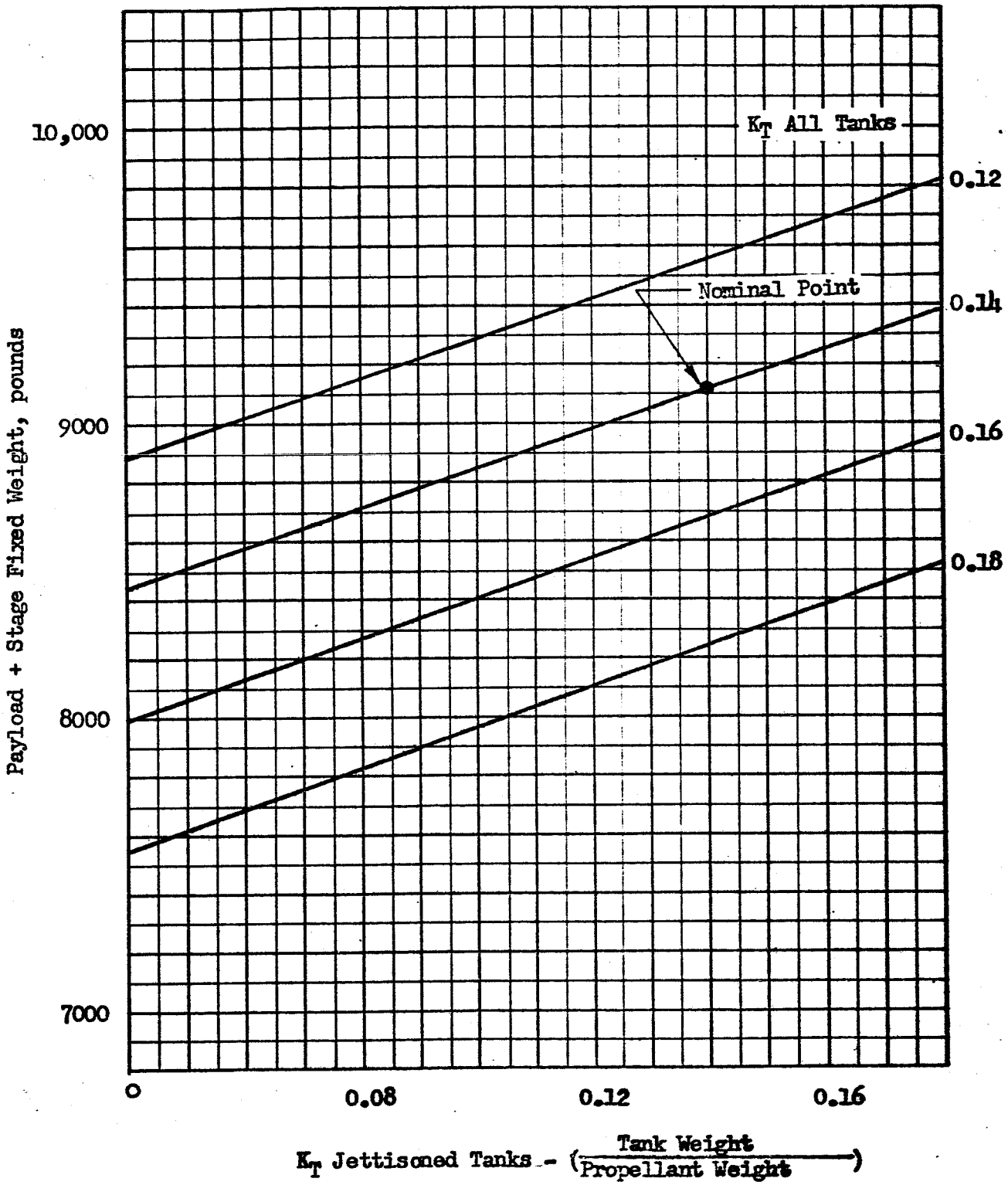

Figure 56. One-Stage Vehicle with Jettisoned Tanks, Pump-Fed O_2/H_2 Propellants.

K_T of the jettisoned tanks equals zero show payloads which would result if no tanks were jettisoned on the surface. Other points on the curves can be compared to these points to determine the advantage gained by jettisoning tanks.

TABLE 1

STAGE INERT WEIGHT FACTORS

	Noncryogenic		O_2/H_2	
	Pump-Fed	Pressure-Fed	Pump-Fed	Pressure-Fed
Tank Weight Factor (K_T)	0.05	0.08	0.14	0.21
Engine Weight Factor (K_E)	0.02	0.04	0.025	0.040

Thrust Optimization. Thrust optimization analysis was conducted for a nominal lunar landing-from-orbit stage, a takeoff-to-orbit stage, and a single stage that performs both functions. Both noncryogenic and high-energy cryogenic propellants were considered. Characteristics of the nominal landing stage systems are described in Table 2 .

TABLE 2

LANDING STAGE NOMINAL PARAMETERS

	Noncryogenic Propellant	O_2/H_2
Initial Gross Weight, pounds	35,000	35,000
Specific Impulse, seconds	320	420
Thrust Dependent Weight Factor (K_E, lb/lb thrust)		
Pump-fed	0.020	0.025
Pressure-fed	0.040	0.040
Propellant Dependent Weight Factor (K_T, lb/lb propellant)		
Pump-fed	0.05	0.14
Pressure-fed	0.08	0.21

The values presented above, utilized in conjunction with the appropriate velocity requirement data yielded the results shown in Figure 57 and 58 . Optimum values of thrust-to-(Earth) weight ratios are indicated below:

	Noncryogenic	O_2/H_2
Pump-fed	0.60	0.55
Pressure-fed	0.50	0.50

It should be noted that these optima are applicable as propulsion design criteria only if the subsequent (return-to-orbit) maneuver is performed by some other propulsion system; i.e., only if the landing stage is the first stage of a two-stage vehicle.

The results for the lunar takeoff-to-orbit stage are shown in Figure 59 and 60 . The term, fixed weight, as used in these figures, includes all inert weight which is neither thrust nor propellant dependent. The amount of fixed weights is dependent on the particulars of any specific stage design*, but the breakdown between payload and fixed weight (not thrust-dependent) does not influence thrust level selection. The optimum thrust-to-(Earth) weight ratios for the takeoff stages considered are:

	Noncryogenic	Cryogenic
Pump-fed	0.75	0.65
Pressure-fed	0.55	0.55

These optimum values represent appropriate design criteria for the second stage of a two-stage landing-takeoff vehicle.

Analysis of single stage vehicles for the landing/takeoff mission included the ground rule that 850 pounds are jettisoned on the lunar surface prior to takeoff. Results are presented in Figure 61 and 62 , and the optimum thrust-to-(Earth) weight ratios are:

	Noncryogenic	Cryogenic
Pump-fed	0.65	0.55
Pressure-fed	0.50	0.50

* and on semantics, considering that an item such as a guidance system sometimes is, and sometimes is not, counted as part of the useful payload..

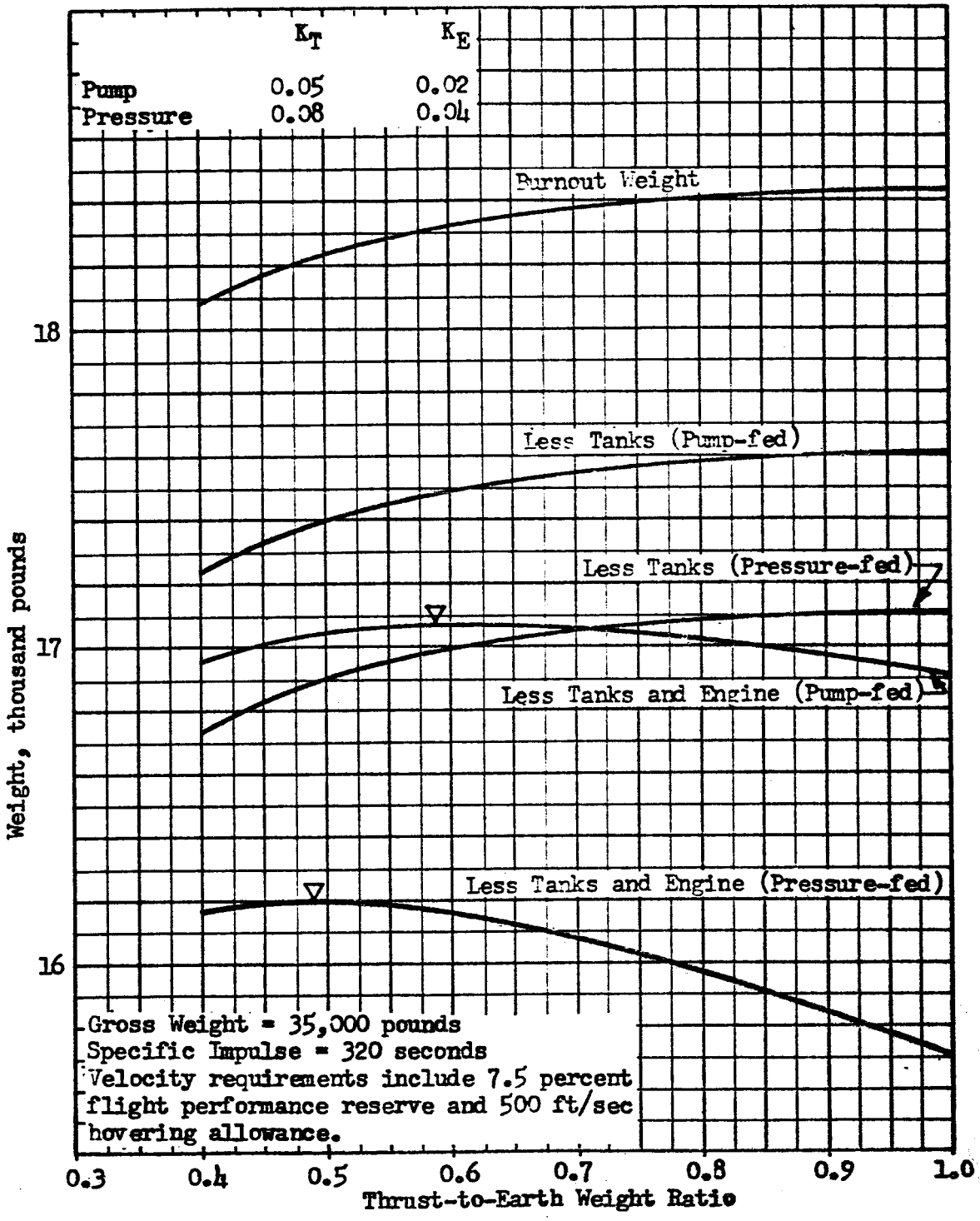

Figure 57. Thrust Level Selection for Orbital Descent Vehicle

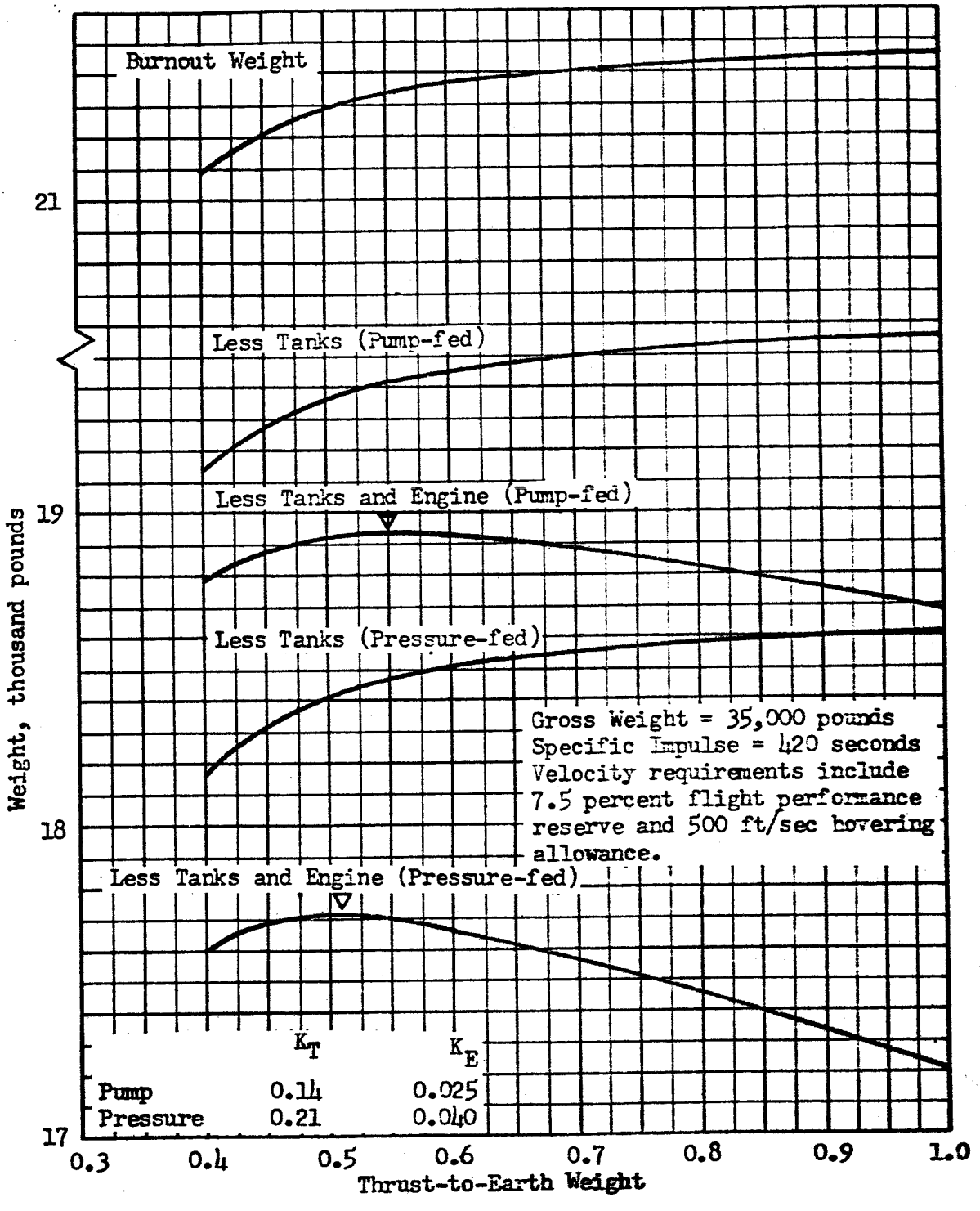

Figure 58. Thrust Level Selection for Orbital Descent Vehicle

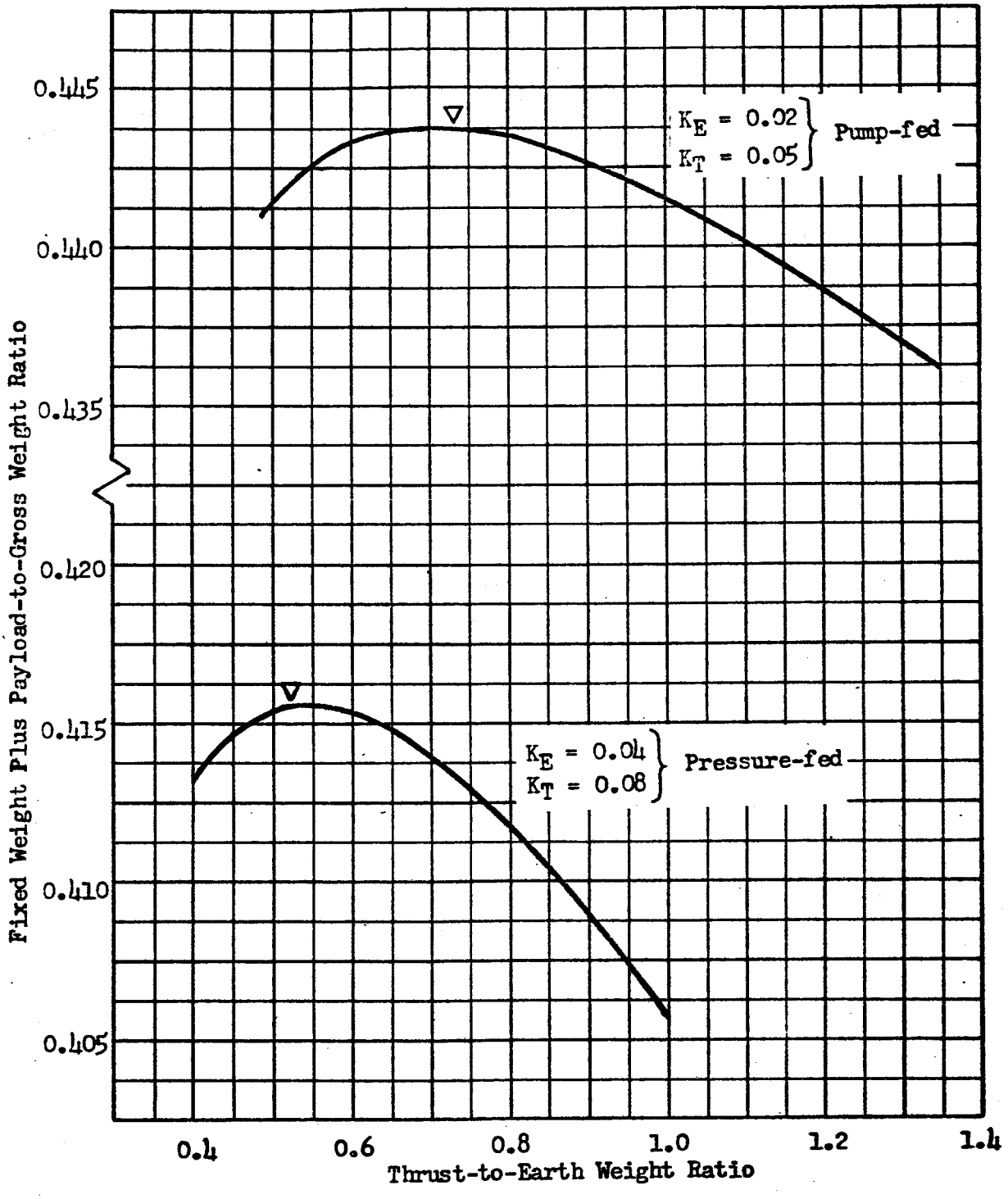

Figure 59. Thrust Level Selection for Noncryogenic Lunar Takeoff Vehicle

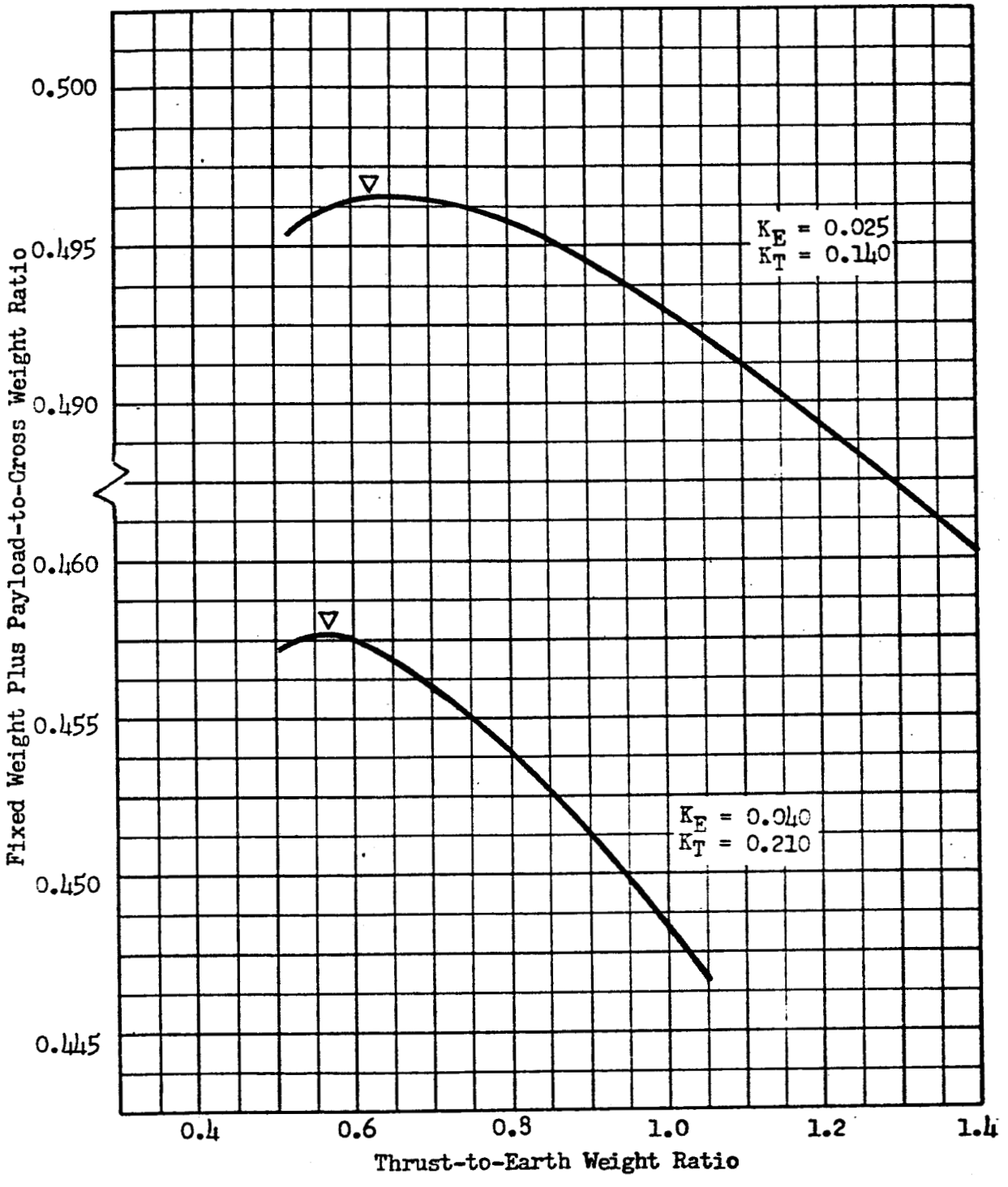

Figure 60. Thrust Level Selection for O_2/H_2 Lunar Takeoff Vehicle

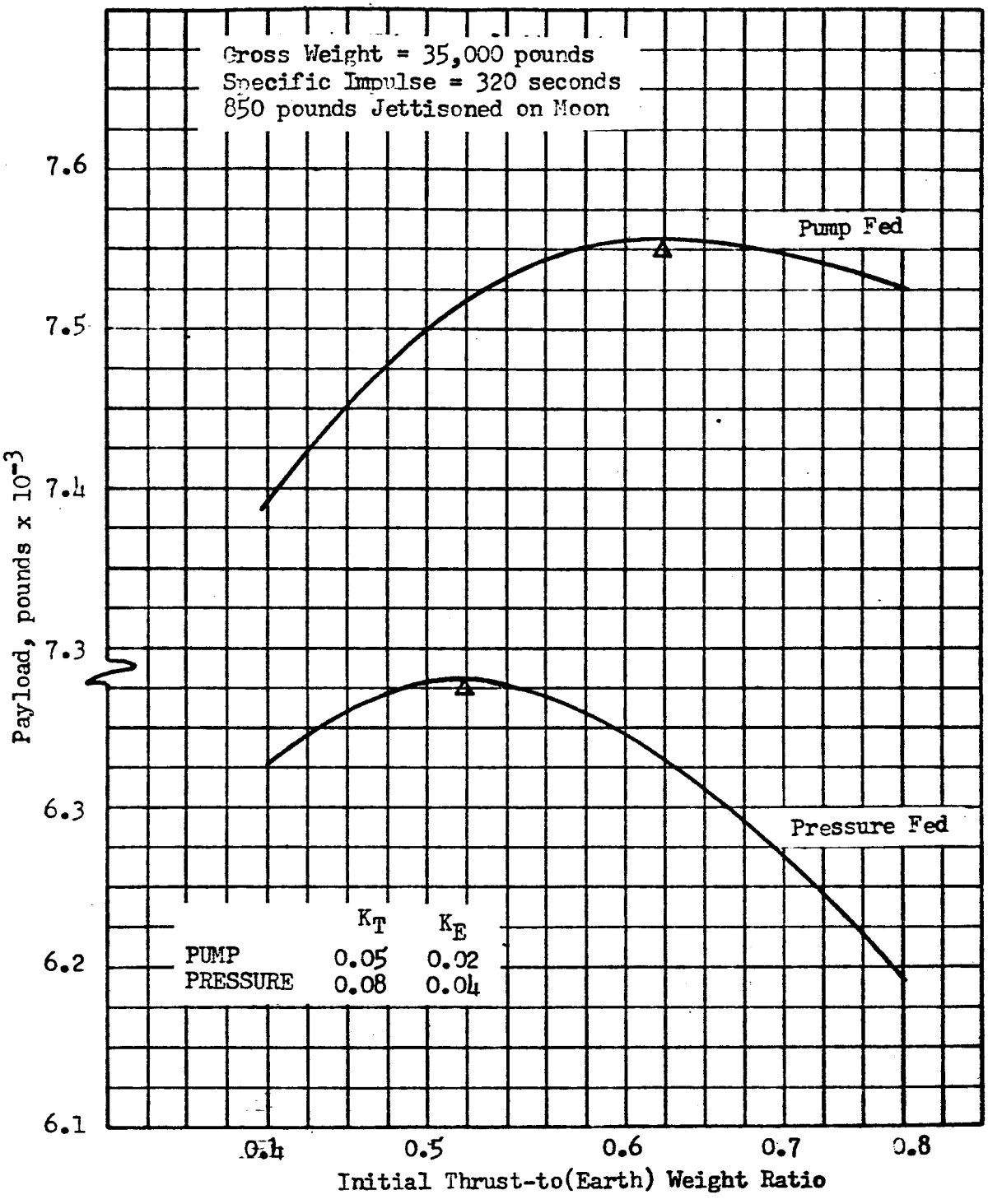

Figure 61. Thrust Level Selection for Lunar Descent and Reorbit Vehicle

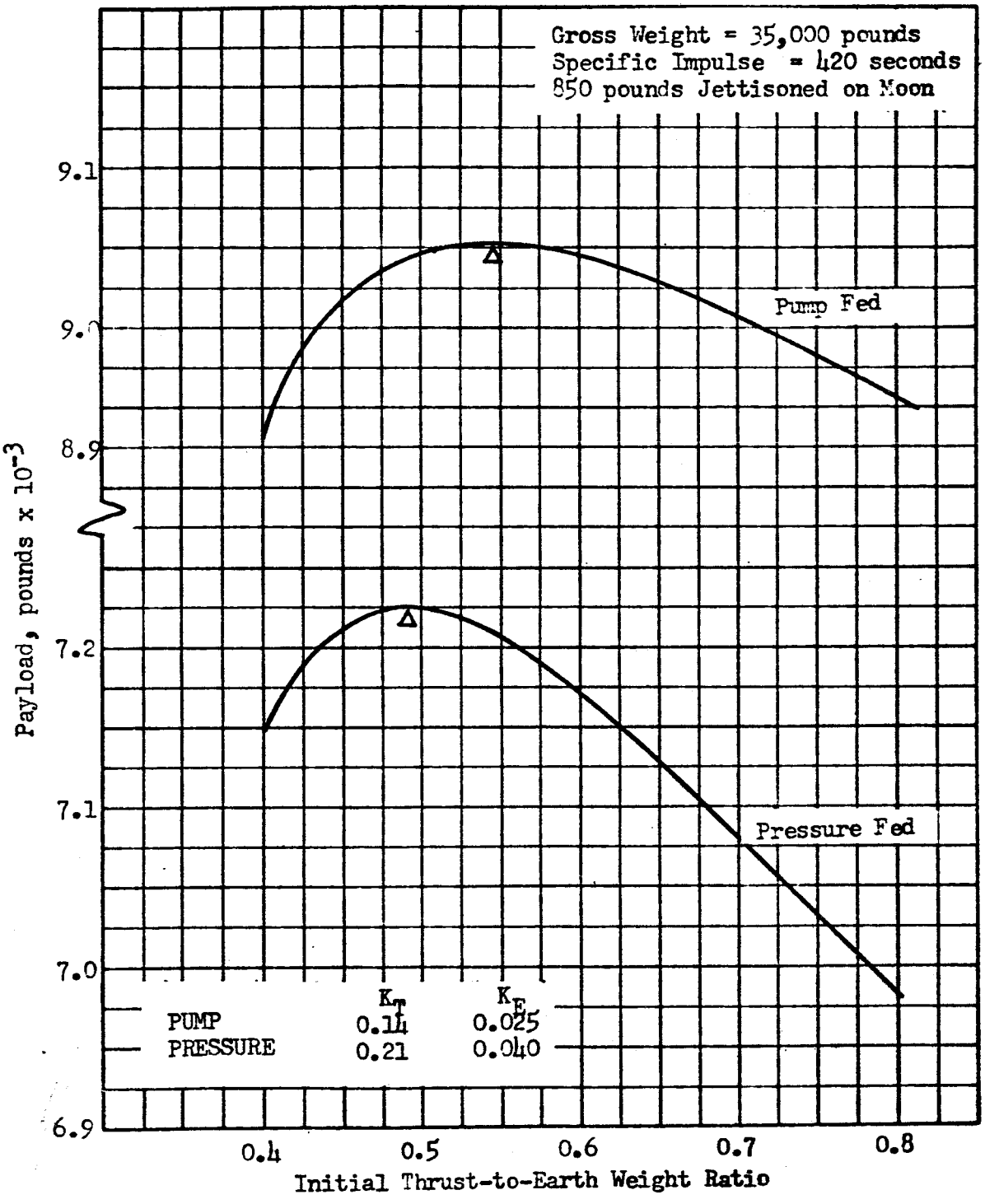

Figure 62 . Thrust Level Selection for Lunar Descent and Reorbit Vehicle

A significant point regarding the thrust-to-weight optima is that in a relatively wide band about the optimum point (approximately 0.08 thrust-to-weight ratio units in most of the cases presented) the payload is practically constant.

In this investigation, nominal values of thrust-dependent and propellant-dependent weight factors were assumed. These values, representing typical stage designs, are subject to wide variation with material selection, redundancy philosophy, etc., and have an important influence on the selection of thrust level.

Parametric analysis was conducted to provide trade-off data describing the influence of thrust-dependent and propellant-dependent weight on the optimization of thrust level. In this analysis, propulsion was provided by engines which ranged from relatively light weight (i.e., $K_E = 0.01$) to relatively heavy (i.e., $K_E = 0.04$). For the second (takeoff) stage of a two-stage vehicle, a large change in propellant-dependent weight factor was introduced in order to evaluate its effect on thrust level selection. Only noncryogenic propellant systems were considered. Additionally at this juncture, fixed stage weights were introduced, in amounts suitable to yield logical stage propellant fractions, in order to provide payload values representative of actual vehicle capabilities.

Results for a lunar landing stage are presented in Figure 63 . To illustrate an important point cited earlier, the curve represented in $K_E = 0.025$ is considered. The maximum payload, 14,974 pounds, occurs when the thrust level is 19,600 pounds. However, to obtain a payload within 75 pounds, or 0.5 percent of maximum, the thrust level can range from 14,400 pounds to 26,500 pounds. The larger thrust-dependent weight factors result in lower optimum thrust-to-weight ratios caused by the higher weight penalties associated with higher thrust levels for systems having larger values of K_E.

Similar results for a lunar takeoff stage are presented in Figure 64 . For comparison purposes, the tank weight factor used in Figure 64 was tripled, and the data shown in Figure 65 was computed. The increase in optimum thrust-to-weight ratio at increased tank weight factor (for a given thrust-dependent weight factor) simply expresses the tendency of the system to seek an operating point where less propellant is required and thereby minimize the onus of high tank weight factor. For the magnitude of tank weight-factor change utilized, the effect on optimum thrust level selection is fairly small.

Characteristics of the single-stage vehicle for performance of the overall mission are presented in Figure 66 . For $K_E = 0.02$, the optimum thrust level is 22,900 pounds, but values between 19,300 pounds and 27,300 pounds can be employed without imposing so much as 0.5 percent payload penalty.

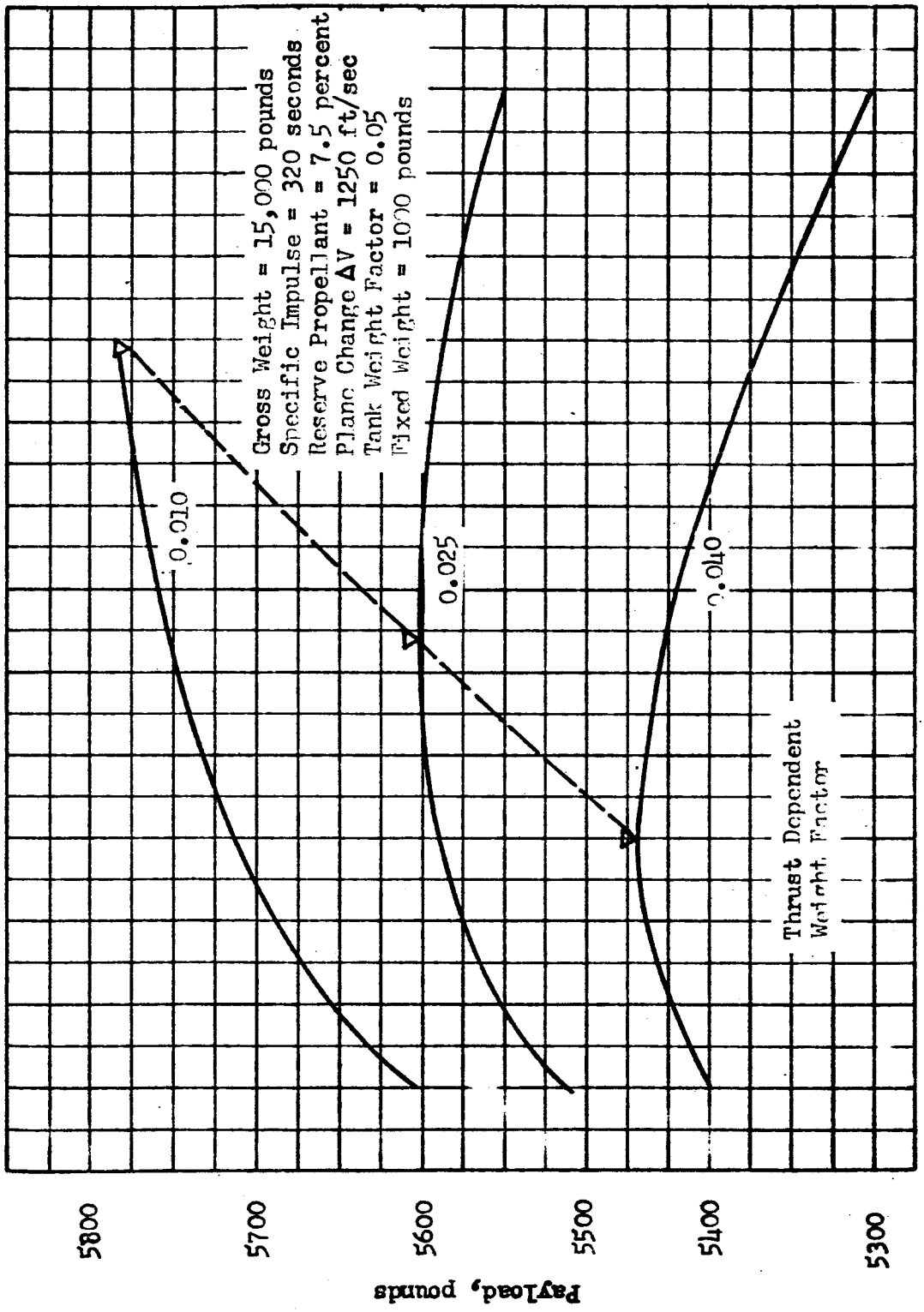

Figure 63 . Thrust Selection for Lunar Takeoff-to-Orbit

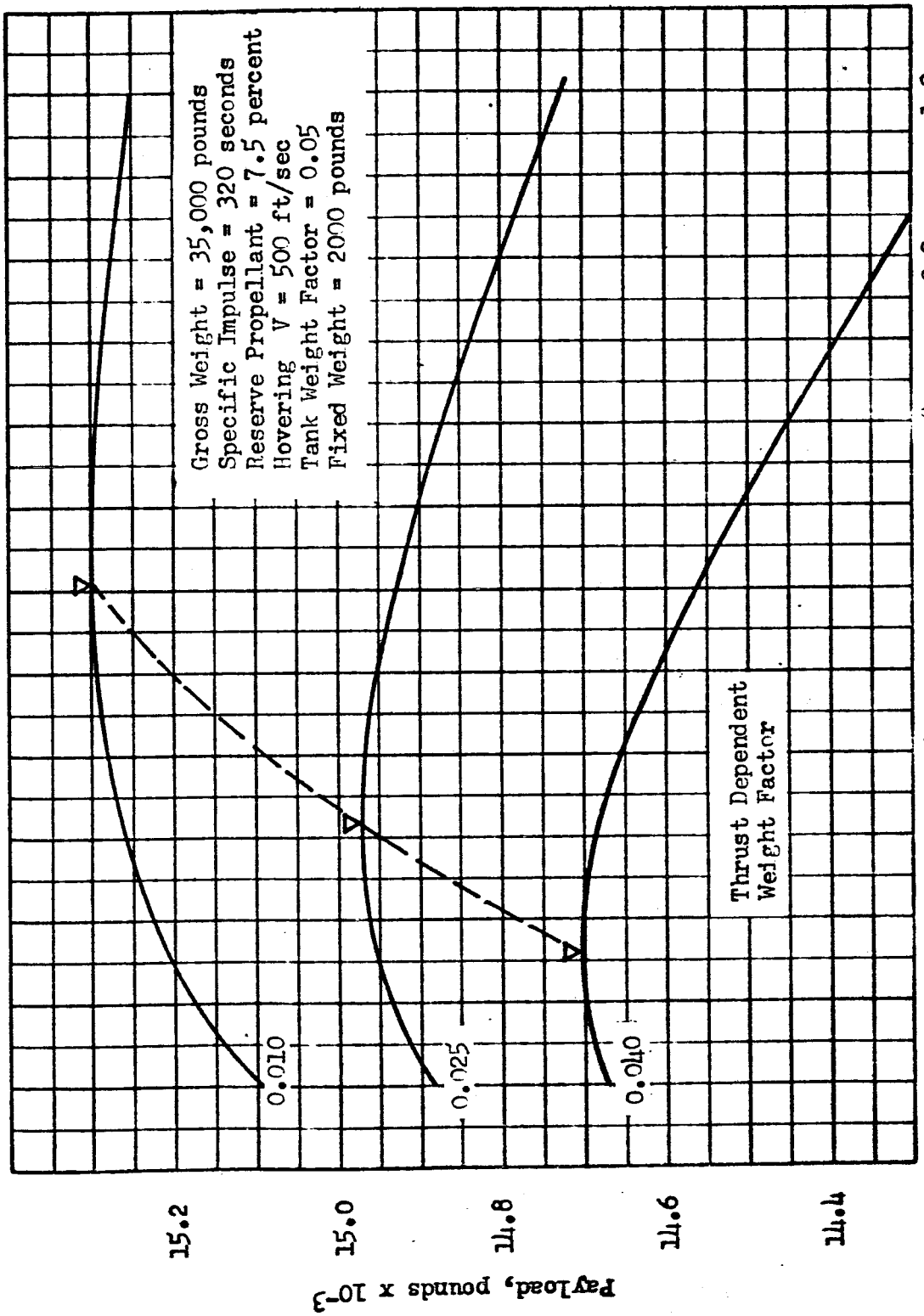

Figure 64. Thrust Selection for Landing from Lunar Orbit

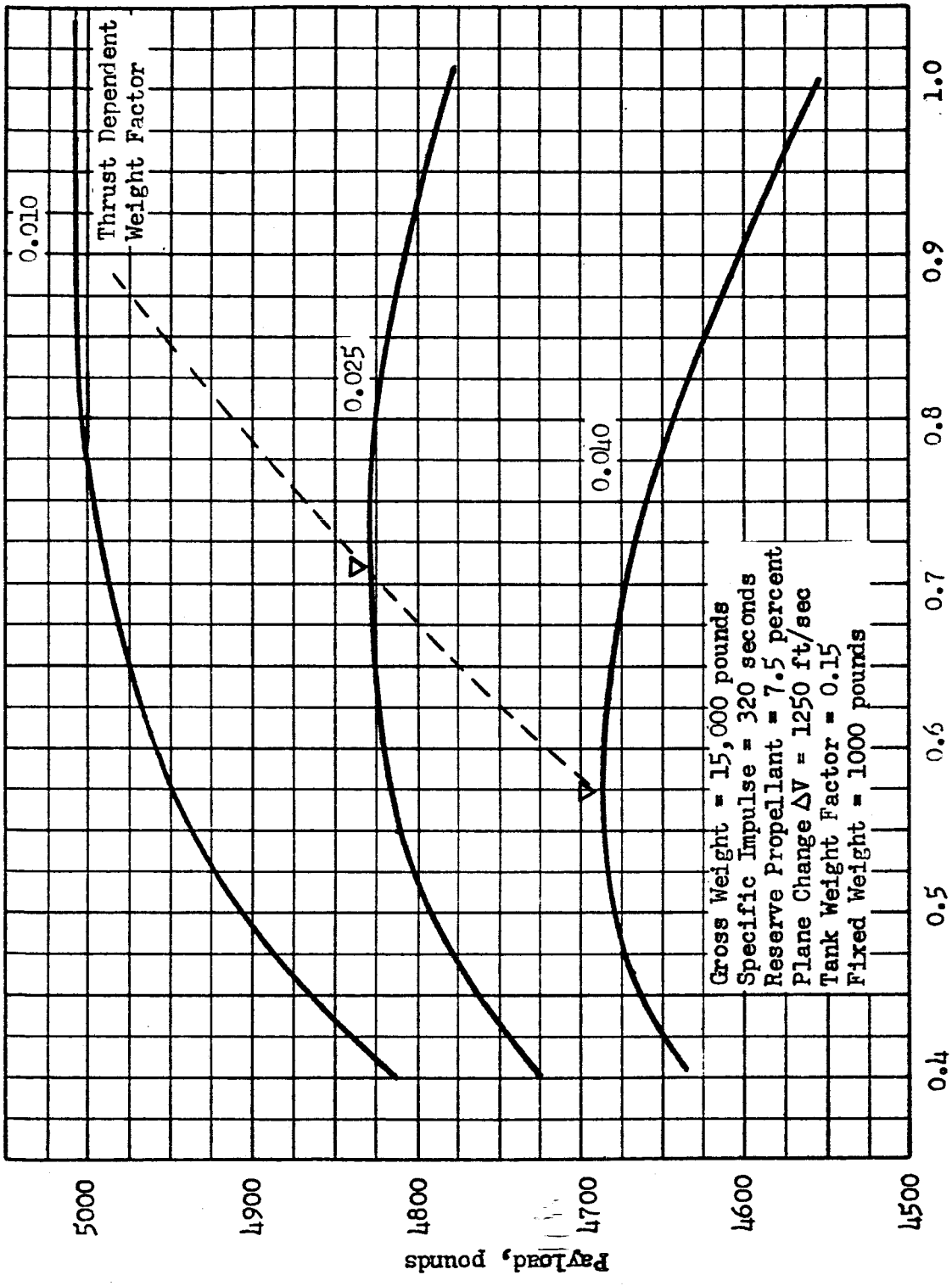

Figure 65. Thrust Selection for Lunar Takeoff-to-Orbit

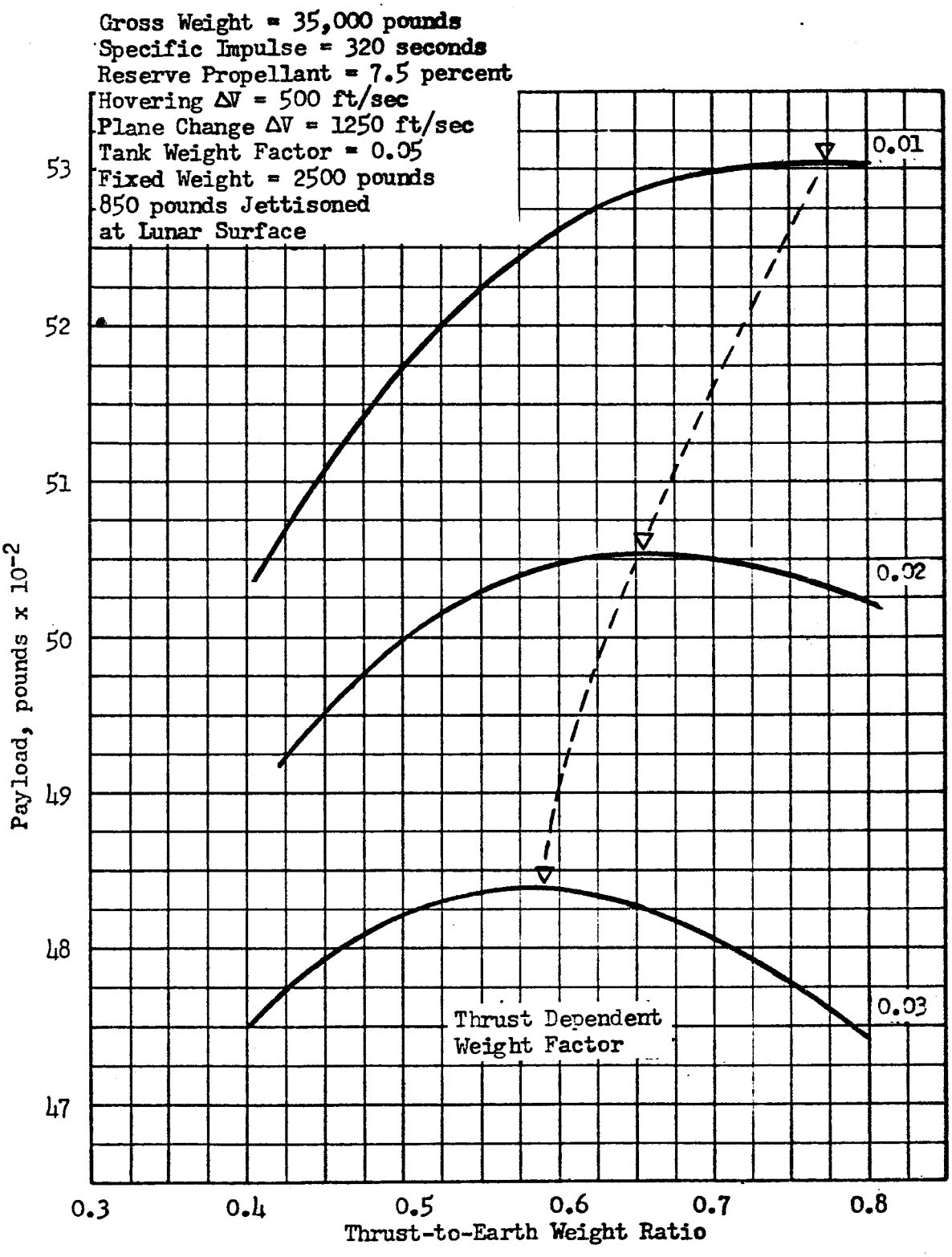

Figure 66. Thrust Selection for Lunar Descent and Reorbit

In this preliminary investigation, the effect of interstage structure weight was not included. If the interstage structure remained with the subject stage after separation from the previous expended stage, the effect would be equivalent to increasing the thrust dependent weight factor, K_E. Thus, the optimum thrust would tend to be lowered. If the interstage remained attached to the previous stage after separation, two design philosophies are possible for the subject stage. First, the subject stage may be considered by itself. By so doing, the interstage has no effect on the stage optimization. Second, the interactions between the two stages may be considered. In this case, the interstage weight would tend to lower the optimum thrust of the second stage by diminishing the allowable gross weight of the stage.

The thrust-to-lunar weight ratio at the end of the descent from orbit maneuver versus initial thrust-to-(Earth) weight is shown in Figure 67. (To achieve a 1:1 thrust-to-lunar weight, for hovering, for example, an engine throttling ratio equal to the terminal thrust-to-lunar weight indicated must be employed).

Nominal Vehicle Systems. Payload comparisons based on typical designs for several vehicle configurations are presented in Figure 68 for one- and two-stage landing-takeoff vehicles based on an initial weight in orbit of 35,000 pounds. The propellant fraction, λ_p, ranges associated with each line represent the probable variations in design of each system. Estimated values of specific impulse of each system are indicated on the graph. The ability to leave part of the inert weight on the surface results in the two-stage vehicles exhibiting better performance. Other general conclusions are the superiority of O_2/H_2 over noncryogenic propellants and of pump-fed systems over pressurized-gas-feed systems. However, it should be noted that considerations other than payload, (e.g., cost, reliability) must be evaluated in the selection of a propulsion system.

Table 3 and 4 present propulsion system thrust, thrust range, payload, and throttling requirements to achieve a 1:1 thrust-to-lunar weight ratio for hovering for landing-takeoff vehicles having gross weights of 35,000 pounds. Both one-and two-stage vehicles were considered, as well as pump- and pressure-fed systems. K_E and K_T result from different design features of pump and pressure-fed systems. These data may be scaled to establish preliminary design trends for larger vehicle sizes.

The gross weight requirements of the noncryogenic propellant landing-takeoff vehicle are shown in Figure 69 as a function of the payload, based on λ_p's of 0.91 and 0.86 for the pump- and pressure-fed systems respectively. The optimum thrust and the thrust range which will result in less than 1 percent payload loss (compared to the payload with optimum thrust) are also indicated. The figure indicates that a thrust level may be selected for

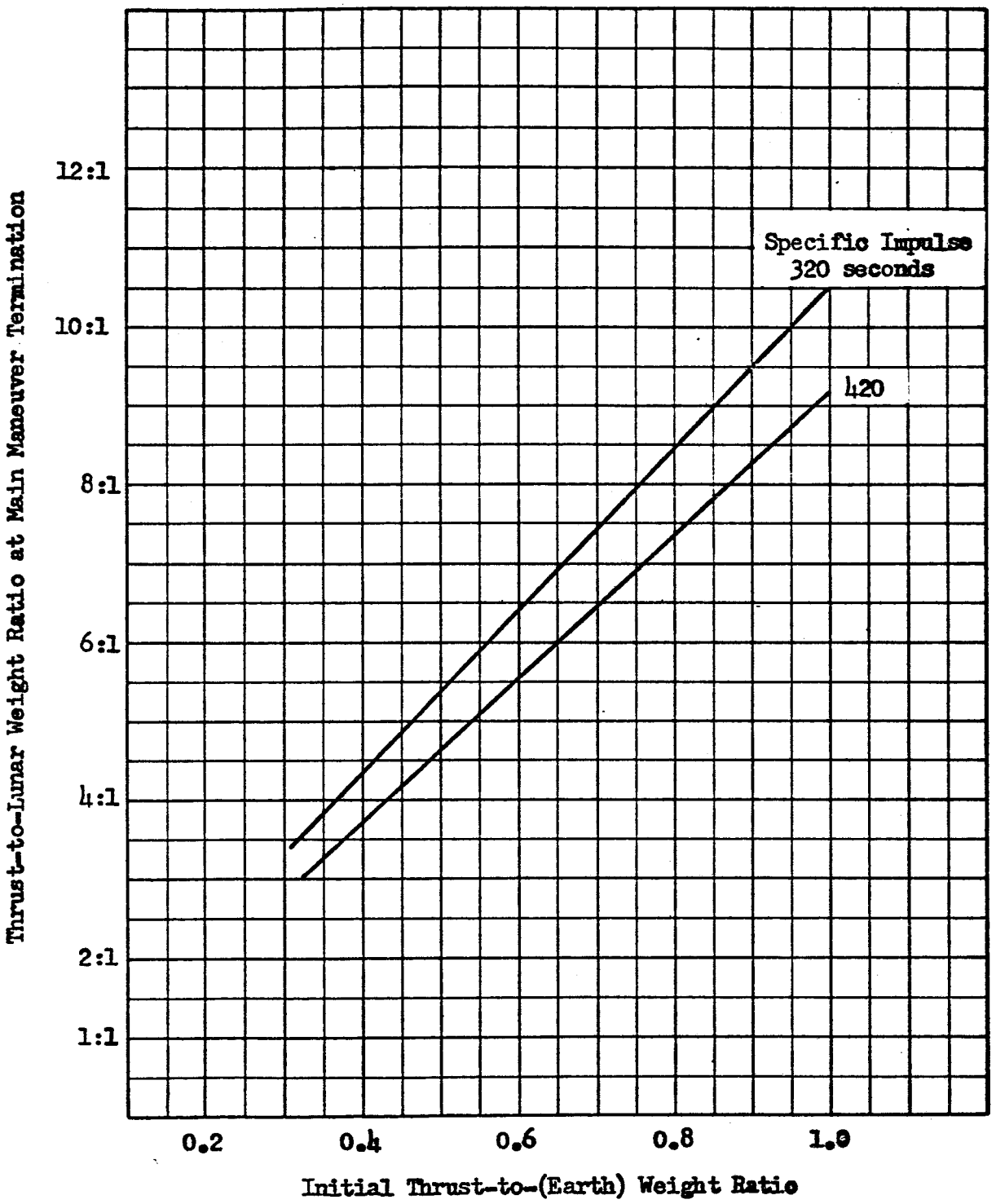

Figure 67. Throttling Ratio Required to Achieve Thrust Equal to Lunar Weight: Lunar Landing-from-Orbit.

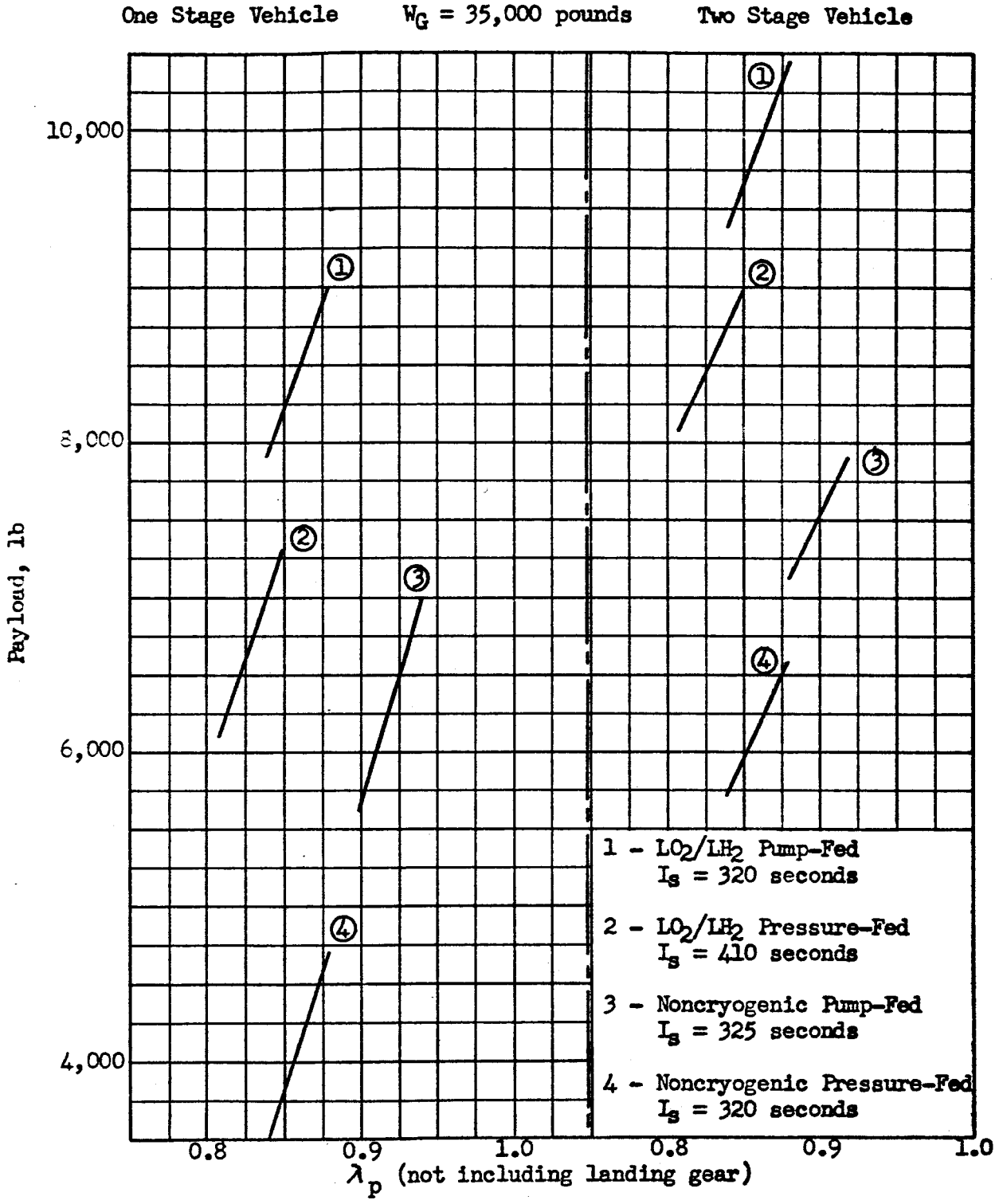

Figure 68. Payload Comparisons for Various Vehicles and Propulsion Systems.

TABLE 3

NONCRYOGENIC PROPELLANT LUNAR LANDING/TAKEOFF VEHICLES

	Two Stage		Single Stage
	Landing	Takeoff	
Initial Weight, pounds	35,000	15,800 pump-fed* 14,600 pressure-fed	35,000
Specific Impulse, seconds	320	320	320
Thrust-Dependent Weight Factor	0.02 0.04	0.02 0.04	0.02 0.04
Propellant-Dependent Weight Factor	0.05 0.08	0.05 0.08	0.05 0.08
Optimum Thrust, pounds	21,000 16,800	10,900 8,100	22,900 19,300
Payload, pounds	16,200 14,600	7,300 6,100	6,000 4,000
Thrust for Payload within 1 percent of Maximum, pounds	15.4K - 28.9K 13K - 22.1K	8.2K - 14.8K 6.4K - 10.5K	19.3K - 27.3K 15.8K - 25.0K
Throttling Ratio for Optimum Thrust Engine	6.4:1 5.2:1		6.8:1 5.8:1
Propellant Weight in Optimum Thrust System, pounds	16,670 16,780	7,800 7,650	16440 + 9060** 16710 + 9090
Duration of Optimum Thrust System, seconds***	334 396	229 302	314 + 127 356 + 151

* Pairs of number indicate pump/pressure throughout Table

** Division separates landing and takeoff phases

*** Includes 94 seconds of hovering for landing phases

TABLE 4

O_2/H_2 LUNAR LANDING/TAKEOFF VEHICLES

	Two Stage		Single Stage
	Landing	Takeoff	
Initial Weight, pounds	35,000	18,600 pump-fed* 17,300 pressure-fed	35,000
Specific Impulse, seconds	420	420	420
Thrust-Dependent Weight Factor	0.025 0.040	0.025 0.040	0.025 0.040
Propellant-Dependent Weight Factor	0.14 0.21	0.14 0.21	0.14 0.21
Optimum Thrust, pounds	19,300 17,900	11,700 9,700	19,100 17,200
Payload, pounds	18,600 17,300	9,900 8,500	8,600 6,800
Thrust for Payload Within 1 percent of Maximum, pounds	15.0K - 26.6K 14.4K - 22.4K	9.1K - 17.3K 8K - 13.1K	15.6K - 24.1K 14.9K - 20.1K
Throttling Ratio for Optimum Thrust System, pounds	5.0:1 4.6:1		5.0:1 4.5:1
Propellant Weight in Optimum Thrust System, pounds	13,670 13,700	7,970 7,480	13,680 + 8660** 13,730 + 8660
Duration of Optimum Thrust System, seconds***	373 397	286 324	377 + 190 409 + 212

* Pairs of number indicate pump/pressure throughout Table
** Division separates landing and takeoff phases
*** Includes 94 seconds of hovering for landing phases

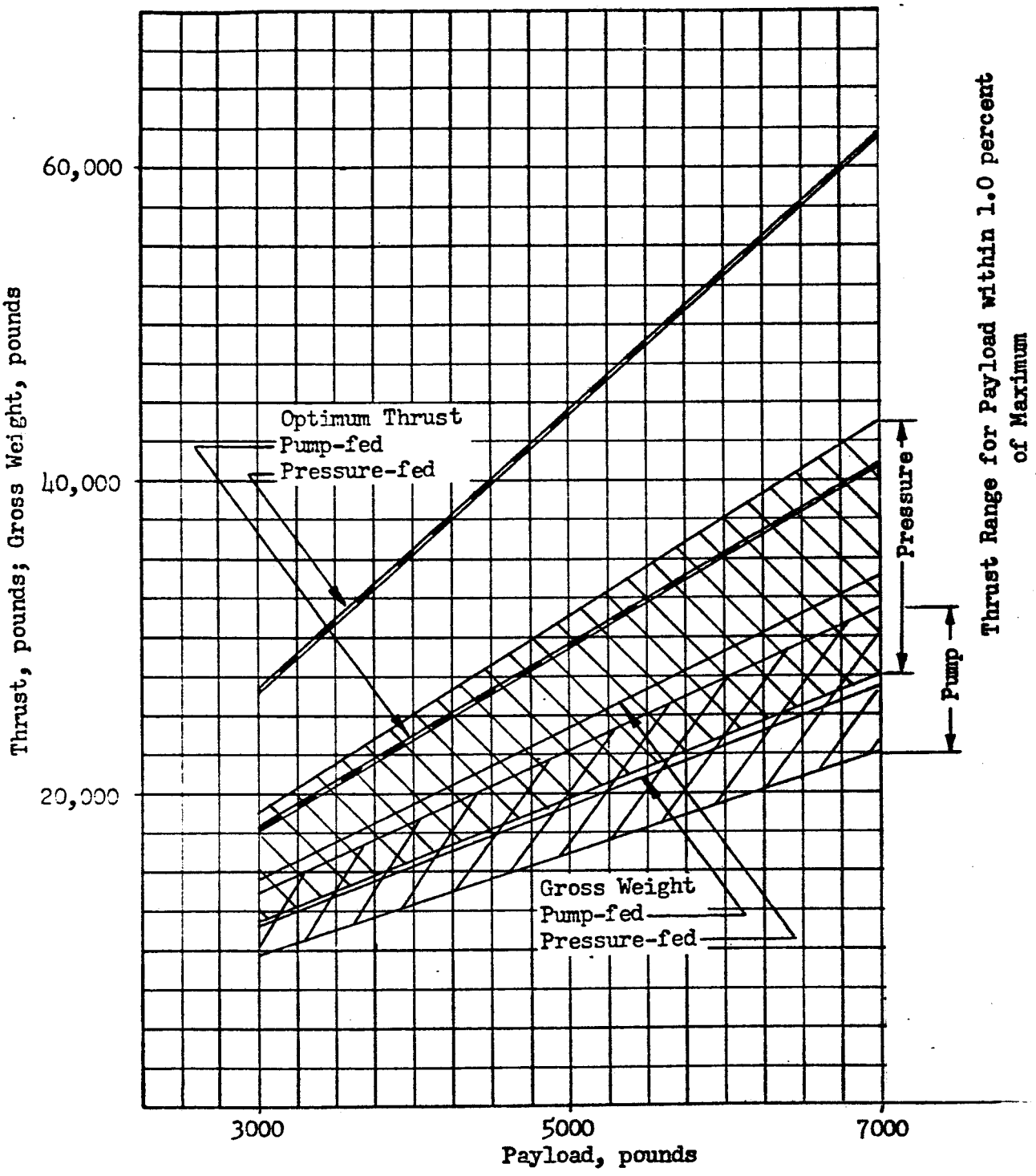

Figure 69. Thrust and Gross Weight Requirements - One-Stage Noncryogenic Propellant Vehicle

preliminary design purposes before a final choice of pump- or pressure-fed systems is made. The flatness of the thrust optimization curves is shown in Figure 70 .

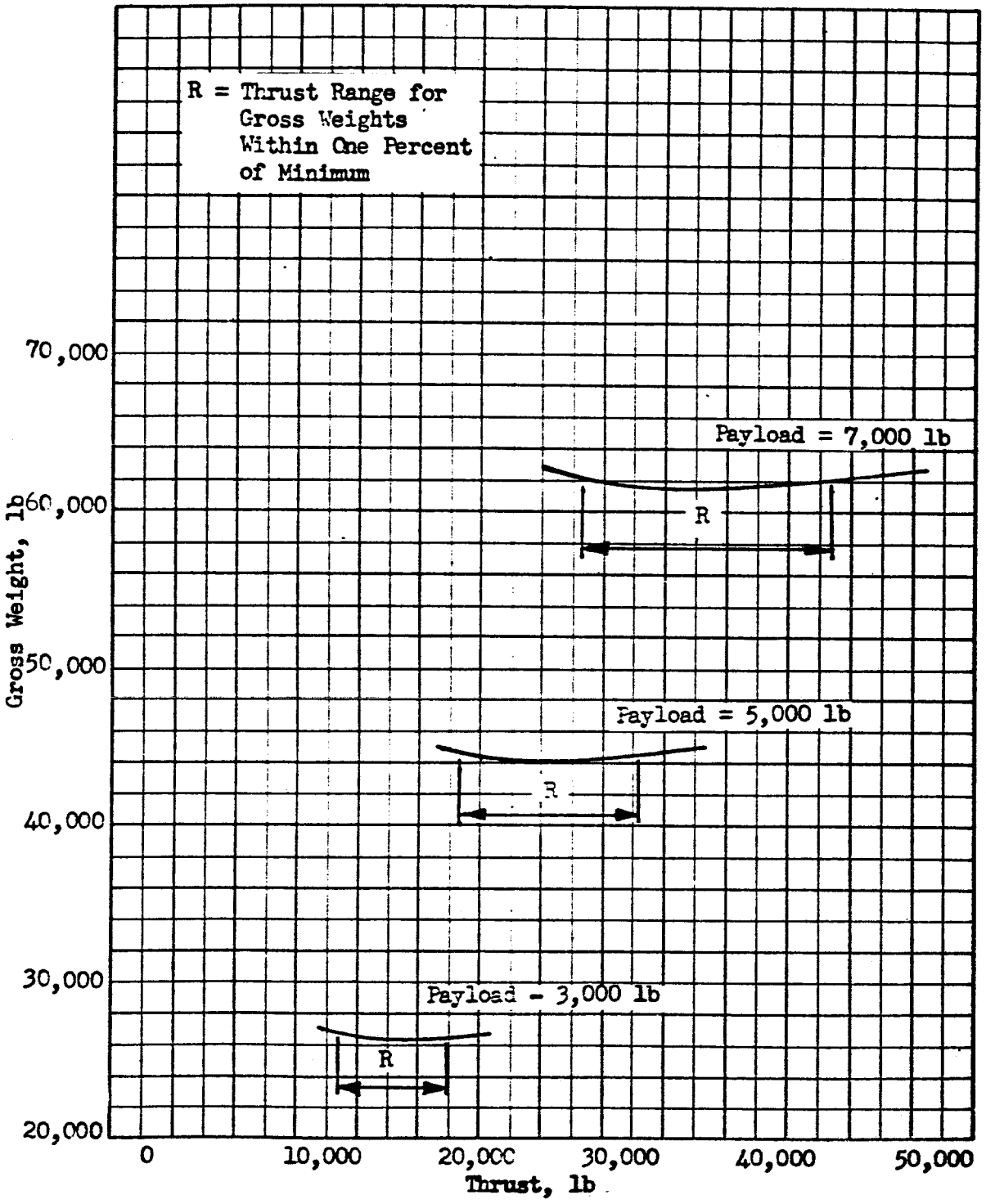

Figure 70 . Gross Weight Variation with Thrust; One Stage Vehicle, Noncryogenic Pressure-Fed Propellants

ERROR ANALYSIS FOR LUNAR LANDING-FROM-ORBIT MANEUVER

The major propulsive phase of landing from a lunar orbit is that portion of the maneuver during which the vehicle is decelerated from high velocity at the periapsis of an elliptical orbit about the body to a hover position near the surface of the body. An evaluation of the errors experienced in reaching a desired hover point if execution of the maneuver deviates in certain respects from nominal (ideal) performance of the maneuver has been made. The errors considered were deviations from nominal thrust, both with and without accompanying variation in specific impulse, ignition prior to or beyond the periapsis of the ellipse, and angular displacement between the thrust and velocity vectors during the propulsive maneuver.

Nominal conditions for this analysis were selected on the basis of results of previous trajectory and thrust optimization studies. Noncryogenic propellants were employed, and an initial thrust-to-(Earth) weight ratio of 0.4 was utilized. Nominal periapsis conditions were 5704 ft/sec velocity and 71,000 feet altitude. Deviations from the nominal periapsis altitude translate directly to deviations from the altitude of the nominal hover point. Characteristics of the nominal thrust-parallel-to-velocity (gravity turn) landing trajectory are presented in Figure 71 . The nominal hover altitude for the selected initial conditions, indicated as zero in Figure 71 , is 5150 feet above the lunar surface.

Thrust Variation

If each of two vehicles, differing only in thrust level, performs a gravity-turn maneuver, the higher thrust vehicle will execute a steeper descent and will come to rest at a hover point higher than, and up-range of, the hover point of the other vehicle; this result is intuitively obvious and results as a consequence of the shorter operating duration of the higher thrust system.

The deviations in range and altitude resulting from off-nominal thrust operation are presented in Figure 72 . Several possible causes exist concerning thrust discrepancies and most of these yield one of the two characteristics shown in Figure 72 . In Case A, specific impulse is unchanged as thrust varies; this condition is characteristic of a change in turbopump speed (regulator setting shift, turbine inlet nozzle obstruction) for a pump-fed system or tank-pressure deviation (regulator shift) for a pressure-fed system. The constancy of specific impulse in these circumstances is not precisely true, but the deviation is barely detectable. In Case B, thrust

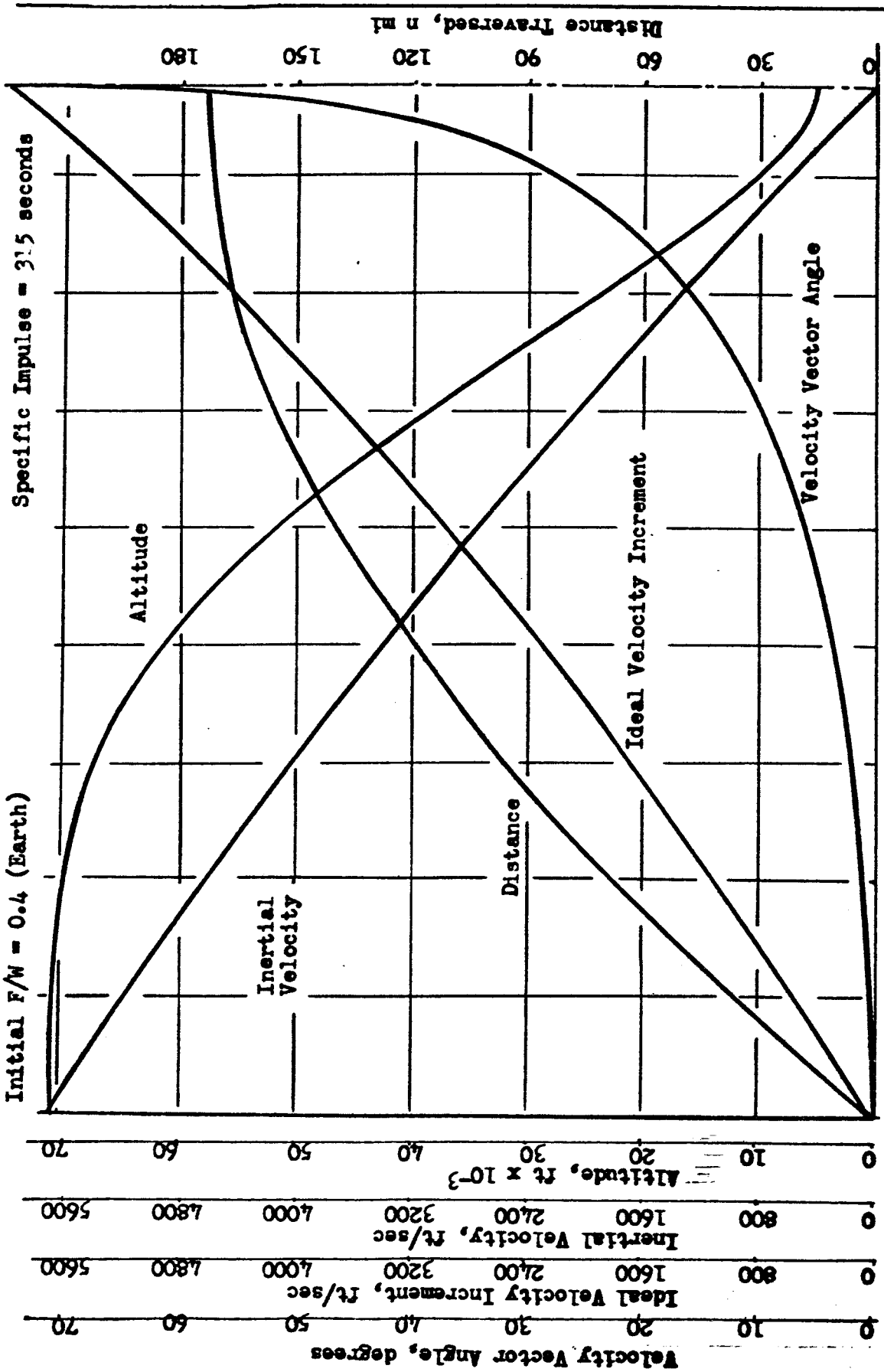

Figure 71. Nominal Lunar Landing Trajectory Characteristics

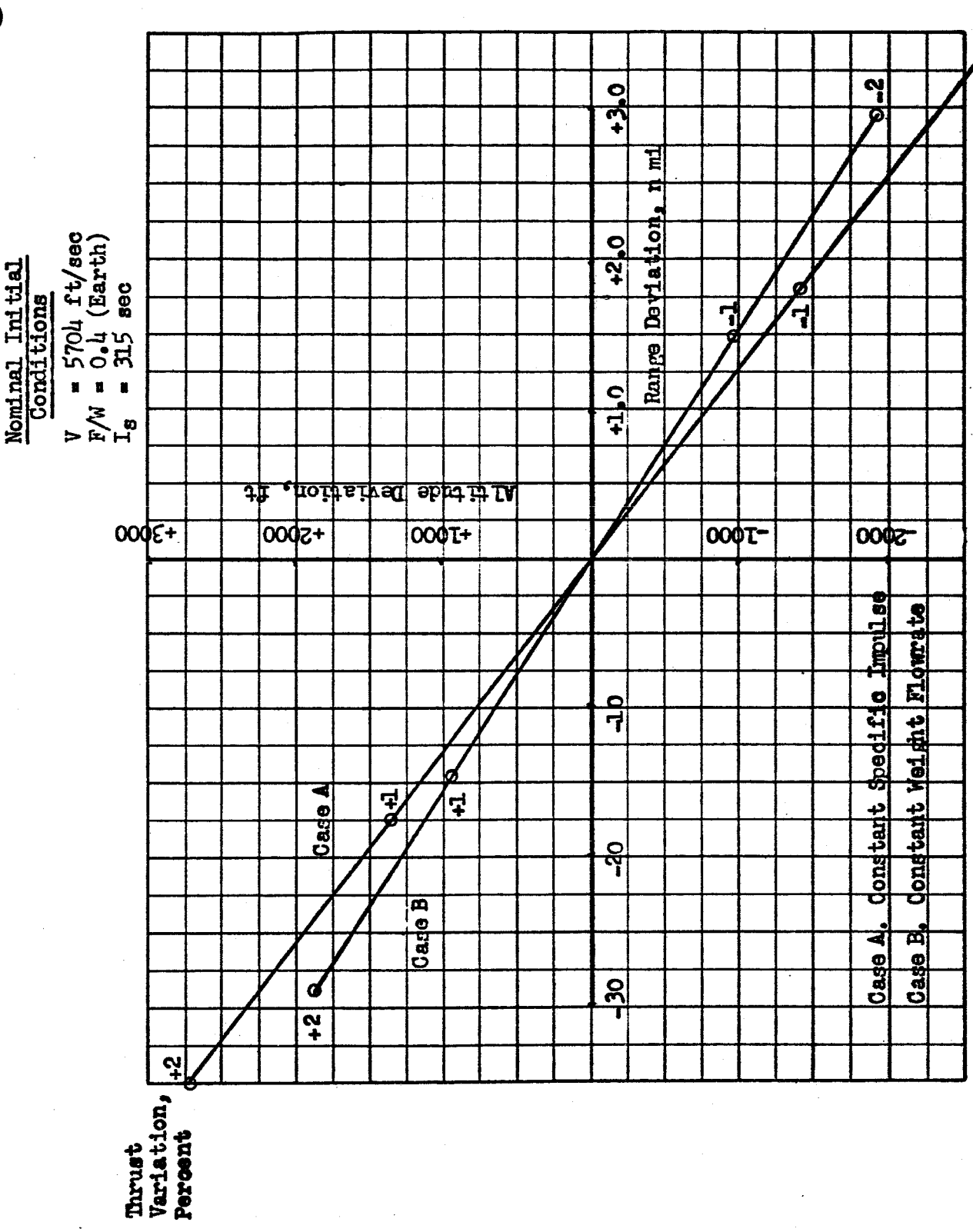

Figure 72. Effect of Thrust Errors on Lunar Landing Maneuver Terminal Position

and specific impulse vary together; the cause may be random variation of combustion efficiency or the presence of a nondestructive mode of combustion instability.

The indicated results do not include the effect of lunar rotation. Since nominal target points on the equator of the moon are moving at a speed of 15.5 ft/sec, deviations from the nominal landing-maneuver duration, resulting from deviations from nominal thrust, cause distance errors up to a value equal to 15.5 times the difference between the nominal and actual landing maneuver durations, $V_s(t-t_{nom})$.* A 1-percent thrust discrepancy is equivalent to approximately a 3-second duration change, resulting in an error of less than 50 feet. Since the 1-percent thrust deviation causes a range error in excess of 10,000 feet, the additional 50 feet is trivial.

The significant conclusion to be drawn from Figure 72 is that small variations in thrust cause substantial deviations in hover point location. Translation maneuver studies have indicated that to reach the nominal hover point from the position reached by a vehicle with a 2-percent thrust discrepancy, the vehicle would require a reserve propellant supply equivalent to approximately 2000 ft/sec of ideal velocity increment.

Trajectory Position at Propulsion System Ignition

The nominal landing maneuver is initiated precisely at the periapsis of an elliptical orbit about the destination body. However, if some guidance system errors exists, ignition might occur at a time prior to, or later than, arrival at periapsis, in which case a landing location error arises due to deviations from the nominal initial position coordinates and velocity vector direction.

The variation of trajectory parameters as the vehicle approaches and passes by the periapsis of its elliptic orbit is shown in Figure 73 . The 40-second interval indicated on either side of the periapsis corresponds to a range-angle error slightly in excess of ± 2 degrees. Velocity variation during the interval, amounting to approximately 0.3 ft/sec, is not shown; it was,

* The maximum effect is experienced for a landing from retrograde, equatorial orbit; the error adds algebraically to the error caused by the thrust discrepancy. For an equatorial orbit in the same direction as the planet rotation, the thrust error is reduced by an amount equal to $V_s(t-t_{nom})$. For nonequatorial orbits, the error is a function of orbit inclination and landing site latitude, and is between the two extremes cited above.

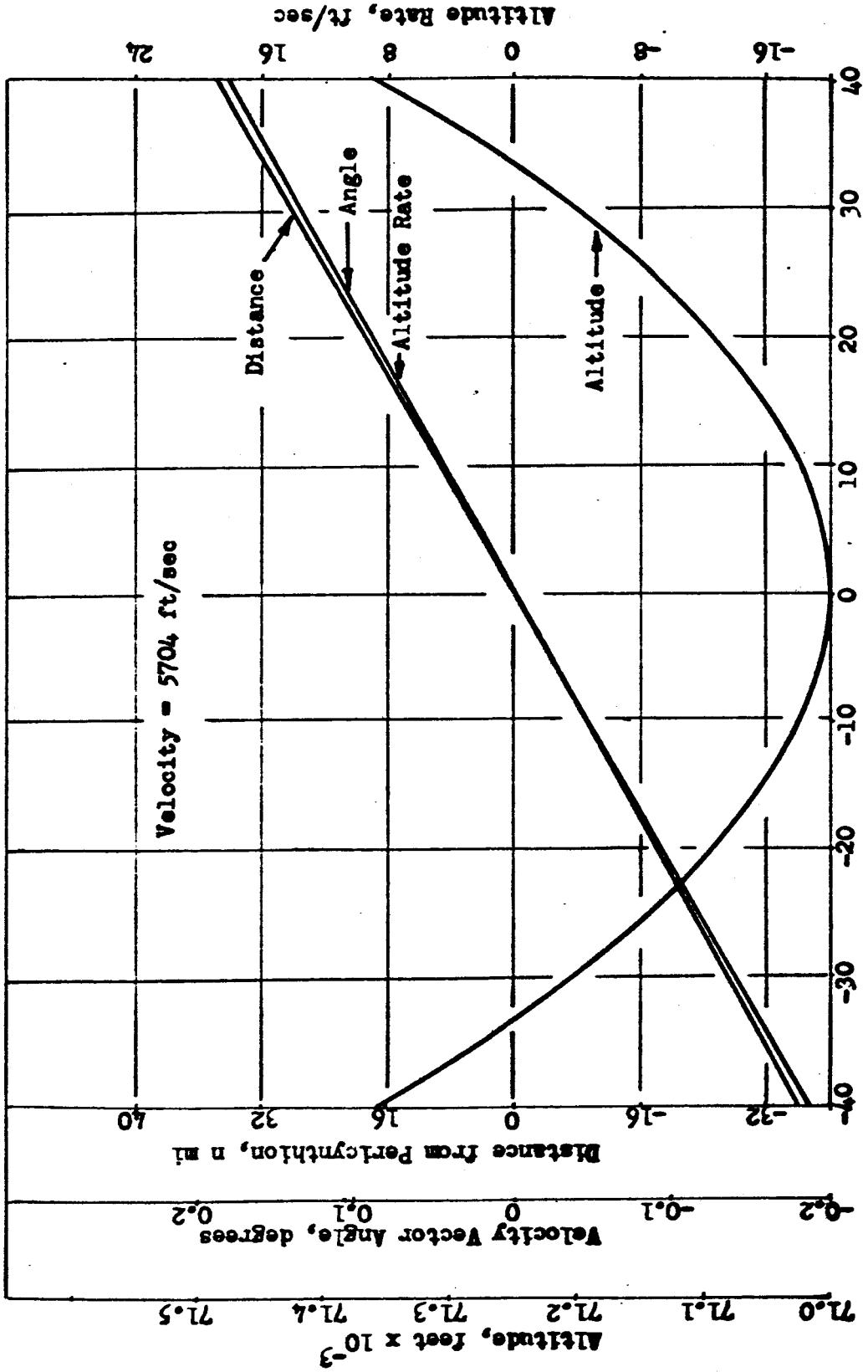

Figure 73. Reference Conditions for Initiation of Lunar Landing Maneuver

however, included as a factor in subsequent analysis. Of the variables indicated in Figure 73 , distance from pericynthion is the most significant; the vehicle traverses, and therefore produces at the lunar surface, a range error amounting to almost one nautical mile each second. The other factors, though important, are less significant in producing final position errors.

Results of the ignition-time analysis are presented in Figure 74 . It is evident that if a particular landing site is the goal of the maneuver, some corrective action is needed to alter the trajectory and thereby to avoid a requirement for substantial translation-maneuver propellant reserves. For early ignition, engine throttling can be employed to correct the trajectory; the penalty (resulting from the need to allow sufficient altitude bias to avoid impact and to perform the descent maneuver at lower-than-nominal thrust-to-weight ratio) is on the order of a few hundred ft/sec of propellant reserve. For late ignition, if reaching a particular site is essential and increased thrust is not available, the options include mission abort (or another orbit), use of surface vehicles, and carrying large (several thousand ft/sec) propellant reserves.

Thrust Vector Misalignment

In the nominal landing maneuver, the propulsion-system thrust vector is directed precisely and continuously opposite to the vehicle velocity vector. The ability of the vehicle to detect the direction of the velocity vector and the ability of the propulsion system to respond to commands to orient the thrust vector accordingly are subject to error. Therefore, an analysis was conducted to evaluate the hover-point position errors induced by misalignment errors, i.e., by inadvertently performing a small angle-of-attack maneuver instead of the desired gravity turn. In addition, the analysis indicates the possible corrections of other errors that can be achieved by the deliberate use of an angle-of-attack descent.

Results of this investigation are presented in Figure 75 . For the range of typical misalignment errors considered, the altitude errors produced have the same order of magnitude as those experienced because of the thrust or ignition-time errors described previously; intentional misalignment therefore offers a means of correcting altitude errors. However, range errors are quite small, in fact, almost insignificant in comparison to the range errors shown in Figures 72 and 74 . This result indicates that deliberate misalignment cannot be used effectively to correct lateral position errors caused by other deviations from nominal conditions.

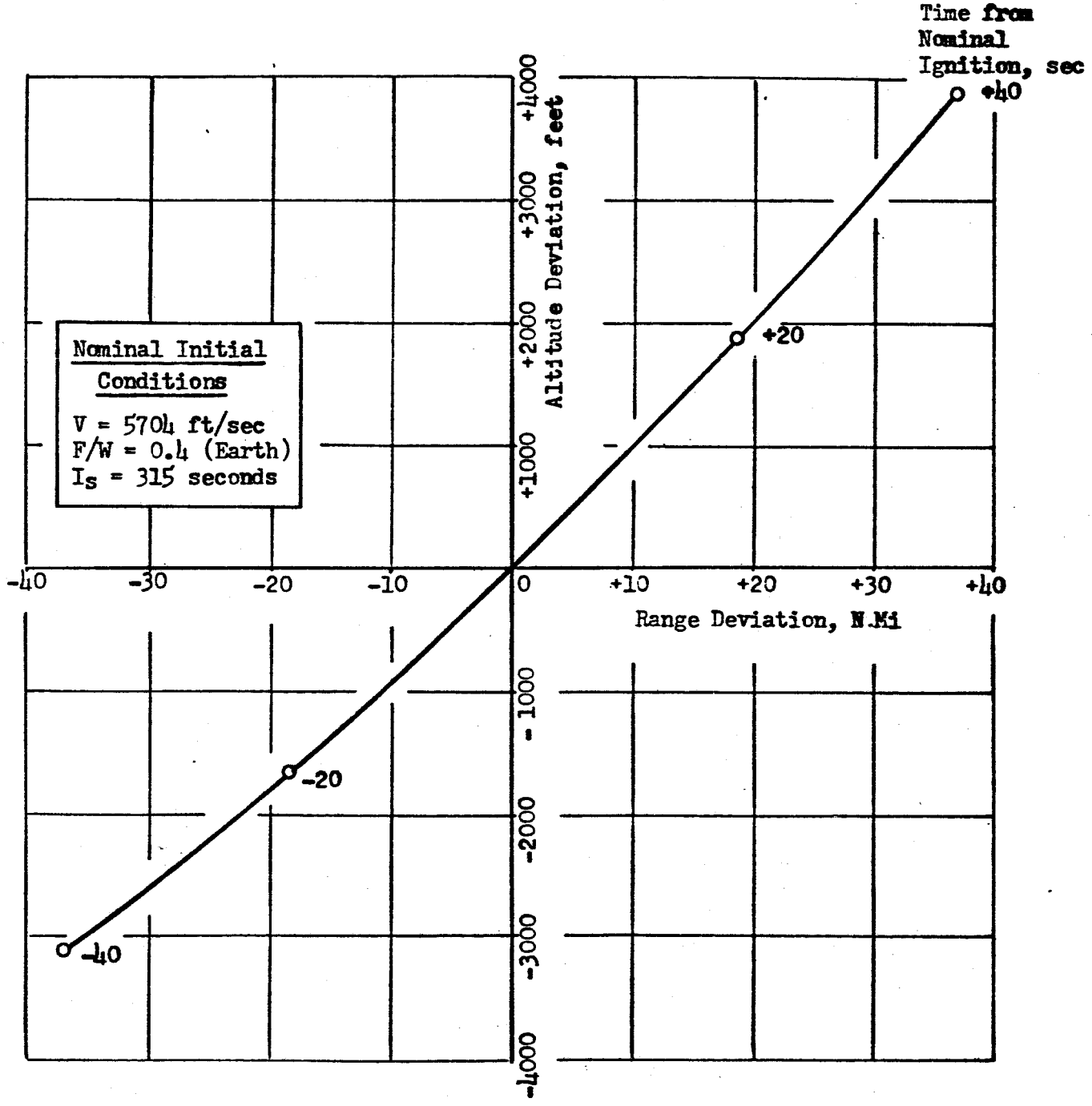

Figure 74. Effects of Propulsion Initiation Time on Lunar Landing Maneuver Terminal Position

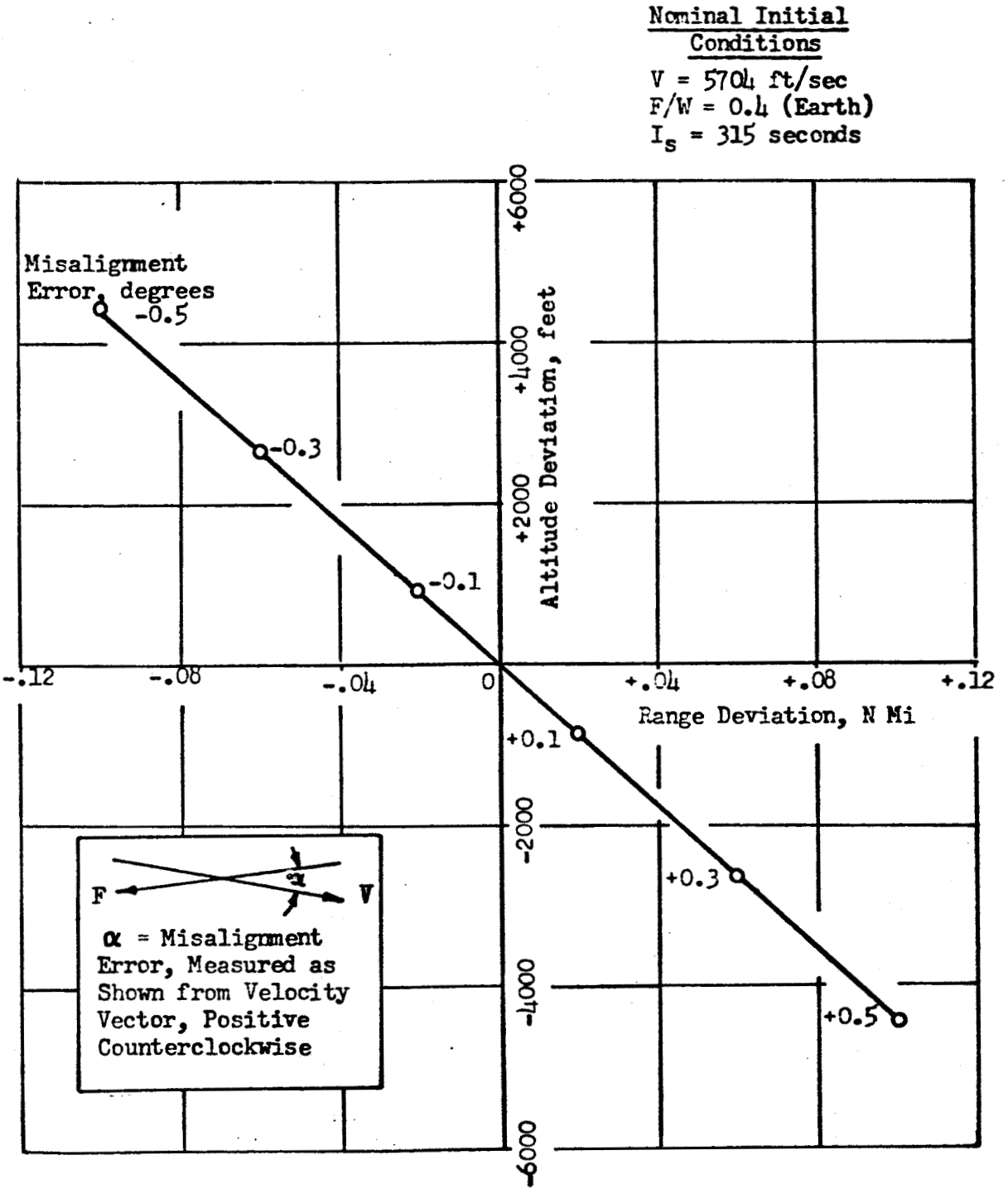

Figure 75. Effects of Thrust Misalignment Errors on Lunar Landing Maneuver Terminal Position

Critique of Gravity Turn Analysis

With the deliberate exception of the misalignment error study, the analyses have been predicated on the ability of the landing vehicle to continuously align the propulsion system thrust vector and the vehicle velocity vector, i.e., to perform a gravity turn correctly regardless of deviations from the nominal values of thrust magnitude or initial position and velocity.

A simpler (from a guidance standpoint) technique for performing the powered descent maneuver may be the use of a preprogrammed thrust orientation profile. In this case, since the profile is based on nominal conditions, the descent trajectory is a gravity turn only if the propulsion system operates at nominal thrust and specific impulse, and ignition occurs precisely at the periapsis of the elliptical orbit. If nominal conditions do not prevail, the programmed thrust-orientation profile does not constitute a gravity turn, and an error, equivalent to a time-variable misalignment error, is introduced. The magnitude of the error at any given time is equal to the difference between the nominal trajectory angle and the corresponding gravity-turn trajectory angle.

The variation in velocity-vector angle (and therefore thrust-vector angle) is presented in Figure 76 for the nominal lunar-orbit descent maneuver and for two thrust deviations from the nominal maneuver (angle is measured positive clockwise from the horizontal). It is evident that for a major portion of the trajectory, the angle vs time characteristics are identical for the three cases. Beyond 160 seconds, however, the characteristics diverge; thereafter, descent in compliance with the nominal curve is, for the high and low thrust conditions, equivalent to having both thrust and misalignment errors.

Misalignment errors, though constant rather than variable, were analyzed earlier, and the results of that study offer a useful, though approximate, insight into the errors introduced by adhering to an inappropriate, preselected thrust-orientation schedule. The instantaneous magnitude of the misalignment error is described in Figure 77 for the two examples described in Figure (note unorthodox ordinate scale on Figure 77). Measurement of the area under either of the two curves between zero and 350 seconds yields an approximate time-average misalignment error of 0.7 degree, which represents an equivalent, constant value of misalignment error.

The use of a time-average misalignment value is far from precise as a means of evaluating errors, but it offers a simple, and qualitatively correct, way to estimate overall landing maneuver errors. Sharing equal significance with time in determining an accurate equivalent value of angular misalignment are altitude rate and range rate, each affecting the respective component of the misalignment-induced error. Thus, because range rate is very small in the

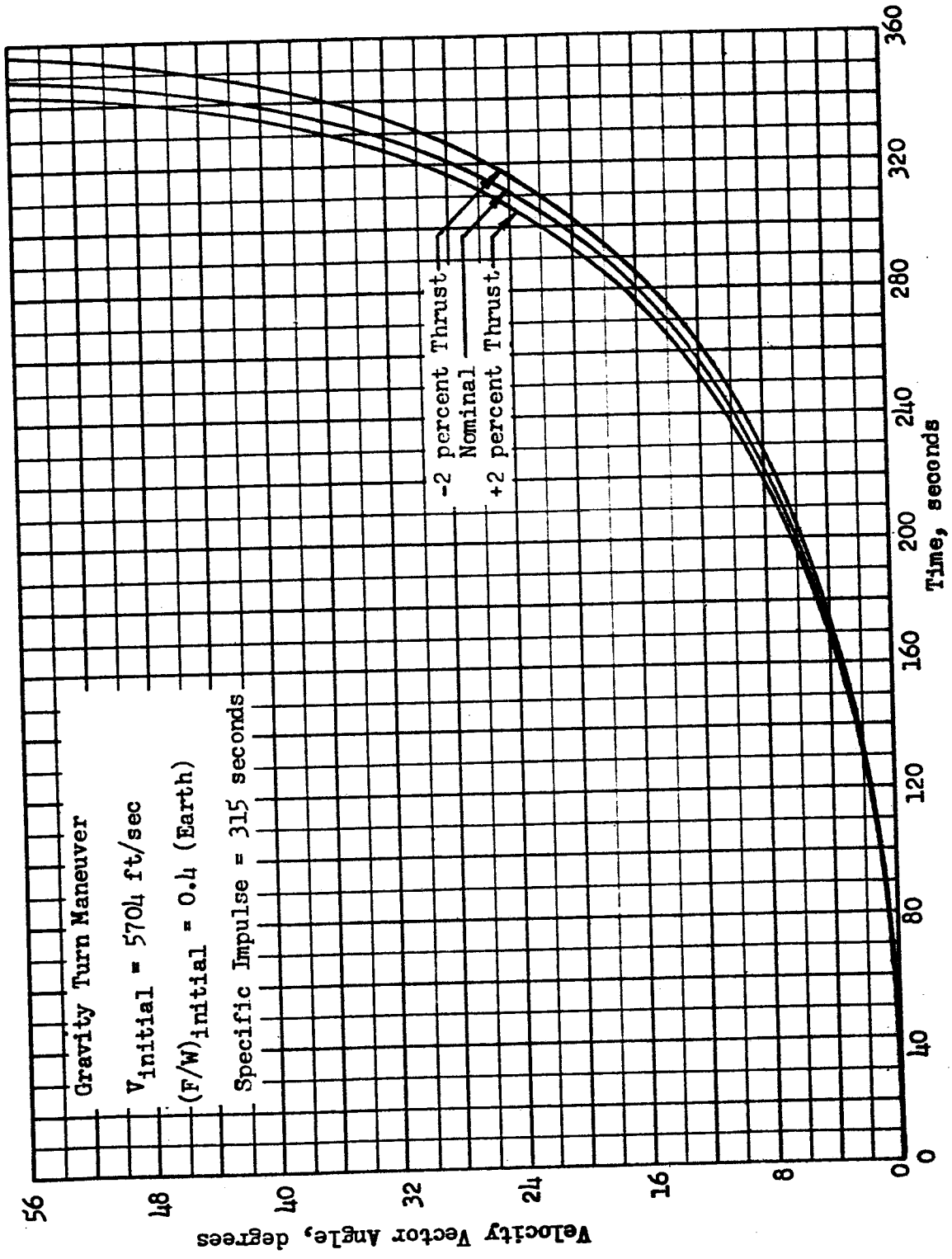

Figure 76. Variation of Velocity Vector Angle During Lunar Orbit Descent

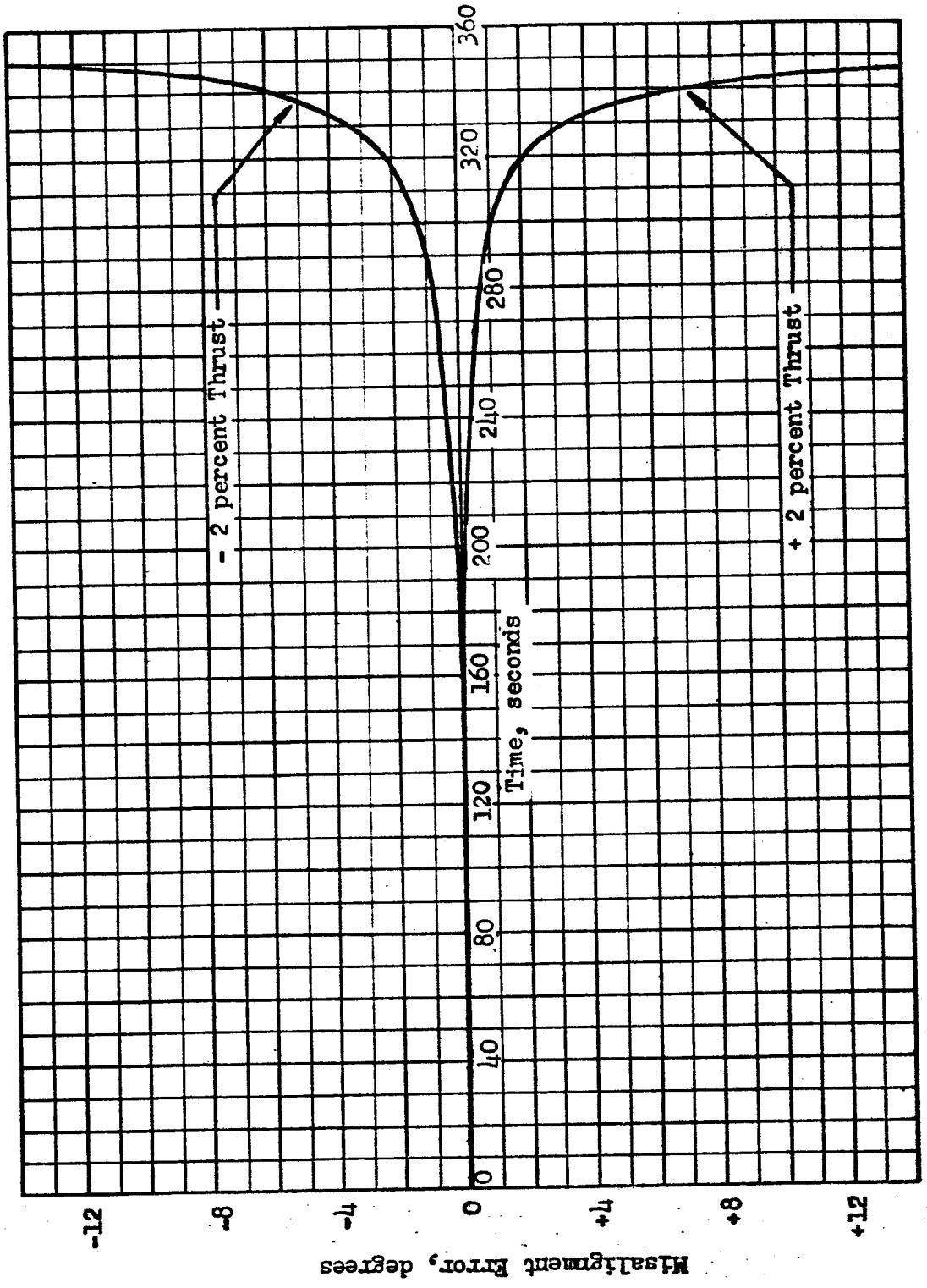

Figure 79. Thrust Misalignment Error for Lunar Landing Maneuver

region where instantaneous misalignment is greatest, the range error estimated by a time-averaging process tends to be high; however, since altitude rate and instantaneous misalignment are high simultaneously in the latter portion of the trajectory (except for the final 30 seconds), the misalignment-induced altitude error is greater than the time-averaging method indicates.

For any given set of conditions, the overall error in trajectory terminal position can be estimated by superimposing the separate errors caused by individual error factors; thus, for the +2-percent thrust case, errors of +2700 feet altitude and -3.5 nautical mile range are indicated in Figure 72 caused by excessive thrust, and, using the time-averaged misalignment value, Figure 75 (extrapolated) indicates errors of -6000 feet altitude and +0.2 nautical miles range due to misalignment. The net result is an approximate terminal position 3300 feet below and 3.3 nautical miles short of the nominal hover point.

For early or late ignition (i.e., deviations from ignition at periapsis) the nominal trajectory again differs from the appropriate gravity-turn maneuver; the magnitude of the deviation is shown in Figure 78 (compare this with Figure 77). In this case, the time-averaged misalignment error is approximately 0.15 degrees and an early-ignition (40 seconds) trajectory attains a hover point 1300 feet below and 0.03 miles beyond the point that would be reached if a gravity-turn maneuver were employed. Note that in this example, early ignition and misalignment both lower the hover point below the nominal altitude; in the high thrust case, misalignment lowered the hover point while the added thrust raised it.

Results

For all of the errors considered (see Table 5), the ideal velocity requirements needed to decelerate the landing vehicle to a hover position were within a band defined by 5984 + 20 ft/sec. Thus, the significant influence that propulsion errors have on propellant requirements is related to the displacement of the hover position, rather than to the propulsion requirement to attain zero velocity.

Values of displacement from the nominal hover point are presented in Table 5 for representative deviations from nominal performance of lunar-orbit landing maneuvers.

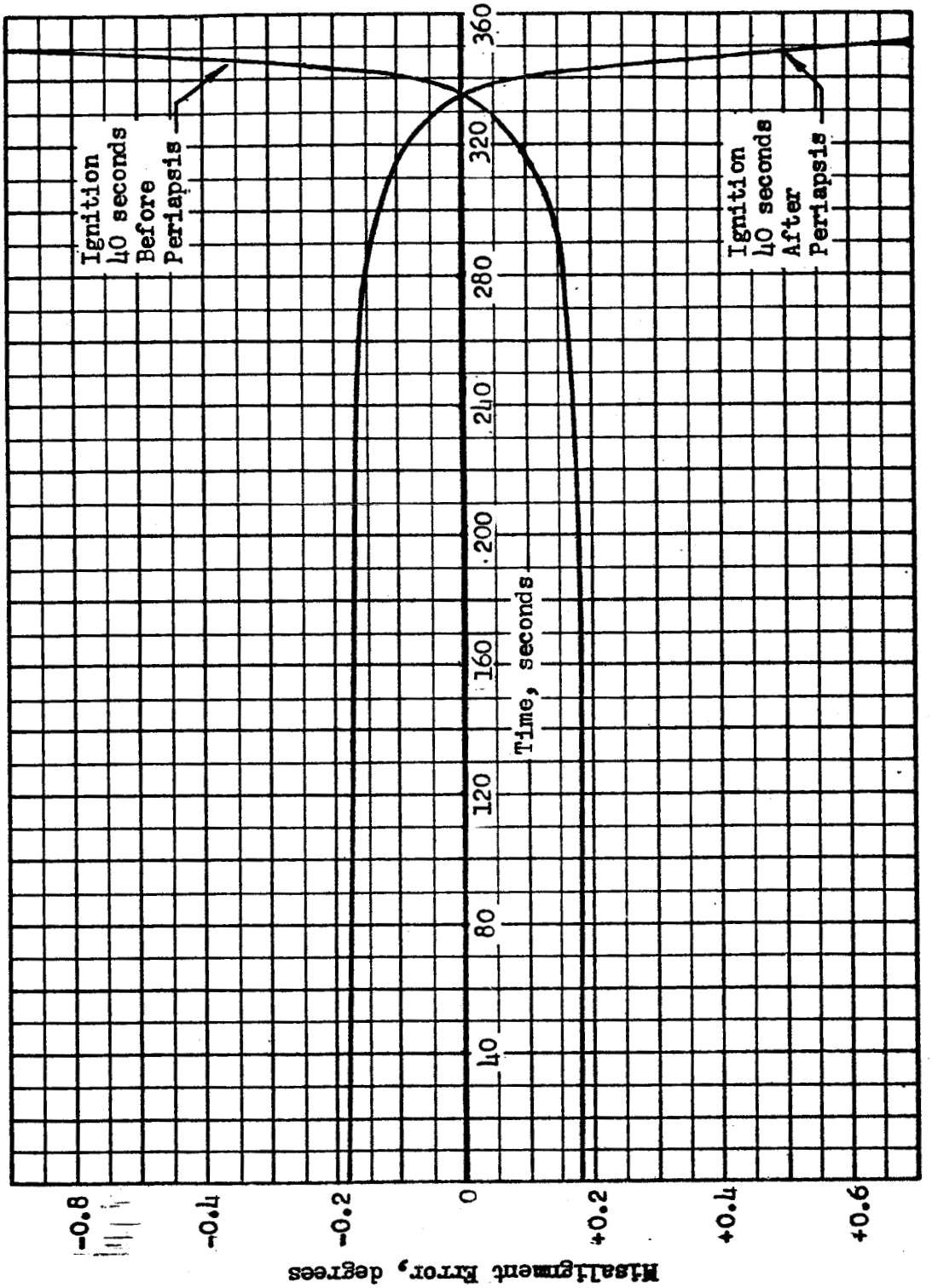

Figure 78. Effect of Initial Position on Lunar Landing Misalignment Error

TABLE 5

HOVER POINT POSITION ERRORS

Error	ΔAltitude, feet	ΔRange, n mi
+2 percent Thrust; Specific Impulse Constant	+2710	-3.48
+2 percent Thrust; +2 percent Specific Impulse	+1890	-2.88
Ignition 20 seconds Early	+1890	-2.88
+0.5 degree Misalignment	-444	+0.10

To account for altitude deviations introduced by the propulsion or trajectory errors considered, the nominal hover position should be approximately 5000 feet above the lunar surface. Errors in elliptic orbit periapsis altitude, not evaluated in this study, should be added to these values. The propulsion requirements for translation and descent to the nominal landing site from the positions indicated above are on the order of several thousand ft/sec in most instances, and therefore corrective measures such as engine throttling should be initiated during the main propulsion phase rather than after reaching the hover point. The vehicle can descend from the hover point during the subsequent translation maneuver; the altitude would then be on the order of a few hundred feet when the vehicle arrived at a point directly above the desired landing site.

MISSION ABORT

Provision of mission abort capability in a lunar or planetary landing vehicle requires that the available propulsion systems be sufficient to perform not only the maneuvers associated with a successful mission, but also the maneuvers required to implement an abort decision. A "brute force" solution would be to provide an independent abort propulsion system (which would be discarded if no abort were required). A more efficient approach is to supplement the landing and/or takeoff propulsion systems, by addition, if necessary, of propellant capacity and/or suitable selection of thrust levels, so as to enhance their capabilities sufficiently to encompass abort requirements as well as routine landing and takeoff requirements.

Lunar Landing Abort

Landing from lunar orbit may be divided into three phases: (1) conversion of the circular orbit to an ellipse with a low altitude pericynthion; (2) powered descent from pericynthion to hover altitude; (3) translation and descent. The present analysis was concerned with abort during the second phase. The purpose of the abort maneuver was to place the vehicle in a 50-n mi circular orbit. Other terminal conditions could have been chosen (e.g., different circular orbit altitudes or various ellipses which do not intersect the lunar surface); however, the selected terminal conditions are reasonable, particularly when the lunar rendezvous concept is considered.

In the present study, abort propulsion requirements were evaluated for one- and two-stage vehicles performing the landing-from-orbit and return-to-orbit maneuvers of a lunar mission. For the two-stage vehicle, separate analyses were conducted to determine the modifications needed if abort is to be performed 1) by the landing stage, and 2) by the takeoff stage.

The representative landing trajectory from which abort occurs was the same for both vehicle configurations considered; vehicle flight parameters are shown in Figure 79. The trajectory is for a landing vehicle which applies retrothrust antiparallel to the velocity vector. The curves present, for any point along the descent trajectory, the orientation of the vehicle with respect to the local horizontal, the decrease of the selenocentric inertial velocity of the vehicle and the increase in vehicle thrust-to-(Earth) weight ratio. The vehicle considered had a specific impulse of 315 seconds and an Earth thrust-to-weight ratio of 0.4 at the start of the descent maneuver approximately 66,000 feet above the lunar surface. At the final point of descent, the vehicle reaches zero velocity and is oriented in a vertical position. A bias altitude can be superimposed on the altitude characteristic to provide for hover-translation maneuvers. It was additionally assumed that at the instant the abort decision is made, the vehicle reorients to the desired abort maneuver attitude and applies thrust (the value of which is dependent on the particular analysis involved) until sufficient velocity is generated to transform the trajectory to an ellipse with a 50-n mi apocynthion. After coasting to apocynthion, a final propulsive maneuver is executed to circularize the orbit.

Single Stage Landing-Takeoff Vehicle. For the single stage vehicle, impulsive ($F/W = \infty$) abort maneuvers were first studied. The vehicle velocity vector (V) is known at each point on the landing trajectory as is the velocity vector (V_p) required to make that point the pericynthion of a Hohmann transfer ellipse

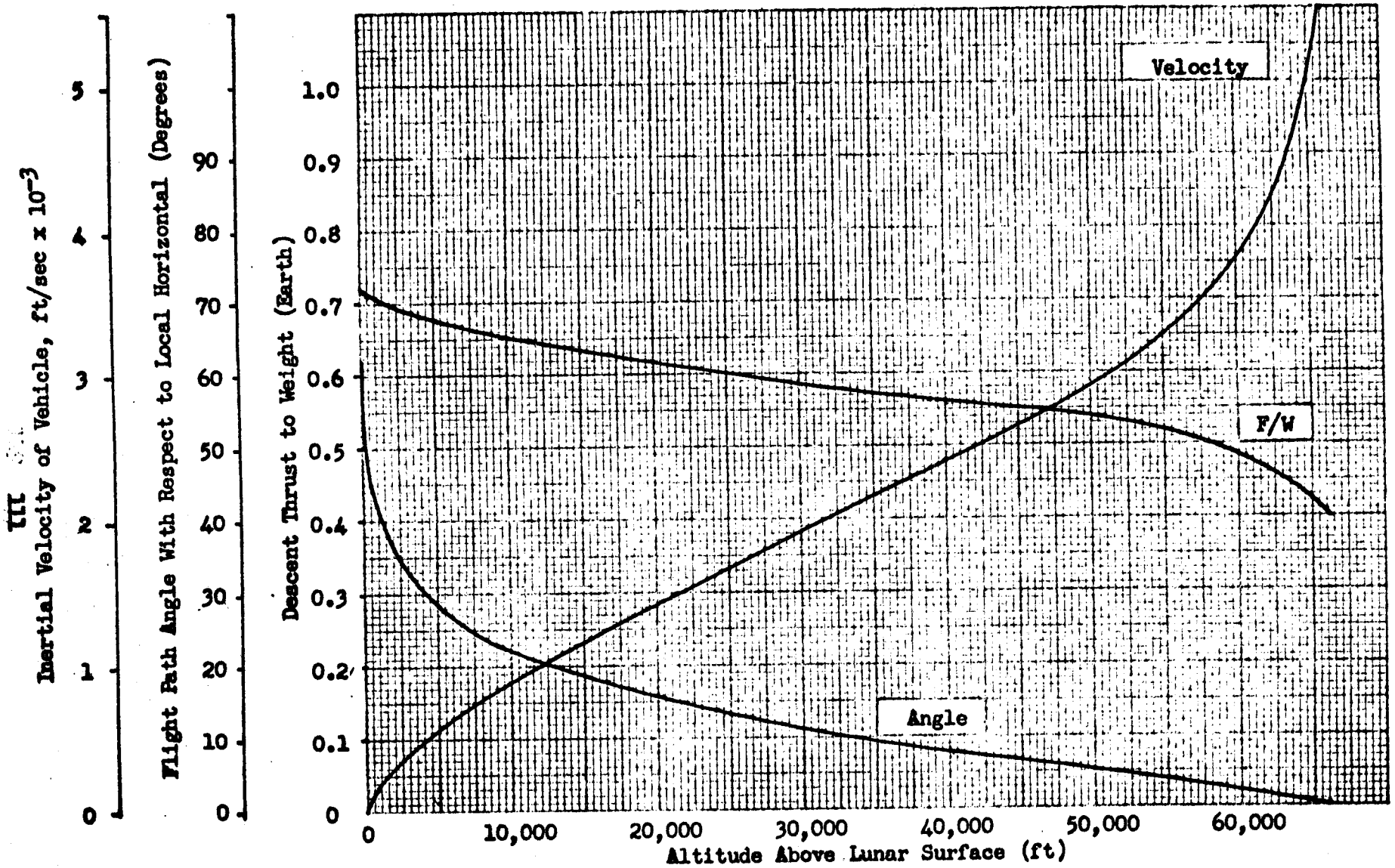

Figure 79 Vehicle Flight Parameters for a Typical Lunar Landing Trajectory (Vehicle Thrust Anti-Parallel to Velocity).

to 50 n mi. The difference of these two vectors is the impulsive (minimum) velocity (ΔV_i) requirement at pericynthion. The sketch below presents the velocity vector diagram for the impulsive pericynthion maneuver. An additional velocity increment must be added at apocynthion. The impulsive value of this increment is approximately 75 ft/sec.

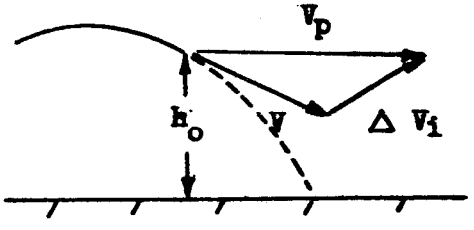

Figure 80 is a plot of the sum of the two impulsive velocity increments required as a function of the point (altitude) on the landing trajectory at which abort is initiated. The curve does not intersect the ΔV_i axis because even if abort were initiated simultaneously with the powered-descent maneuver, there would still be a velocity increment required at apocynthion.

During the early phases of the landing trajectory, velocity is reduced without much altitude loss. (In fact, a slight increase occurs.) This is reflected in the steep nature of the abort velocity requirement curve at high altitudes. Lower abort altitudes correspond to lower vehicle velocity vectors and thus to higher abort velocity requirements. The vehicle velocity is zero at the surface and the velocity shown at that point in Figure 80 is the impulsive velocity requirement for takeoff to the 50-n mi orbit altitude.

Use of nonimpulsive abort maneuvers was next considered. The vehicle began the abort maneuver with the F/W existing at the time of abort. Thus, lower altitude aborts had the advantage of higher values of F/W. The simplification was again made that the vehicle was capable of instantaneous reorientation of the vehicle thrust vector at the time of abort. After this reorientation, the thrust vector was maintained at a constant attitude (with respect to the local vertical) throughout the abort maneuver. The effect of thrust vector orientation during abort on the abort trajectory and velocity requirements was also studied.

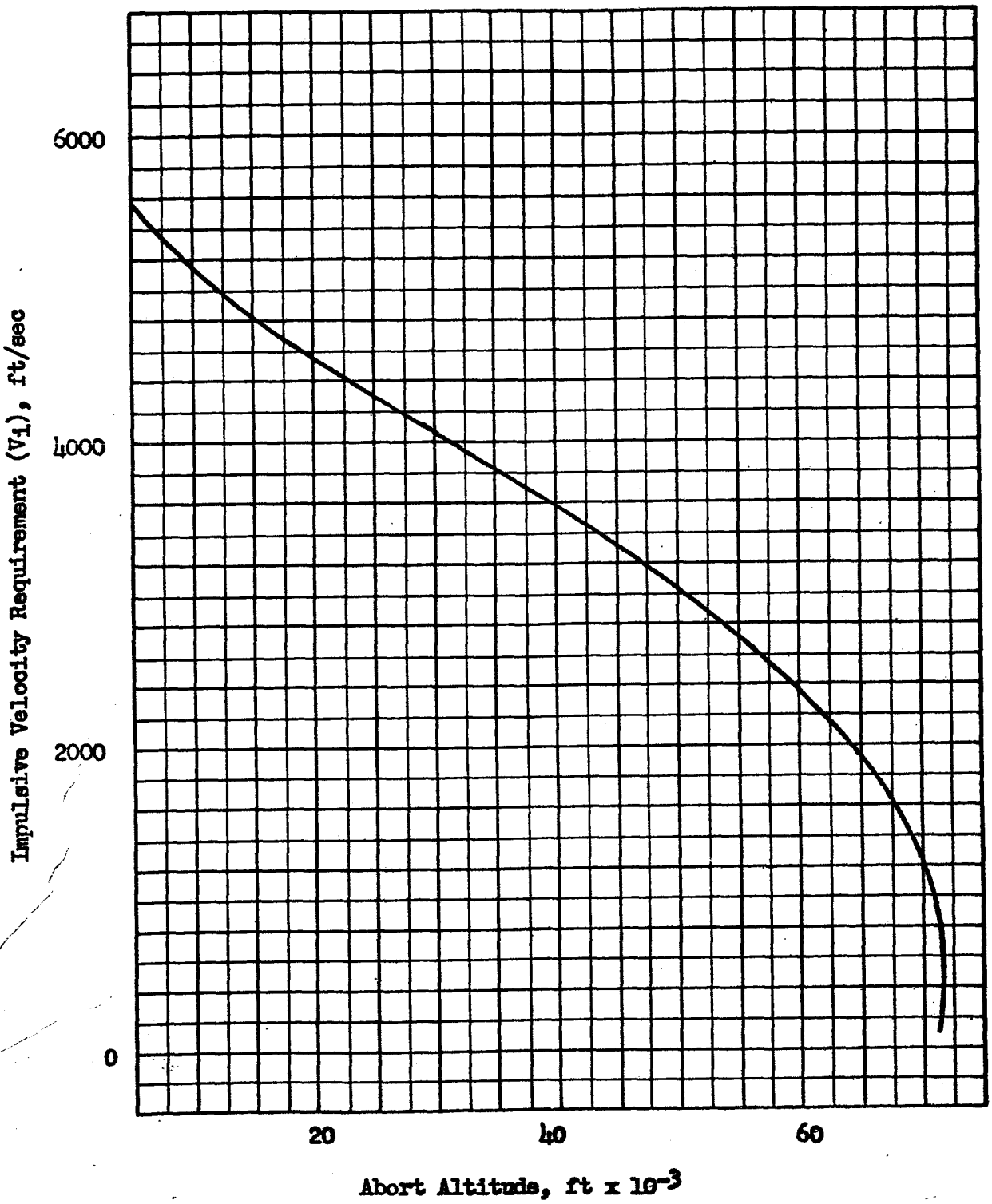

Figure 80. Impulsive Velocity Requirements for Abort from Lunar Landing Versus Altitude at Initiation of Abort.

A typical landing-abort trajectory is sketched below and indicates that the altitude where abort is initiated, h_o, is not the minimum altitude, h_{min}, to which the vehicle descends during the maneuver. The altitude loss $(h_o - h_{min})$ can be minimized by pointing the thrust vector straight up. However, this is not an efficient maneuver as it results in high velocity requirements.

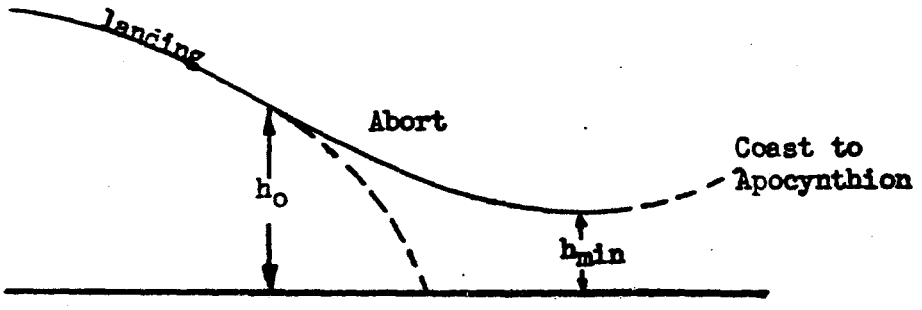

The impulsive velocity requirement curve of Figure 80 is reproduced in Figure 81 . The dashed lines in this figure connect the abort altitude, h_o, on the impulsive curve with the minimum loss value of h_{min}, obtained by using a vertical thrust orientation vector. The upper terminus of each dashed line may be referred to, somewhat paradoxically, as $(h_{min})_{max}$. The locus of these points is plotted in Figure 81 . The significant increase in abort velocity requirement above the impulsive value is also indicated by this curve. These velocity losses may be reduced by orienting the velocity vector in a more horizontal direction. The disadvantage of this thrust orientation is that a more horizontal thrust vector results in lower values of h_{min}. This effect is shown for three specific abort points in Figure 81.

A summary of Figure 81 may be made by considering the points A, B, C on the figure. Point A indicates that the abort was initiated at an altitude of 25,000 feet. If impulsive thrust were available, this would be the minimum altitude, and the velocity requirement would be 4065 ft/sec. Using the actual F/W which was in existence at the instant of abort (0.60) the maneuver can be performed without descending below 20,600 feet by vertical orientation of the thrust vector as shown by point B. The ideal velocity

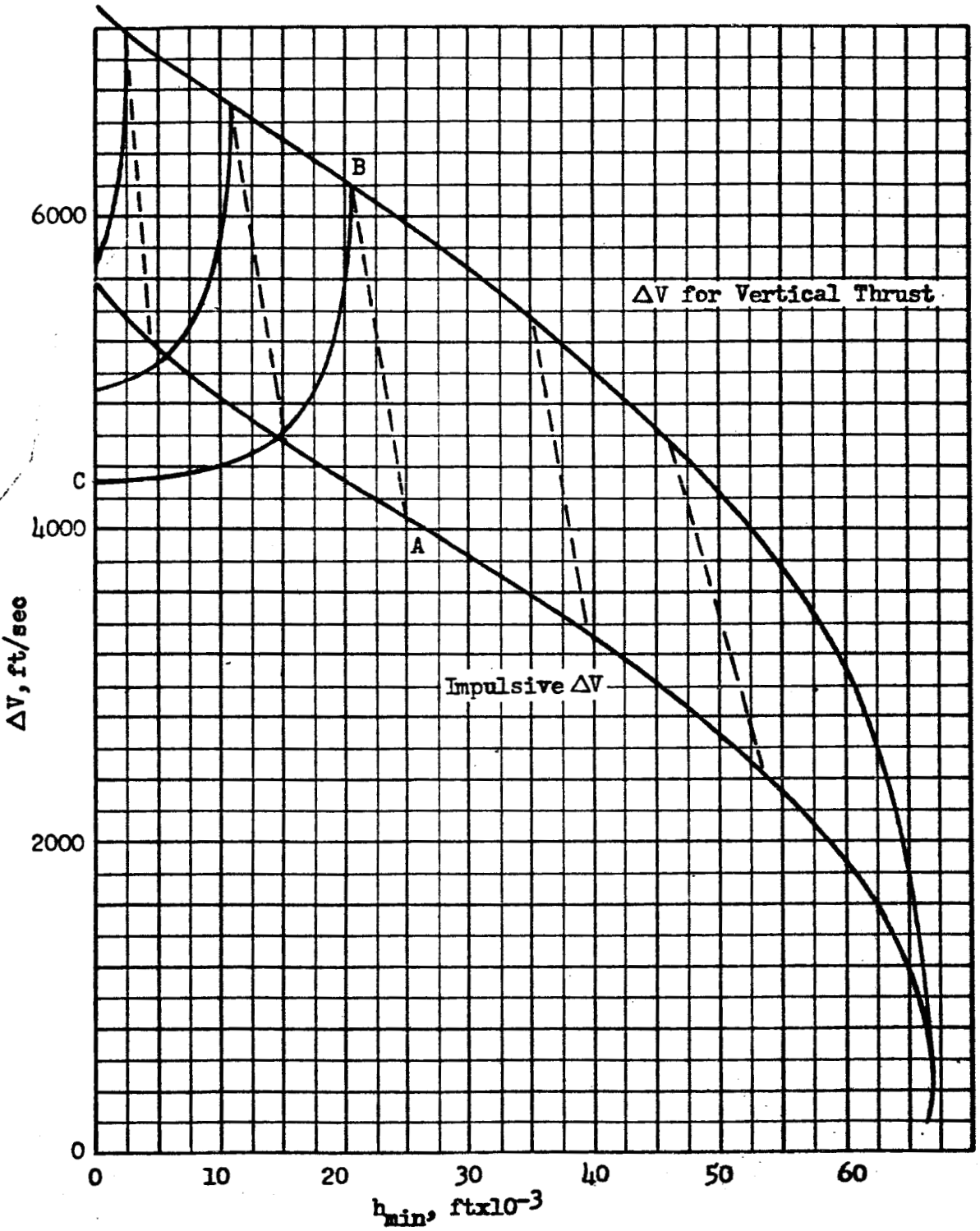

Figure 81. Velocity Requirements for Abort from Lunar Landing vs Minimum Abort Trajectory Altitude

required by this maneuver was 6200 ft/sec. By orienting the thrust vector such that the abort trajectory was tangent to the surface (point C; i.e., $h_{min} = 0$) the velocity requirements could be reduced to 4310 ft/sec.

Two-Stage Vehicle. The two-stage vehicle selected for analysis nominally employs the first stage for the landing-from-orbit and hover-translation maneuvers and the second stage for takeoff-to-orbit. Several alternative modes of vehicle modification exist for providing the ability to perform an abort operation. These are:

1) Modify landing-stage capabilities to assure that it is sufficient by itself to accomplish abort

2) Modify both stages to guarantee that between them, they can meet any abort requirements

3) Modify takeoff stage to provide it with adequate abort capability for any point along the landing trajectory

The first and third alternatives were selected for detailed investigation in the present study.

Implementation of an abort operation can be achieved by various abort maneuvers utilizing different thrust programs and trajectories. For example, the vehicle can either return immediately to the original parking orbit, re-establish another parking orbit near the abort altitude, or keep descending to a point near the lunar surface where a low altitude grazing encounter may take place before ascending to a predetermined orbit. The term, "graze", refers to trajectories such as those illustrated in Figure which pass close to the lunar surface during the abort maneuver. For this abort trajectory, the sum of the gravity and thrust vector misalignment losses are near minimum.

Landing Stage for Abort. The initial study was directed at evaluating the feasibility of utilizing the landing-stage propulsion system for performance of the abort maneuver. The two extreme conditions are immediately apparent. First, if the abort is initiated very early in the descent phase, the landing stage has consumed only a small amount of propellant, and vehicle velocity is still quite high; it is therefore evident that the remaining propellant for the landing maneuver is more than adequate to perform the abort maneuver without recourse to any supplementary propulsive capability.

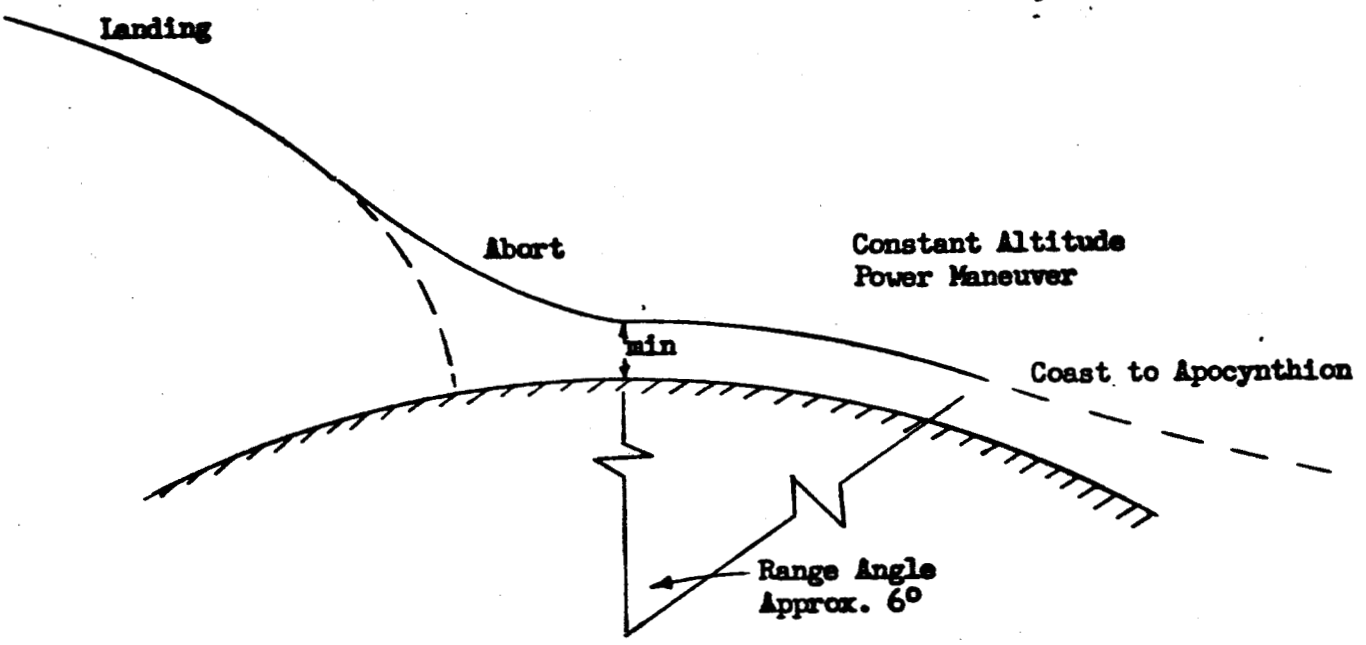

(b) Grazing-Circularization
Abort Trajectory

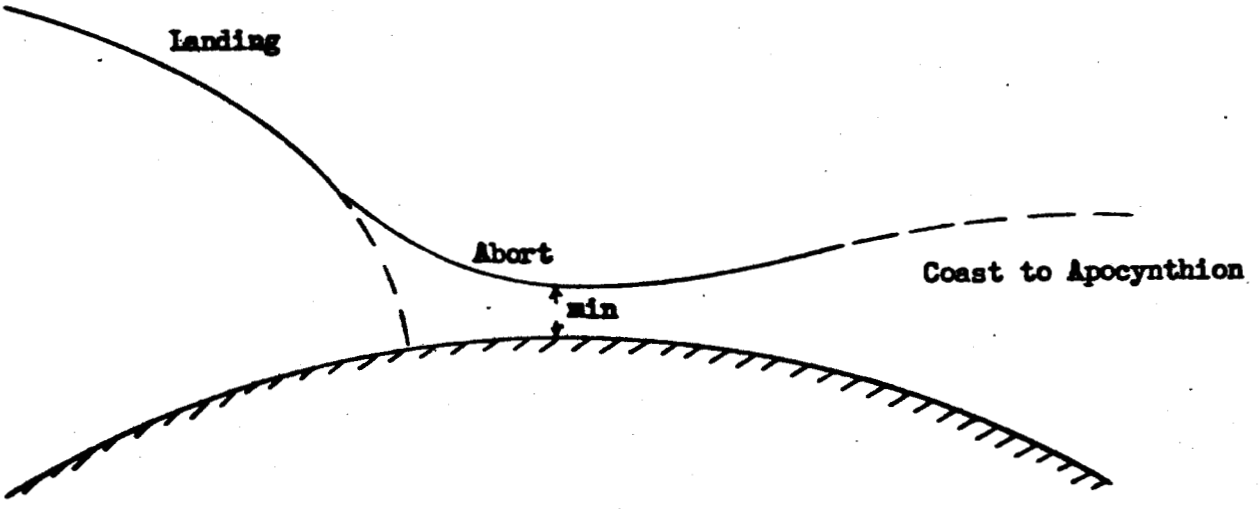

(a) Grazing Abort Trajectory

Figure 82. Typical Lunar Landing - Abort Trajectories

At the other extreme, near the termination of the landing maneuver, the landing stage has exhausted its propellant supply and reduced vehicle velocity to nearly zero, and abort executed by the landing stage at this point would require a supplementary velocity capability approximately equal to the capability of the takeoff stage; this redundancy is equivalent to the "brute force" approach mentioned earlier. Between these extremes, there exists a region in which the landing stage can perform the abort maneuver without, or with modest, supplementary propulsive capability.

Three trajectory types were examined for abort performed by the landing stage. The first case assumed the thrust vector of the vehicle was rotated instantaneously to 90 degrees with respect to the local horizontal (straight up) and remained in that position until the achievement of sufficient velocity for the coast phase to 50 n mi. This type of maneuver establishes the 50-n mi orbit with a minimum loss in elevation and in the quickest time; however, the velocity requirements are high. A decrease in abort velocity requirements occurs with the use of the grazing trajectory shown in Figure 82 . In this trajectory (second case) the vehicle thrust vector was rotated to a particular constant angle, smaller than 90 degrees, which allowed the vehicle to graze the lunar surface prior to coasting to the 50-n mi altitude. The trajectory (third case) shown in Figure 82 offers the lowest abort velocity requirements. In the abort trajectory shown by Figure 82 , the thrust vector was instantaneously rotated to a prescribed position and allowed to remain in that position until the vehicle reached the lowest point of a grazing trajectory, considered to be ten percent of the initial abort altitude. When the abort vehicle reached this minimum altitude, the thrust vector was reoriented to a position which assured constant, low altitude flight above the lunar surface until sufficient velocity was acquired for coast to the 50-n mi apocynthion height.

The reduction in remaining velocity capability (assuming no hovering allowance) for a landing stage traversing its landing trajectory and the corresponding increase in abort velocity requirements (for abort trajectory type 3) is presented in Figure 83. It is evident that the stage capability is adequate for abort maneuvers initiated above 46,000 feet; thereafter, supplementary capability equal to the difference between the two curves is required if the landing stage is to perform the abort maneuver.

For these three types of abort trajectories considered, the ideal velocity requirements needed to establish a 50-n mi orbit as a function of initial abort altitude are shown in Figure 84 . Initial thrust-to-weight ratios for each abort maneuver corresponded to the descent thrust-to-weight ratios

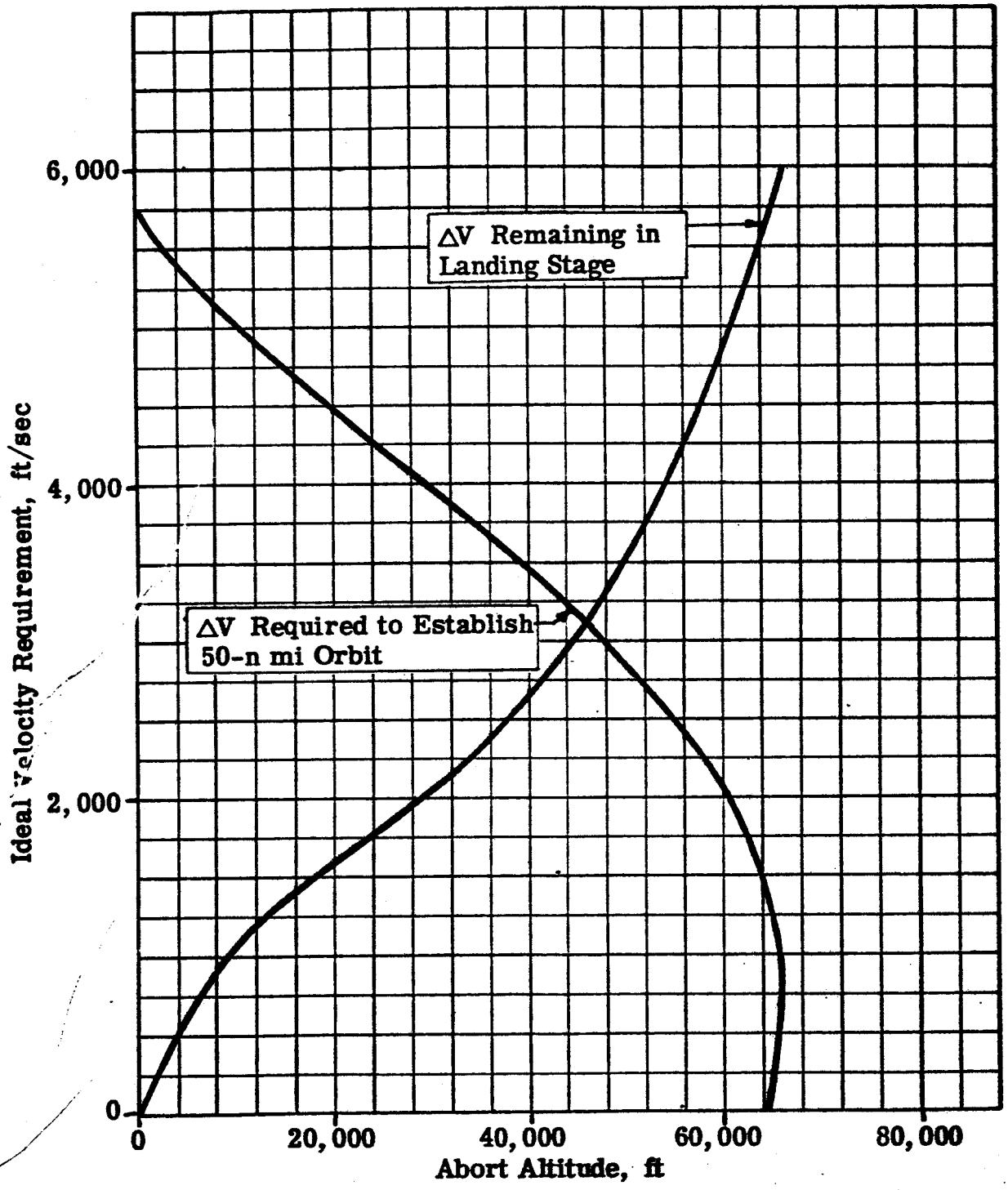

Fig. 83 . Nominal Landing and Minimum Abort Velocity Requirements vs Abort Altitude

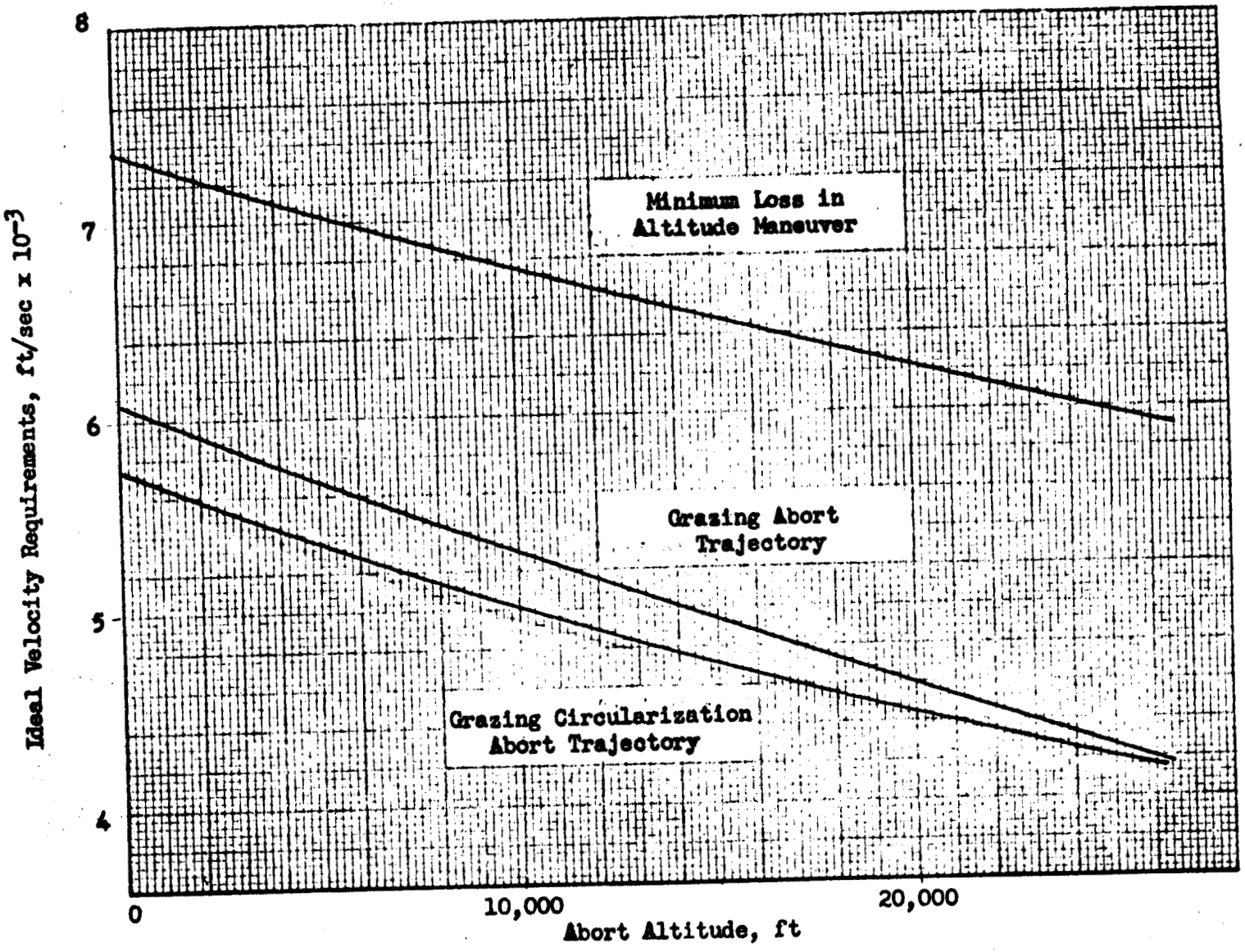

Figure 84. Abort Velocity Requirements Needed to Establish 50 n mi Circumlunar Orbit vs Abort Distance Above Lunar Surface, (Performed by Landing Stage).

of the vehicle at the abort point. This, of course, is equal the thrust-to-weight ratio of the landing stage at the abort point.

The differences in abort trajectories between the lunar graze trajectory which maintains a constant thrust-vector angle and the lunar-graze trajectory which utilizes a variable thrust-vector angle are illustrated in Figure 85. Changes in altitude and range, or distance covered above the lunar surface, before the coast phase to 50-n mi are shown for a vehicle which aborts at an altitude of 4200 feet above the lunar surface. The range distance of 83.2 n mi covered by the vehicle while building up sufficient velocity to coast to 50-n mi corresponds to a lunar arc angle or approximately 5 degrees.

Takeoff Stage for Abort. Use of the takeoff stage for abort is strongly suggested by the fact that the landing stage might not be available (i.e., the need for abort might have been precipitated by a landing propulsion system malfunction) and the takeoff stage has its entire propulsive capability available throughout the landing maneuver. The lunar takeoff stage may perform an abort maneuver at any point of the descent trajectory provided the thrust-to-weight ratio and velocity requirements for the takeoff stage are satisfied for each abort point. It is not immediately apparent how the takeoff propulsive capability could be anything but adequate for the abort maneuver; however, near the lunar surface, it is possible to formulate a situation in which the takeoff stage F/W is inadequate to propel the vehicle upward before inertia of the vehicle carries it to impact at the surface. Shown in Figure 86 are the ideal velocity increments, expressed as a function of abort altitude and initial takeoff stage (abort stage) thrust-to-weight ratio, required by the takeoff stage to establish a 50-n mi circumlunar orbit. The results of the plot were based upon a grazing circularization abort trajectory. Assumed in the abort maneuver was instantaneous jettisoning of the landing stage and instantaneous orientation of the thrust vector to the prescribed abort position. The dotted lines in Figure 86 indicate the initial constant orientation of the abort stage (takeoff stage) or thrust-vector angle with respect to the local horizontal during the lunar descent portion of the abort trajectory. Thus, if it were necessary to perform an abort maneuver at an altitude of 20,000 feet with a takeoff stage having an initial thrust-to-weight ratio of 0.5, the thrust vector angle would initially be rotated to 30 degrees. This angle will cause the vehicle to graze the lunar surface.

The minimum thrust-to-weight ratio for abort as a function of abort altitude based upon the previously defined grazing-circularization abort trajectory is illustrated in Figure 87. The plot is based upon zero-hover altitude, and a comparison between the normal increase in vehicle descent thrust-to-weight and the minimum allowable thrust-to-weight ratio for abort is illustrated. This minimum thrust-to-weight ratio which is allowable

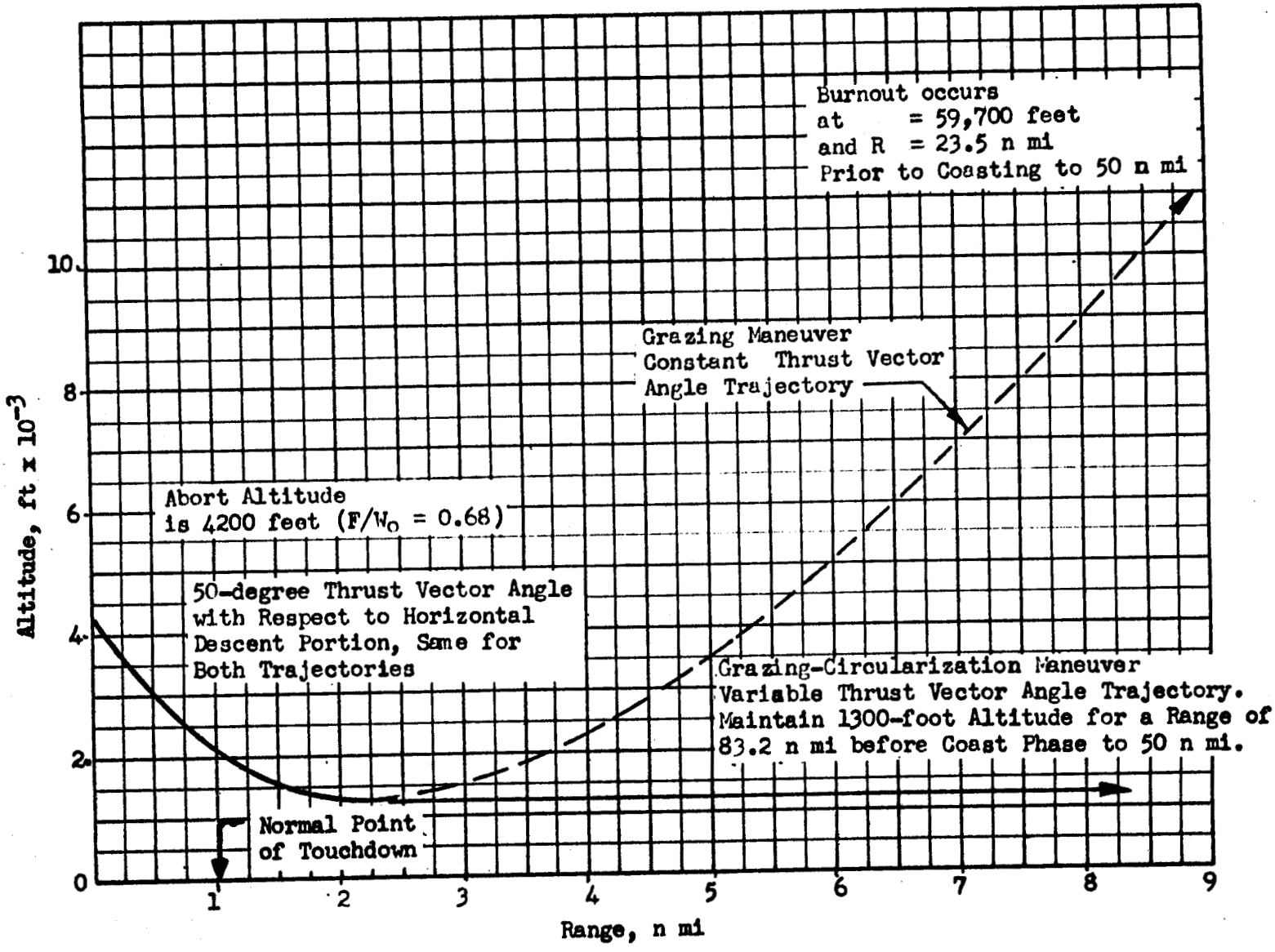

Figure 85. Typical Abort Trajectories to Re-establish 50-n mi Lunar Orbit

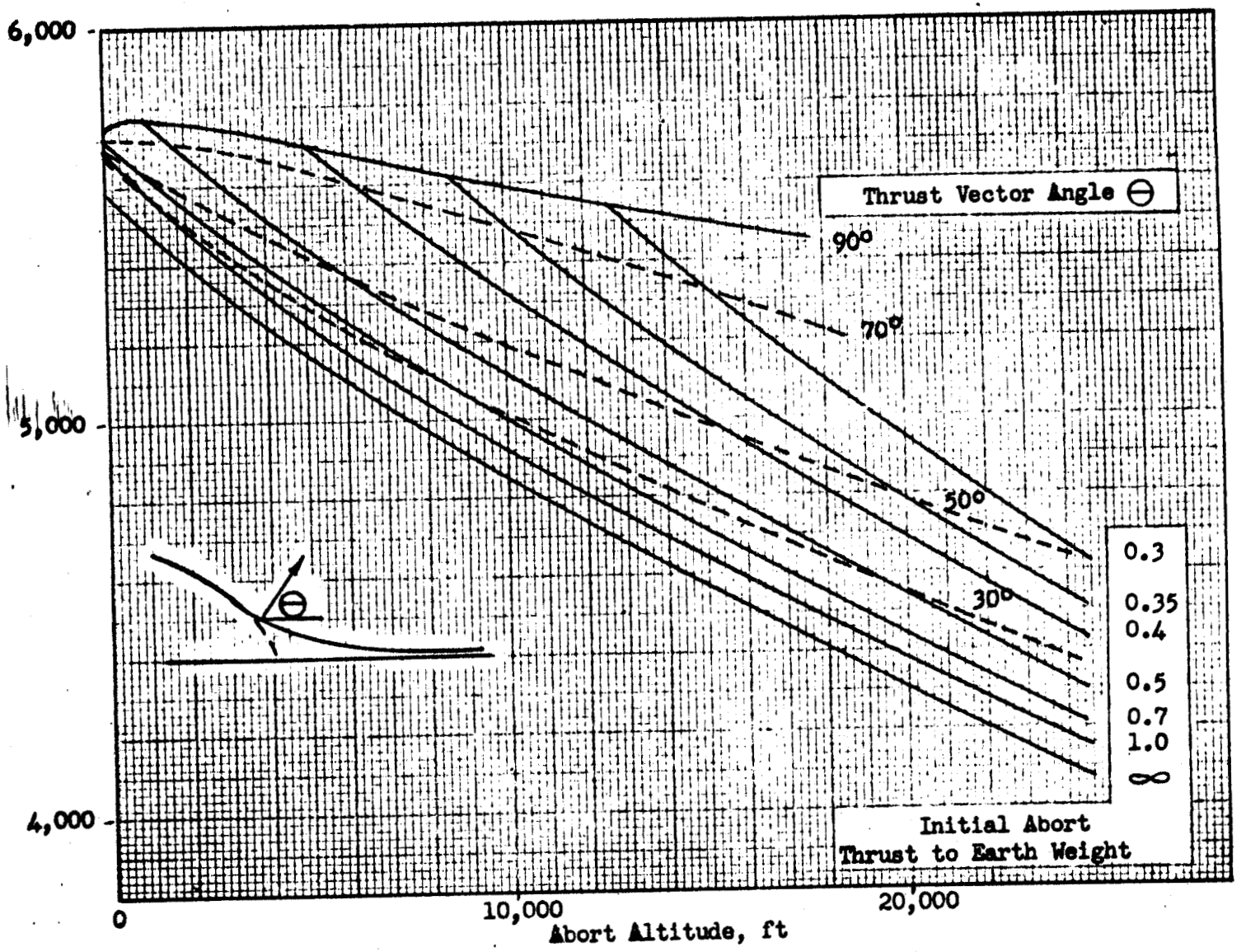

Figure 86. Ideal Grazing-Circularization Velocity Requirements Needed to Establish a 50 n mi Circumlunar Orbit as a Function of Abort Altitude and Initial Abort Stage Thrust to Weight. (For Zero Hover Altitude).

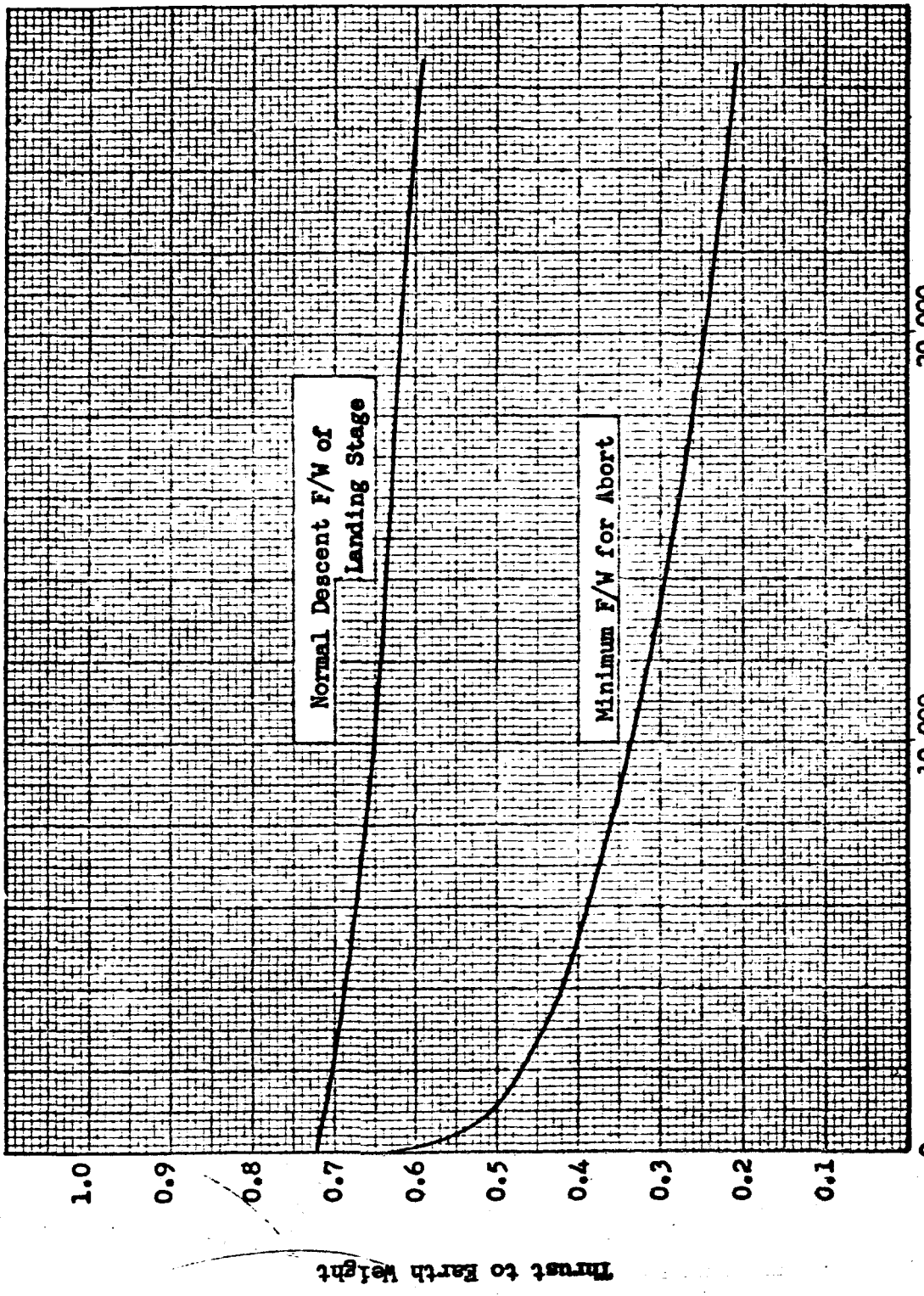

Figure 87. Thrust to Weight Requirements vs Abort Altitude
(No Hover Altitude)

corresponds to the thrust vector angle pointing vertically upward during the early descent portion of the grazing-circularization maneuver. Analysis of the data presented in Figure 87 indicates that the abort stage or lunar-takeoff stage should be designed for an initial thrust-to-weight ratio equal to or greater than the vertical component of the thrust-to-weight ratio of the normal landing stage at the completion of descent. For the descent trajectory utilized in this study, the vehicle orients itself to the vertical position while hovering; the maximum vertical component of thrust-to-Earth-weight ratio is 0.63, which is therefore the required initial thrust-to-weight ratio of the takeoff stage.

The abort thrust-to-weight requirements if no allowances are made for a hover altitude are indicated in Figure 87 . The effects of a hover altitude on abort thrust-to-weight ratio requirements can be seen in Figure 88 . With no hover altitude, the thrust-to-weight ratio requirement for abort increases with decreasing altitude. Thus, for abort capabilities at all altitudes, the minimum design F/W is defined by zero altitude conditions. When a hover altitude is introduced, the minimum allowable thrust-to-weight ratio is shifted to a higher abort altitude. Thus, for the typical descent trajectory shown by Figure 79 , if no allowances were made for a hover altitude, the minimum abort F/W requirement would be 0.63 and would occur at the point of touchdown. Adding a 400-foot hover altitude lowers the minimum abort F/W requirement to 0.43; this value of F/W is required if abort were executed at an altitude of 1800 feet.

The ideal velocity requirements for a nominal lunar takeoff mission are shown in Figure 89 as a function of the initial thrust-to-weight ratio of the vehicle. Orbital velocity for the nominaltakeoff mission was achieved during low constant altitude flight above the lunar surface. An additional velocity increment must be added to the minimum takeoff stage requirements (Figure 89) if abort should be considered at the lower altitudes. If no hover altitude were considered for a lunar takeoff stage which performs an abort maneuver below 2350 feet, the nominal takeoff stage ($F/W_0 = 0.63$) should be designed for an additional ΔV of 50 feet per second as shown in Figure 90 . At any abort altitude above 3100 feet, the normal takeoff capabilities would provide sufficient velocity for abort.

The addition of any hover altitude reduces the thrust-to-weight ratio requirements for the abort stage; however, if thrust-to-weight ratio is decreased, abort velocity-requirement penalties are increased at the lower altitudes. The increases or variations in velocity requirements with abort altitudes are shown in Figure 90 for hover altitudes of 100, 400, 700, 1000 and 1500 feet. The variations in ΔV are relative to the nominal lunar takeoff mission shown in Figure 89 .

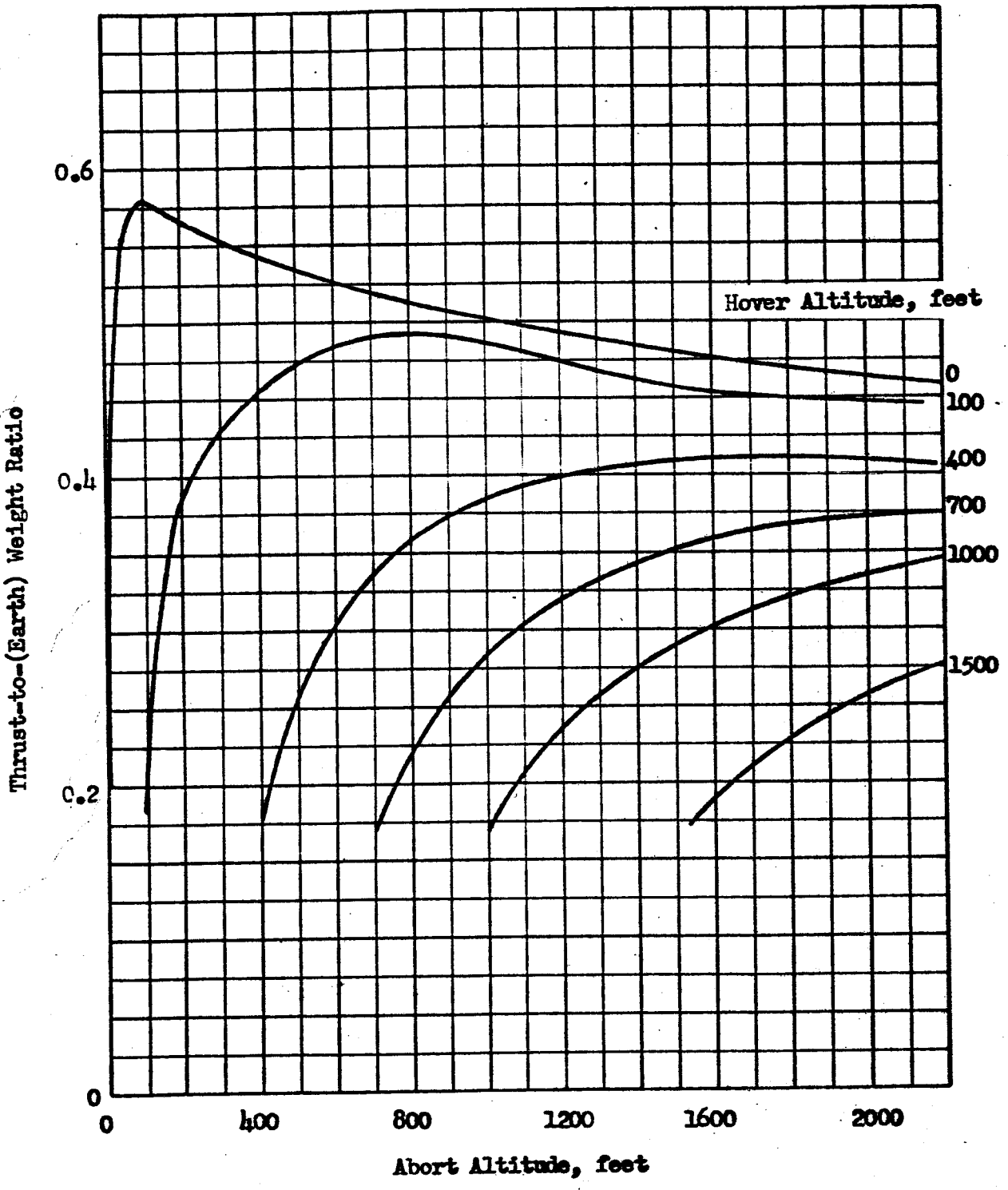

Figure 88. Minimum Abort Thrust-to-Weight Ratio Requirements as a Function of Hover and Abort Altitudes.

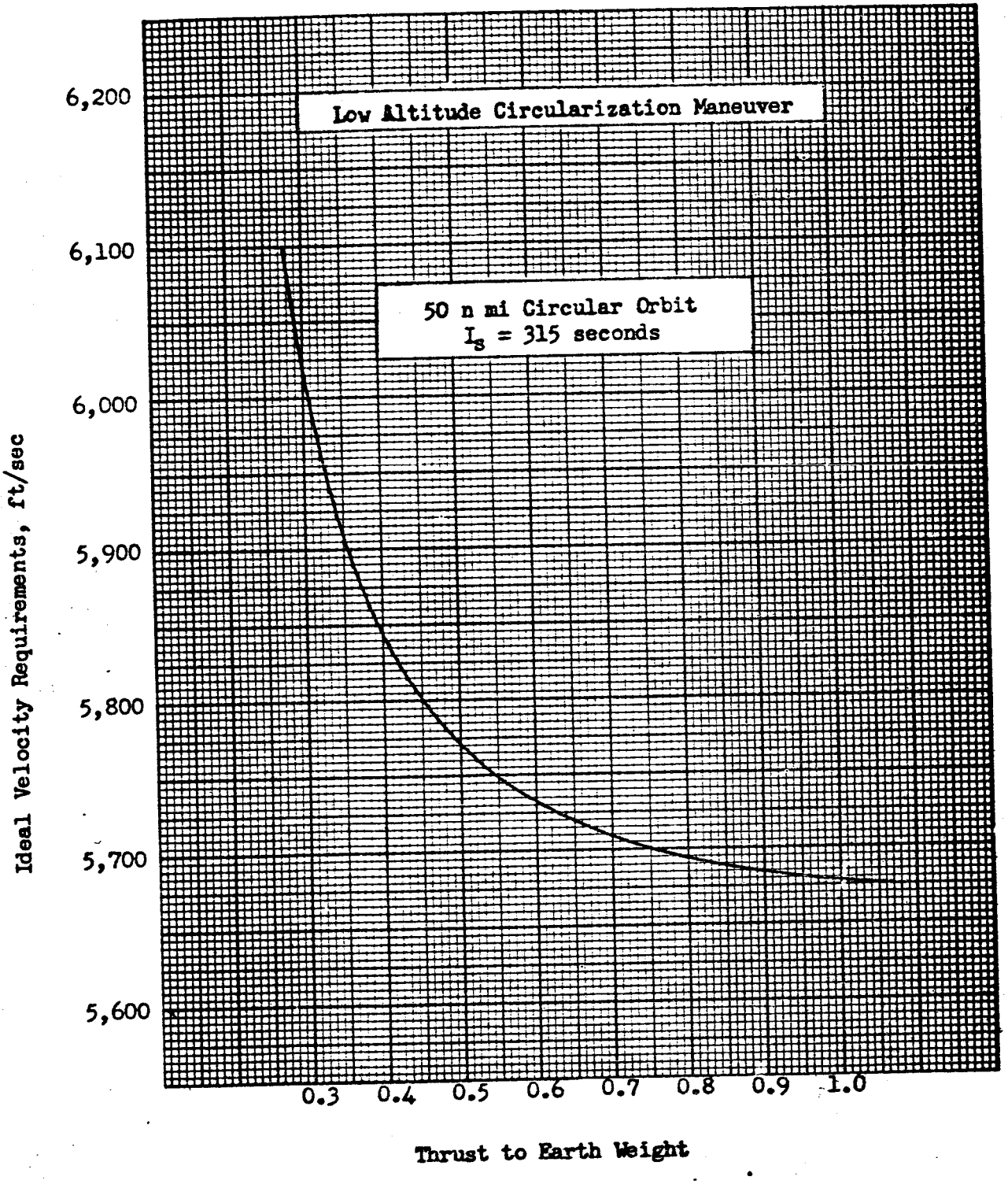

Figure 89. Lunar Takeoff - Ideal Velocity Increment vs. Initial Thrust to Earth Weight Ratio.

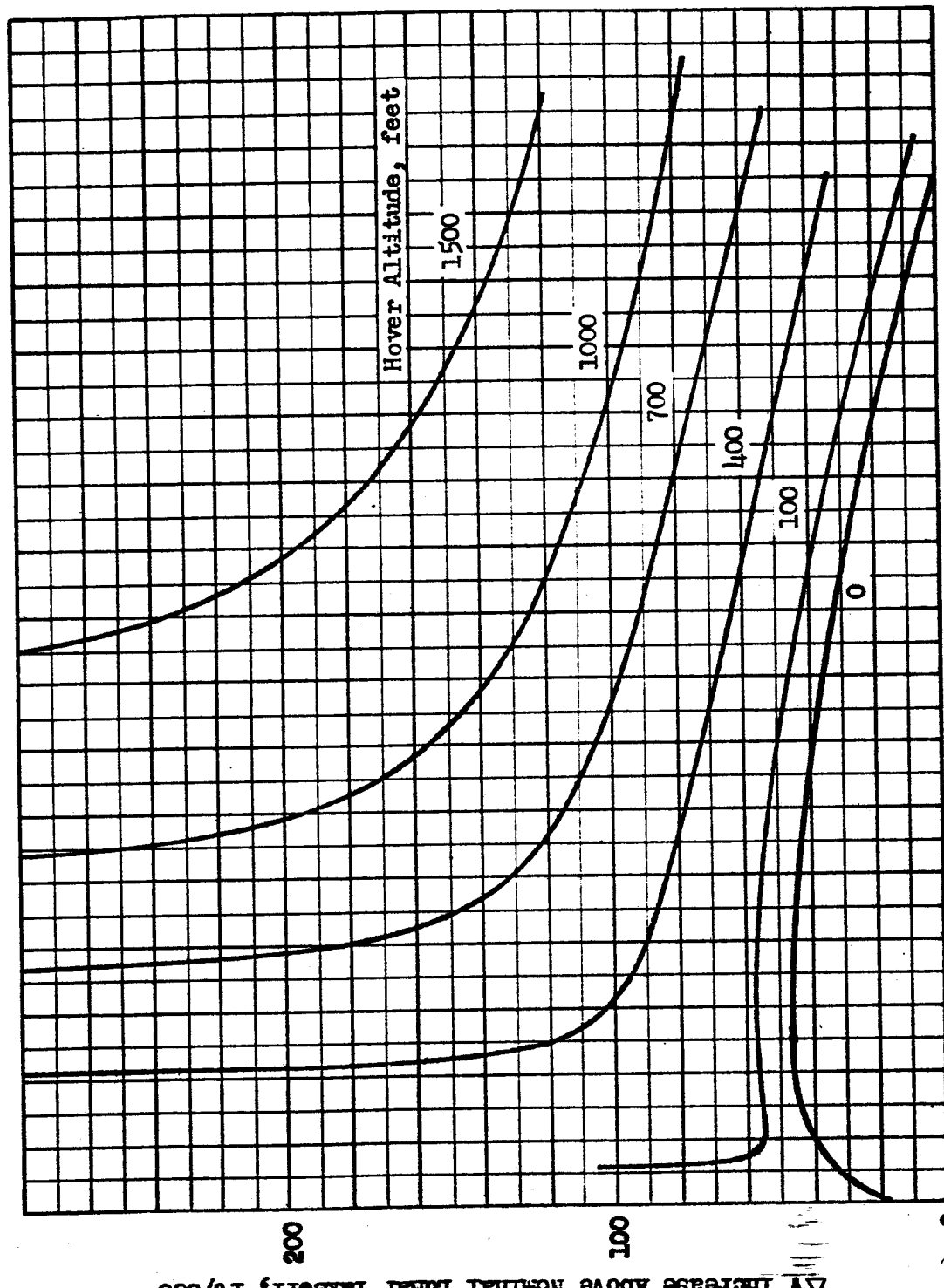

Figure 30. Increase in Abort Velocity Requirements as a Function of Hover and Abort Altitude.

Conclusions. A single-stage landing/takeoff vehicle designed for optimum performance of the landing and takeoff maneuvers is capable of performing an abort maneuver from any point on the landing trajectory.

The landing stage of a two-stage landing/takeoff vehicle cannot perform the abort maneuver below 46,000 feet (for the vehicle and trajectory considered in the analysis) without supplementary propulsive capability above that required for landing. The takeoff stage of a two-stage vehicle is adequate for performing the abort maneuver if its initial thrust-to-weight ratio is at least equal to the vertical component of the final thrust-to-weight ratio of the landing stage; lower thrust-to-weights are permissible if the landing trajectory is biased to achieve zero velocity at a positive distance above the surface.

NEAR-SURFACE TRANSLATION

Maneuver Concepts

For a nonaerodynamic planetary landing mission, it may be desirable, following the major deceleration maneuver, to hover briefly at a point in space while evaluating subsequent action, and then to perform a translation maneuver prior to the actual landing. Landing-site selection, planetary surface survey or need to reach a specific surface location can require a translation maneuver. Several methods for applying rocket propulsion systems to the performance of this maneuver are possible. The two basic propulsion methods are categorized as ballistic or continuous, with the latter capable of providing horizontal translation. Horizontal translation can be performed with a multiengine system or a single engine system. The general characteristics of the methods are described in Figure 91; a coast phase is possible in either the multiengine or single-engine system, although it is shown only for the multiengine system.

As indicated in the landing-from-orbit error analysis presented earlier, the vehicle may be several thousand feet above the lunar surface at the start of the translation maneuver; it would in this case be desirable to descend concurrently while performing the translation maneuver. If, however, the translation maneuver is initiated at a point a short distance above the surface, a constant-altitude maneuver would be required. Both these possibilities exist, and have therefore been considered in the analysis of translation maneuvers.

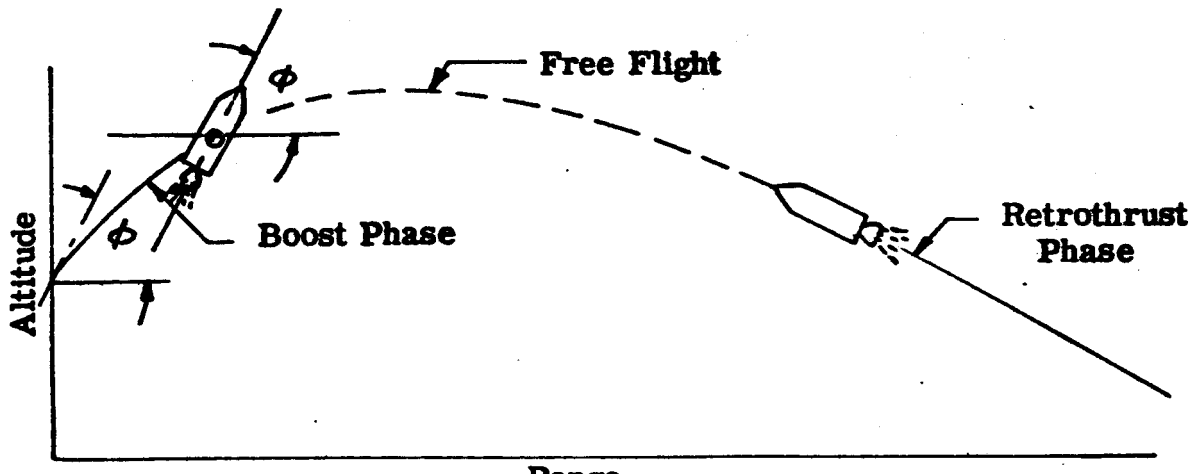

Ballistic Maneuver

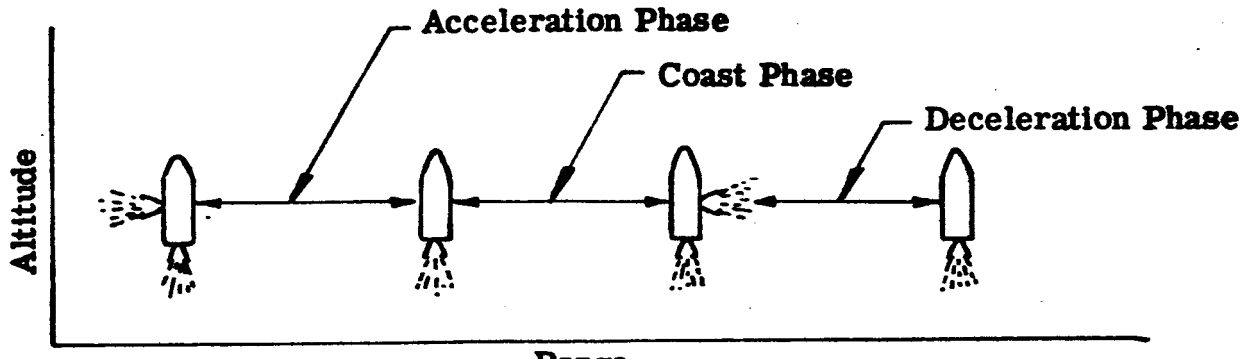

Multiengine System

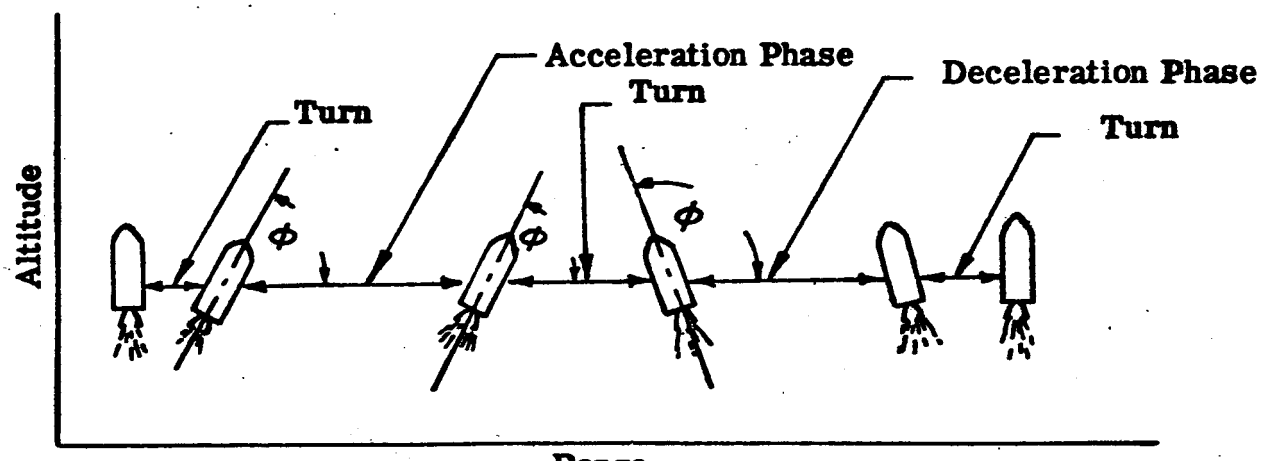

Single Engine System

Fig.91. Methods of Translation

Hovering. Prior to, or perhaps following, a lunar translation maneuver a hovering (constant altitude) maneuver may be required for pilot orientation or other purposes. To achieve constant altitude, an initial thrust-to-lunar weight ratio of 1:1 must be employed, and the engine thrust must be decreased during the hovering as propellant is consumed. The ΔV may be calculated by:

$$\Delta V = g \cdot t$$

where: g = lunar surface gravity, 5.31 ft/sec^2
t = hover time, seconds

The propellant consumed (W_p) is:

$$\frac{W_p}{W_G} = 1 - e^{-\Delta V/32.2(I_s)}$$

The throttling ratio (T'/T) during the hover phase is determined by

$$T'/T = e^{\Delta V/32.2(I_s)}$$

For a variation in hover time, the throttling ratio is indicated in Figure 92 for lunar (near-surface) hovering. This hovering ΔV and throttling required must be included with the main descent phase, translation phase, and final descent phase requirements.

Ballistic Maneuver. The ballistic maneuver is described in detail in Reference 4 and begins after the vehicle has been brought to a hover or near-hover condition. The vehicle is first rotated to the proper firing angle. Thrust is then initiated and maintained while the thrust vector angle is held constant. At the end of the boost phase, thrust is terminated and the vehicle is allowed to coast to the retrorocket firing altitude where the vehicle is aligned along the velocity vector and thrust is applied parallel to velocity to ensure that zero horizontal and vertical velocities are attained simultaneously.

This maneuver has several undesirable features. It requires that the vehicle be turned through a very large angle just prior to retrorocket firing, and it also requires that the engine be restarted; failure to restart could be disastrous. Also, the translation distance cannot be easily altered after the initial firing phase.

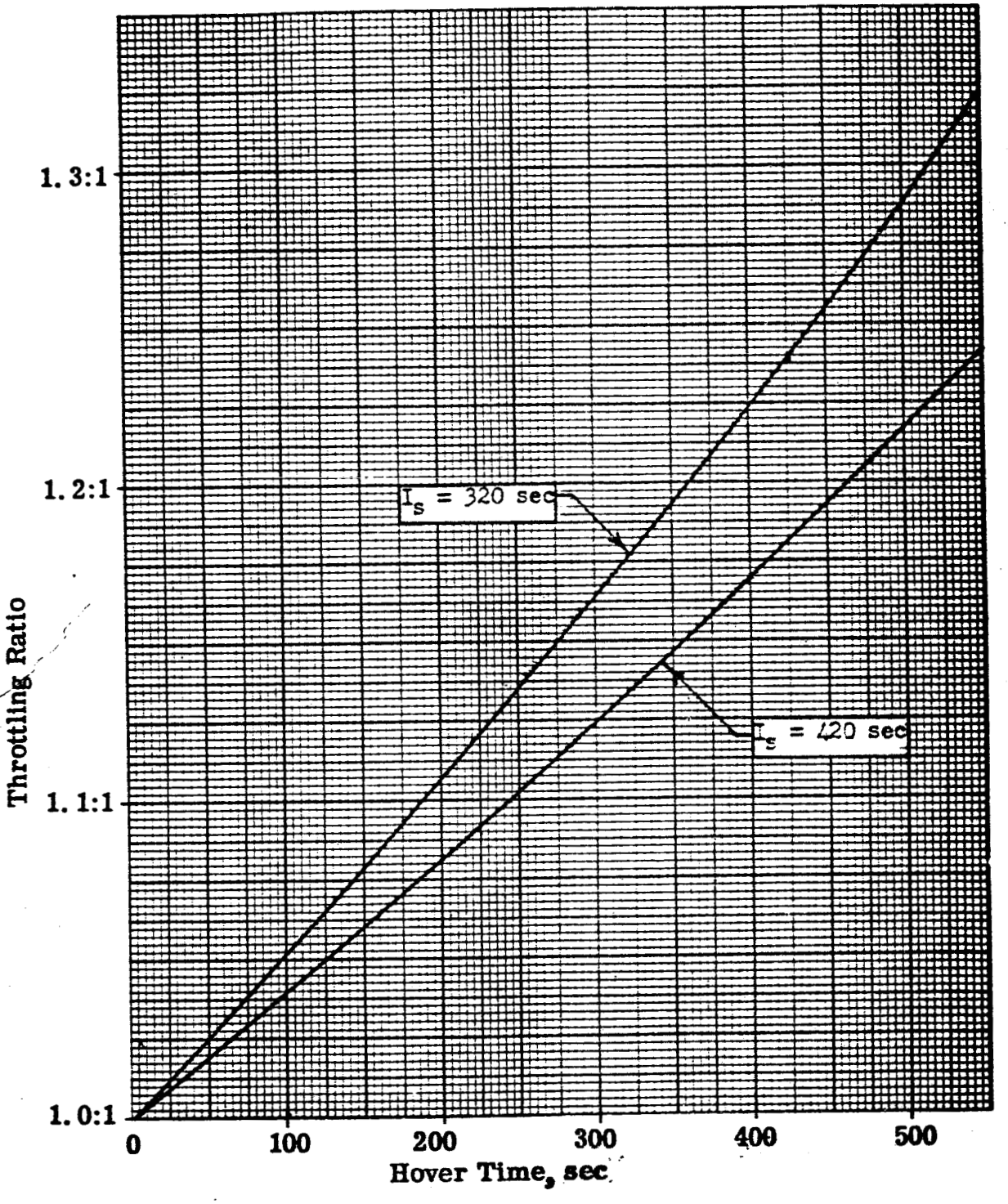

Fig. 92. Throttling Requirements During Hovering

Continuous Propulsion Maneuver. This maneuver can be performed at near-constant altitude with a vehicle that provides separate engines for the vertical and horizontal thrust requirements, or with a vehicle that orients itself to allow a single engine to provide both thrust components.

Multiengine System. With the multiengine system, the maneuver is initiated from a hovering position, and horizontal acceleration is provided by a horizontally mounted engine. After the required horizontal velocity is attained, the engine is shut off, and a coast phase (optional) begins. The vehicle is then decelerated to a hover condition by rotating 180 degrees and using the same horizontal engine; alternatively, a diametrically opposed horizontal engine could be used to apply the decelerating thrust.

Some of the undesirable characteristics of the multiengine system are the requirements that the horizontal engine be restarted and/or the vehicle rotated through 180 degrees for the deceleration phase. Also, a weight penalty due to the auxiliary engine system is incurred. In Reference 4, it is shown that a single engine system is more efficient since one engine provides both the horizontal and vertical thrust components that are required, providing a saving in propellant necessary to perform the maneuver.

Single-Engine System. For the single-engine system, the horizontal acceleration is provided by tilting the vehicle downrange. The process is reversed approximately midway through the maneuver to stop the horizontal translation at the desired distance. In the tilted position, the vertical thrust component can, by proper selection of thrust level and vehicle orientation, be adjusted to be equal to, greater or less than the system weight.

If the thrust is constant and is equal to or less than the vehicle weight, then in the rotated position, the vertical thrust component is less than the weight, and the vehicle descends during the translation maneuver; conversely, if the thrust is sufficiently great so that after tilting the vertical component is greater than the weight, the vehicle rises during the translation. By selecting a suitable initial thrust for a desired translation maneuver, the change in vehicle weight as propellant is consumed causes the vehicle to descend during the acceleration phase and then rise during the deceleration phase, resulting in a near-constant altitude for the overall maneuver. A continuously constant altitude maneuver can be obtained, if required, by the use of engine thrust control to increase the thrust after

tilting to maintain a vertical thrust-to-weight ratio of 1.0. A variable-thrust, single-engine maneuver is evaluated in Reference 4, and is discussed later in a comparison of various translation maneuver techniques.

A power-on coast phase, with vertically-directed thrust used to maintain (or alter in a desired manner) the altitude, may be introduced between the downrange acceleration and deceleration phases. This coast phase requires that the vehicle first be rotated and accelerated downrange, then turned to a vertical position for the coast. Following the coast phase, the orientation procedure is reversed to decelerate the vehicle.

Constant Thrust Analysis

Analysis was conducted to investigate the use of constant thrust during the entire lunar translation maneuver. This analysis was performed to evaluate the feasibility of the method and thereby to indicate whether adjustments of thrust level are necessary during translation. The study includes investigation of the effects of engine gimbal capability, vehicle orientation and the presence of an intermediate coast phase on characteristics of the translation maneuver.

Maneuver Method. In the translation analysis conducted, the thrust is constant during the entire translation maneuver. The maneuver profile is illustrated in Figure 93. The vehicle is initially in a vertical hover or near-hover position with no horizontal velocity. It is then rotated to the required orientation angle (measured from the local horizontal) by gimbaling the main engine. When the vehicle has rotated through half of the desired angle, the engine is gimbaled in the opposite direction to apply a decelerating moment to stop the rotation at the desired orientation angle. The thrust vector is then directed through the vehicle center of gravity. In the tilted position, the horizontal thrust component provides the horizontal acceleration. The vehicle then accelerates in the horizontal direction for a specified time. The rotation procedure is then reversed by engine gimbaling to attain the desired orientation angle for horizontal deceleration. The vehicle decelerates until the horizontal velocity is such that if the vehicle begins to rotate back to a vertical position at this point, it will have a zero horizontal velocity when it reaches the vertical position. The final descent to the planetary surface can then be made.

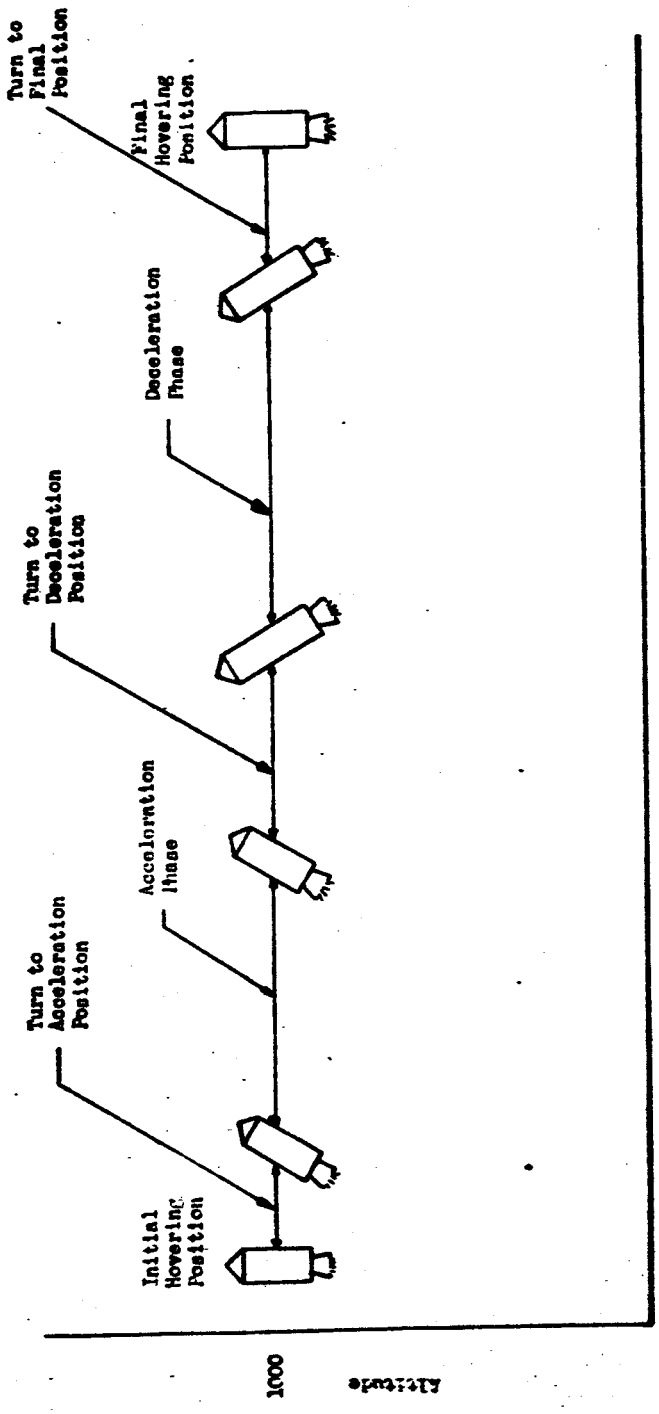

Figure 93 - Schematic Representation of Single Engine Translation Maneuver at Constant Altitude

Engine Gimbaling. The analysis of the single-engine, constant thrust translation technique includes a finite interval for vehicle orientation, but it assumes that engine gimbaling is instantaneous. For a typical translation maneuver, the vehicle turning requires approximately 3 to 4 seconds, while the engine gimbaling time is 0.2 to 0.3 seconds. If transient motion of the engine were considered, torque on the vehicle, and therefore vehicle angular acceleration, would reach the nominal value during the finite time required to gimbal the engine rather than instantaneously, as assumed; the analysis model vehicle therefore receives slightly more angular impulse than it would in reality, and it performs the turn maneuver slightly faster than it actually could. This effect was examined by using a slightly smaller vehicle angular acceleration during the turning maneuvers. Results indicated that a small change in angular acceleration has a very small effect on the overall trajectory and translation times, which justifies the assumption of instantaneous gimbal motion in subsequent analysis.

The significance of the magnitude of engine-gimbal angle on the overall translation trajectory was evaluated. For relatively small angles, representative of the normal range of rocket engine gimbal capabilities, gimbal angle is directly proportional to vehicle angular acceleration, and therefore governs the dynamics of the turn portions of translation maneuvers.

Comparison of Figure 94 and 95 show that for an increase in gimbal angle, the same horizontal distance is covered in a slightly shorter time for the higher gimbal angle, based on the same vehicle orientation angle. Also for the higher gimbal angle, the loss in altitude during the translation maneuver is slightly greater since the rotation intervals, during which the vertical component of thrust is greatest, are shorter.

Vehicle Orientation Angle. At a given thrust level, the horizontal thrust component is greater for smaller vehicle orientation angles; as a result greater horizontal velocities and distances are attained in the same maneuver duration. The data presented in Figure 96 can be compared with Figure 94 to show the effect of vehicle orientation angle. The data are for an initial vehicle thrust-to-weight ratio of 1.0. With the smaller vehicle orientation angle, there is less vertical thrust component, and the vehicle loses more altitude during the translation maneuver. If descent is not desired when smaller vehicle orientation angles are used, the thrust-to-weight ratio could be increased such that the vertical component of thrust-to-weight ratio is slightly less than 1.0. This will result in near-constant altitude during the translation maneuver.

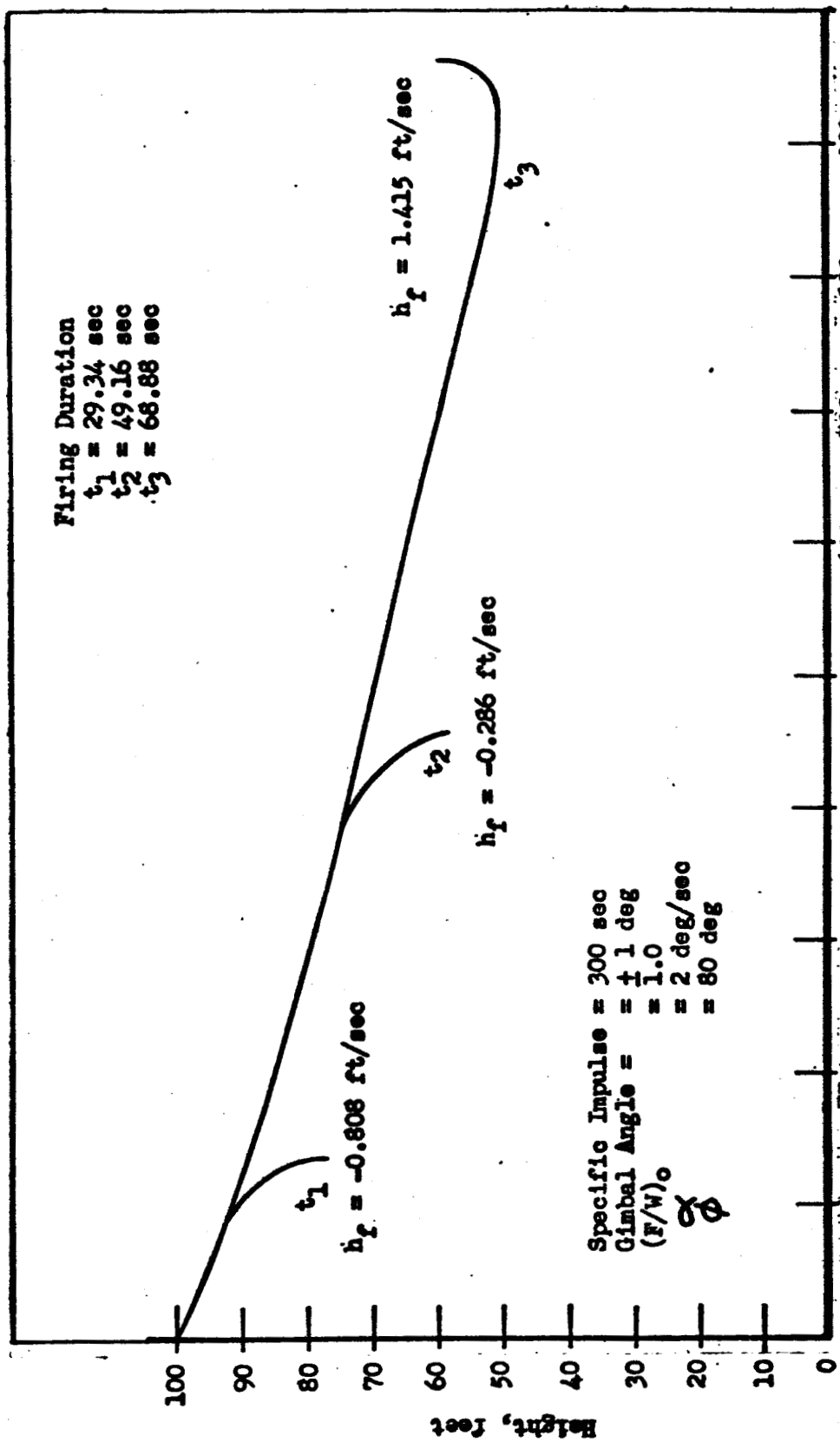

Figure 94 . Height vs Horisontal Distance for Lunar Landing Translation Trajectories

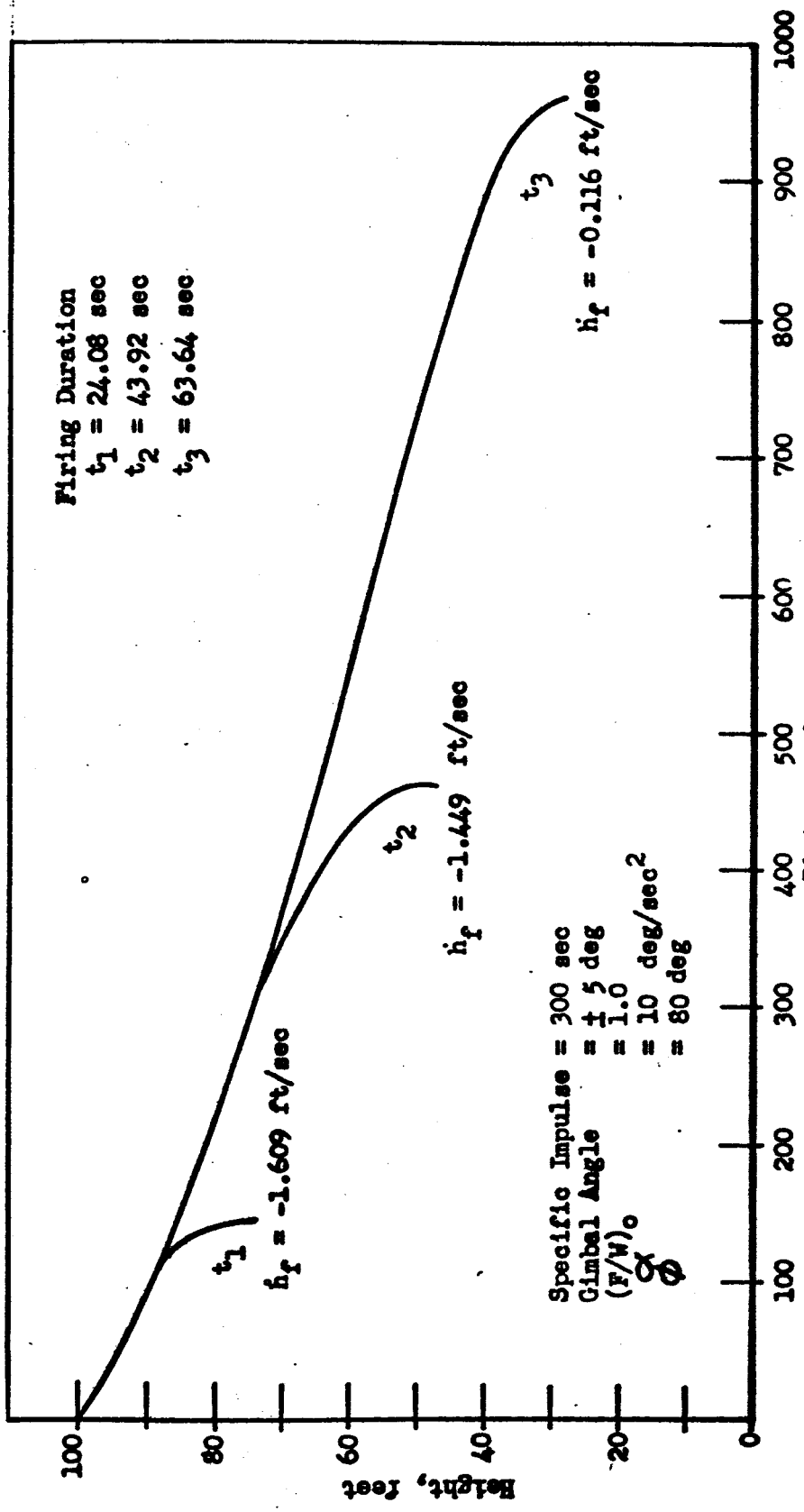

Figure 95. Height vs Horizontal Distance for Lunar Landing Translation Trajectories

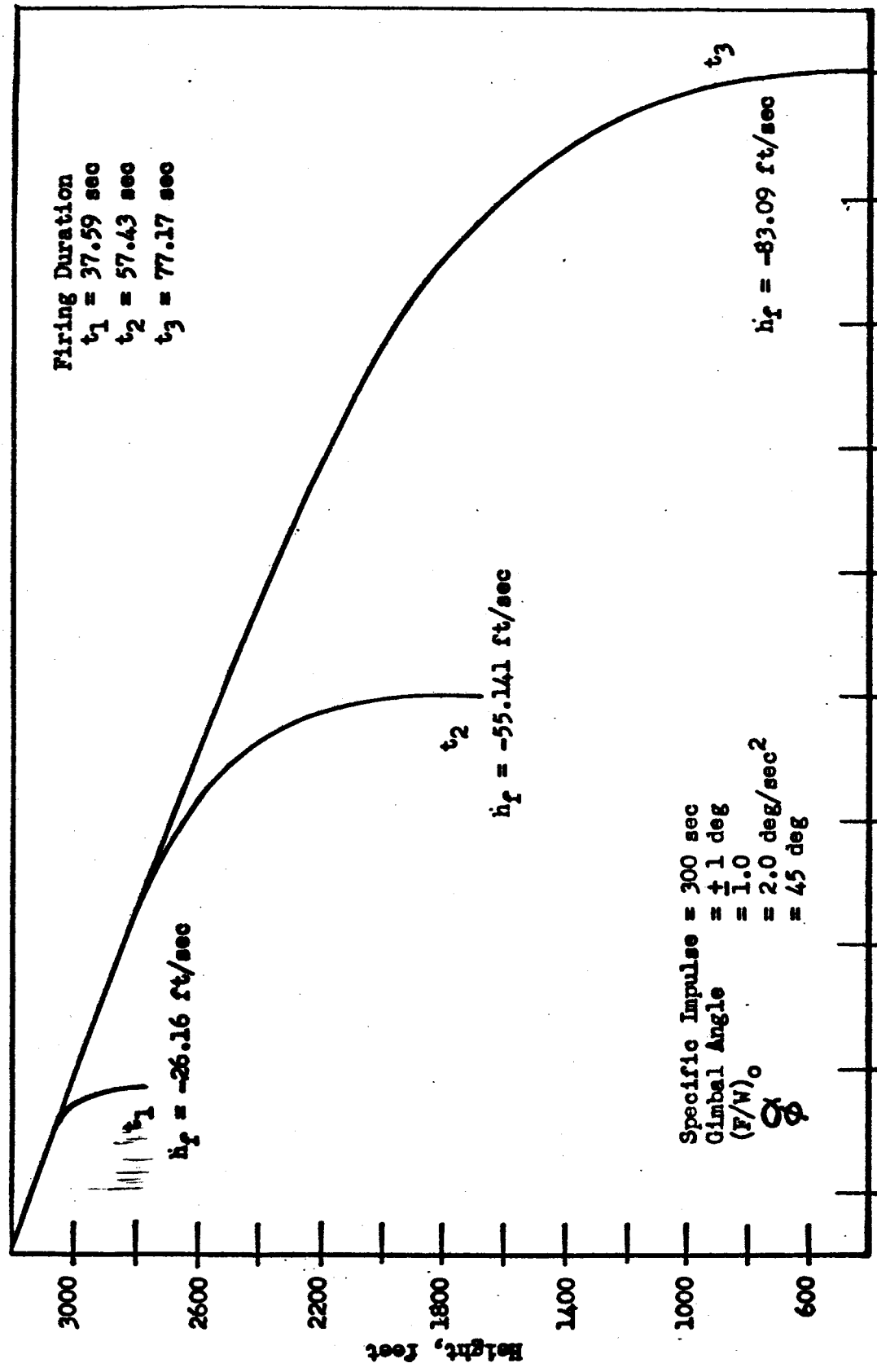

Figure 96 . Height vs Horizontal Distance for Lunar Landing Translation Trajectories

Constant Altitude Translation. An analysis of the feasibility of maintaining a near-constant altitude during the translation maneuver was made. A vehicle orientation angle of 60 degrees, a gimbal angle of ±5degrees and vehicle angular acceleration of 10 deg/sec^2 were used. Representative results are presented in Figure 97 . An initial thrust-to-weight ratio greater than 1.0 was employed so that after the vehicle assumed an angle 30 degrees from the vertical, the vertical component of thrust-to-weight ratio was slightly less than 1.0. This allowed the vehicle to rise slightly during the tilting procedure and then descend during the acceleration phase. Then, because vehicle weight decreased as propellant was consumed, a gradual ascent occurred during the deceleration phase.

The analysis results indicate that a near-constant altitude translation maneuver can be accomplished above the surface by applying a constant thrust throughout the maneuver. The restrictions are simply that the thrust and/or vehicle orientation angle must be selected so that the correct vertical component of thrust-to-weight ratio is obtained.

Intermediate Coast Phase. One alternative to the near-constant altitude translation maneuver described above is a coast phase introduced between the acceleration and deceleration phases. Analysis of coast phase indicates that it offers few advantages other than a longer translation time, which provides more time for surveillance, and a small saving in propellant if the optimum orientation angle and coast time are used.

A comparison of the propellant consumption for coast and no-coast translation maneuvers is presented in Figure 98 . The comparison, based on results from Reference 4 , shows that there is a small saving in propellant attributable to the coast phase. The penalties or benefits associated with a coast phase for the constant thrust method were evaluated by interrupting a translation trajectory between the deceleration and acceleration phases by a coast phase. During coast, the vehicle was vertically oriented.

A constant altitude trajectory similar to that shown in Figure 97 was selected for analysis. A coast phase at constant velocity was introduced for a specified translation distance. During the coast phase, a thrust-to-weight ratio of 1.0 was used to maintain a constant altitude (throttling required). At the end of the coast phase, the braking and final rotation maneuver were completed. A comparison of fuel consumption for an acceleration-deceleration translation versus an acceleration-coast-deceleration translation is shown in Table 6 .

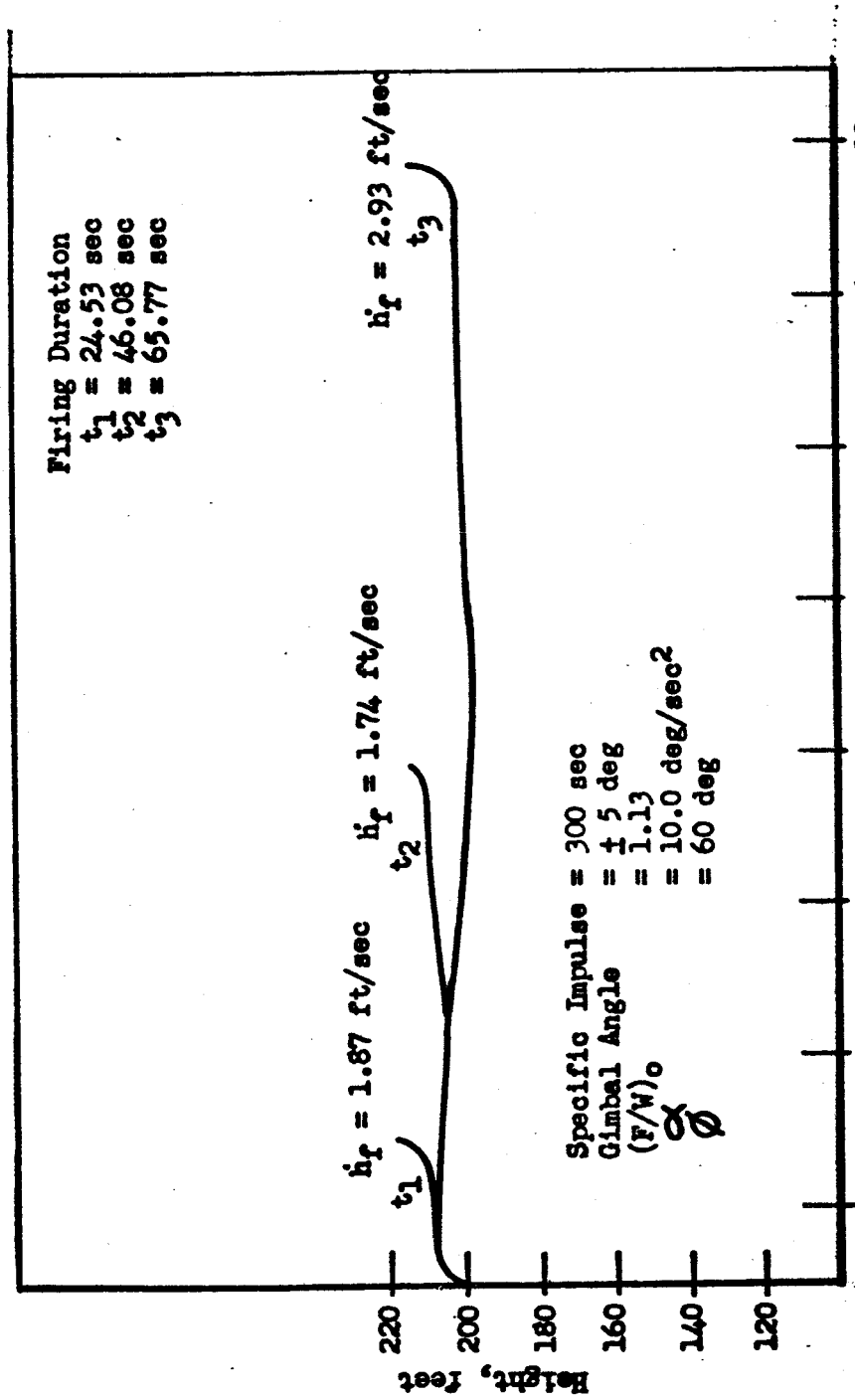

Figure 97 . Height vs Horizontal Distance for Lunar Landing Translation Trajectories

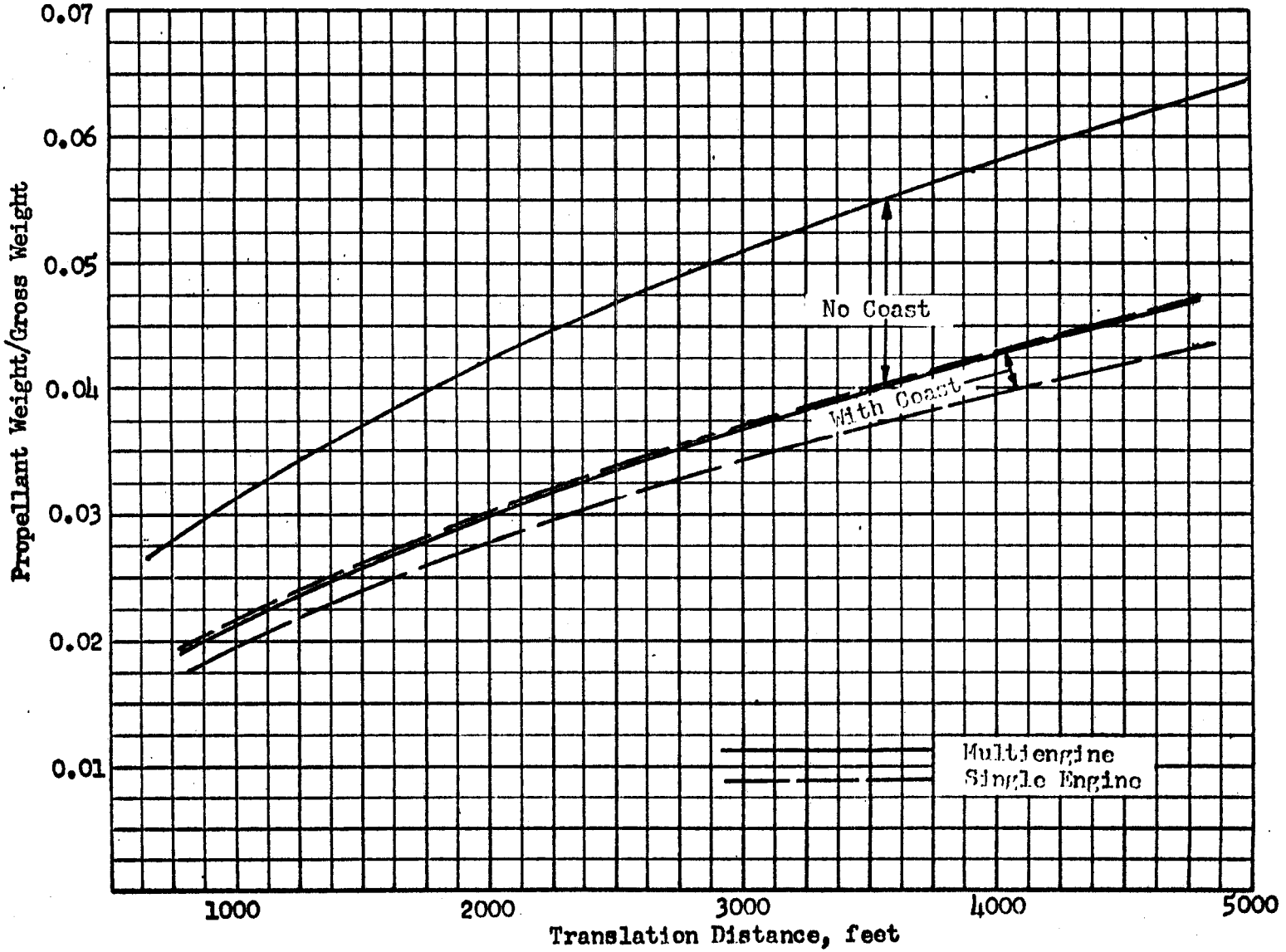

Figure 98. Comparison of Coast and No-Coast Translation Trajectories

TABLE 6

PROPELLANT CONSUMPTION (W_p) FOR A COAST VERSUS A NO-COAST TRANSLATION

Orientation Angle, degrees	Translation Distance, feet	W_p With Coast, pounds	W_p, No-Coast, pounds
60	2940	423	408
60	5112	614	529
45	5025	481	485
45	8649	669	625
30	8437	616	670
30	14530	837	860

The results (Table 6) show that as the orientation angle is reduced to an angle of 45 degrees or smaller, there is a savings in propellant realized by use of a coast phase; but as coast distances are increased, study results indicate that this benefit is reduced and the no-coast translation eventually becomes desirable for any given orientation angle. This indicates that there is an optimum orientation angle, probably near 30 degrees, and also an optimum coast time, associated with trajectories employing a coast phase. Precise optimum values were not determined in this study, since it was felt that the larger orientation angles (near vertical vehicle orientation) were of greater importance and more practical. Also, if the coast phase is used, midmaneuver throttling must be provided in order to reduce the thrust-to-weight ratio to 1.0 during the coast. Departure from the constant-thrust feature of this translation method detracts somewhat from its attractiveness.

Vehicle Orientation - Constant Altitude Maneuver. Study results indicated that a vehicle orientation angle of 45 degrees was optimum with respect to propellant consumption for translations without a coast phase. The result is shown graphically in Figure 99 for an arbitrary planetary body; optimum orientation was independent of the local gravity constant. If a coast phase is introduced, the

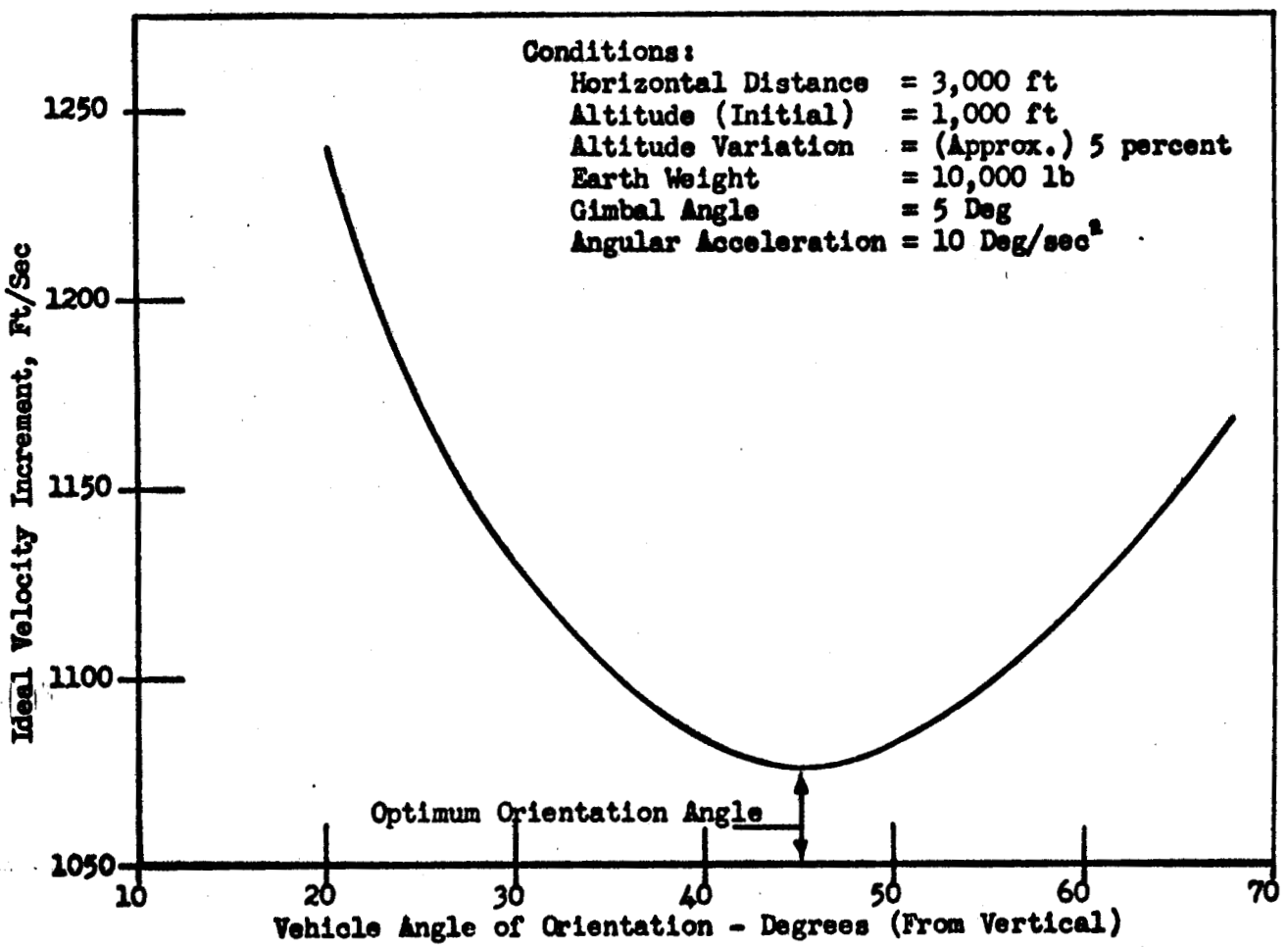

Figure 99 . Ideal Velocity Increment vs Angle of Orientation for Gravity Constant = 35 Constant Altitude Translation Maneuver.

optimum orientation angle was less than 45 degrees, although, as mentioned above, precise values were not determined.

However, there are considerations which make the larger orientation angles appear more practical. With the smaller or near-optimum orientation angles, the horizontal thrust-to-weight-ratio component approaches unity and the horizontal accelerations become quite large. This may make translations of short distances very difficult, if not impossible, since some range is attained during turning. For translations of greater distances, the horizontal velocity can become so great that the ability to select a landing site or to avoid local obstacles might be impaired. Tipping the vehicle over to the smaller orientation angles also might prevent, if it suddenly became necessary, the execution of an abort maneuver.

A comparison of two orientation angles to show their effects on horizontal velocities and translation distances for the acceleration phase of a translation maneuver are presented in Figure 100. The propellant weight, time, and maximum velocity attained for several constant-altitude translation distances and two orientation angles are presented in Table 7 .

TABLE 7

EFFECTS OF VEHICLE ORIENTATION ANGLE (Ø) ON CONSTANT ALTITUDE TRANSLATIONS

Translation Distance, feet	Propellant Weight* pounds		Time, Seconds		Maximum Velocity Attained, ft/sec	
Ø, degrees	45	70	45	70	45	70
500	165	195	23	34	47	32
2000	318	383	44	66	97	59
5000	480	625	67	110	145	96

*the propellant weights given are based on a 10,000-pound vehicle.

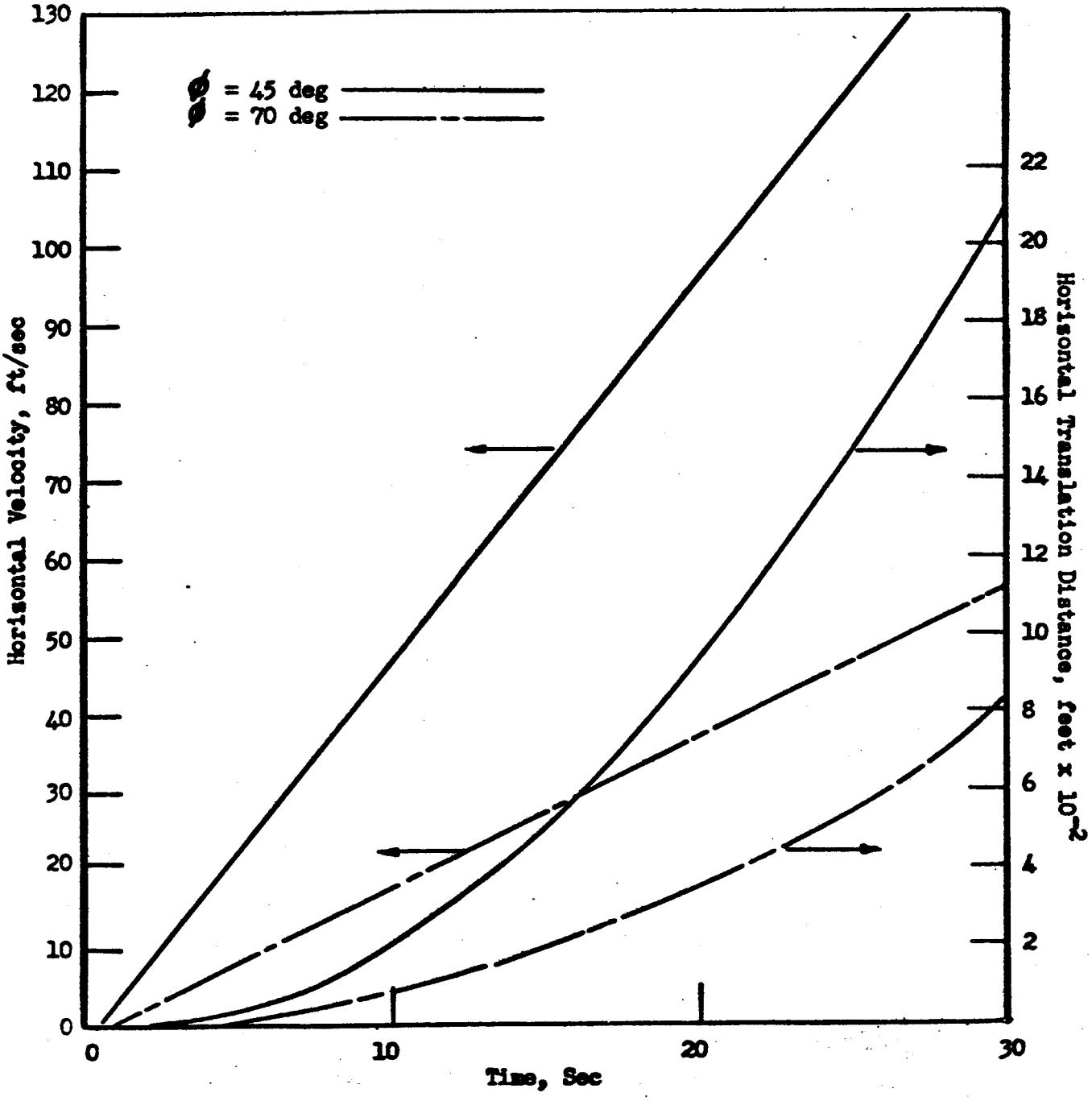

Figure 100. Effect of Vehicle Orientation Angle on Horizontal Velocity And Translation Distance for Acceleration Phase of Constant Altitude Translation

Effect of Gravity Constant. A representative set of translation maneuver conditions was formulated to evaluate the effect of gravity constant on velocity requirements for a selected maneuver, and thereby to obtain a basis for comparison of the propulsion requirements for lunar translation maneuvers, which have been analyzed extensively, and translation maneuvers on other planetary bodies. Thrust was held constant in all cases at a value selected to provide a near-constant altitude maneuver. An intermediate coast phase was not utilized. The vehicle was oriented at 30 degrees from the vertical during the acceleration and deceleration phases of the maneuver; other pertinent data are listed below.

Horizontal distance	3000 feet
Altitude (initial)	1000 feet
Vehicle (Earth) weight	10,000 pounds
Gimbal angle	$\pm$ 5 degrees
Vehicle angular acceleration ( )	10 deg/sec^2
Specific Impulse (I_s)	300 seconds

Results of the study are presented in Figure 101. It is interesting to note that the selected maneuver requires 390 ft/sec ΔV at the moon and 1070 ft/sec at Earth; the ratio is far from the 6:1 ratio of gravity constants. Thus, though the propulsion system has six times the thrust, and expends six times as much propellant at Earth as at the moon to maintain a constant altitude, it simultaneously benefits by having six times the capability for horizontal acceleration and deceleration. As a result, the given translation distance is traversed faster on the Earth than on the moon, and the ΔV requirements depart markedly from a 6:1 ratio.

Performance Summary

Figure 102 presents Lunar translation distances and loss in altitude versus propellant weight or firing time for various vehicle orientation angles. This data is based on an initial vehicle thrust-to-weight ratio of 1.0 and constant thrust throughout the maneuver. (In this case, no attempt was made to maintain a constant altitude.) In all of the examples presented, an initial vehicle Earth weight of 10,000 pounds was used.

A comparison of propellant weight versus constant-altitude translation distance is presented in Figure 103 for various methods of translation. Curves 1 to 5, normalized to a specific impulse of 300 seconds for comparison to the results of the present study, were obtained from Reference . Curve 1 is for a ballistic maneuver system. The results drawn in Curves 2 and 3 are for

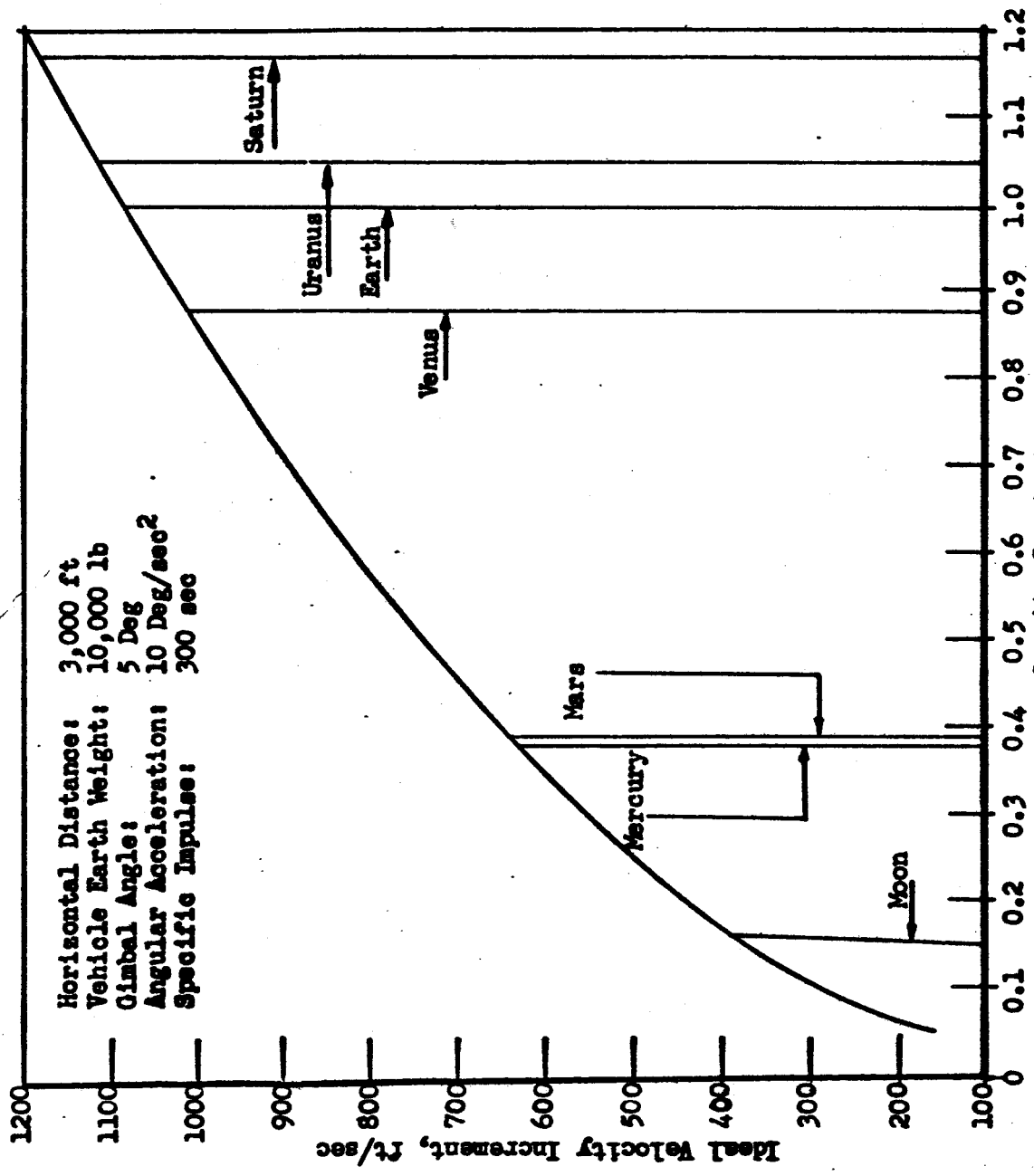

Figure 101. Ideal Velocity Increment vs Gravity Constant
Constant Altitude Translation Maneuver

ϕ = Vehicle Orientation Angle
F/W = 1.0
I_s = 300 seconds
Gimbal Angle = 5.0 degrees
α = 10.0 deg/sec^2
W_0 = 10,000 pounds

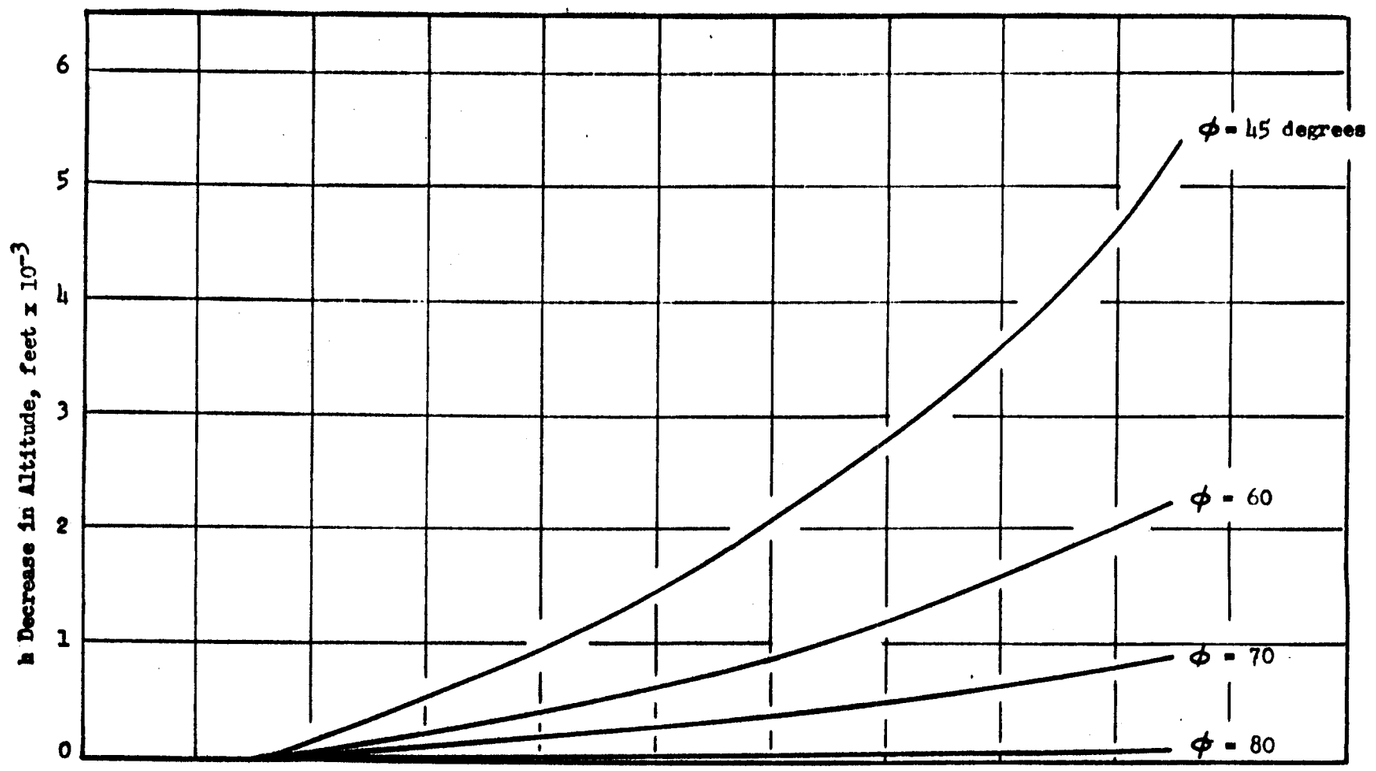

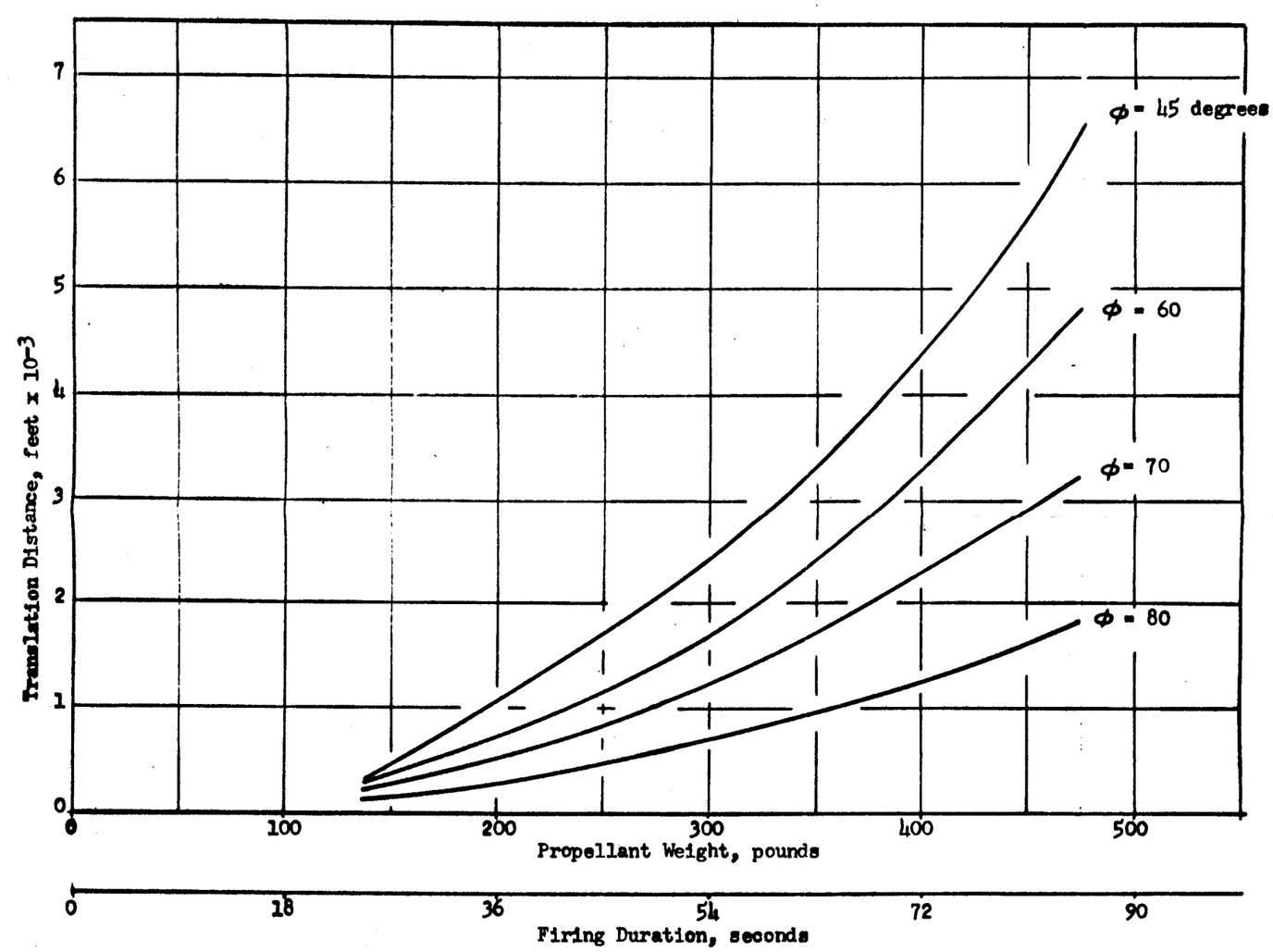

Figure 102. Lunar Translation Distance and Decrease in Altitude vs Propellant Weight

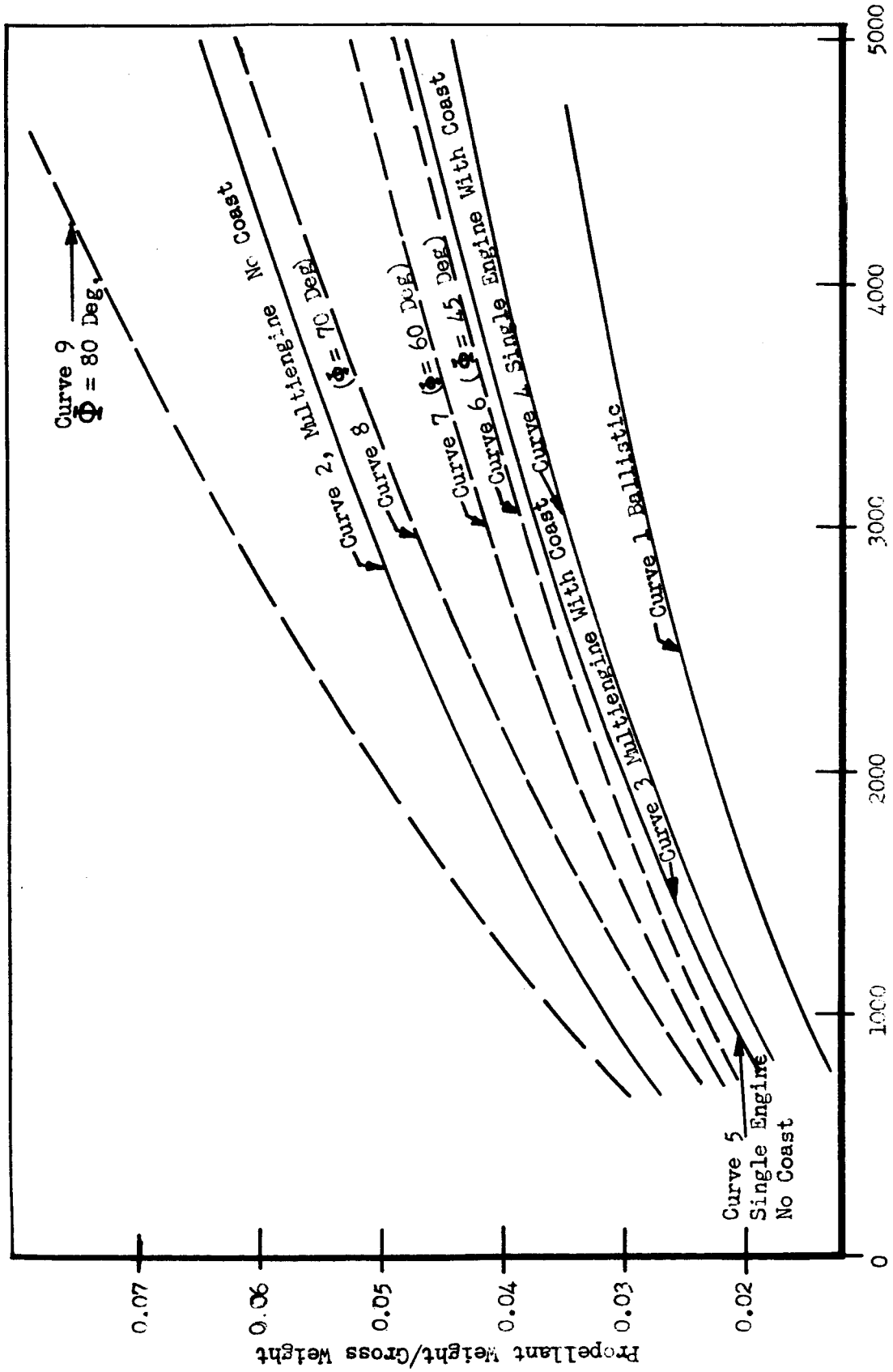

Figure 103. Comparison of Propellant Weight vs Constant Altitude Translation Distance For Various Methods of Translation

constant-altitude translation with the multiple-engine concept. Curves 4 and 5 are for the single engine (throttleable) constant-altitude translation system. (The optimum vehicle orientation angles are 45 degrees without a coast phase and 30 degrees from horizontal with the coast phase.)

The curves 6 to 9 are for the near-constant altitude, constant-thrust systems without a coast phase. The appropriate thrust level was used for each orientation angle. A slightly greater propellant consumption is indicated in curve 6 than in curve 5, although they are basically the same system. However, curve 5 is based on the assumption that the vehicle rotation time is zero; therefore, the curve does not reflect propellant burned during the turning operations. In the analysis it was found that for rotation rates of practical interest, the turning operations required from 2 to 6 seconds and the entire maneuver required three (four with an intermediate coast phase) turning operations. Since for the smaller orientation angles, larger thrusts are required to maintain a constant altitude during translation, the propellant used while turning the vehicle could be significant. If the propellant used to rotate the vehicle is considered, the single engine system of Reference 5 compares very closely, with respect to propellant consumed, to the method analyzed.

Review of the analysis and results indicates that the ballistic system offers the most favorable propellant economy for down-range translation (approximately 25 percent less propellant than a single-engine, continuous-powered system for a given maneuver). However, several disadvantages exist: engine restarts are required; large vehicle tilt angles can exist; the downrange distance cannot be changed enroute; and high altitude trajectories preventing surveillance can result.

For the multiengine horizontal translation system, however, the system has the disadvantage of requiring additional restartable engines, and the auxiliary engine must be located at the vehicle cg to prevent vehicle rotation, or the main engine must be gimballed to maintain a constant attitude.

The single engine continuous-powered translation method appears to be the best with respect to simplicity, reliability, and versatility. This method eliminates the requirement of engine restart. Use of a throttleable main engine allows a continuous constant altitude, but requires thrust adjustment during the maneuver. The optimum angles for single engine translation maneuvers (45 degrees if no intermediate coast phase is employed; 30 degrees with coast) are somewhat high for short translation distances,

the horizontal velocity with these tilt angles might be excessive for ground surveillance. The propellant-consumption decrease obtainable by the use of coast phase does not appear to warrant the additional rotation maneuvers required.

The investigation of constant thrust translation showed that translation with either increasing, decreasing, or approximately constant altitude can be achieved with a constant engine thrust. However, the thrust at initiation of the maneuver must be the amount specified to achieve the desired translation trajectory. An intermediate horizontal coast phase between the acceleration and deceleration phases was examined and found to require throttling to prevent altitude change, and, in general, did not offer significant benefits.

The engine gimballing conditions (angles and rates) do not appear to be a critical factor. Changes in engine gimballing produce only very slight changes in the overall translation maneuver. Vehicle orientation (tilt) angles are not critical for short translation distances, but in general have a pronounced effect on translation trajectory characteristics.

FINAL-DESCENT PHASE OF A LUNAR LANDING

The final propulsive maneuver in the course of landing a space vehicle on the surface of the moon will very likely be a vertical descent from a position a few feet to a few hundred feet directly above the desired landing site (the terminal point of a translation maneuver). For ideal execution of the maneuver, the velocity will reach zero precisely at touchdown; for nonideal cases, reasonable velocities can be mechanically absorbed by various types of landing gear. It is strongly probable that the main landing engine will be utilized for the vertical-descent maneuver.

Analysis of Velocity Requirements

The velocity requirement (ΔV) for performance of the descent maneuver is dependent on the following parameters:

1. Initial altitude
2. Initial descent rate
3. Maximum thrust available
4. Throttling ratio

For any values of initial altitude and descent rate, the descent maneuver requires least propellant if it is divided into a free-fall phase (which is equivalent to an infinitely throttled engine) followed by an impulsive velocity addition (which is equivalent to infinite maximum thrust). The former condition is generally unacceptable, since there is no practical possibility of safe abort if, following free-fall, engine ignition fails to occur. The closest alternative to free-fall is to use the landing engine throttled to its lowest thrust level. For the second phase, the maximum thrust is the optimum value selected for the major braking maneuver. Thus, the high-thrust portion of the descent maneuver is performed by the landing engine in an unthrottled condition.

Alternatives to this two-step thrust program can be formulated; e.g., velocity can be cancelled uniformly if desired by suitable application of continuous throttling capability. This approach, however, is less economical than the two-step approach; the only gain is a reduction in deceleration forces, and these are already quite small in comparison to human or equipment tolerance limits.

The effects of throttling ratio and initial altitude are presented in Figure 104 . (The indicated value of F/W max (6.0) is typical of the burnout thrust-to-weight ratio of an optimized direct landing or landing-from-orbit stage. The F/W max represents the product of the initial stage thrust-to-weight ratio and the ratio of initial stage weight, including payload, to stage weight at the start of the vertical descent phase). The rapid ΔV increase accompanying reduction of throttling ratio to values below 10:1 indicates that the net force on the vehicle (i.e., lunar gravity force minus thrust) is too small in this region to promote adequate downward motion. (A pilot might appreciate the gentleness and related sense of security of this landing, but the propellant penalty associated with prolonging the descent must be classed as an extravagance in a mission where weight is critical). One curve of Figure 104 was extended to infinite throttling ratio to indicate the magnitude of gain realized by improving adequate (i.e., approximately 15:1) throttling to complete (i.e., engine off) throttling. The difference is only 5 ft/sec.

In each of the curves of Figure 104, a narrow range of throttling ratio is indicated in which a rapid transition from high to low values of change in velocity requirement per unit throttling ratio (e.g., 31 ft/sec change in ΔV as throttling ratio change from 7:1 to 8:1 on the 150-feet altitude curve, but a change of only 3 ft/sec as throttling ratio changes from 11:1 to 12:1) occurs. The approximate centerpoint of this region, or "knee" (which might be either more or less pronounced in its appearance and displaced somewhat along the abscissa if the coordinate scales were different from the presentation in Figure 104), is relatively insensitive to initial altitude, ranging from approximately 9:1 for an altitude of 50 feet to about 11:1 for 500 feet. The location of the knee represents a useful estimate of the design point for a landing propulsion system. More significant in determining where the knee occurs is the initial value of F/W, as shown in Figure 105. The middle curve is repeated from Figure 104 . As initial F/W varies from 4 to 8, the knee (indicated Δ) ranges over throttling ratios of approximately 7:1 to 12:1.

Descent characteristics for a representative case are illustrated in Figure 106. It is apparent that maximum velocity attained increases with throttling ratio, with free-fall representing the limiting condition. However, propellant consumption decreases as throttling ratio increases; therefore, a closely controlled descent (e.g., one comparable to the 8:1 throttling ratio curve, which at no time exceeds 20 ft/sec), however beneficial from a pilot point of view, requires a propellant expenditure greater than that required for a faster descent maneuver.

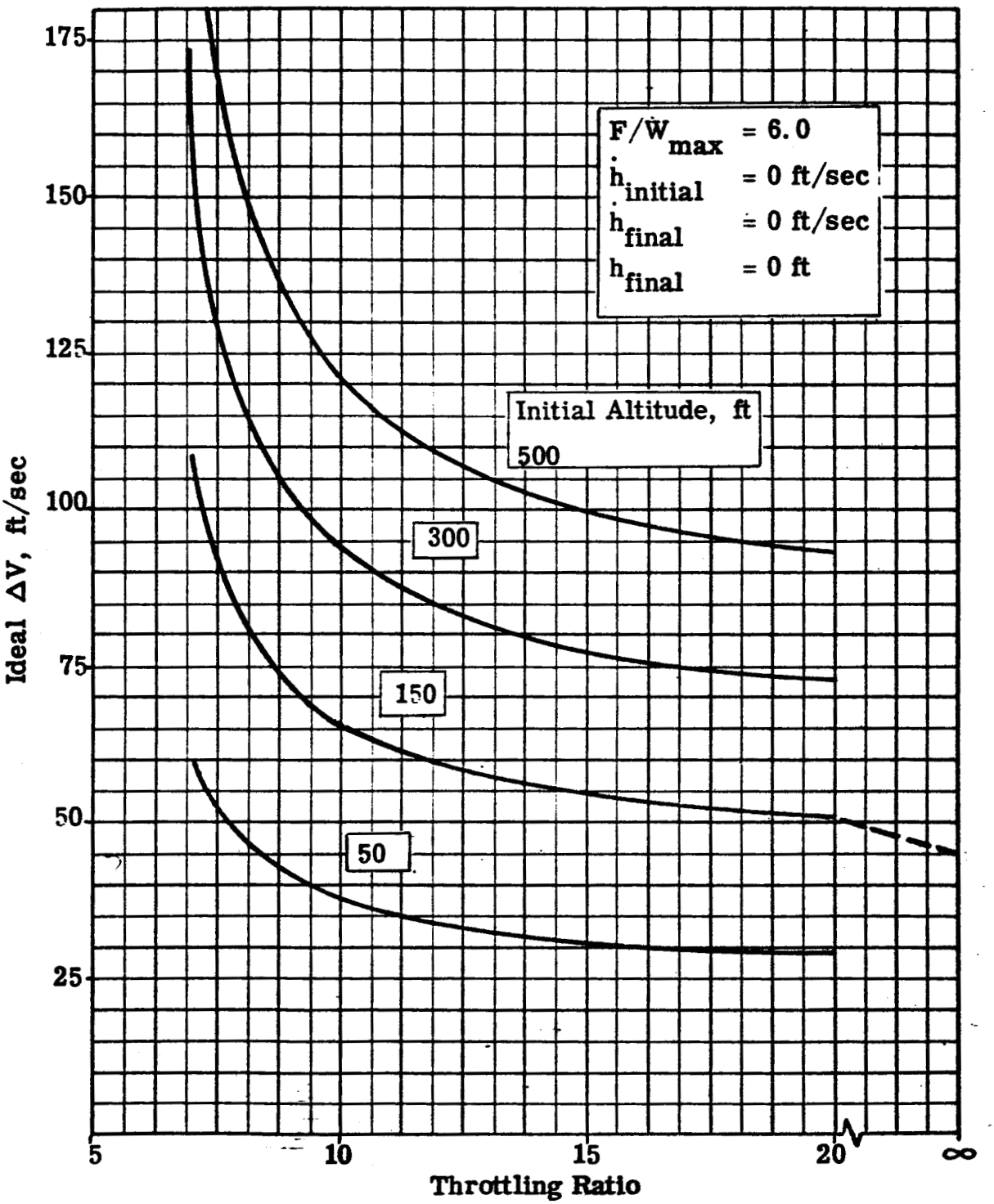

Fig. 104. Effect of Throttling Ratio and Initial Altitude on Vertical Descent Maneuver Propulsion Requirements

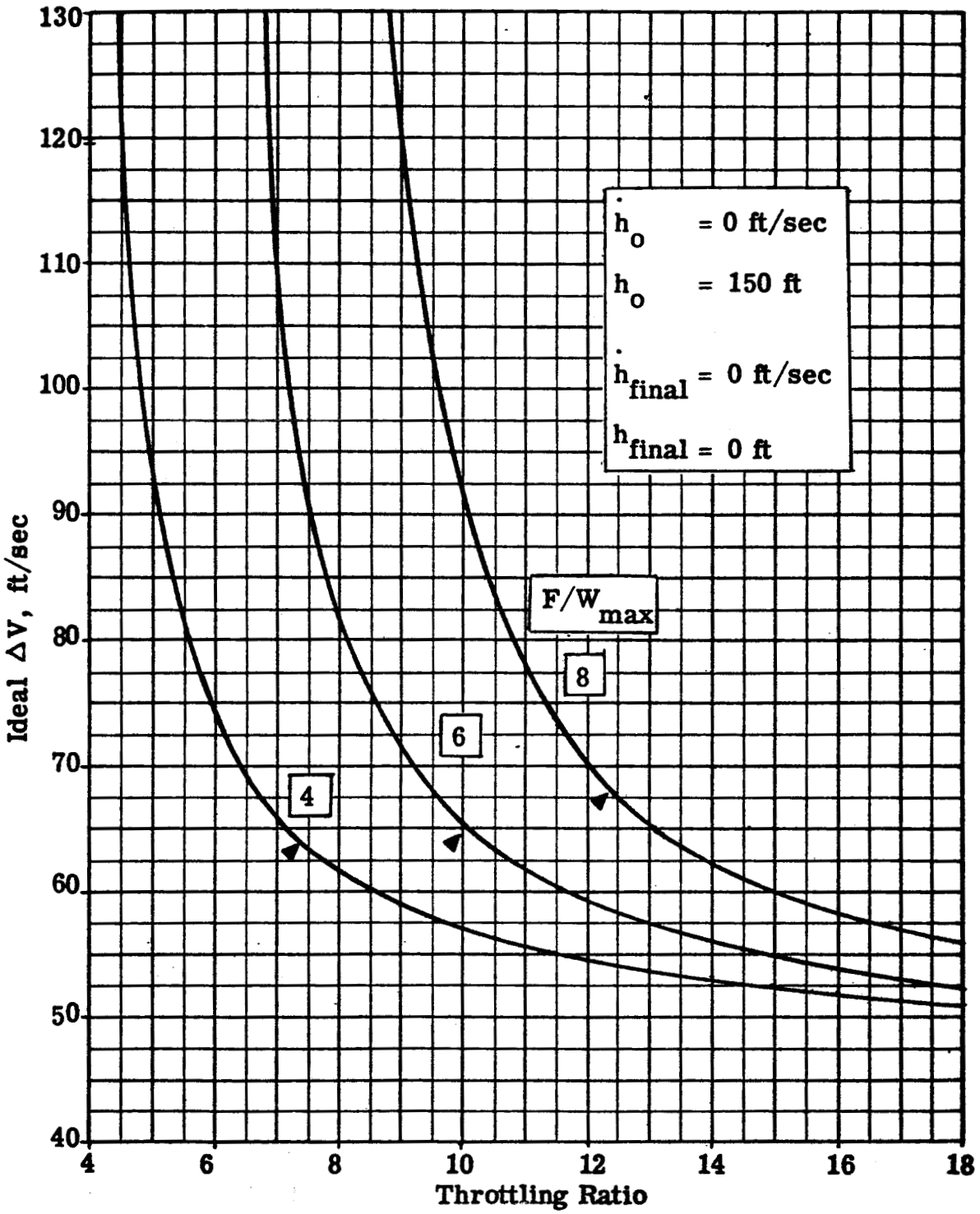

Fig. 105. Effect of Maximum Thrust-to-Weight Ratio on Vertical Descent Maneuver Propulsion Requirements

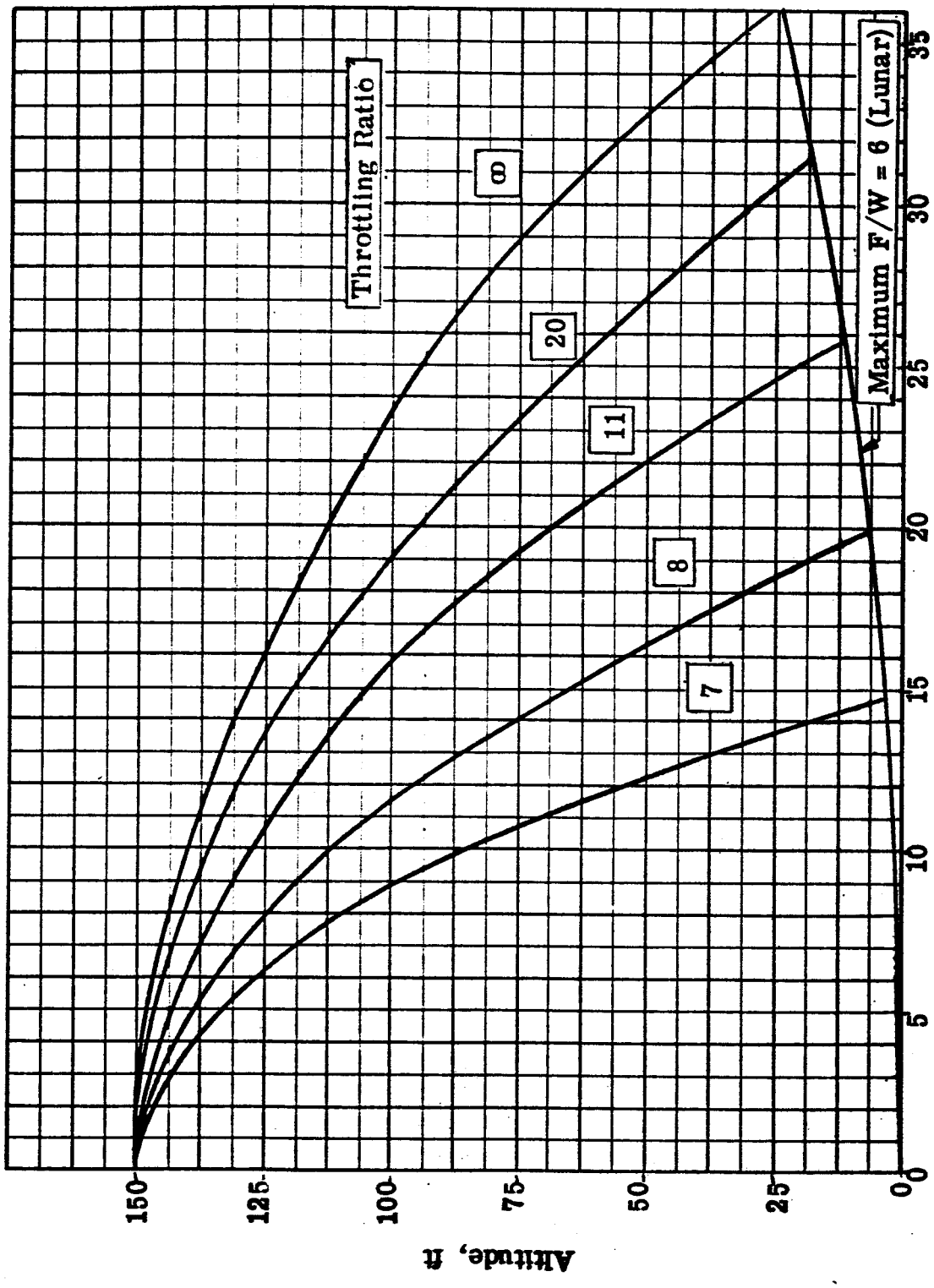

Fig. 106. Final Descent Characteristics for Lunar Landing

The effect of initial descent rate is illustrated in Figure 107. For descent rates in excess of 25 ft/sec, the reason for the upward ΔV trend shown in Figure 107 is obvious; a higher velocity initially requires that a greater velocity be cancelled propulsively. The existence of optima on the indicated curves is, however, not so self-evident. Their presence reveals that the propulsion system can achieve greater overall efficiency, despite the need to cancel additional velocity, if the duration of the descent maneuver (and with it, gravity loss) is reduced by the presence of a nonzero initial descent rate. The optimum initial descent rate is far more pronounced when the minimum thrust level is close to the weight of the landing vehicle (i.e., when throttling capability is limited). An additional characteristic to be noted on Figure 107 is that the curves terminate at an initial descent rate of 75 ft/sec. The reason is that as initial descent rate increases, a point is reached where the constraint that velocity and altitude reach zero simultaneously can be satisfied only if the high thrust level is employed exclusively; at still higher initial descent rates, the constraint cannot be satisfied.

The effects of the high-level and low-level F/W values on the descent maneuver velocity requirements are presented in Figure 108. At low values of the upper thrust level, $(F/W)_{max}$, thrust is insufficient to perform the second phase of the descent efficiently; velocity requirements are therefore high. At high values of $(F/W)_{max}$, the related lower thrust level (equal to maximum thrust divided by throttling ratio) is too high to permit efficient performance of the first phase of the descent; again velocity requirements are high. Between these extremes, an optimum $(F/W)_{max}$ exists for each value of throttling ratio. The limiting (lowest) value of ΔV possible occurs when both thrust and throttling ratio are infinite; for the set of initial and final conditions stated in Figure 108, the minimum ΔV is approximately 45 ft/sec.

It is evident from the data presented in Figures 104, 105, 107, and 108 that the propellant requirements associated with the vertical-descent phase of a lunar landing are small in comparison to the propellant required for the braking and translation maneuvers. The vertical-descent phase is, however, of primary importance in determining the throttling ratio required in the engine design. In a detailed system evaluation, the velocity reduction provided by increased depth of throttling must be weighed against the weight, and possibly reliability, panalties accompanying the use of a more flexible system.

Figure 109 is presented to illustrate the effect of the gravitational constant on vertical-descent-maneuver velocity requirements. Unlike the major braking maneuver, whose comparative Earth:moon velocity requirement does not deviate too far from the 6:1 ratio of gravity constants, the ΔV for vertical descent at Earth is, over the indicated range of throttling ratios, less than 3 times the comparable value for the moon. The reason is simply that the two systems considered are identical when first- and second-phase accelerations are compared in units of local g's, but widely

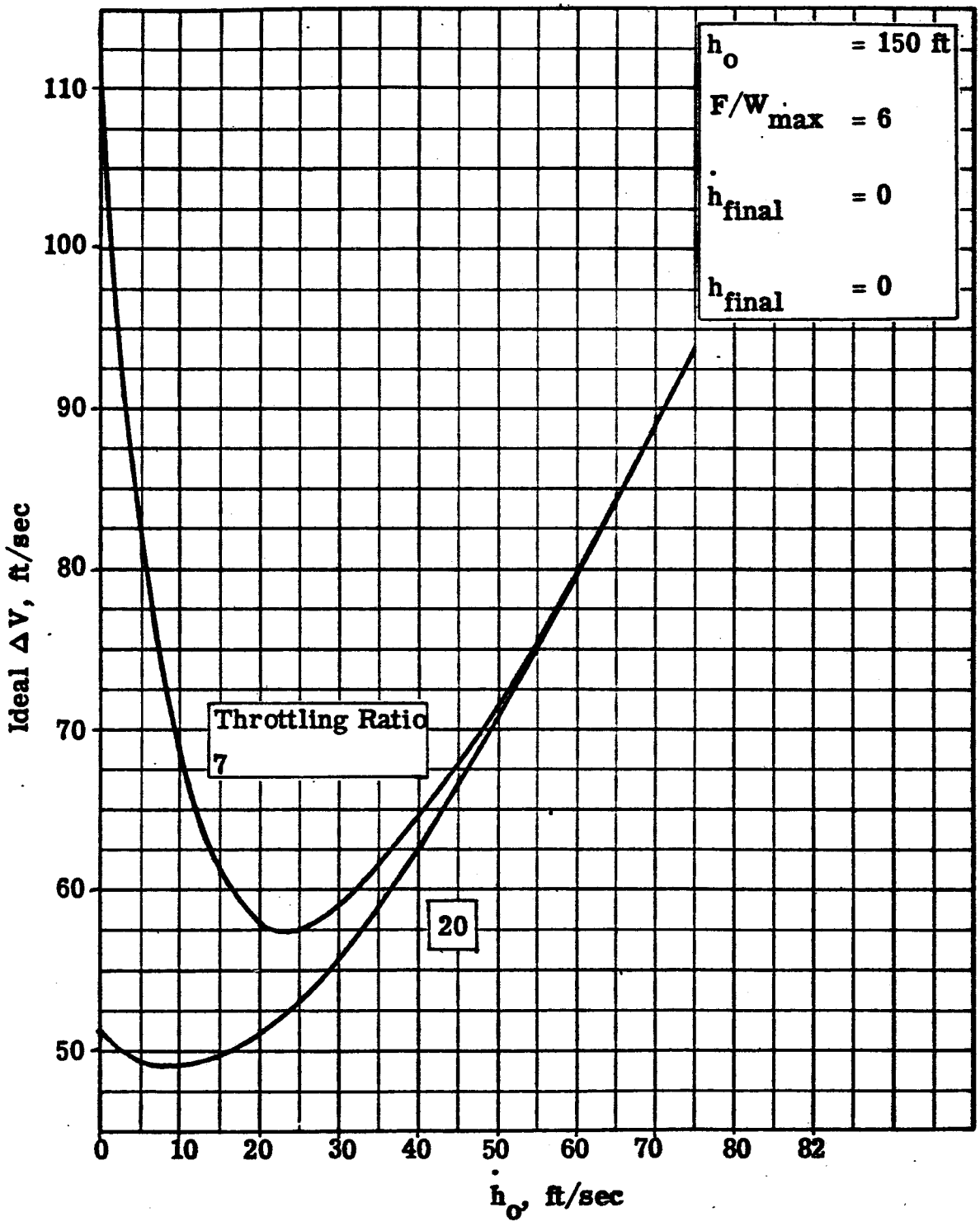

Fig. 107. Effect of Initial Descent Rate on Vertical Descent Maneuver Propulsion Requirements

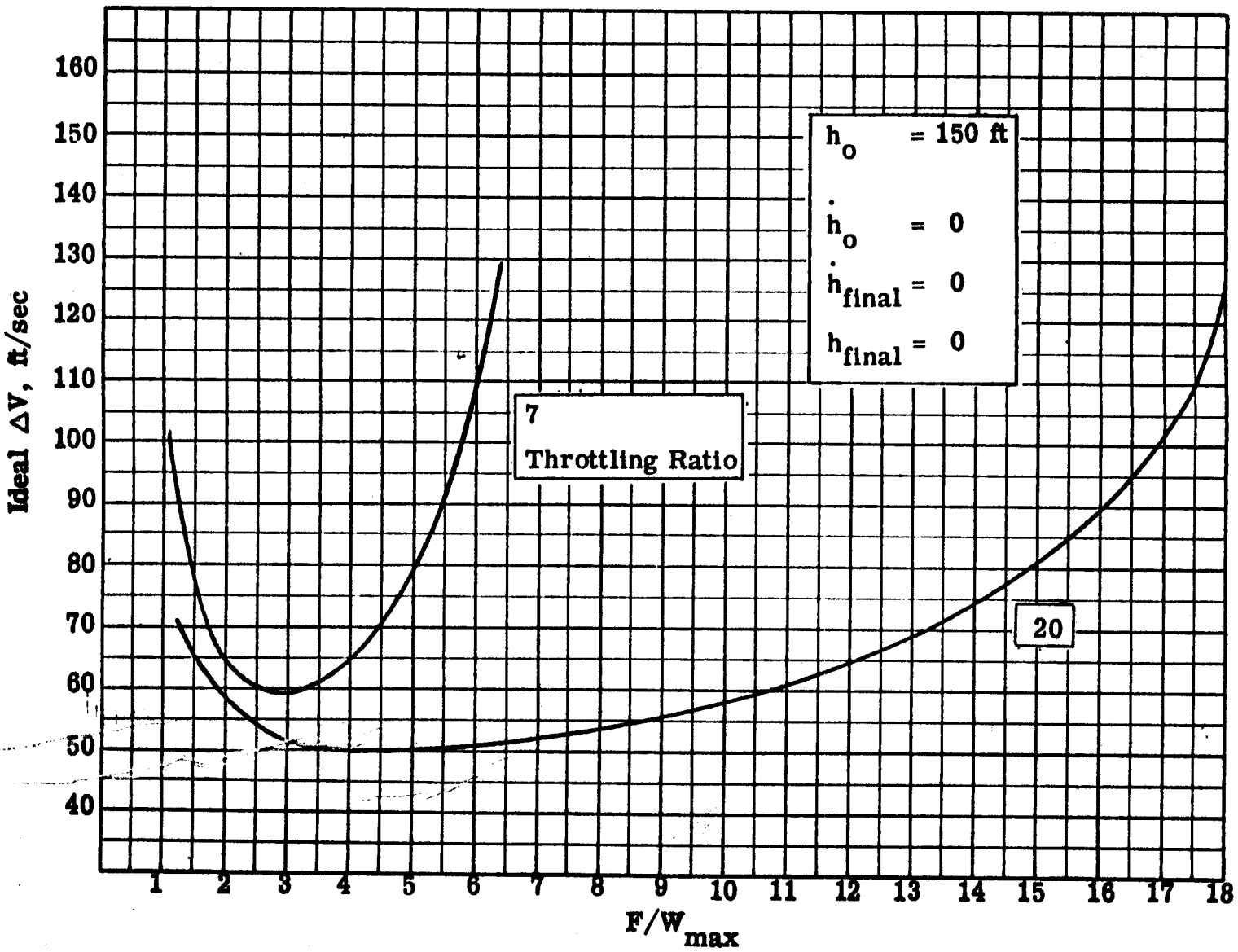

Fig. 108. Effect of Maximum Thrust Level on Vertical Descent Maneuver Propulsion Requirements

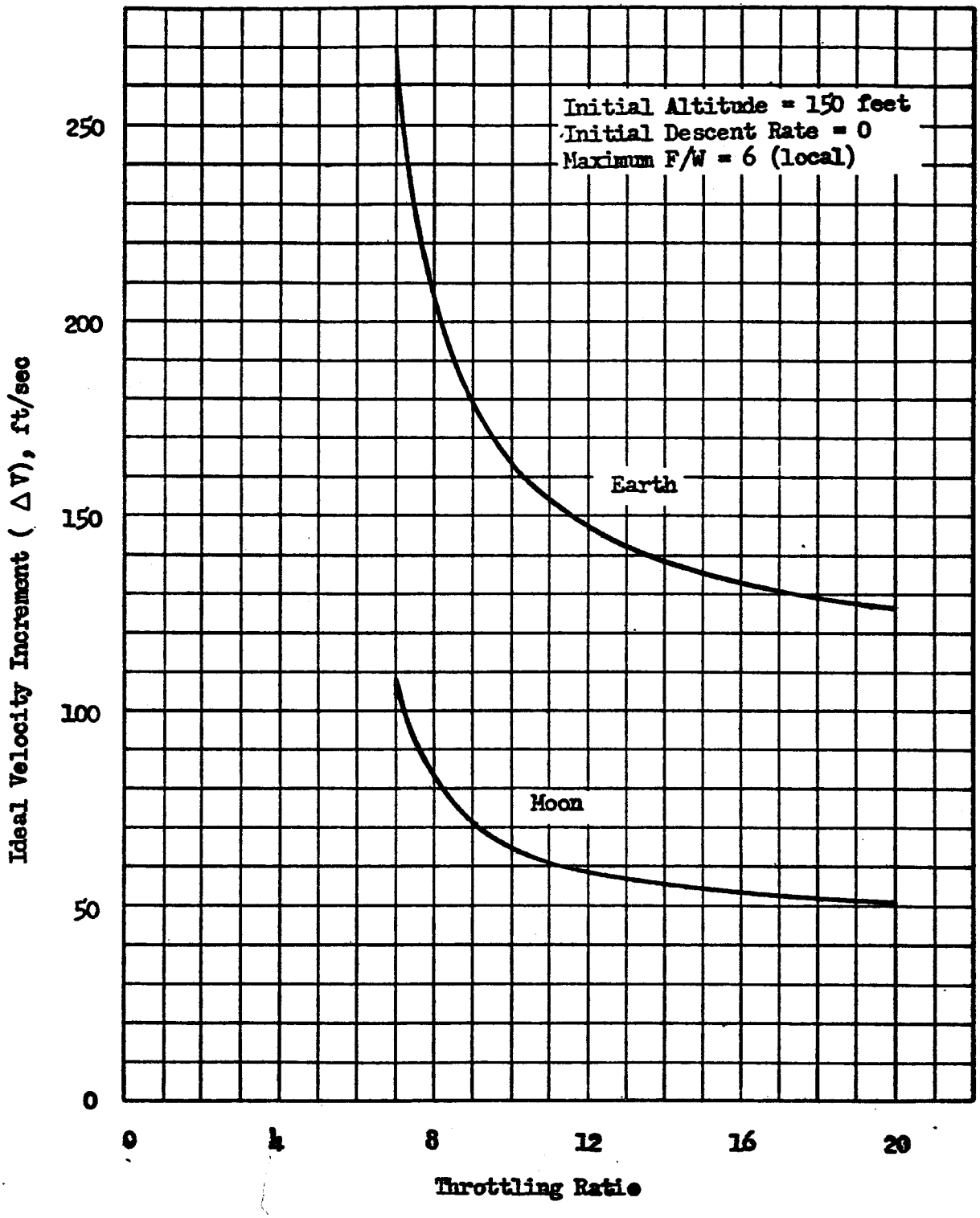

Figure 109. Velocity Requirements for Vertical Descent Maneuvers

different in terms of distance/time squared acceleration units. Thus, the vertical descent, whose first phase actually benefits from high acceleration, reflects the advantage of performing the maneuver in the Earth's gravitational field rather than the moon's.

Conclusions

The ideal-velocity capability required for performance of a vertical-descent maneuver to the lunar surface:

1. Is approximately 75 ft/sec for a typical case in which initial altitude is 200 feet, initial descent rate is zero, maximum thrust-to-weight ratio is 6, and throttling ratio is 10:1

2. Decreases as throttling ratio increases, although for most cases, throttling capability beyond 10:1 provides only small benefits.

3. Increases with increasing initial altitude (e.g., approximately 125 ft/sec for descent from 500 ft altitude).

4. Is less for relatively low non-zero initial descent rates than it is for a zero initial rate of descent. An optimum initial descent rate exists, and is dependent on initial altitude, maximum thrust and throttling ratio.

5. Is a function of maximum F/W, and displays an optimum which is dependent primarily on throttling ratio.

The maximum velocity achieved during a vertical descent maneuver increases with increasing throttling ratio. However, deliberate reduction of maximum velocity, attained by employing less-than-available throttling, imposes an increased propellant requirement on the vehicle system.

TOUCHDOWN STABILITY

An analysis was conducted to evaluate the trajectory, terrain and vehicle factors governing touchdown stability of an assumed lunar landing vehicle. The vehicle stability criterion was based on the condition that angular kinetic energy of the vehicle at impact be sufficient to rotate the vehicle to an unstable position.

The vehicle impacts the surface with an initial kinetic energy which is the result of a residual vehicle velocity (V). Since the landing legs have the ability (by design) to absorb energy, the energy associated with the velocity component (V_L) along the leg is assumed to be completely absorbed. The energy acting to tip the vehicle is associated with the velocity component (V_R) perpendicular to the leg (see illustration below). This energy is equated to the potential energy required to lift the center of gravity (cg) to the point of instability; that is, the vehicle rotates about the point of impact until the cg swings through the vertical (point of instability), and the vehicle falls on its side.

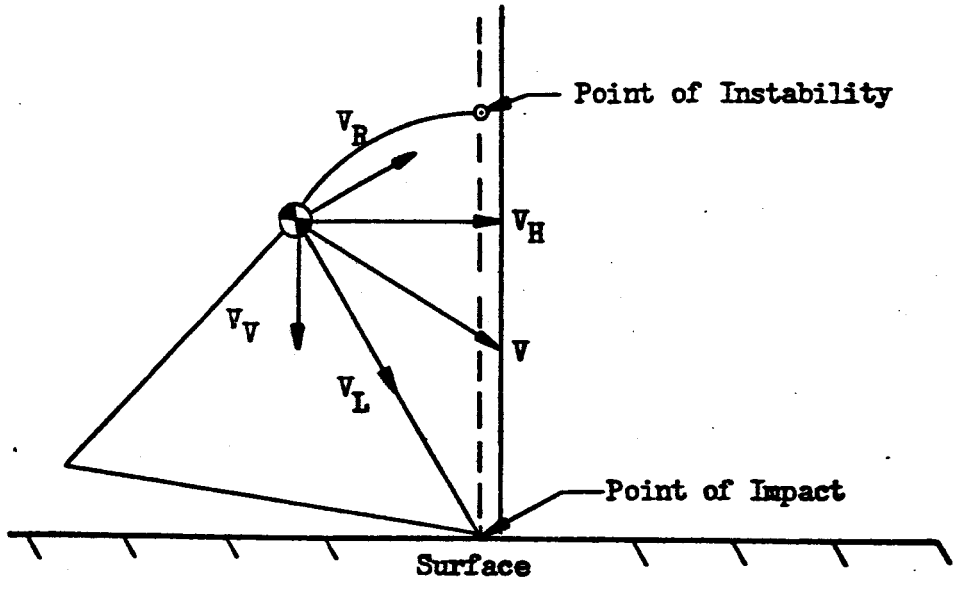

Once V_R is determined, V may be determined, which yields V_H and V_V, the components of the vehicle velocity vector in the horizontal and vertical directions, respectively.

In the case of hindleg impact, first the hindleg strikes the ground and then the foreleg. In each instance, the kinetic energy associated with the velocity component directed along each leg is assumed to be completely absorbed. Downhill impact is analyzed because the vehicle is inherently less stable on a downgrade than on an upgrade.

The vehicle parameters utilized are described in the figures below.

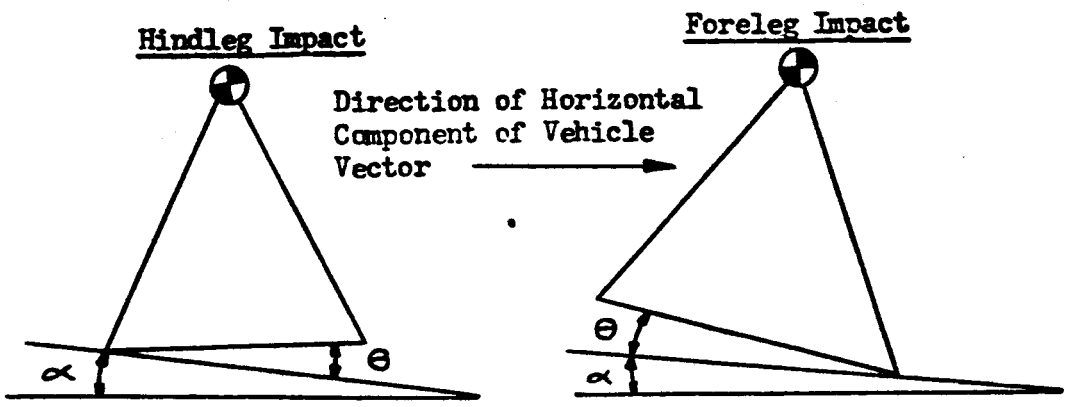

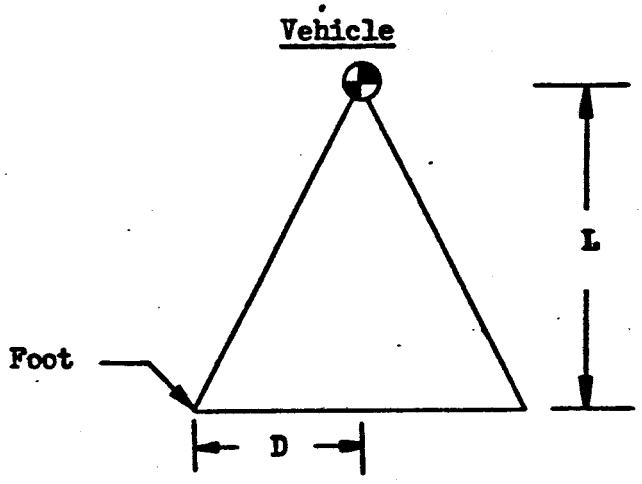

L : Vertical distance to cg from base

D : Distance from foot to center of base

α : Surface inclination from horizontal

θ : Angle of impact (angle between base and surface at point of impact)

V : Vehicle velocity vector

The angular kinetic energy, E_K, at impact is

$$E_K = \frac{1}{2} I \frac{(V_V^2 + V_H^2)}{(D^2 + L^2)} \sin^2 \left[\alpha + \theta + \arctan (L/D) - \arctan \left(\frac{V_V}{V_H}\right)\right]$$

where I is the moment of inertia about the point of impact, and the other terms are as defined previously. In the case of foreleg impact, the vehicle will tip over if E_K exceeds the potential energy, E_p, which is defined by the expression,

$$E_P = mg (D^2 + L^2)^{\frac{1}{2}} \left\{1 - \sin\left[\left[\alpha + \theta + \arctan (L/D)\right]\right]\right\}$$

where m = vehicle mass
g = local gravitational constant

The case of hindleg impact differs in that the angular kinetic energy increases as the vehicle rotates from the hindleg to the foreleg contact position. The foreleg subsequently absorbs energy directed along its length; the stability of the vehicle is governed by the remaining velocity component perpendicular to the foreleg.

For the selected example, nominal vehicle parameters were:

L = 20 feet
D = 14 feet
α = 0, 15 degrees
θ = 0, 5, 10, 15, 20 degrees
I = 525,700 slug-ft^2
W = 35,000 pounds

Each of the parameters previously defined affects vehicle stability. The analysis was conducted to evaluate the effect on V_V and V_H of L, D, I, α, and θ.

Regions of stability and instability are indicated in Figures 110 through 112. Each line defines the vehicle velocity limits if the vehicle is to remain upright after impact. The actual vehicle velocity vector is represented by the directed line segment from the origin (0, 0) to the point (V_H, V_V). Both magnitude and direction are shown on the plot. It is evident that for a particular value of descent rate at impact, the allowable lateral velocity component decreases as impact angle increases.

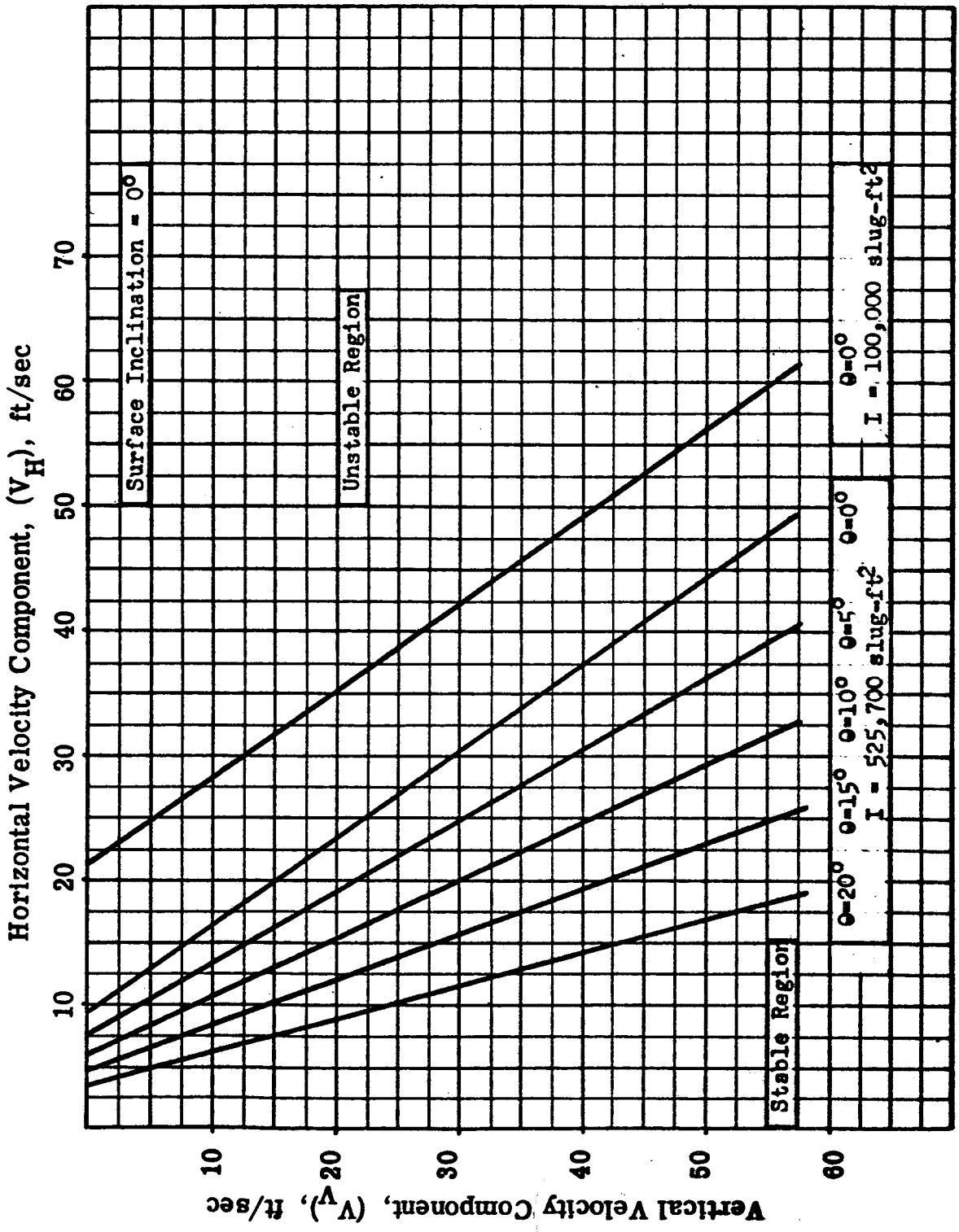

Fig. 110. Fore-leg Impact of Lunar Landing Vehicle

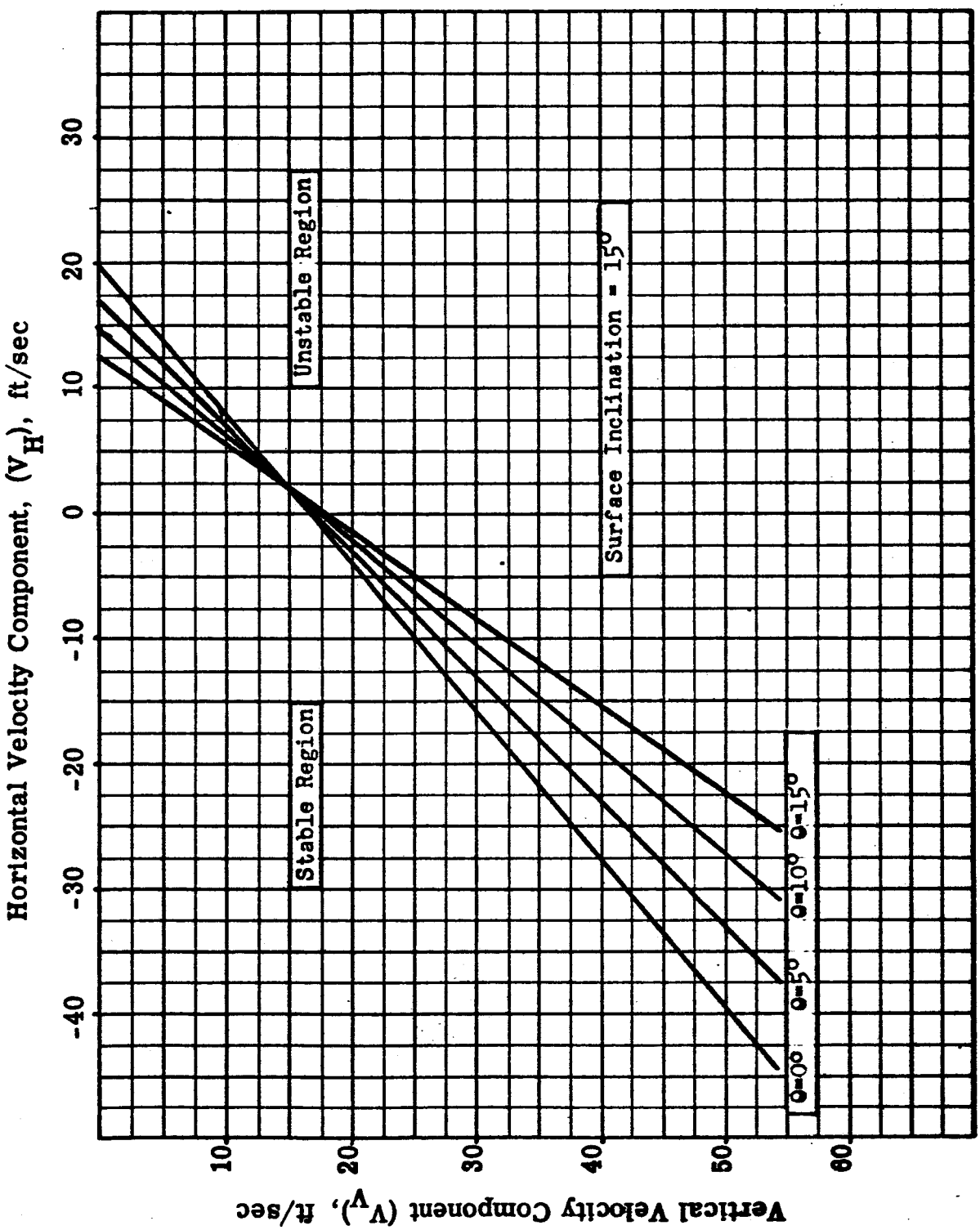

Fig. 112. Hindleg Impact of Lunar Landing Vehicle

266

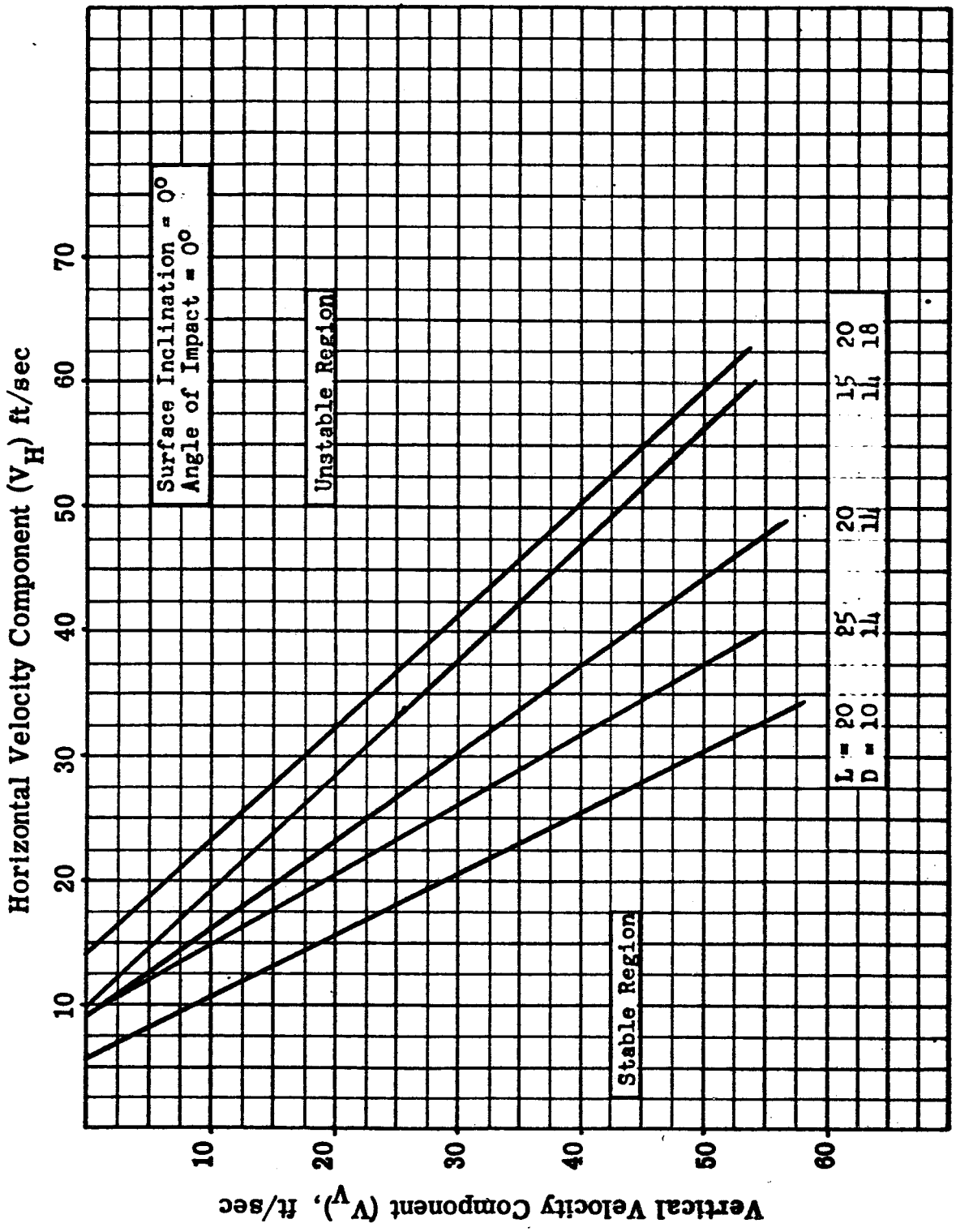

Fig. 112, Effect of Vehicle Geometry on Lunar Landing Stability Regions

A case when the moment of inertia is 100,000 slug-ft^2 is shown in Figure 110 for purposes of comparison with the nominal value of moment of inertia. It can be seen that the vehicle becomes more stable as the moment of inertia decreases.

In the case of hindleg impact, part of the initial energy is absorbed by the rear legs and part by the front legs. Kinetic energy is added (due to the potential energy decrease of the cg) as the vehicle rotates about the hindlegs and impacts on the front legs. Part of this energy addition shows up as increased velocity available to tip the vehicle. Thus, the vehicle stability curves have a different appearance in the case for hindleg impact.

The results of L and D perturbations are shown in Figure 112. The reference line is for L = 20 and D = 14. The effect of vehicle geometry can be seen since all other parameters were held constant.

The energy required to tip the vehicle is presented in Figure 113 as a function of the angles between the vehicle, the surface, and the horizontal. The energy values are obtained from potential energy considerations.

A comparison was made between the results of this analysis and those obtained in an analytical and experimental study on a particular small landing vehicle (Reference 5). Reasonable agreement between results is shown by the curves of Figure 114. The differences can be attributed to the sliding (a factor which was not included in this study) of the experimental vehicle, which made the vehicle more stable.Thee presence or absence of sliding is strongly dependent on surface terrain, and the assumption that sliding does not occur, which is equivalent to an assumption of an infinite friction coefficient, is therefore a conservative approach for selection of safe limits for the terminal velocity components of a landing vehicle.

Although only one value of the gravity constant is pertinent to a lunar analysis, it is significant to note that for a particular landing vehicle configuration, the velocity conditions which provide stable impact are dependent on the local gravitational constant; i.e., on the planetary body upon which the landing is performed. Thus, allowable terminal velocity components specified to yield stable impact on the moon may be inappropriate as specifications for landings on other planetary bodies.

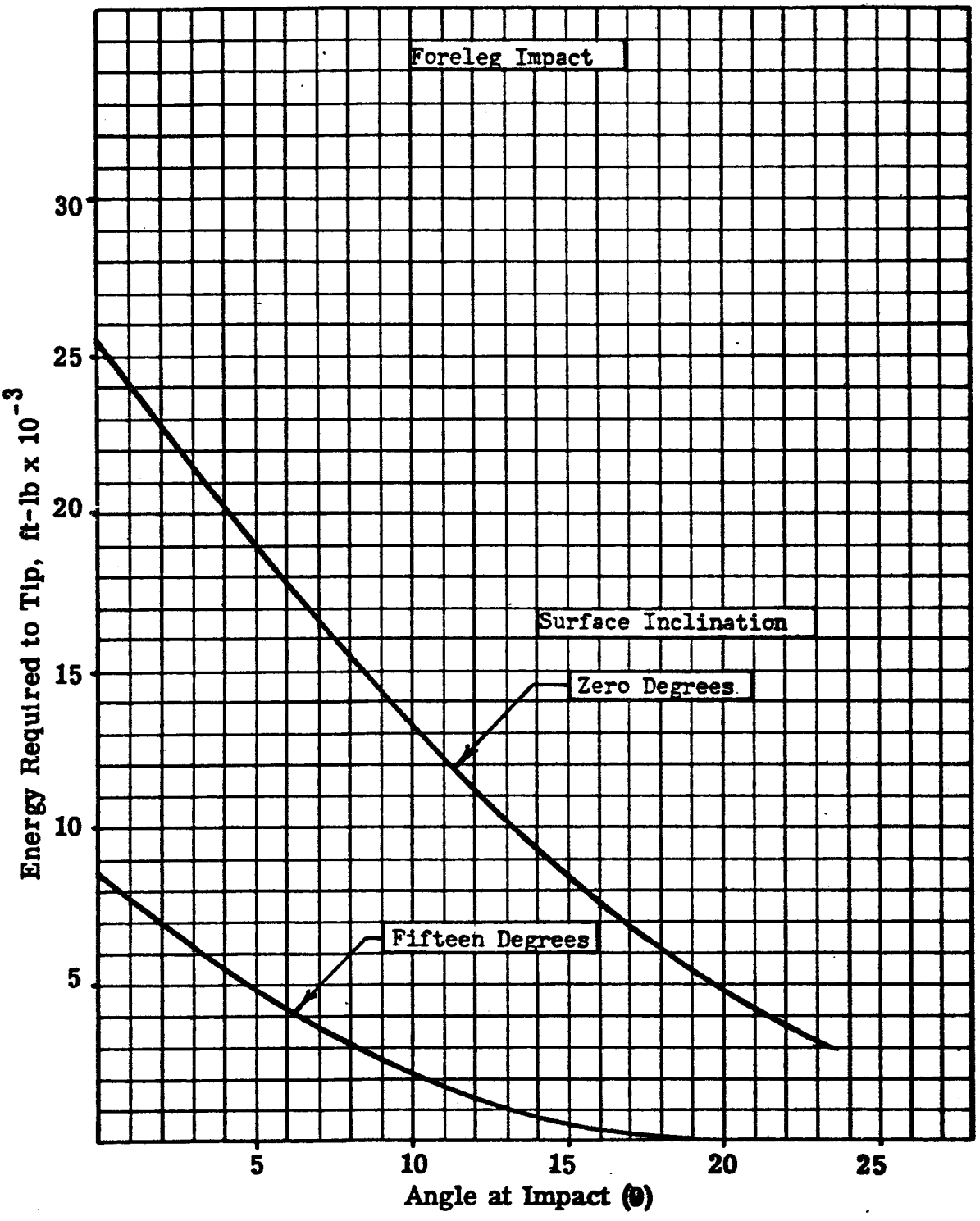

Fig. 113. Maximum Energy for Stable Lunar Landing

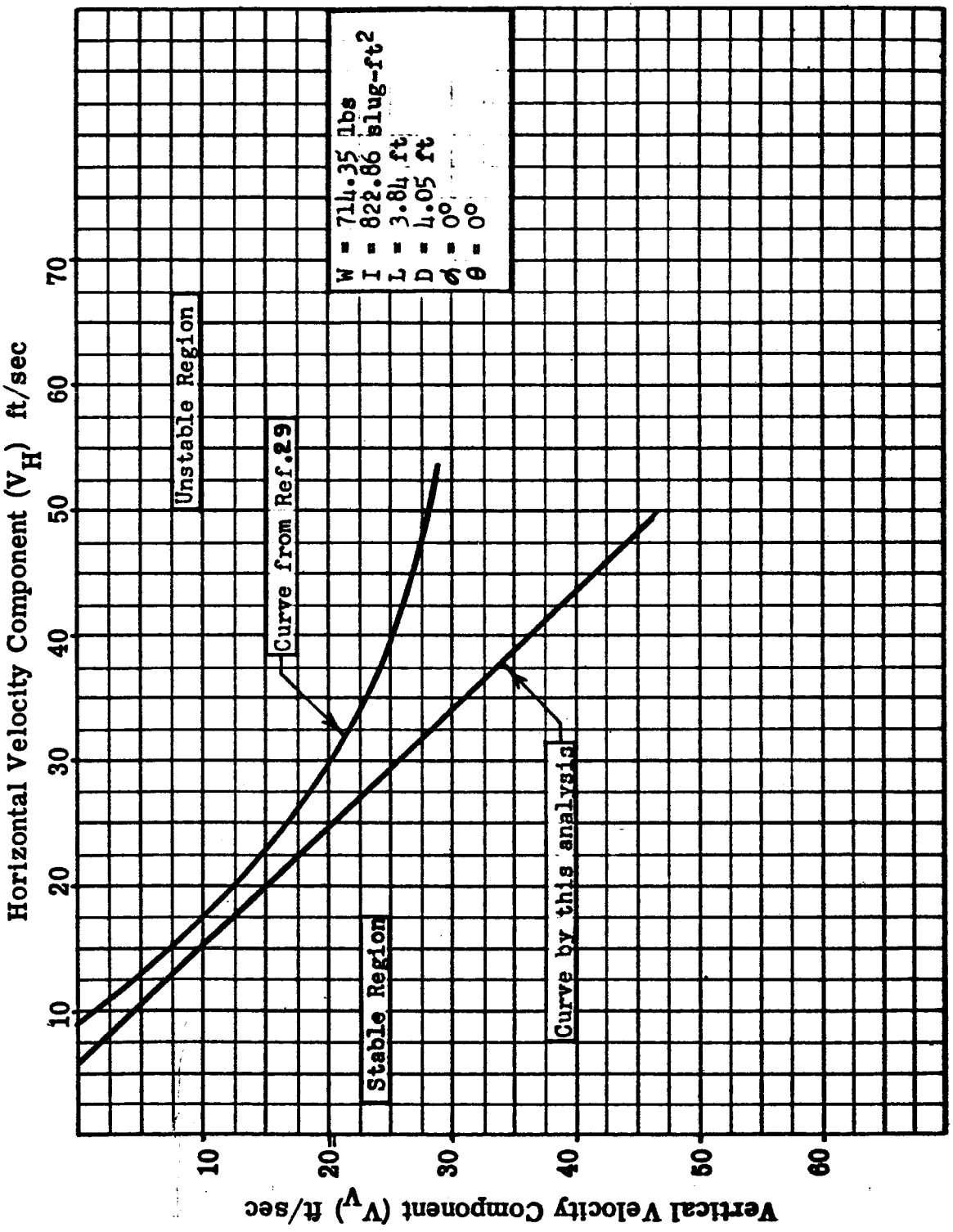

Fig. 11b. Comparison of Analytical Results

The results of a study of the effect of gravitational constant on impact stability are summarized in Figure 115. The term, critical lateral velocity, represents the maximum horizontal velocity component which can be tolerated (in conjunction with the indicated vertical velocity component) if the vehicle is to come to rest in an upright position. It is evident that for a given landing vehicle weight and geometry, the allowable velocity limits for stable impact are higher in a stronger gravitational field. This condition results from the fact that the increase in potential energy required to tip a vehicle is directly proportional to the local gravitational acceleration.

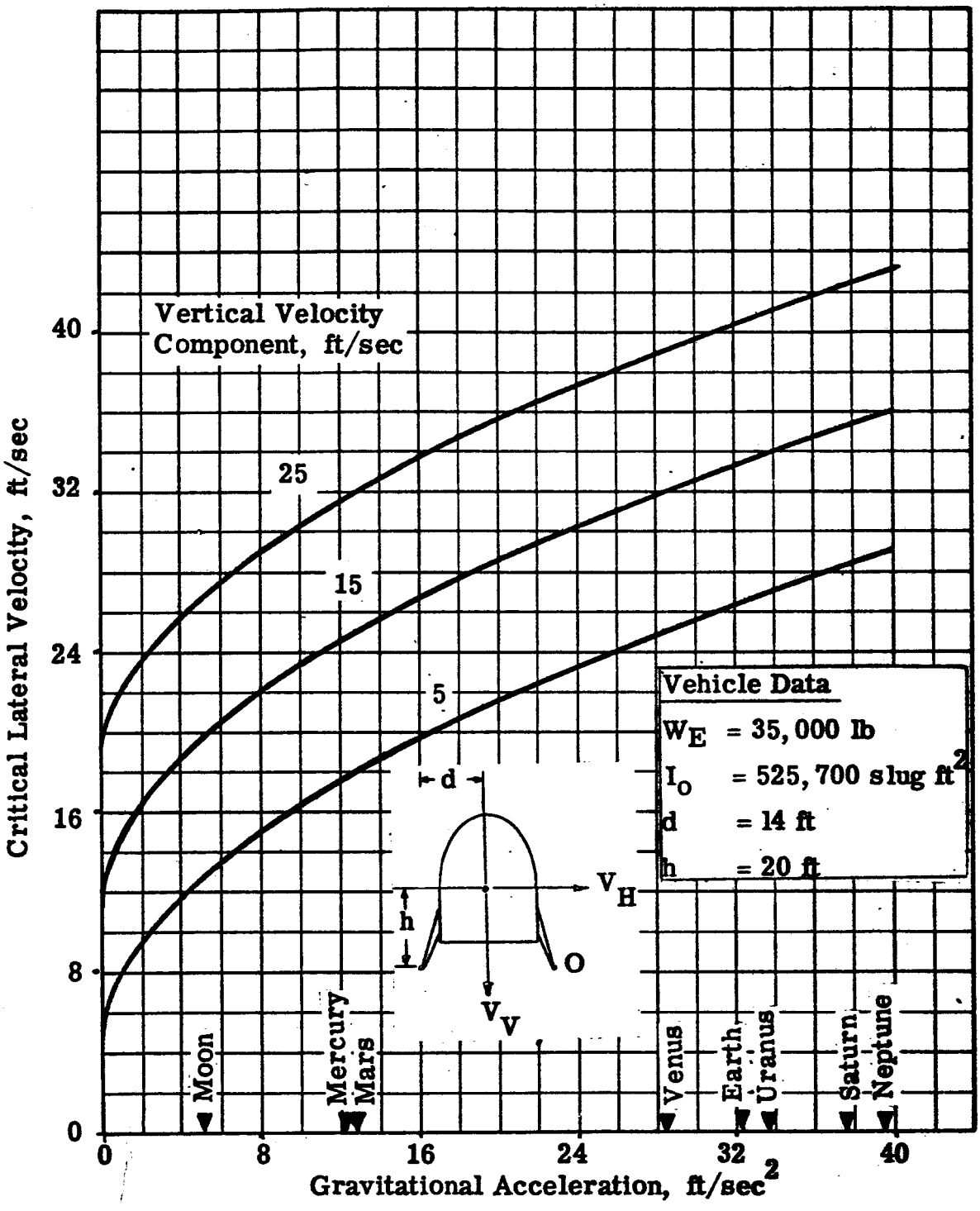

Fig. 115. Effect of Surface Gravity on Landing Vehicle Stability

EARTH-MERCURY MISSIONS

TRANSFER PHASE

Selection of an interplanetary trajectory for a Mercury mission is strongly dependent on the nature of the mission; e.g., an unmanned probe whose function is the collection of data enroute to, and in the immediate vicinity of, Mercury (and which subsequently goes into solar orbit or impacts the Sun or Mercury) requires a trajectory which minimizes Earth-departure propulsion requirements and disregards Mercury arrival conditions, while a soft-landing vehicle, either manned or unmanned, requires a trajectory which minimizes the combined propulsion requirements for the Earth-departure and Mercury-landing phases.

For a selected probe mission, the Earth-departure velocity requirements are presented in Figure 116 for a 1966 launch at near-minimum Earth departure velocity conditions. A 100-day transfer initiated on 15 December 1966 requires an Earth hyperbolic excess velocity of 21,500 ft/sec. The arrival velocity for this mission is 53,000 ft/sec.

In contrast to a probe mission, for a soft-landing mission, it is desirable to find trajectories such that the arrival velocity is lowered while increasing the launch velocity in order to minimize overall velocity requirements. From an optimum vehicle-system standpoint, it might be preferable to utilize trajectories biased toward higher-than-optimum departure velocity requirements in return for reductions in arrival velocity requirements, thereby reducing the amount of propellant which must be stored and shielded for approximately three months in the space environment.

Since detailed three-dimensional Mercury trajectory data are not presently available, an analysis of Mercury orbit establishment missions for the 1970-75 time period was performed using a Rocketdyne ballistic interplanetary trajectory program. The program calculates hyperbolic departure (V_h) and arrival velocities (V_a) for three-dimensional heliocentric conic section trajectories.

The results are presented in terms of hyperbolic velocities, and also as the impulsive velocity increments for the cases of departure from 300-n mi Earth orbit and establishment of 300-n mi Mercurian orbit. The hyperbolic velocity is related to impulsive velocity for orbit-establishment by:

$$V_I = (V_h^2 + V_p^2)^{1/2} - V_{co}$$

where V_{co} is the circular orbit velocity and V_p is the planetary escape velocity at the parking orbit altitude.

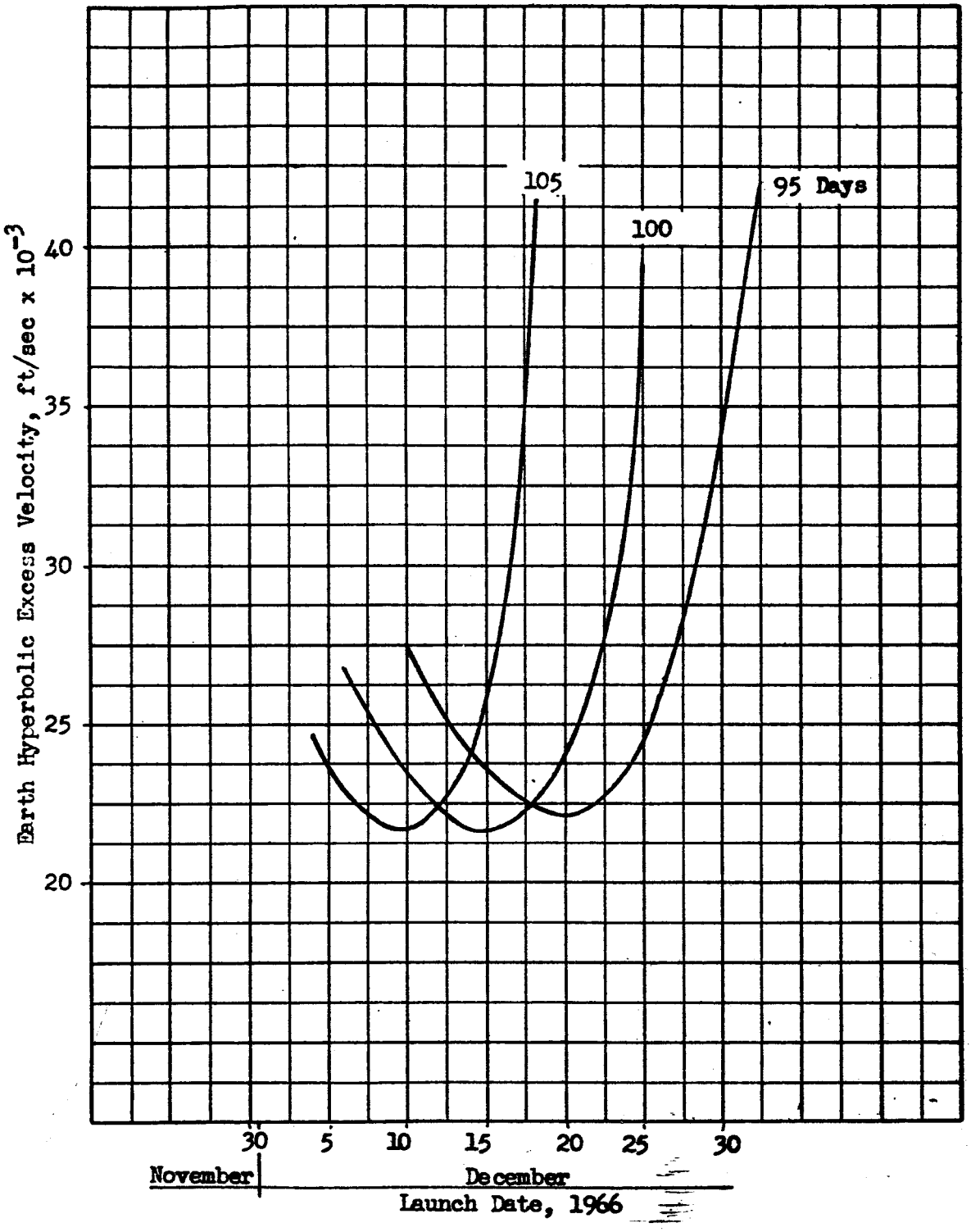

Figure 116. Earth-Departure Velocity Requirements for Mercury Missions

Transfer Trajectory Criteria

The analysis was based on a transfer trajectory in a plane defined by the vehicle (at Earth launch), the Sun, and the rendezvous position at the target planet. Therefore, because of the inclination angle (7 deg 0 min) between the orbital plane of Mercury and the ecliptic, a plane-change from the ecliptic is required. To minimize guidance requirements, this plane change is made at launch for the missions considered; therefore, as the angular travel of the trajectories approaches 180 degrees, the inclination of the transfer plane with respect to the ecliptic approaches 90 degrees. As this occurs, the Earth's heliocentric orbital velocity provides a progressively smaller fraction of the vehicle transfer velocity, and the energy requirements increase correspondingly. Of course, if the transfer is made from node to node, the three defining points lie on a straight line, and therefore, the trajectory plane may have any desired inclination.

The goal of the probe mission trajectory was to minimize the launch velocity. This was achieved by finding trajectories in which the vehicle reached Mercury near its aphelion, after approximately 160 degrees of angular travel about the Sun. An ecliptic projection sketch of this trajectory is depicted in Figure 117. For this trajectory, there is a fairly large angle between the velocity vectors of the vehicle and Mercury at rendezvous. At this time, the magnitude of the (heliocentric) velocity of the vehicle is 167,000 ft/sec, and that of Mercury is 128,000 ft/sec.

To achieve a suitable trajectory for a Mercury landing mission, it is necessary to (a) reduce the angle between the two velocity vectors and (b) reduce the difference in magnitude of the two velocities, thereby reducing the vector difference of the velocities, which is the hyperbolic arrival velocity.

The angle between the velocity vectors may be reduced in the desired trajectory by launching at a nodal point such that the vehicle is injected into the plane of the orbit of Mercury and traverses an angular travel such that the orbits are nearly cotangent at rendezvous.

The possibility of such a nodal transfer was investigated for the 1970-1975 time period. Trajectory computations indicated that, while no exact nodal transfer cotangent to the orbit of the Earth at launch and the orbit of Mercury at arrival can occur in the time period considered, a near-nodal trip may be performed in 1973, launching at the descending node.

By launching at the descending node in 1973, the vehicle is injected into the plane of Mercury and then the total vehicle angular travel is made as near 180 degrees as the aforementioned constraints will allow. The transfer

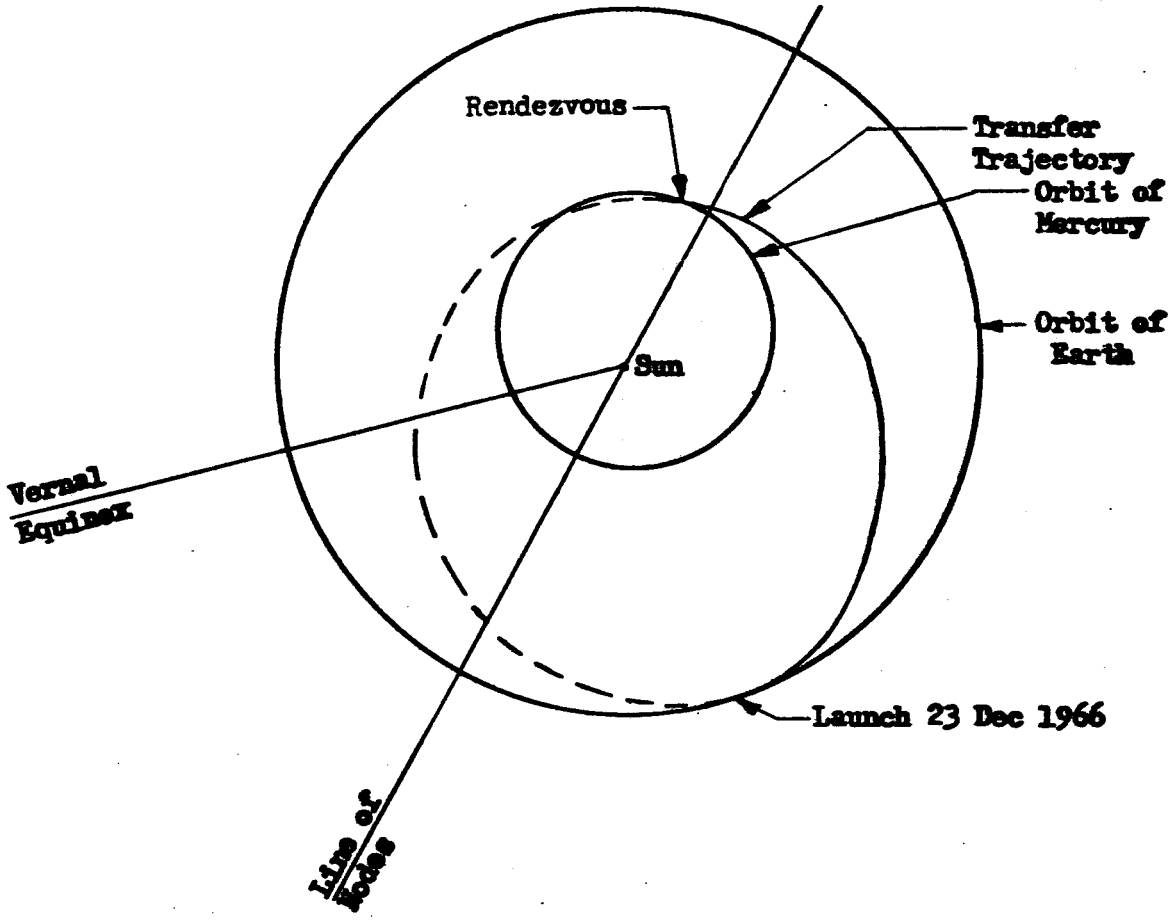

Fig. 117.100-Day Earth-Mercury Trajectory

is thereby made as near to minimum-energy (Hohmann) as possible. This transfer trajectory is illustrated in Figure 118. By launching the vehicle approximately at the node, it is injected very nearly into the orbit of Mercury. In addition, the orbits are nearly cotangent at rendezvous.

Selected Transfer Trajectory

Earth-Mercury trajectories are characterized by the fact that a small variance in trip time and/or launch date produces sharp increases in energy requirements. Since precise launch dates are difficult to guarantee, an array of trajectories was computed about this nodal launch to indicate the effects of varying launch date and trip time. The results are presented in Figures 119 and 120 in the form of contour charts.

The minimum energy transfer in this array is a 90-day trip, launched on 10 May 1973. The trajectory is characterized by a hyperbolic departure velocity of 31,000 ft/sec, (a 22,000 ft/sec impulsive ideal velocity increment to depart from a 300-n mi Earth parking orbit). The hyperbolic arrival velocity is 27,000 ft/sec, (a 21,000 ft/sec impulsive velocity increment establishes a 300-n mi Mercurian circular orbit).

The hyperbolic arrival velocity magnitude is 30,000 ft/sec or less if the launch occurs in the interval 6 May to 13 May 1973 (Figure 121). There is infrequent cyclic repetition for this mission; the next time a fairly-similar transfer can be accomplished is 1986. For intervening launch dates, minimum hyperbolic arrival velocities will be considerably higher (on the order of 50,000 ft/sec).

MERCURY ORBIT ESTABLISHMENT

Deceleration from the Earth-Mercury transfer trajectory (30,000 ft/sec hyperbolic arrival velocity) into a 300-n mile circular, Mercurian orbit requires a velocity change in excess of 23,000 ft/sec. For finite thrust systems of practical interest, this corresponds to an ideal velocity increment close to 24,000 ft/sec. Single stage systems for this maneuver were analyzed; however, this magnitude of ΔV represents essentially the practical limit of capability for single stage propulsion systems. The task is better suited to two-stage (or staged propellant tanks) vehicle systems, which were also evaluated.

Single Stage Analysis

For the analysis of single stage propulsion systems, the nonographs presented in Figures 122 and 123 (in conjunction with techniques described previously for Earth orbit-establishment maneuvers) were utilized. The

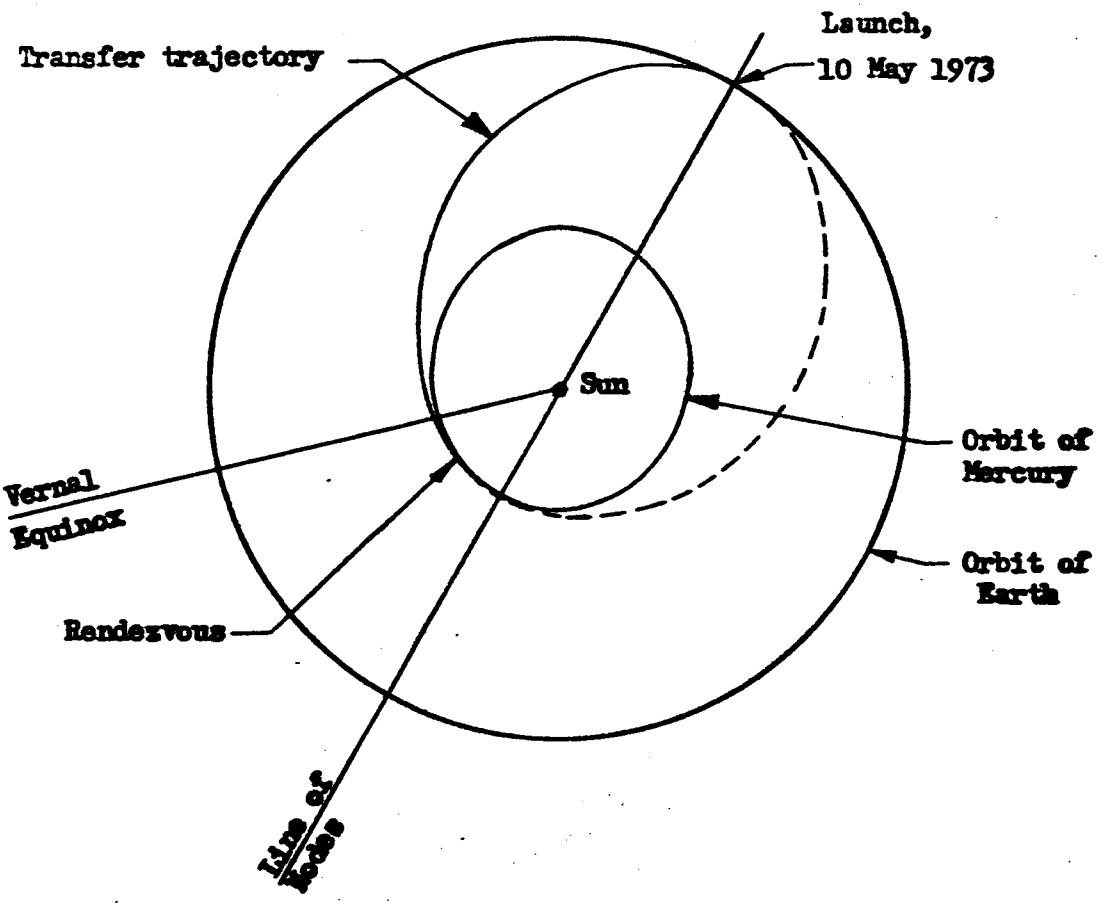

Fig.118. 90-Day Earth-Mercury Trajectory

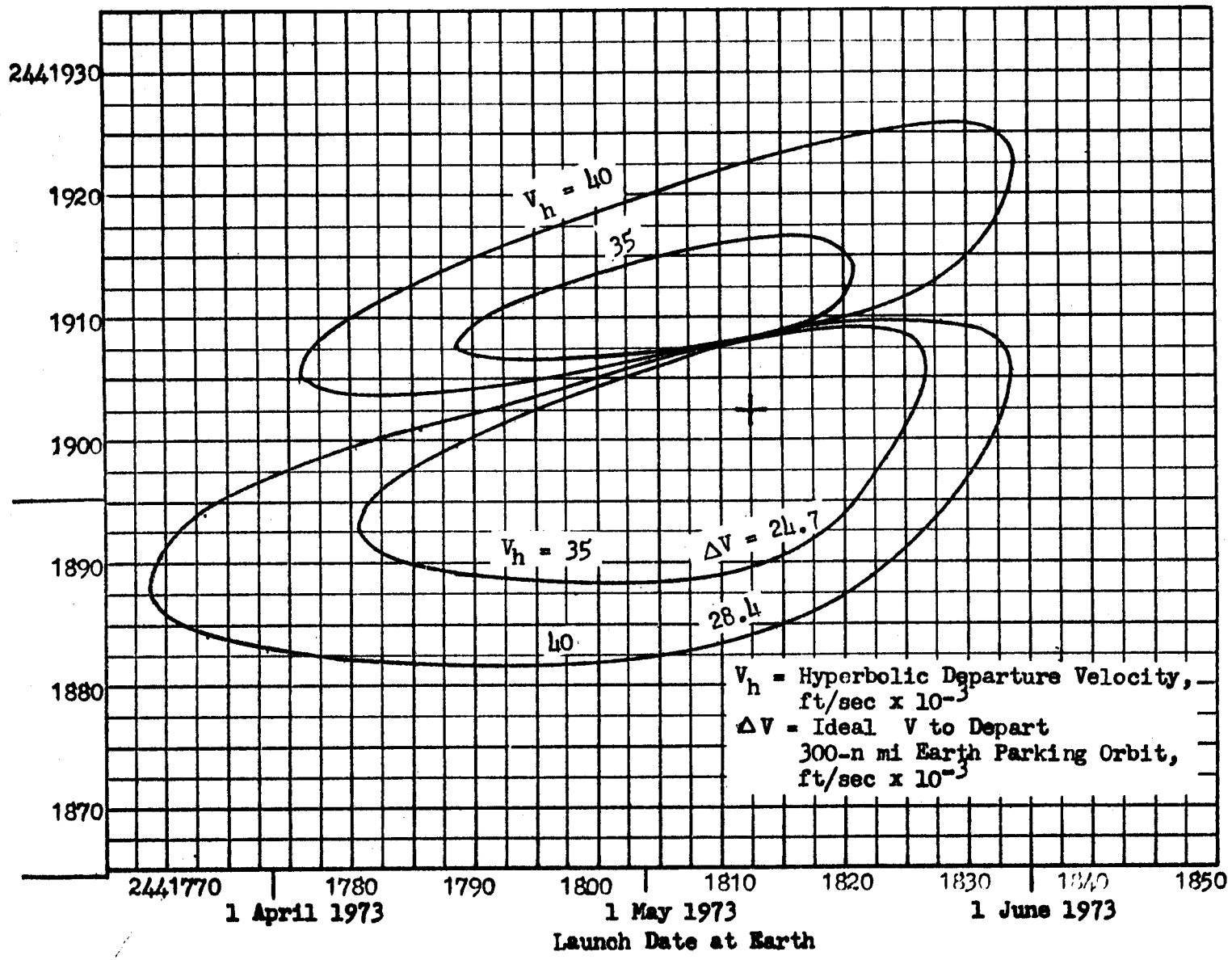

Figure 119 . Earth Departure Velocity Contours

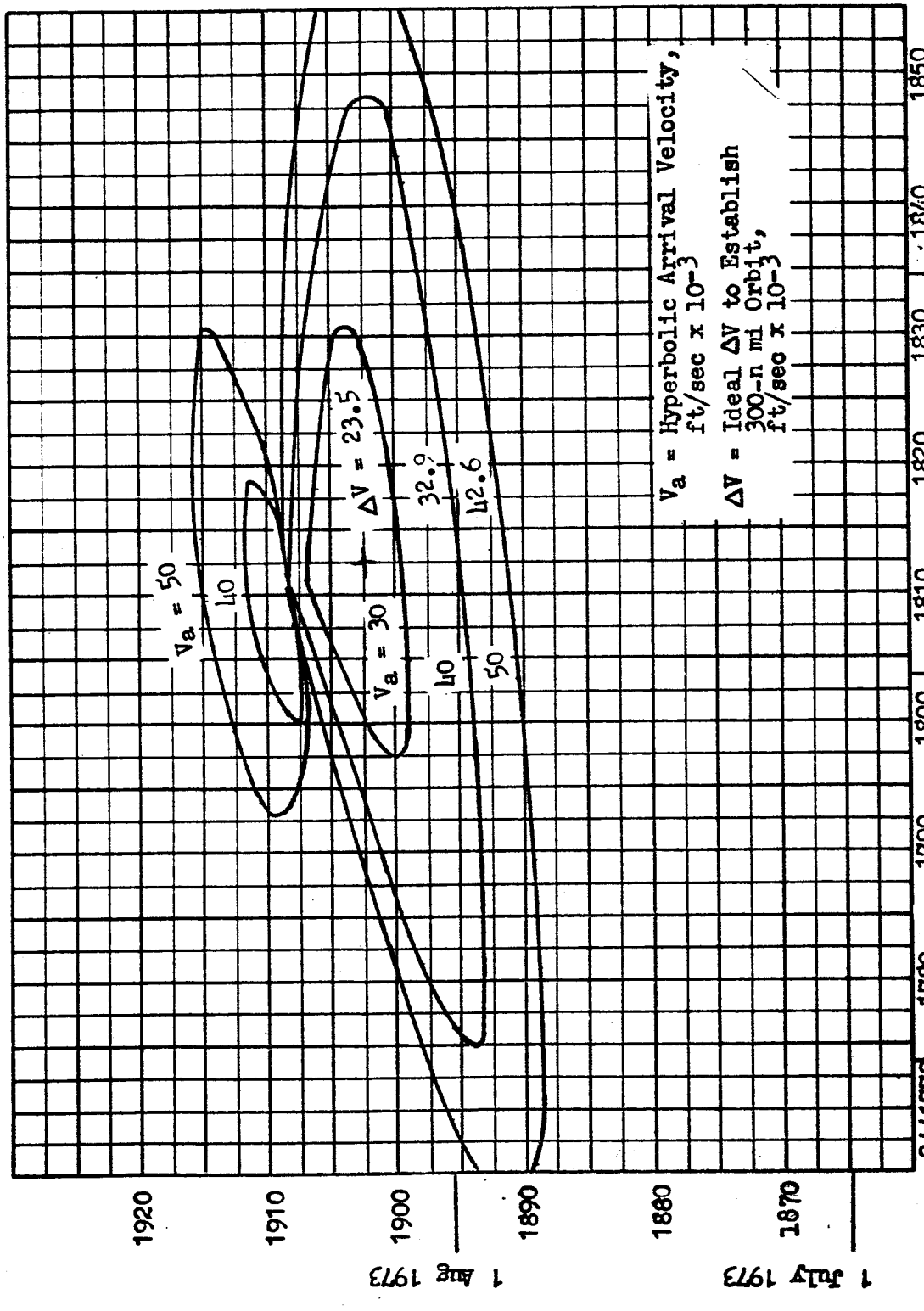

Figure 120 . Mercury Arrival Velocity Contours

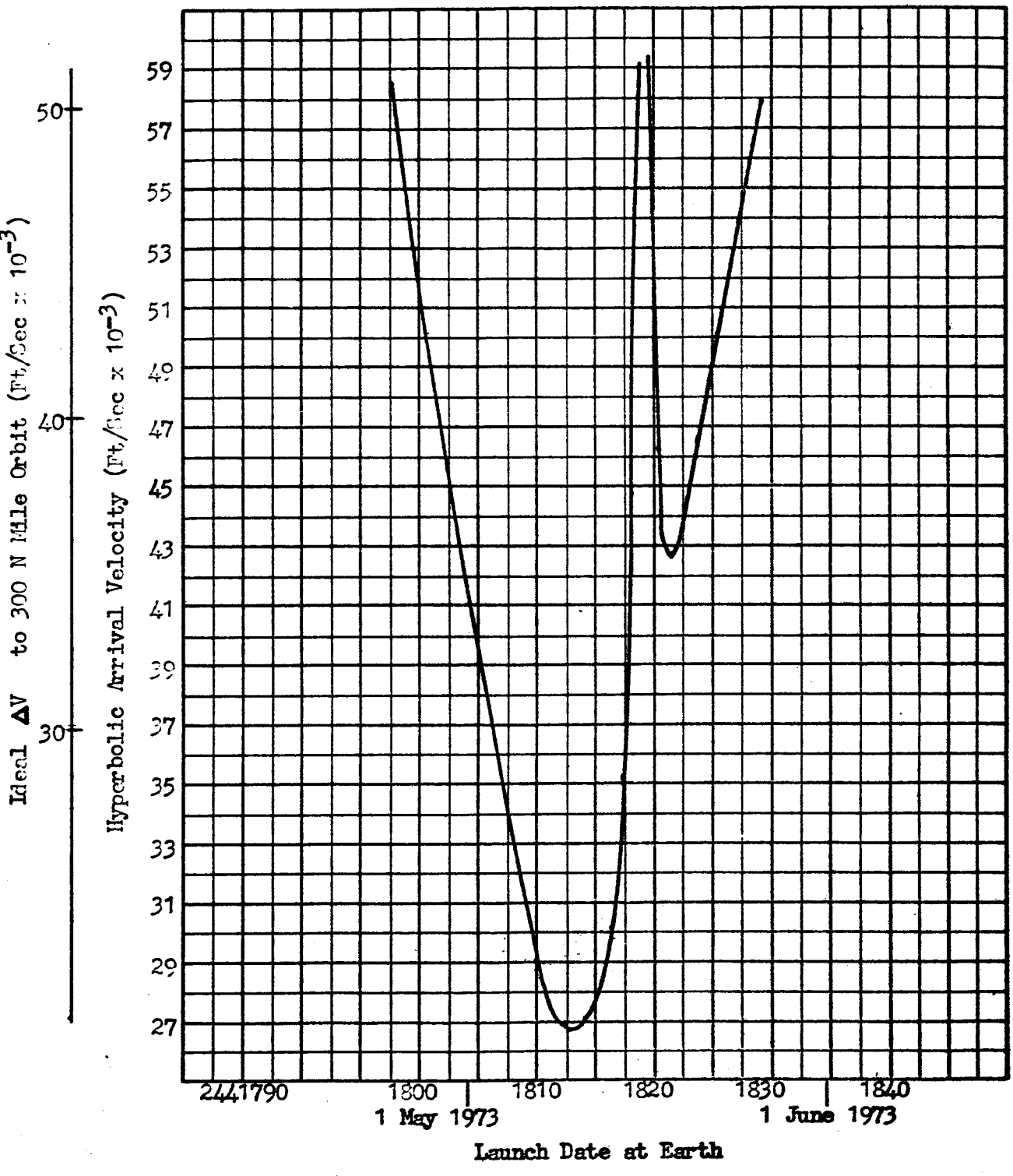

Fig. 121. 90-Day Earth-Mercury Trajectory Data

CONSTANT THRUST
CONSTANT SPECIFIC IMPULSE
TANGENTIAL THRUST PROGRAM

CURVE "A"

SPECIFIC IMPULSE, SEC

800
700
600
500
400
300
200

500 480 460 440 420 400 380 360 340 320 300 280 260 240 220 200 180 160 140 120 100 80 0

10,000 20,000 30,000

TOTAL IMPULSE-TO-WEIGHT RATIO (FT/W_o), LB-SEC/LB

MERCURY HYPERBOLIC EXCESS VELOCITY (V_∞), FT/SEC

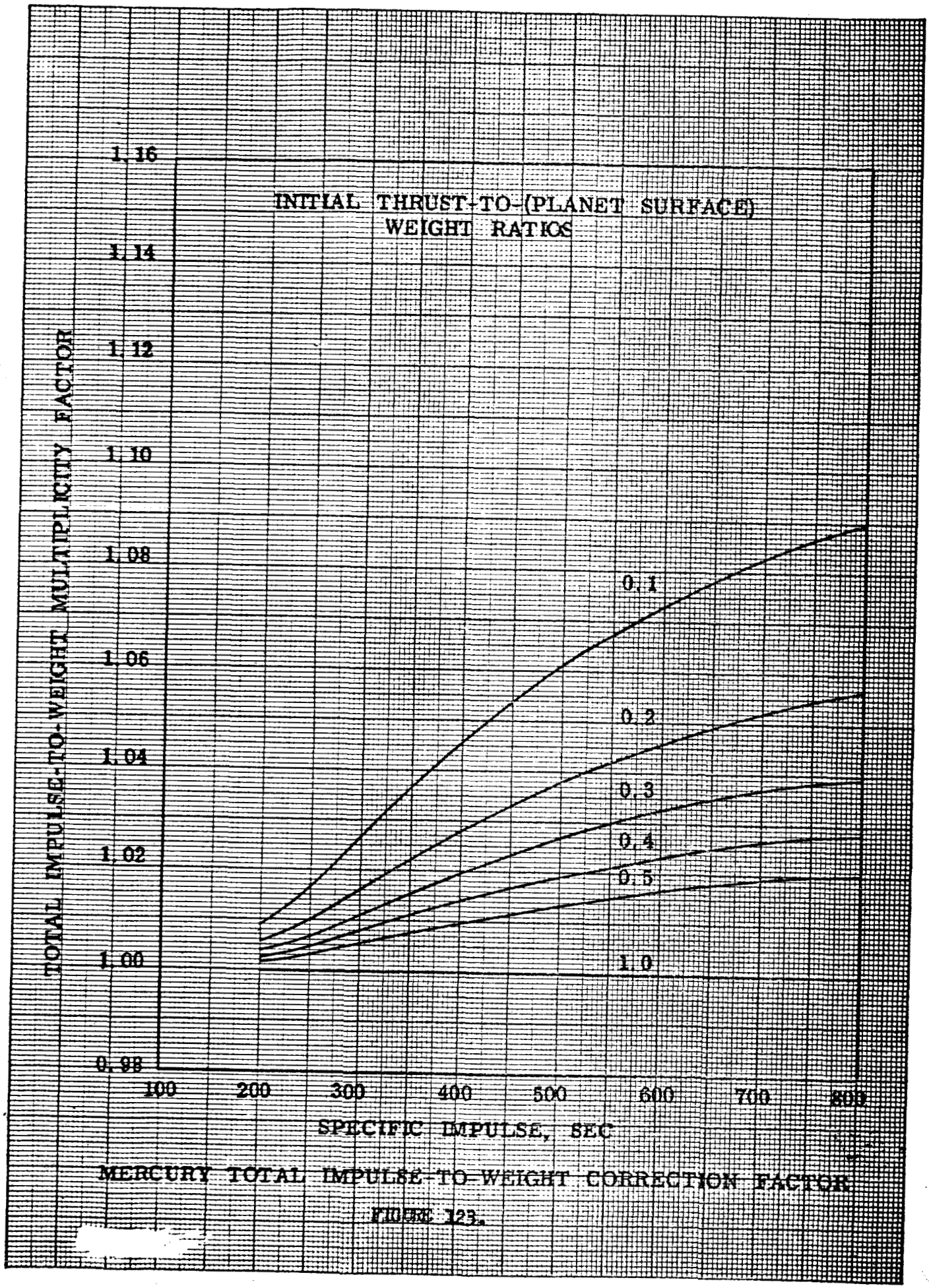

MERCURY TOTAL IMPULSE-TO-WEIGHT CORRECTION FACTOR

FIGURE 123.

results for a propulsion system representative of a pump-fed O_2/H_2 system are presented in Figure 124 . It is important to note that most of the indicated payloads are negative; for the best case shown, only one percent of the initial transfer vehicle becomes useful payload in Mercury orbit. This result points to a need for more efficient systems than single stage chemical rockets for use in Mercury orbit establishment maneuvers.

Multistage Analysis

Because the 23,560 ft/sec impulsive ideal velocity requirement for establishment of a 300-n mi Mercury orbit from a 30,000 ft/sec hyperbolic arrival velocity is a rather high ideal velocity to be supplied by a single stage using conventional chemical propellants, a study was conducted to evaluate the payload advantage of a vehicle with tank staging or a two-state vehicle in comparison to a reference single stage vehicle. The purpose was also to determine the optimum thrust-to-weight ratios for the three systems.

The vehicle comparisons presented are for a system with 400 seconds specific impulse; this I_s value was selected to be representative of various high-energy propellants. Orbit establishment was accomplished by means of a thrust-parallel-to-velocity maneuver. Vehicle jettisoned weights were assumed equal to the sum of a propellant-dependent weight and a thrust-dependent weight, where propellant-dependent weight = 0.08 x stage propellant weight, and thrust-dependent weight = 0.02 x stage thrust level.

A higher payload than that obtained by the use of a conventional single stage vehicle can be achieved if the stage propellant is stored in several tanks, and each tank is jettisoned (tank staging) when its propellant has been consued. For the single stage vehicles with tank staging, the propellant was assumed to be divided between two or more tank units with all tank units of equal volume. The weight of the tank units was determined using the propellant-dependent weight factor. No additional inert weight was included for the added fixtures which a jettisonable tank unit would require, which results in somewhat optimistic values of payload for tank-staged vehicles. The thrust-dependent weight was added to the final tank unit which remained at the end of the propulsive phase to obtain final vehicle burnout weight.

Results of Investigation

The ideal velocity requirement for a 300-n mi Mercury orbit establishment maneuver is presented in Figure 125 for a single stage vehicle and for a vehicle with continuous tank staging (emptied tanks are jettisoned an infinite number of times). The ideal velocity requirements are almost identical. The results presented in Figure 126 show payload-to-gross weight

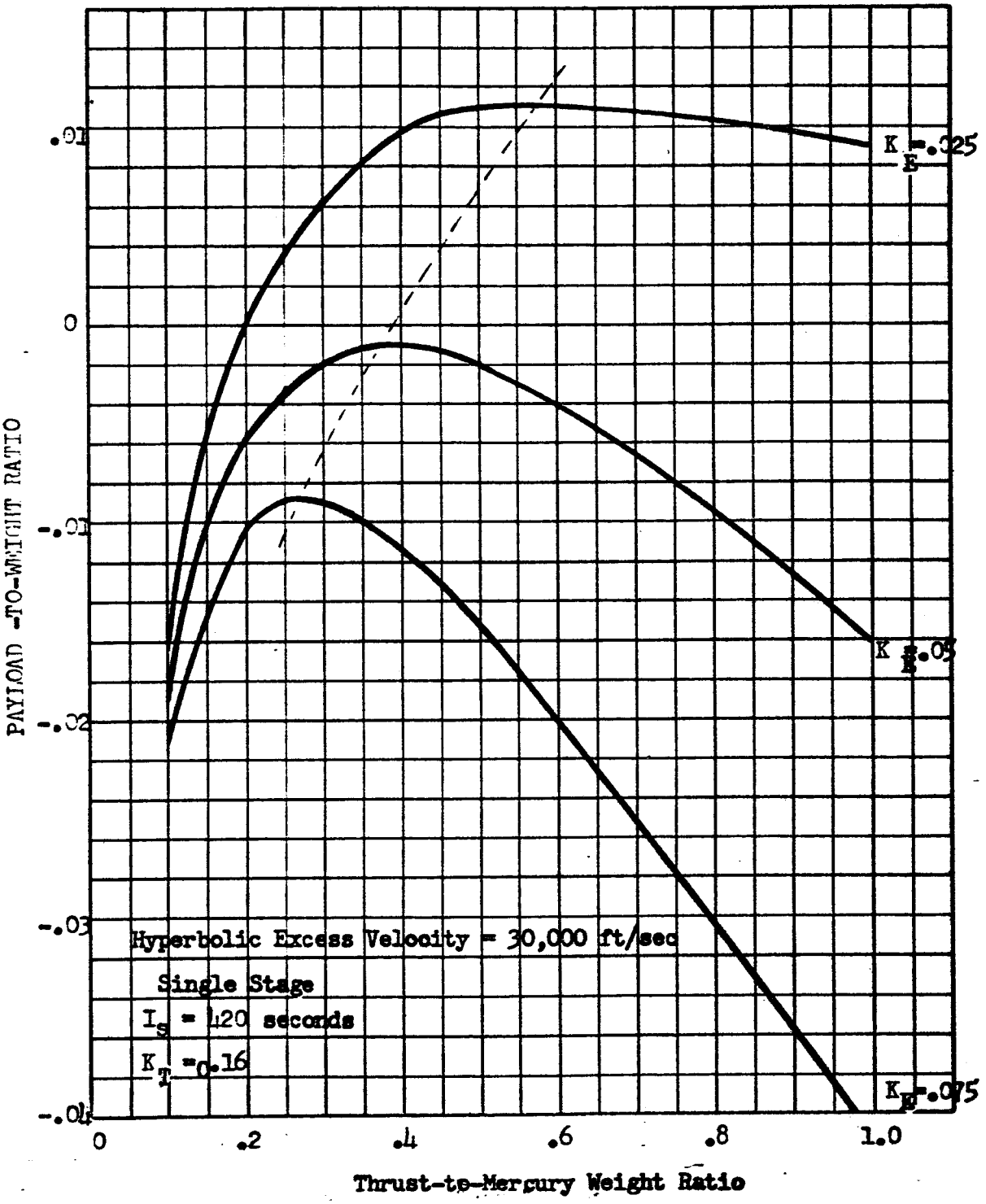

Figure 124. Orbit Establishment Maneuver Thrust-to-Weight Optimization for Mercury

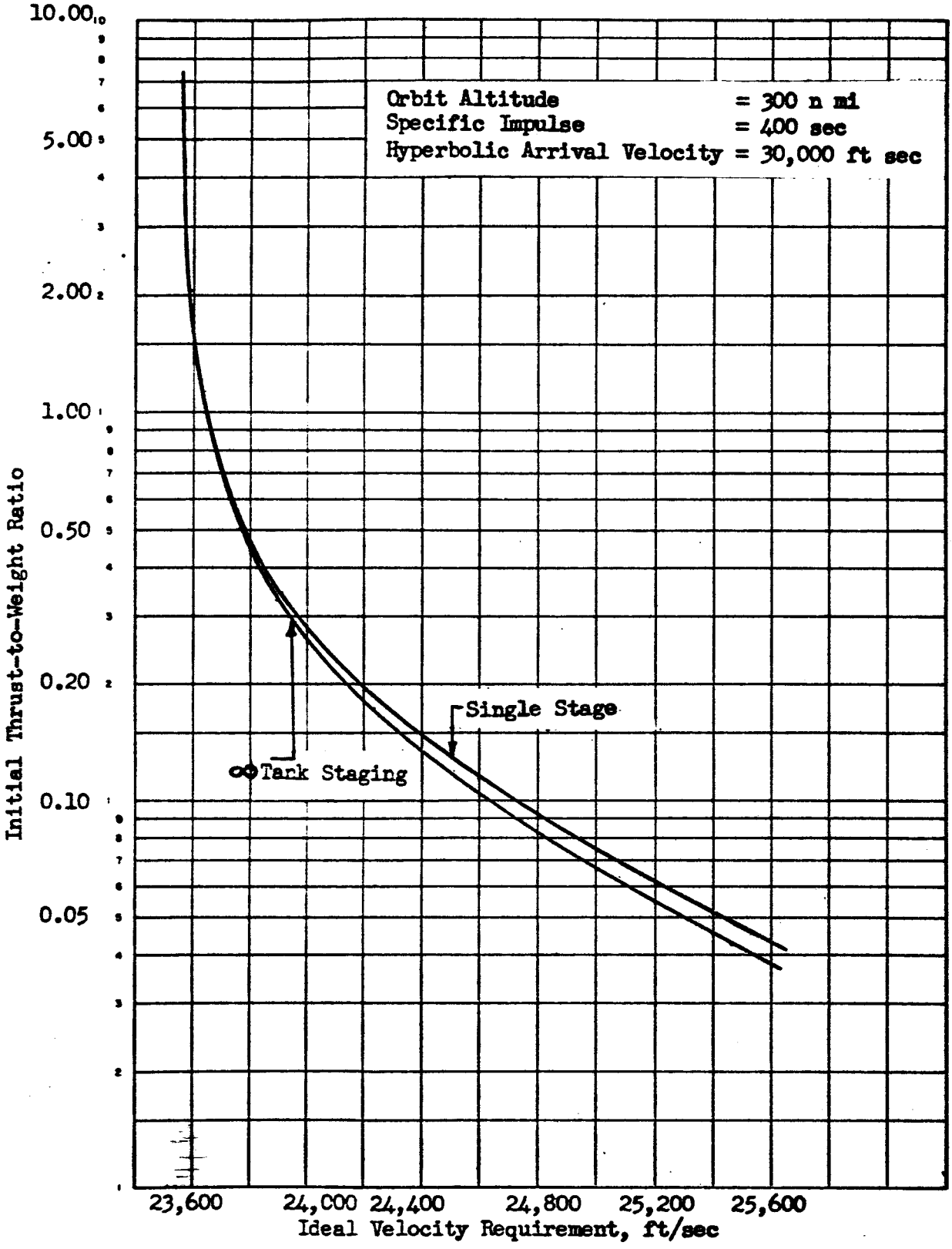

Figure 125 . Mercury Orbit Establishment
Ideal Velocity Requirement

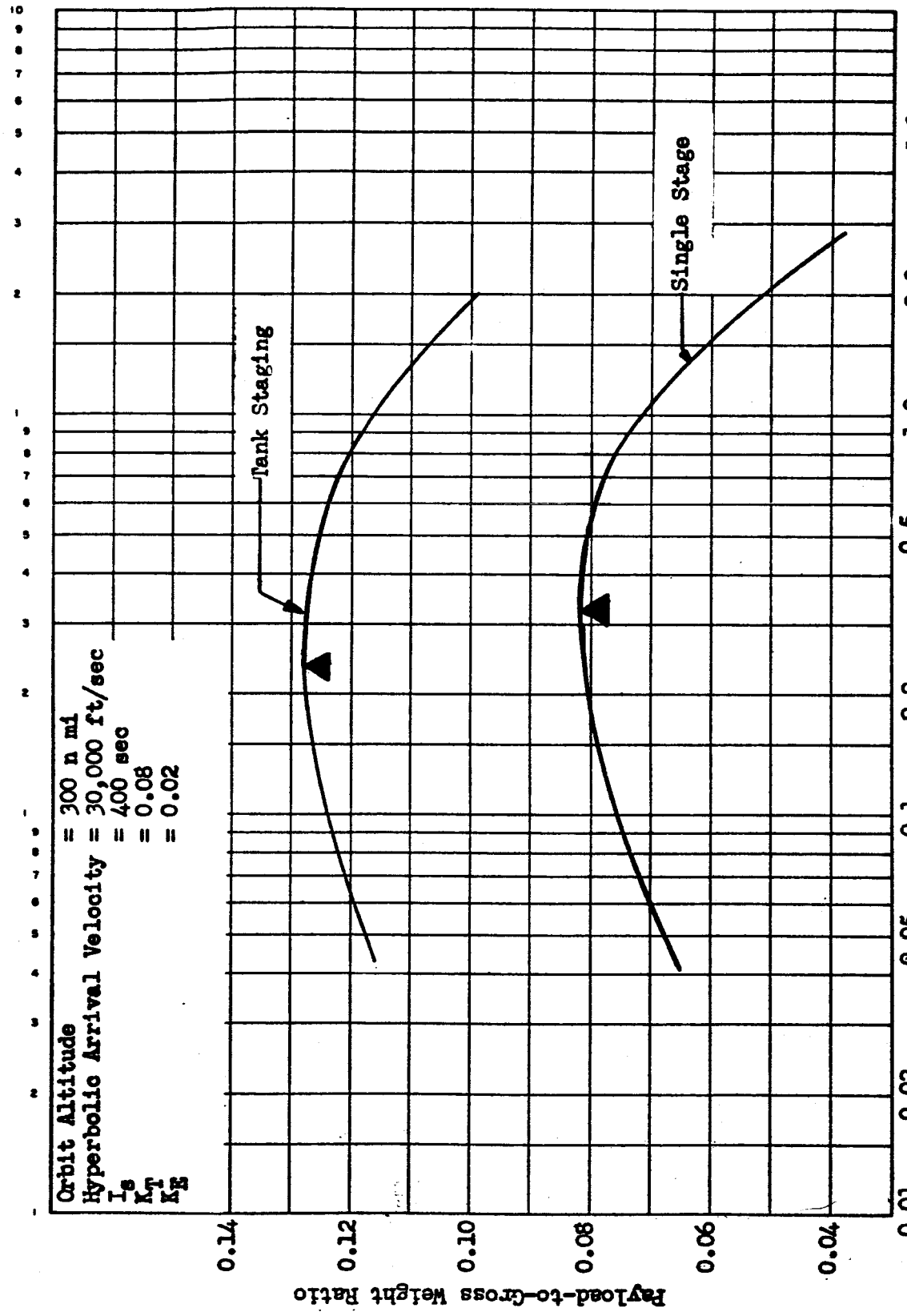

Figure 126. Mercury Orbit Establishment Vehicle Payload-to-Gross Weight Ratio

ratio as a function of initial thrust-to-weight ratio for each of these two orbit-establishment systems. For the single-stage vehicle, the optimum thrust-to-Earth weight ratio is 0.31 and the corresponding maximum payload-to-gross weight ratio is 0.081, while for the continuous tank-staging vehicle, the optimum thrust-to-weight ratio is 0.24, and the payload to-gross weight is 0.127.

In figure 127,payload-to-gross-weight ratio is presented as a function of the number of times tanks are jettisoned. (This figure was based on the assumption that all the tank-staging vehicles required an ideal velocity requirement equal to that of the single stage vehicle.) An initial thrust-to-weight ratio of 0.3 was utilized to obtain the data presented in Figure 127; the results shown in Figure 126 indicate that this initial thrust-to-weight ratio gives very nearly maximum values of payload-to-gross weight ratio for both single-stage and tank-staging vehicles.

For the two-stage Mercury orbit establishment vehicle, the ideal velocity requirement depends upon the thrust-to-weight ratios of both stages.

Ideal velocity requirement versus initial first stage thrust-to-Earth weight ratio, for four different ratios of second stage/first stage thrust-to-weight ratios are presented in Figure 128. For the two-stage vehicles, the total mission ideal velocity requirement is divided evenly between the two stages. In Figure 129, the variation of payload-to-gross weight ratio with initial first stage thrust-to-weight ratio for two-stage orbit-establishment vehicles is shown. These data indicate that the maximum vehicle payload-to-gross weight ratio results when both stages have thrust-to-stage weight ratios of 0.5.

Though primary emphasis was on a hyperbolic arrival velocity of 30,000 ft/sec, the effect of hyperbolic arrival velocity on vehicle performance was evaluated for the three types of vehicles considered in this study. Vehicle payload-to-gross weight ratios are presented in Table 8 for hyperbolic arrival velocities of 20,000, 30,000, 40,000 and 50,000 ft/sec. The single-stage and infinite tank-staging vehicles both have initial thrust-to-weight ratios of 0.3. The two-stage vehicle has an initial thrust-to-weight ratio of 0.5 in each stage.

Orbit-Establishment Vehicle Comparison. A single-stage vehicle, a two-stage vehicle, and a tank-staging vehicle are compared in Tables 9 and 10 for the 30,000 ft/sec hyperbolic arrival velocity Mercury orbit-establishment mission. An optimum thrust-to-weight ratio and the range of thrust-to-weight ratios which could be used and deliver a payload which is within 2 percent of the optimum payload value are presented in Table 9 .

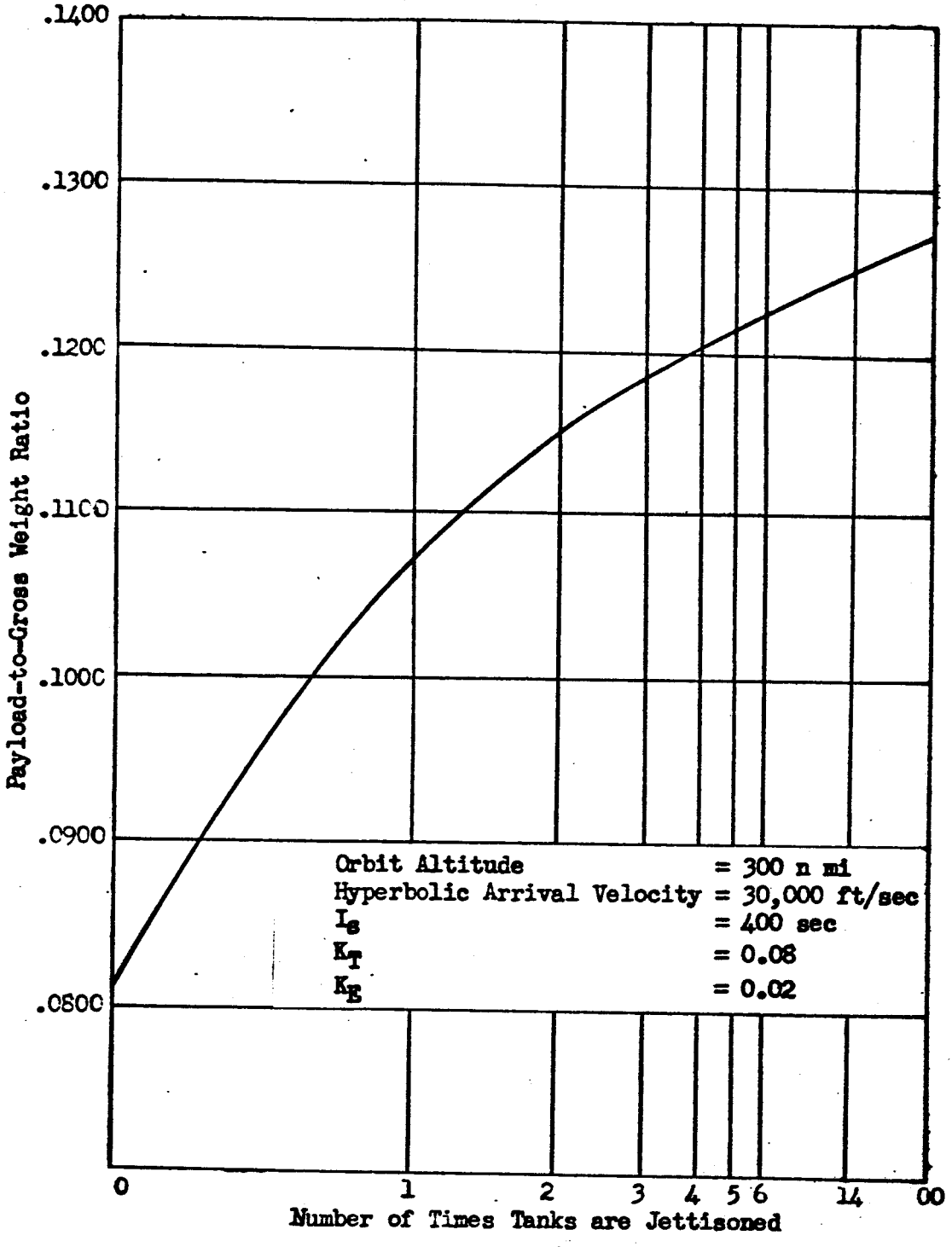

Figure 127 . Mercury Orbit Establishment; Tank Staging Vehicle Payload-to-Gross Weight Ratio

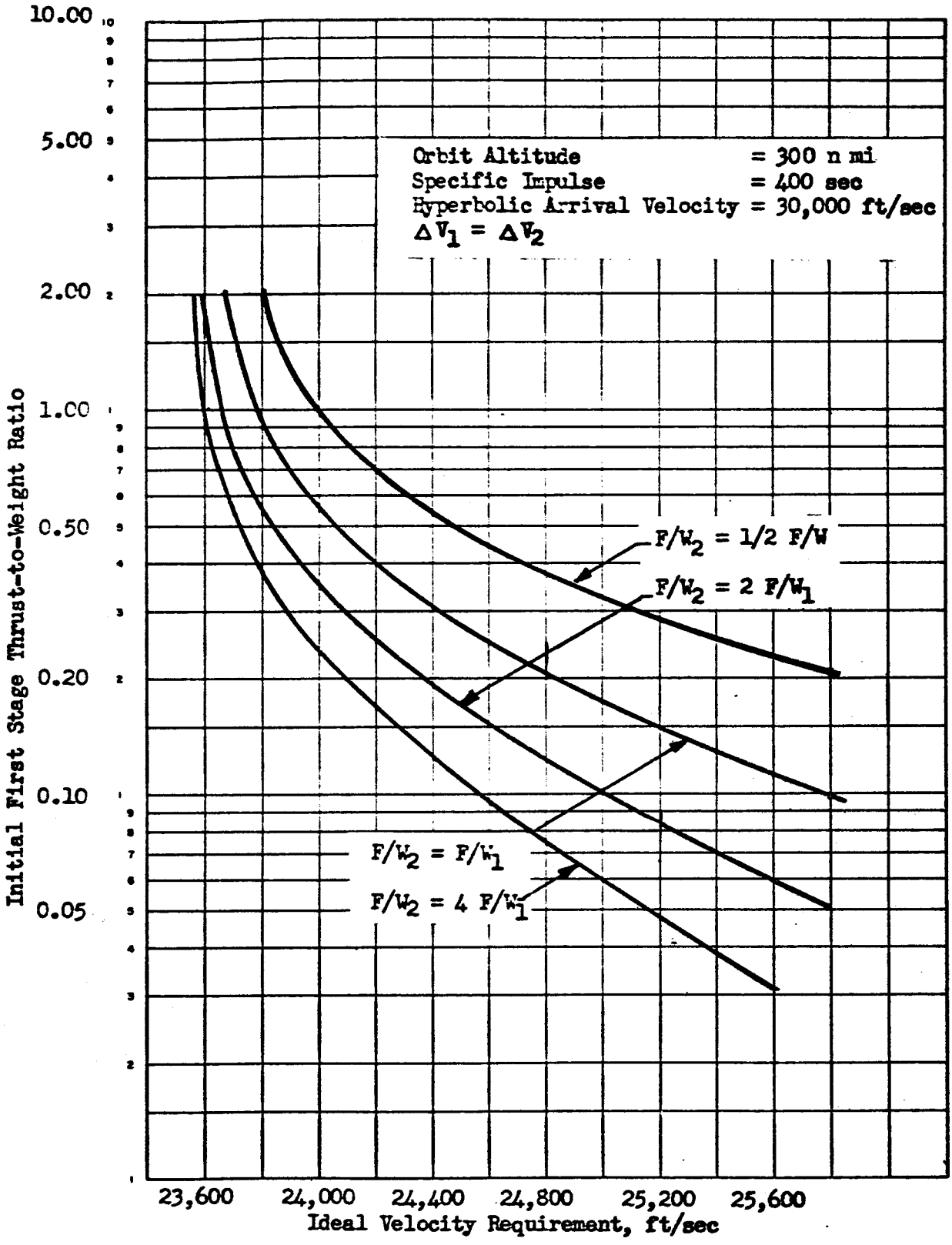

Figure 128. Two-Stage Vehicle Mercury Orbit Establishment Ideal Velocity Requirement

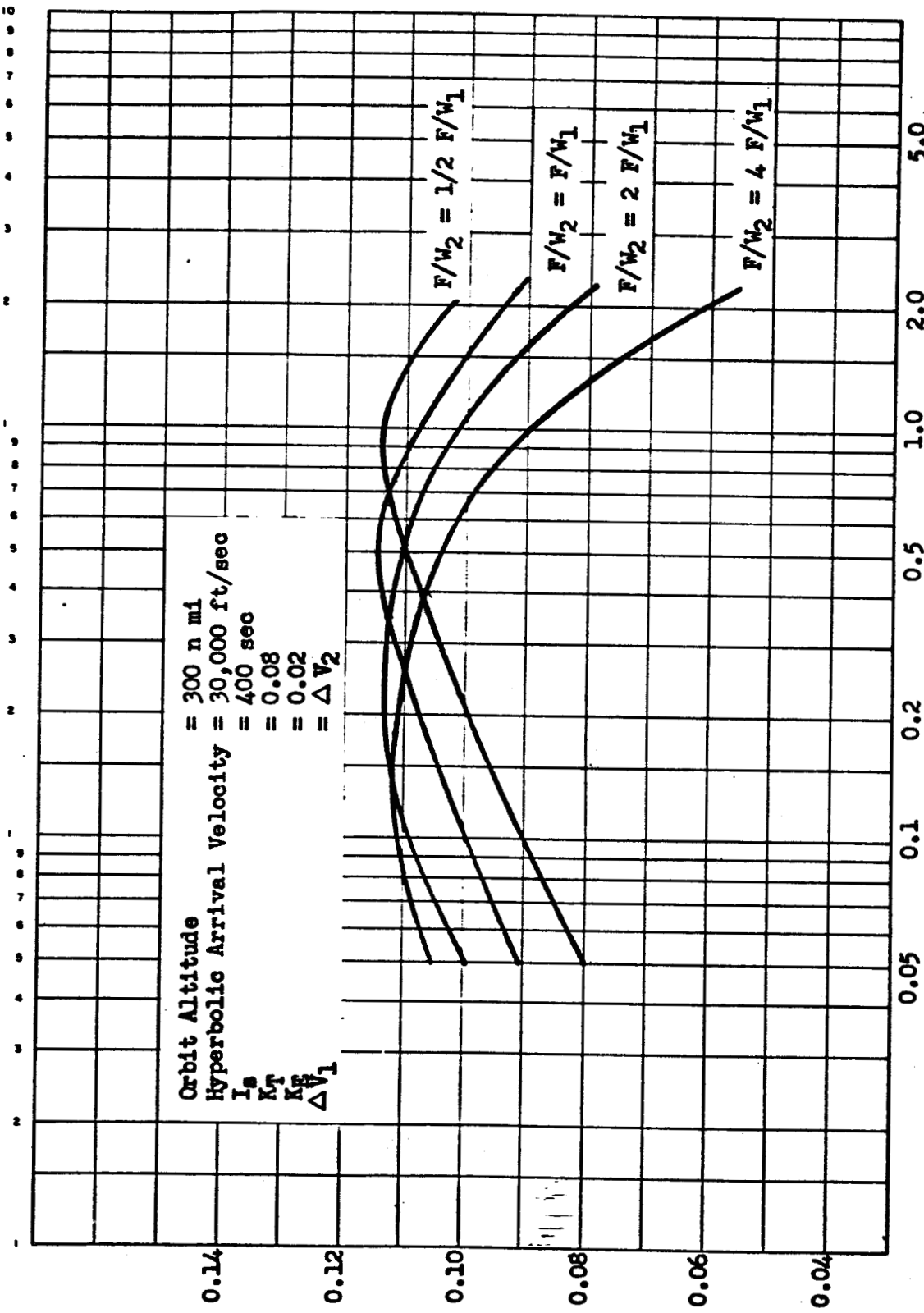

Figure 129 . Two Stage Mercury Orbit Establishment Vehicle
Payload-to-Gross Weight Ratio

TABLE 8

EFFECT OF HYPERBOLIC ARRIVAL VELOCITY ON PAYLOAD

Vehicle	Payload-to-Gross Weight Ratio			
	V_H*=20,000	V_H=30,000	V_H=40,000	V_H=50,000
Single Stage	0.251	0.081	-0.006	-0.048
Two-Stage	0.265	0.114	0.041	0.012
oo Tank Staging	0.279	0.128	0.055	0.021

Vehicle	Percent of V_H = 30,000 Payload			
	V_H=20,000	V_H=30,000	V_H=40,000	V_H=50,000
Single Stage	310	100	0	0
Two-Stage	230	100	36	10
oo Tank Staging	220	100	43	16

*V_H = Hyperbolic Arrival Velocity ft/sec

TABLE 9

MERCURY ORBIT ESTABLISHMENT VEHICLE

OPTIMUM THRUST - TO - WEIGHT RATIO

Mission: 30,000 ft/sec Hyperbolic Arrival Velocity Orbit Establishment

Vehicle	Optimum Initial F/W*	Initial F/W Range for - 2 percent Payload
Single Stage	0.31	0.17 → 0.53
Two-Stage		
$F/W_2 = 0.5\ F/W_1$		0.66 → 1.20
$F/W_2 = F/W_1$	0.5	0.31 → 0.82
$F/W_2 = 2\ F/W_1$		0.18 → 0.40
$F/W_2 = 4\ F/W_1$		0.15 → 0.20
oo Tank Staging	0.24	0.12 → 0.49

* Thrust-to-Weight Ratio

TABLE 30

MERCURY ORBIT ESTABLISHMENT VEHICLE ΔV AND PAYLOAD

Mission: 30,000 ft/sec Hyperbolic Arrival Velocity Orbit Establishment

Vehicle	Approximate Ideal Velocity Requirement, ft/sec	Payload to Gross Weight Ratio	Percent of Single Stage Payload
Single Stage ($F/W = 0.3$)	24,000	0.081	100
Two-Stage ($F/W_1 = 0.5$) ($F/W_2 = 0.5$)	24,000	0.114	141
Single Stage Tanks Jettisoned One Time ($F/W = 0.3$)	24,000	0.017	132
Single Stage Tanks Jettisoned Four Times ($F/W = 0.3$)	24,000	0.120	148

The data shown in Table 10 present mission ideal velocity requirements and payload-to-gross weight ratios. The principal conclusion here is that the two-stage configuration yields a 41 percent payload gain in comparison to the single stage vehicle for an orbit-establishment mission from 30,000 ft/sec hyperbolic excess velocity.

ORBITAL LANDING AND TAKEOFF

The absence of an atmosphere about the planet Mercury dictates that landing maneuvers be performed entirely propulsively; there is no recourse to aerodynamic assistance. The propulsion requirements for landing from orbit were obtained by computation of simulated landing trajectories and the results were applied to an investigation to determine the optimum vehicle thrust-to-weight ratio for the maneuver. Only single-stage vehicles were considered since the ideal velocity requirements for the landing maneuver, on the order of 11,000 to 12,000 ft/sec, are sufficiently low to preclude the possibility of any sizable benefits by the use of some form of staging.

Simulated-Landing Trajectory

In the trajectory utilized, the vehicle flight was simulated in the opposite direction from which a flight would actually be performed. The simulated flight initiated at the planet surface, and the vehicle operated at a negative propellant-weight flowrate, to the orbit. The vehicle first rose vertically until it reached a velocity of 50 ft/sec. It then turned and the flight continued with the thrust vector directed parallel to vehicle velocity. The angle of the turn was selected to satisfy the constraints that the vehicle be moving as nearly horizontally as possible at the end of this propulsion phase, and that it never experiences a negative altitude rate during the powered maneuver. (Previous lunar-landing trajectory analyses have indicated this method to provide near minimum-energy trajectories). The first propulsive phase was terminated when the vehicle had sufficient velocity to coast to the desired orbital altitude (300 n mi in this study). At apoapsis of the coast phase, a constant-altitude, variable thrust-orientation angle maneuver was used to increase the vehicle velocity to orbital velocity. Thus, the actual flight is performed in a manner similar to a lunar-landing maneuver; the first retro-thrust phase transforms the circular orbit to a low periapsis ellipse, and following coast to periapsis, the propulsion system is restarted and operates until landing is accomplished. Investigation of hovering/translation/final descent requirements is not included.

Thrust-to-Weight Ratio Effects

An ideal velocity requirement versus initial thrust-to-(Earth) weight (in Mercurian orbit) ratio curve for landimg from a 300-n mi circular Mercurian orbit is presented in Figure 130. Two values of specific impulse, representing noncryogenic and high-energy, cryogenic propellants, were considered. The ideal velocity for the first propulsion phase (required to establish the elliptical path from the circular orbit) is illustrated in Figure 131 as a function of periapsis altitude, and Figure 132 shows the velocity at periapsis of the ellipse. Because allowance must be added to provide for translation and descent maneuvers, as well as for a reserve propellant supply, the velocity data presented in Figure 130 must be modified to provide useful design values of required propulsion capability. On the basis of studies of lunar translation and descent, it appears that 600 ft/sec for translation (which provides a capability of 3000 ft translation) 300 ft/sec for vertical descent and 400 ft/sec for reserve, are suitable for a Mercury landing-from-orbit maneuver. Interpolation of Figure 109 (page 161) indicates that a throttling ratio on the order of 9:1 or 10:1 is suitable for performance of the vertical descent maneuver.

The periapsis altitude required to assure that the final braking phase will result in the vehicle reaching the surface with zero velocity is a function of the vehicle F/W. A plot of required-periapsis altitude versus F/W at the initiation of the landing is presented in Figure 133. Available environmental data indicate that the surface of Mercury may be similar to that of the moon; the highest lunar mountains are approximately 26,000 ft, and it may be considered desirable to maintain periapsis altitude above this height for the landing maneuver on Mercury. As indicated in Figure 133 (for a 440-sec specific impulse) only thrust-to-(Earth) weight ratios above about 1.5 require periapsis altitudes below 30,000 feet; therefore, selection of lower F/W designs will circumvent this potential problem.

The thrust-to-Mercury weight ratio at the end of the descent-from-orbit phase represents the throttling ratio required to achieve a 1:1 local F/W at the start of the hover/translation phase. These data are presented as a function of initial thrust-to-Earth weight ratio in Figure 134.

Vehicle Thrust Selection

The computed velocity data were utilized in conjunction with representative vehicle characteristics to determine the optimum thrust-to-weight ratios for typical noncryogenic and cryogenic propellant landing vehicles. The results presented in Figure 135 indicate an optimum thrust-to-(Earth) weight ratio between 0.8 and 0.9. Earlier studies of lunar landing and

ROCKETDYNE
A DIVISION OF NORTH AMERICAN AVIATION, INC

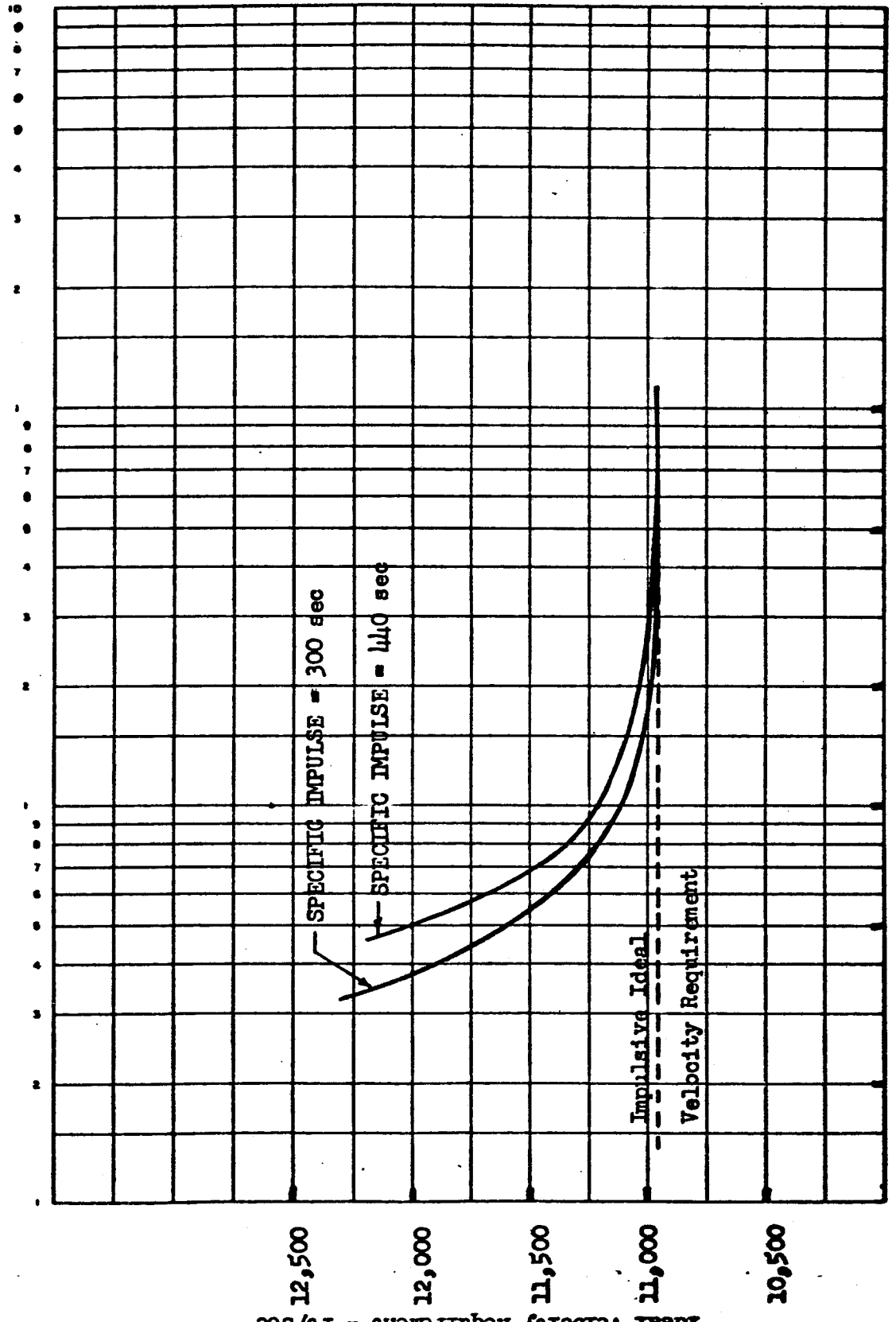

Figure 130. Ideal Velocity Requirements for a Planet Mercury Landing From a 300 N. Mi. Circular Orbit

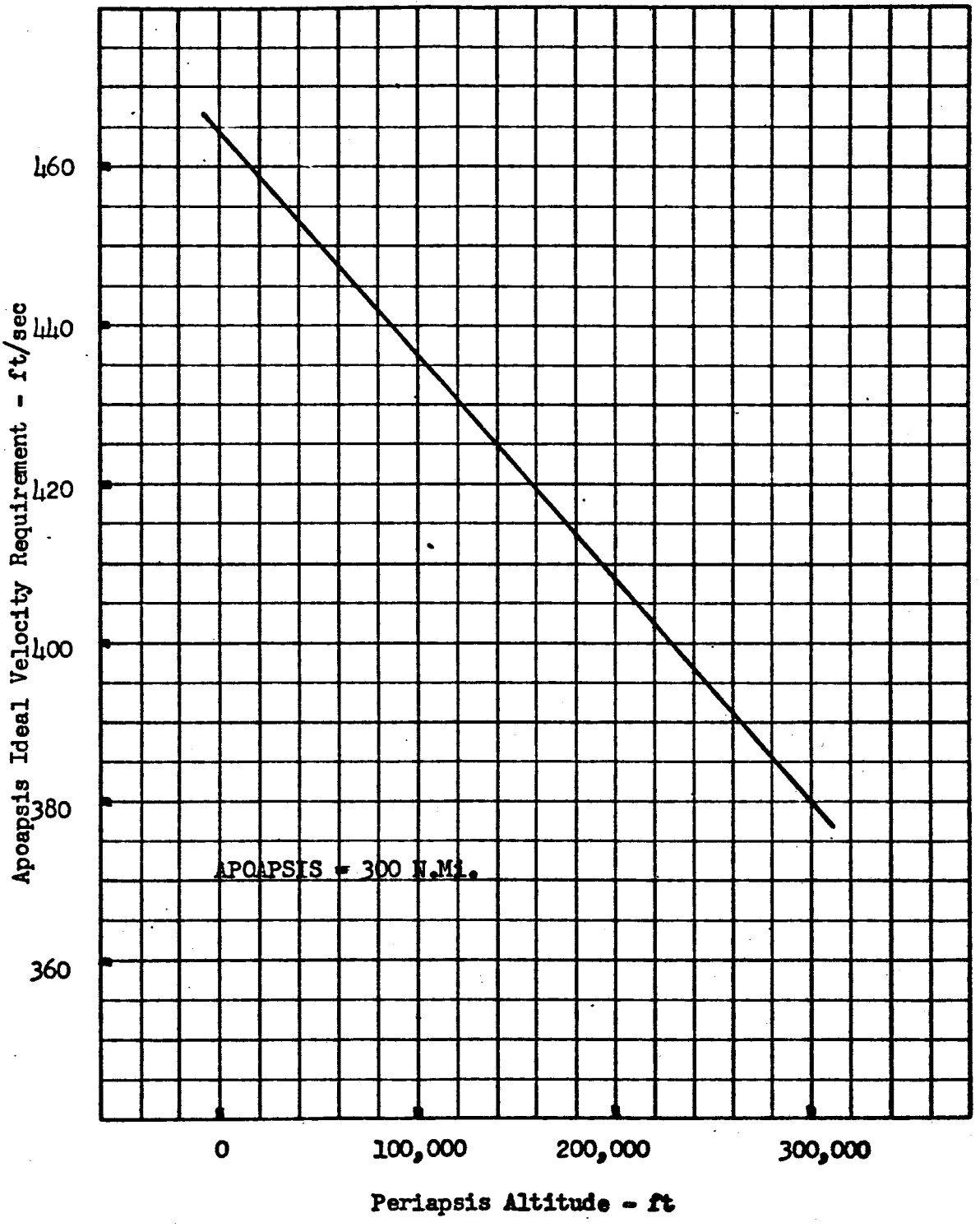

Figure 131. Ideal Velocity Requirement to Establish a Coast Ellipse from a 300 N.Mi. Circular Planet Mercury Orbit.

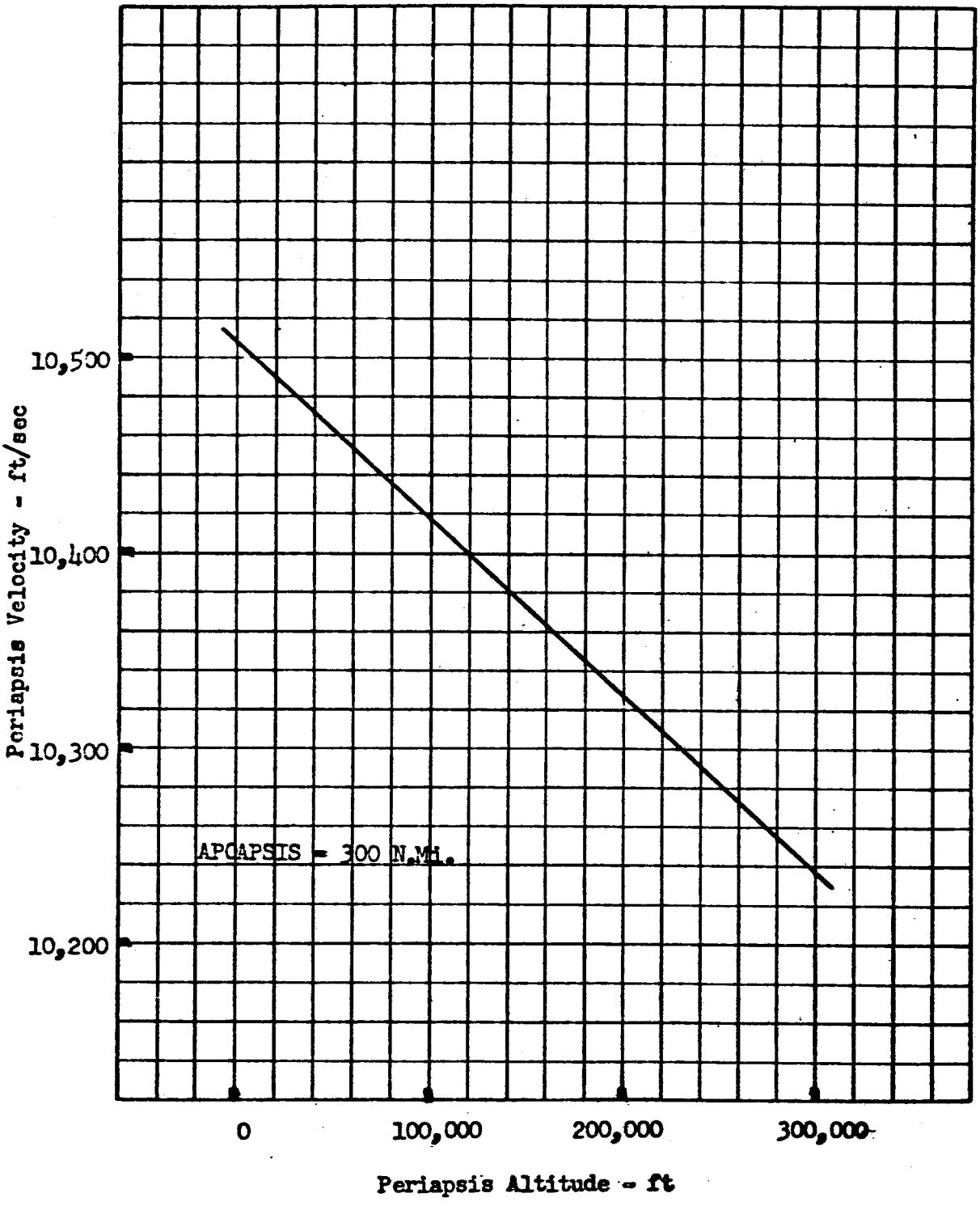

Figure 132. Periapsis Velocity of Intermediate Coast Ellipse for Planet Mercury Landing from Orbit.

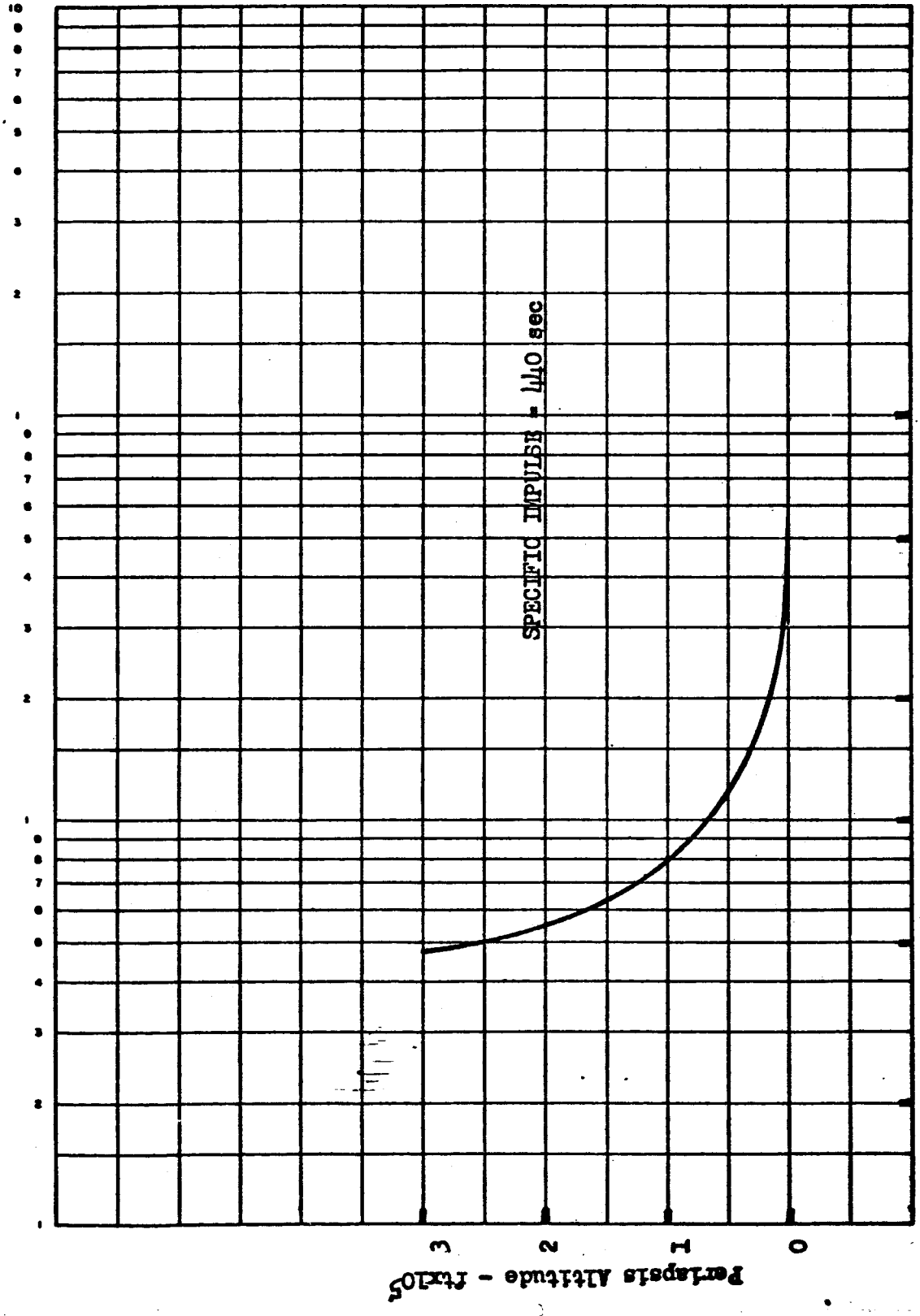

Figure 133. Periapsis of Intermediate Coast Ellipse Planet Mercury Landing From a 300 N.Mi. Circular Orbit.

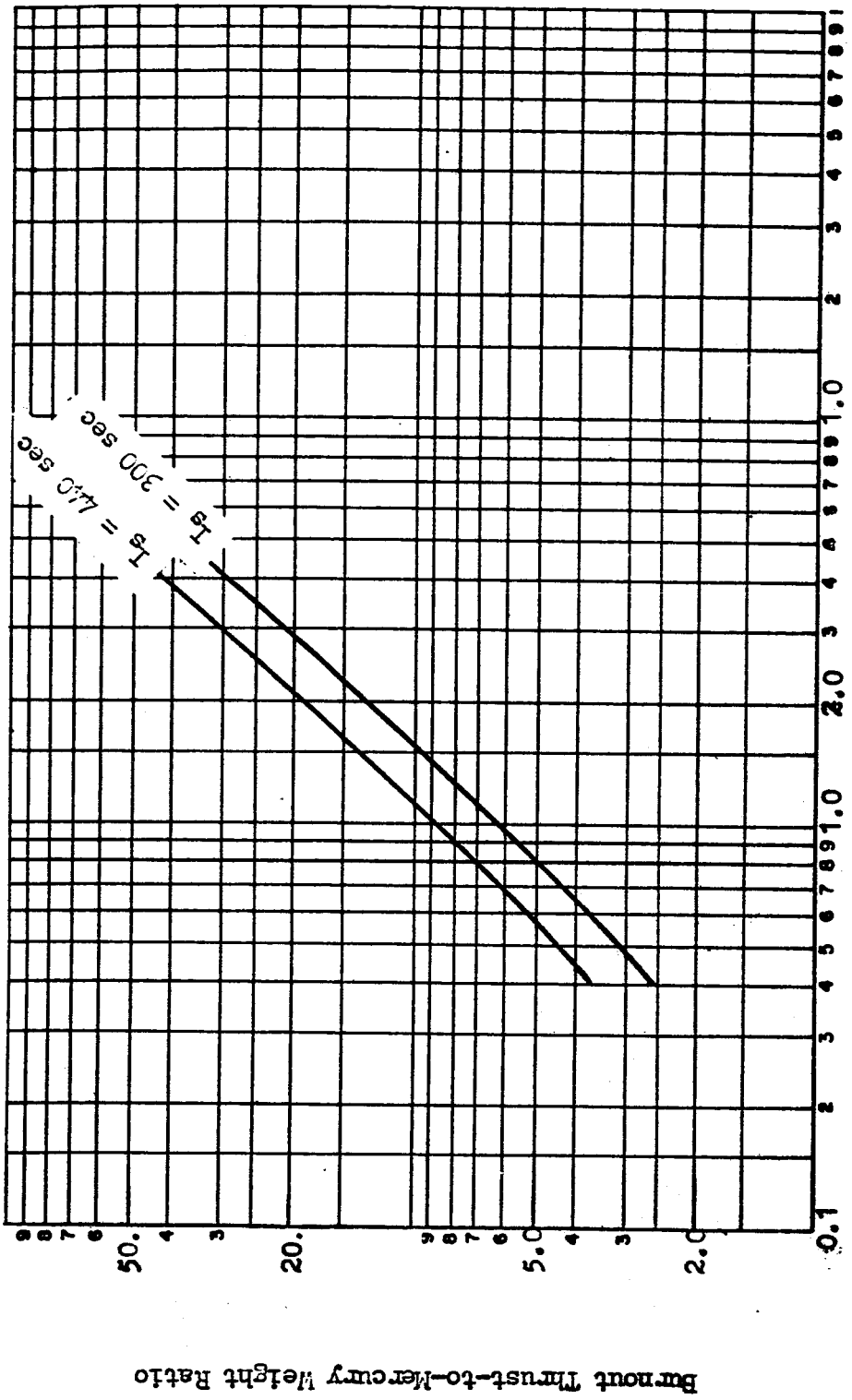

Figure 134. Burnout Thrust-to-Mercury Weight Ratio vs Initial Thrust-to-Earth Weight Ratio for Mercury Landing-from-Orbit Maneuver

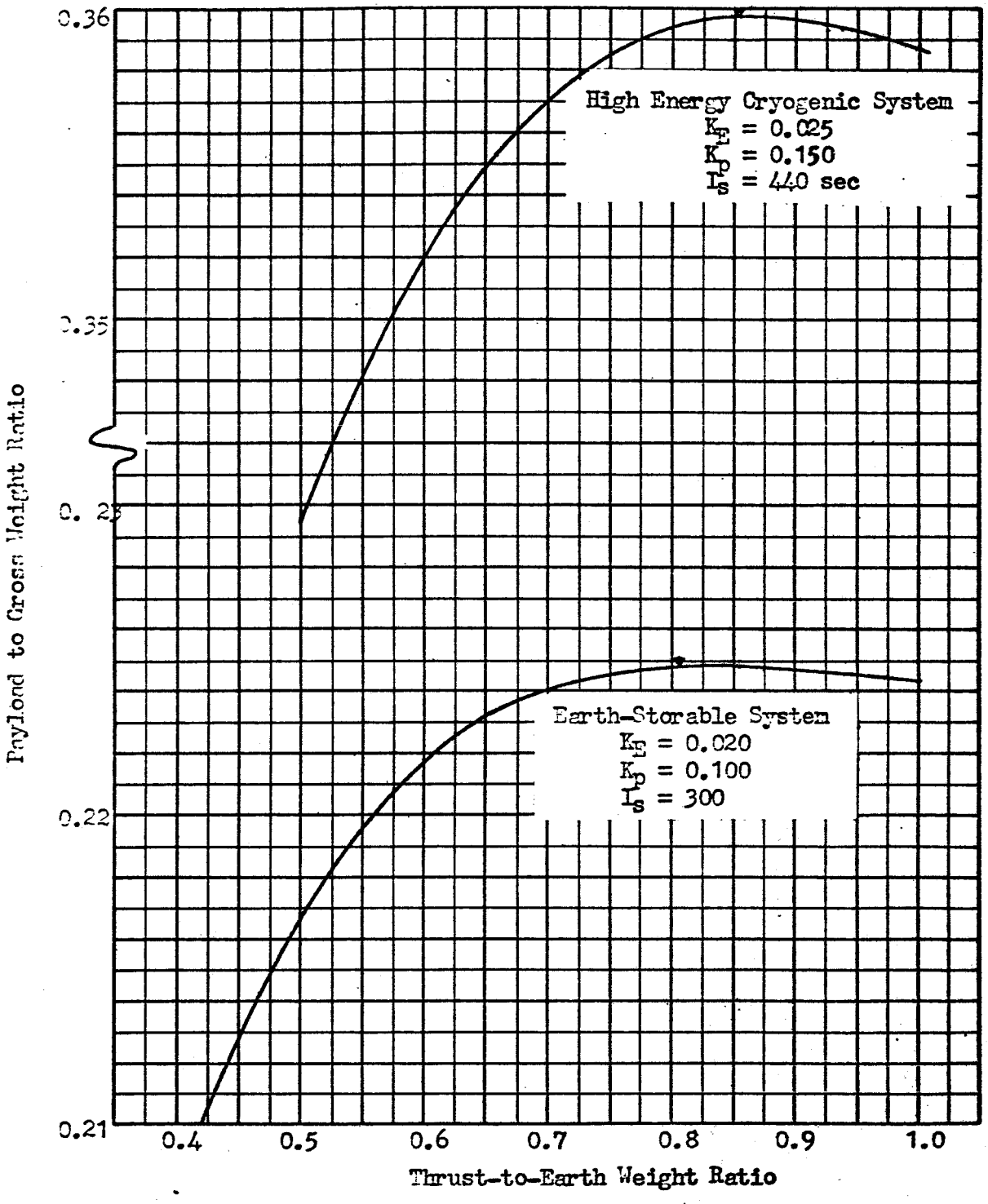

Figure 135. Mercury Landing from 300 N Mi Orbit

planetary orbit establishment or departure maneuvers have demonstrated the effects of various factors such as thrust-dependent or propellant-dependent weights, which govern optimum F/W; a similar parametric analysis will not be repeated here.

Mercurian Takeoff Trajectories

Simulated takeoff trajectories were determined for a vehicle which takes off from the Mercurian surface to establish a 300-n mi circular orbit. In the type of takeoff trajectory considered, the vehicle first rises vertically until it reaches a velocity of 50 ft/sec. The vehicle then performs a turn and the flight continues with thrust parallel to vehicle velocity. In a manner similar to the landing trajectories described above, the angle of the turn is selected so that the vehicle completes the propulsive maneuver oriented as closely as possible to horizontal, but never experiences a negative altitude rate during the propulsive interval. This propulsive phase is terminated when the vehicle has sufficient velocity to coast to the desired orbital altitude. After the coast-to-orbital altitude, a variable thrust-orientation angle, constant-altitude maneuver is used to establish the orbit. This takeoff trajectory is basically the same as the landing trajectory in reverse. In Figure 136 is shown ideal velocity requirement versus thrust-to-weight ratio for the Mercurian takeoff.

ERROR ANALYSIS FOR MERCURY LANDING-FROM-ORBIT MANEUVER

The analysis of landing position errors associated with propulsive landing maneuvers initiated at the periapsis of an elliptical orbit about Mercury was conducted in a manner similar to that employed for lunar landing maneuvers. Nominal conditions appropriate to the high velocity requirements of a Mercury mission were selected; these were:

Orbit Parameters
apoapsis: 300 nautical miles
periapsis: 120,000 feet

Propulsion Parameters
initial thrust-to-(Earth) weight ratio: 0.9
specific impulse: 420 seconds

The characteristics of the nominal gravity-turn landing trajectory are presented in Figure 137 . Though the nominal hover altitude of 42,000 feet is far higher than would be required to assure payload safety, the accuracy of the error data to be presented are not adversely affected by this particular selection; the altitude curve can be vertically displaced over a wide range without introducing a change in study results.

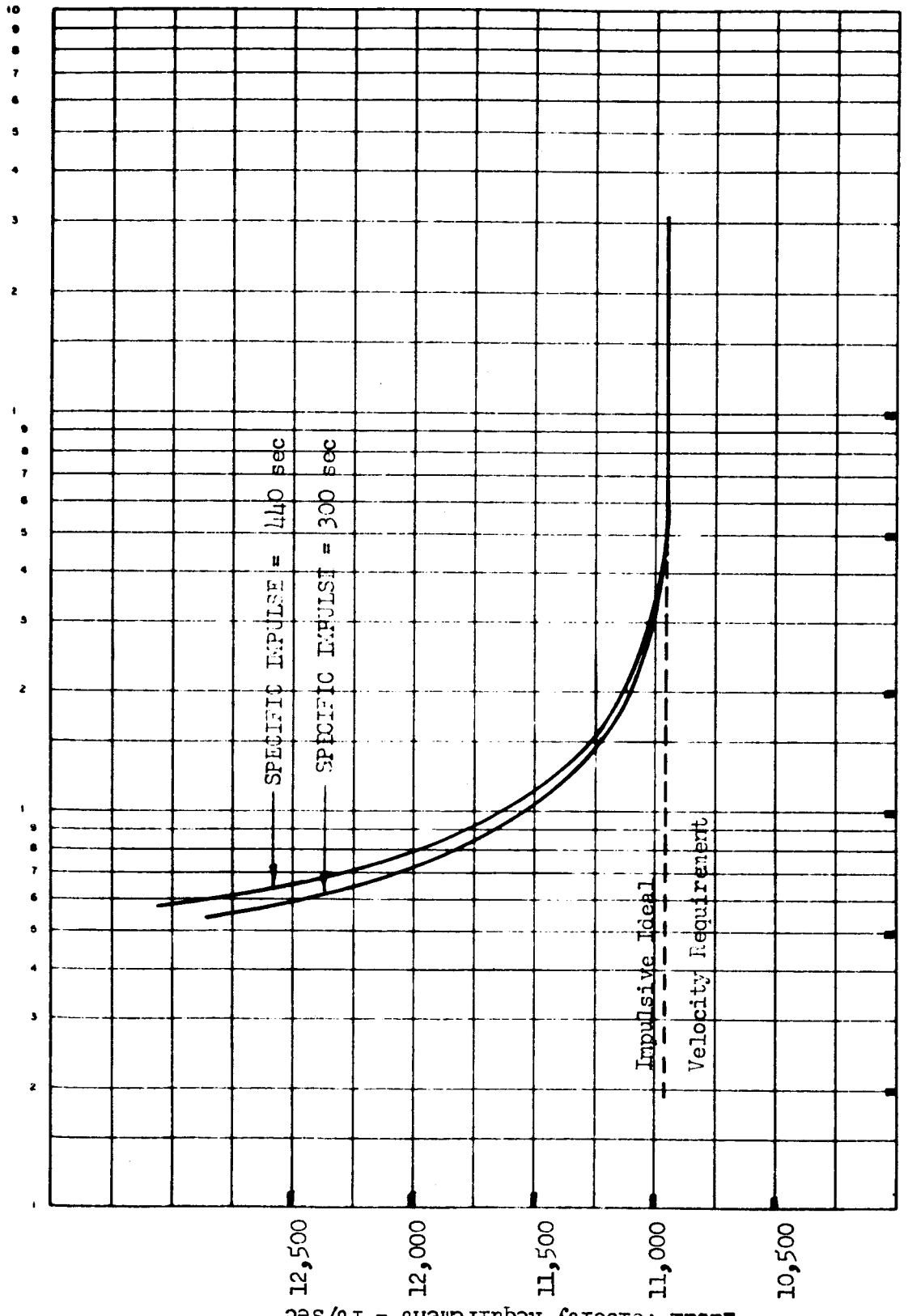

Figure 136. Ideal Velocity Requirement for a Planet Mercury Take-off to a 300 N.Mi. Circular Orbit.

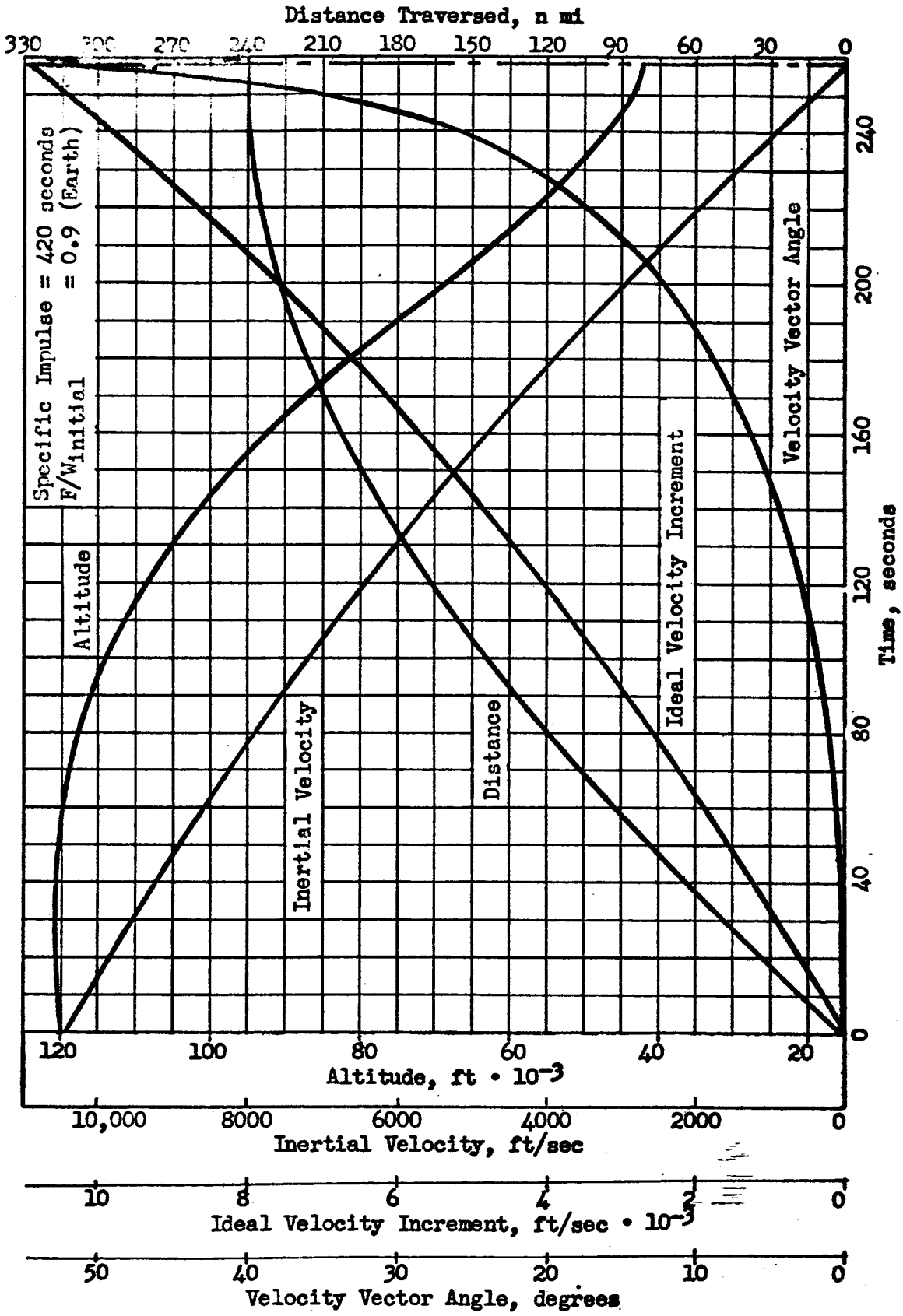

Figure 137 . Nominal Mercury Landing Trajectory Characteristics

Error Analysis

The influence of deviations from nominal thrust on terminal point position is shown in Figure 138. It is evident that when thrust and specific impulse vary in unison, the effect of a given quantitative departure from nominal operation is less pronounced than it is when thrust varies alone.

Coast trajectory conditions in a region on either side of the nominal ignition point are presented in Figure 139. The indicated time span corresponds to a range of ±3 degrees of arc about the ellipse periapsis. The effect of an improperly timed ignition signal on the location of the maneuver terminus is shown in Figure 140. For each second of deviation from the nominal moment for ignition, the error induced is approximately 2 nautical miles in range and 200 feet in altitude (these values are close to twice the values obtained in the analysis of lunar landing).

The influence of departures from a gravity turn maneuver, i.e., an undesirable angle-of-attack, is presented in Figure 141. These results resemble, both qualitatively and quantitatively, the results obtained in the lunar landing analysis.

The variation of velocity vector angle during the landing maneuver is shown in Figure 142 for the nominal case and for the ± 2 percent thrust deviation cases. High thrust yields a shorter-duration, steeper descent as compared to the nominal trajectory, while low thrust prolongs the propulsive maneuver and extends the range traversed during descent.

For a vehicle deliberately constrained to the nominal angle-vs-time characteristic, operation at off-nominal thrust creates a situation in which two distinct errors exist: 1) caused by thrust deviation, and 2) caused by misalignment error, obtained by measuring the distance between curves in Figure 142, is presented in Figure 143. The time-averaged misalignment error is approximately one degree, which yields for +2-percent thrust (by extrapolating Figure 141) errors of -11,000 feet altitude and +0.25 nautical miles range. These, combined with the errors caused by excessive thrust, result in overall position errors of -8000 feet altitude and -4.5 nautical miles range.

A similar disparity in angle-vs-time characteristics exists between the nominal case and the early/late ignition cases. The misalignment error is shown, for 40 second ignition-time errors, in Figure 143 ; a time-averaged value of misalignment is approximately 0.15 degrees. Thus, forced adherence to the nominal vehicle orientation schedule, in the case of late ignition, will add +1700 feet to the altitude error and -0.04 nautical miles to the range error.

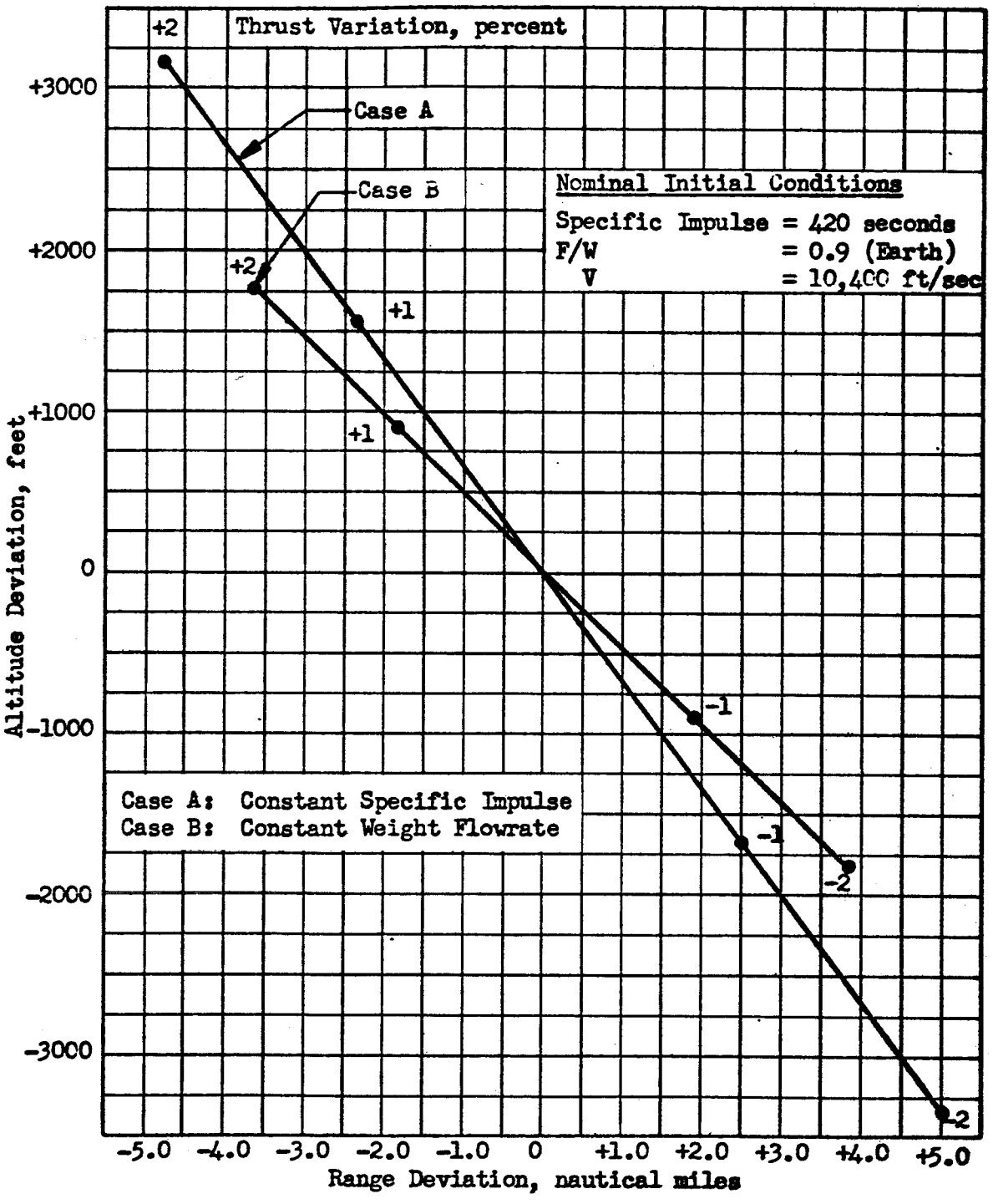

Figure 138. Effects of Thrust Errors on Mercury Landing Maneuver Terminal Position

Figure 139. Reference Conditions for Initiation of Mercury Landing Maneuver

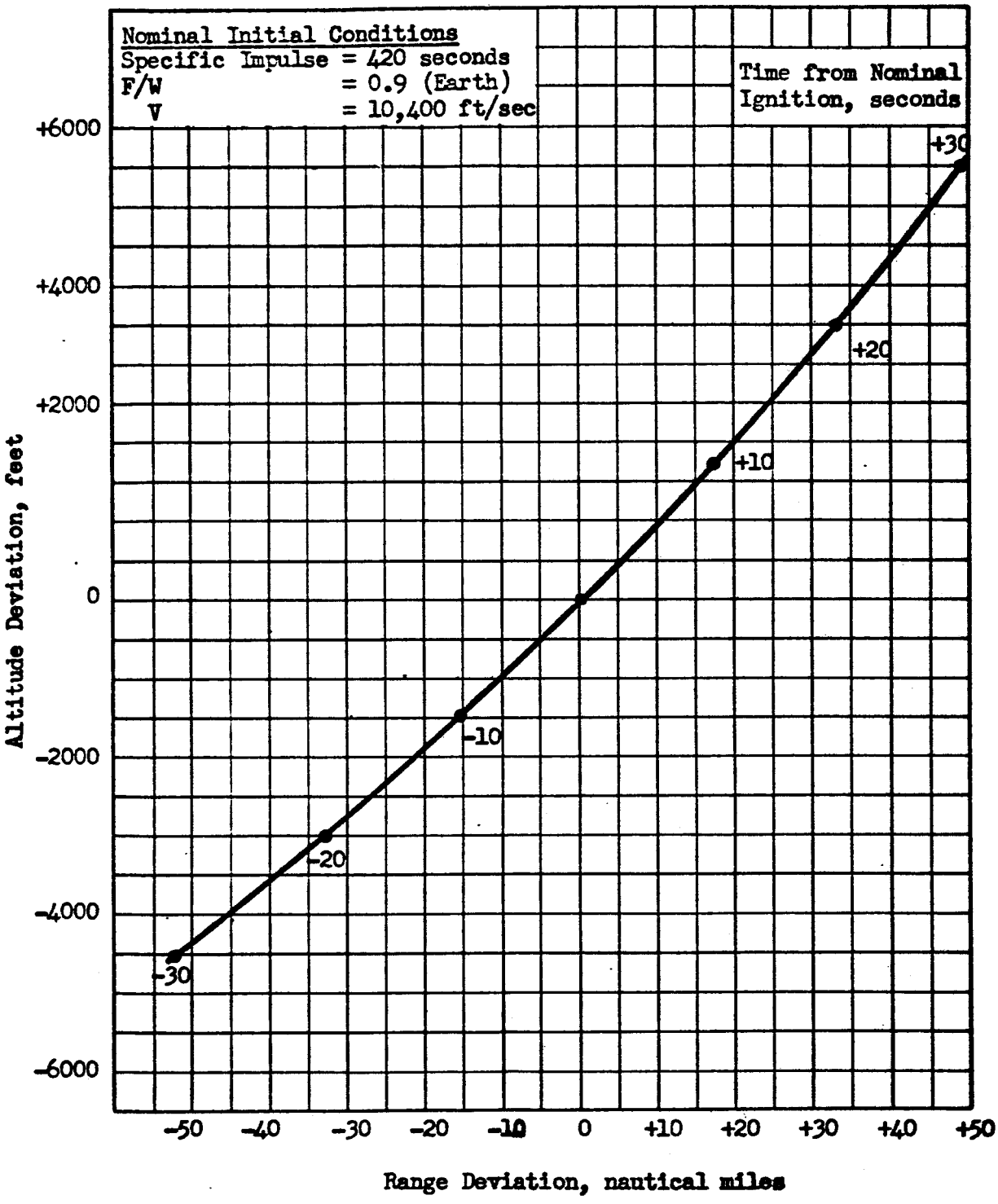

Figure 140. Effects of Propulsion Initiation Time on Mercury Landing Maneuver Terminal Position

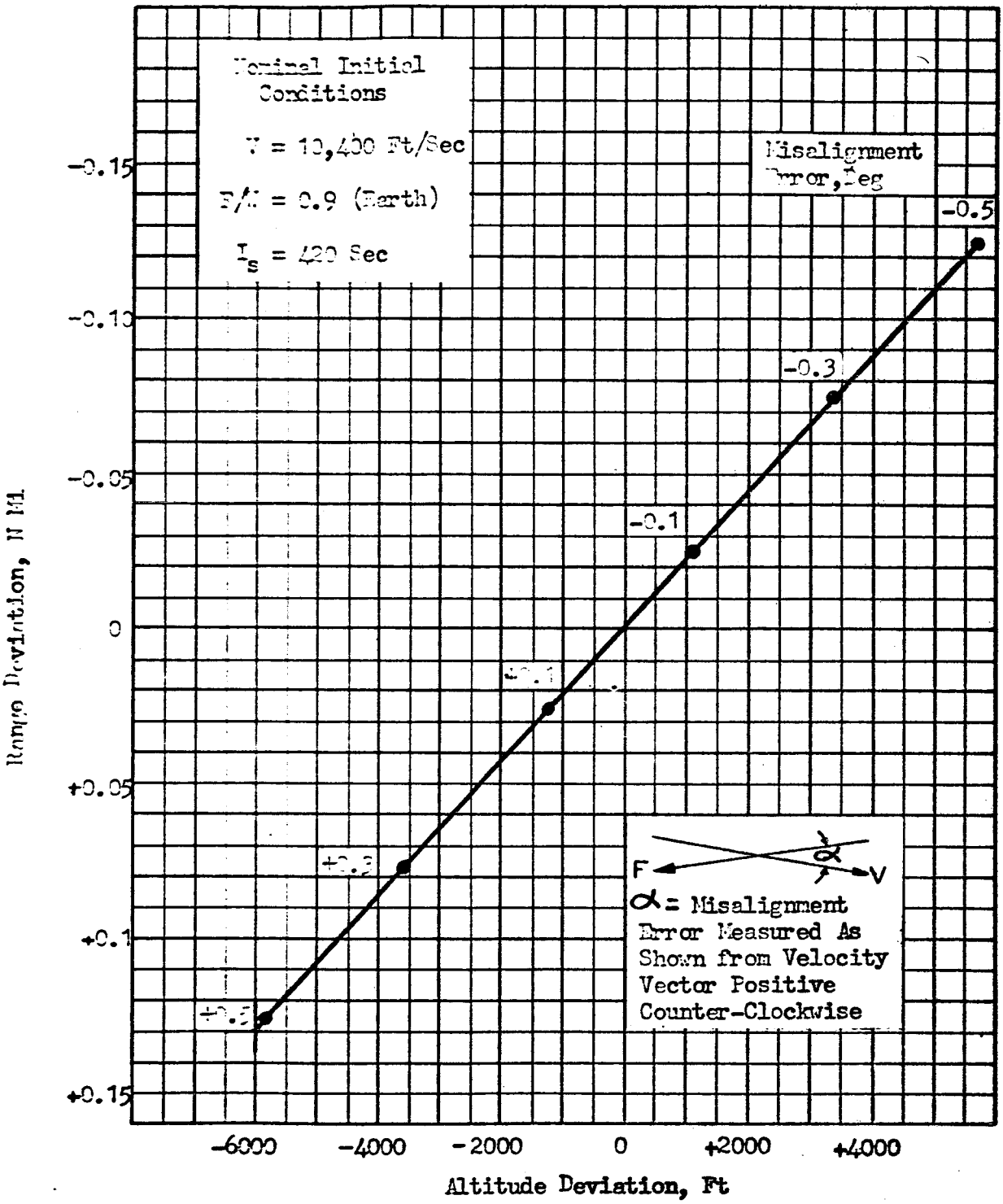

Figure 141. Effects of Thrust Misalignment Errors on Mercury Landing Maneuver Terminal Position

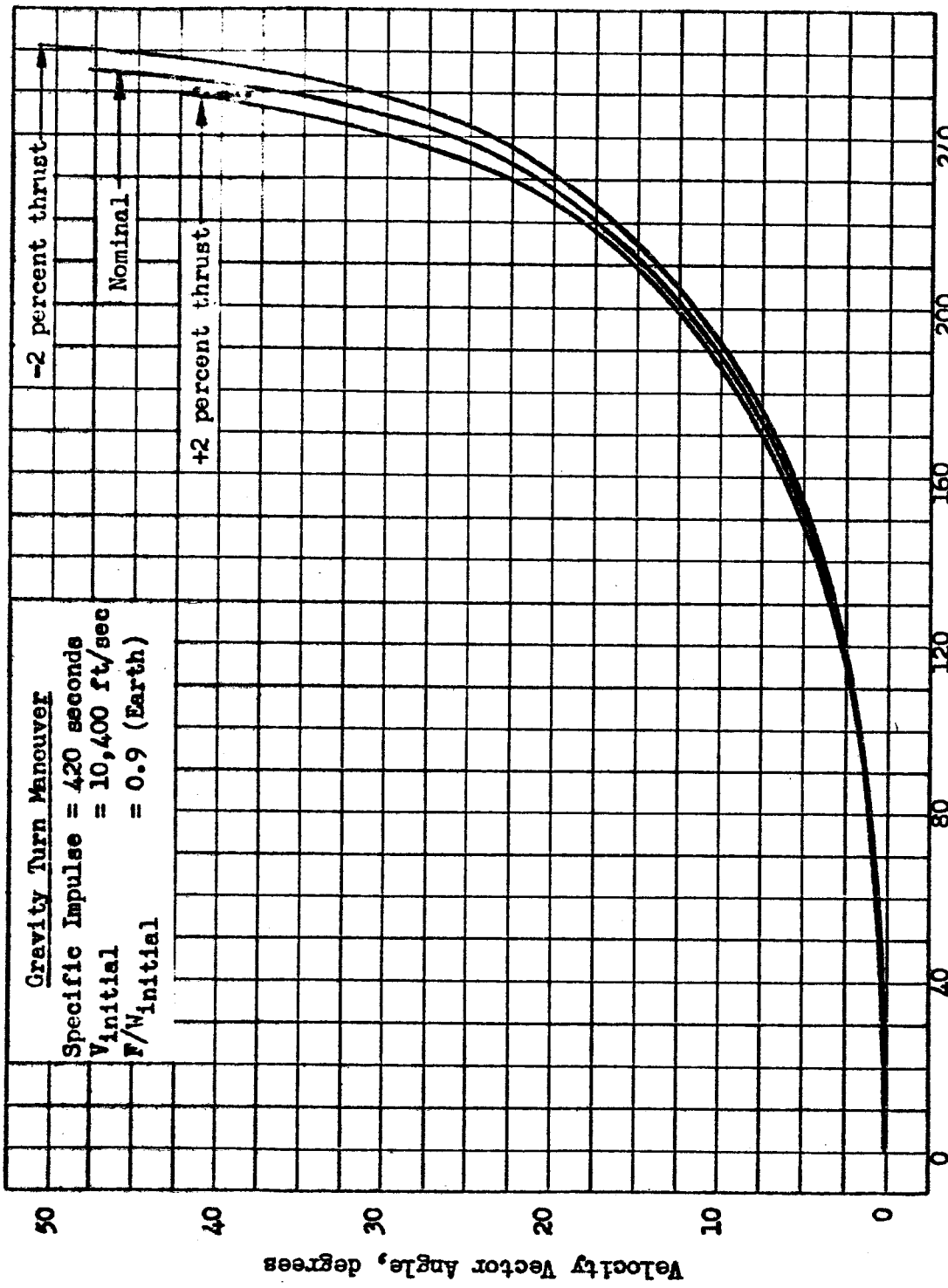

Figure 142 . Variation of Velocity Vector Angle During Mercury Orbit Descent.

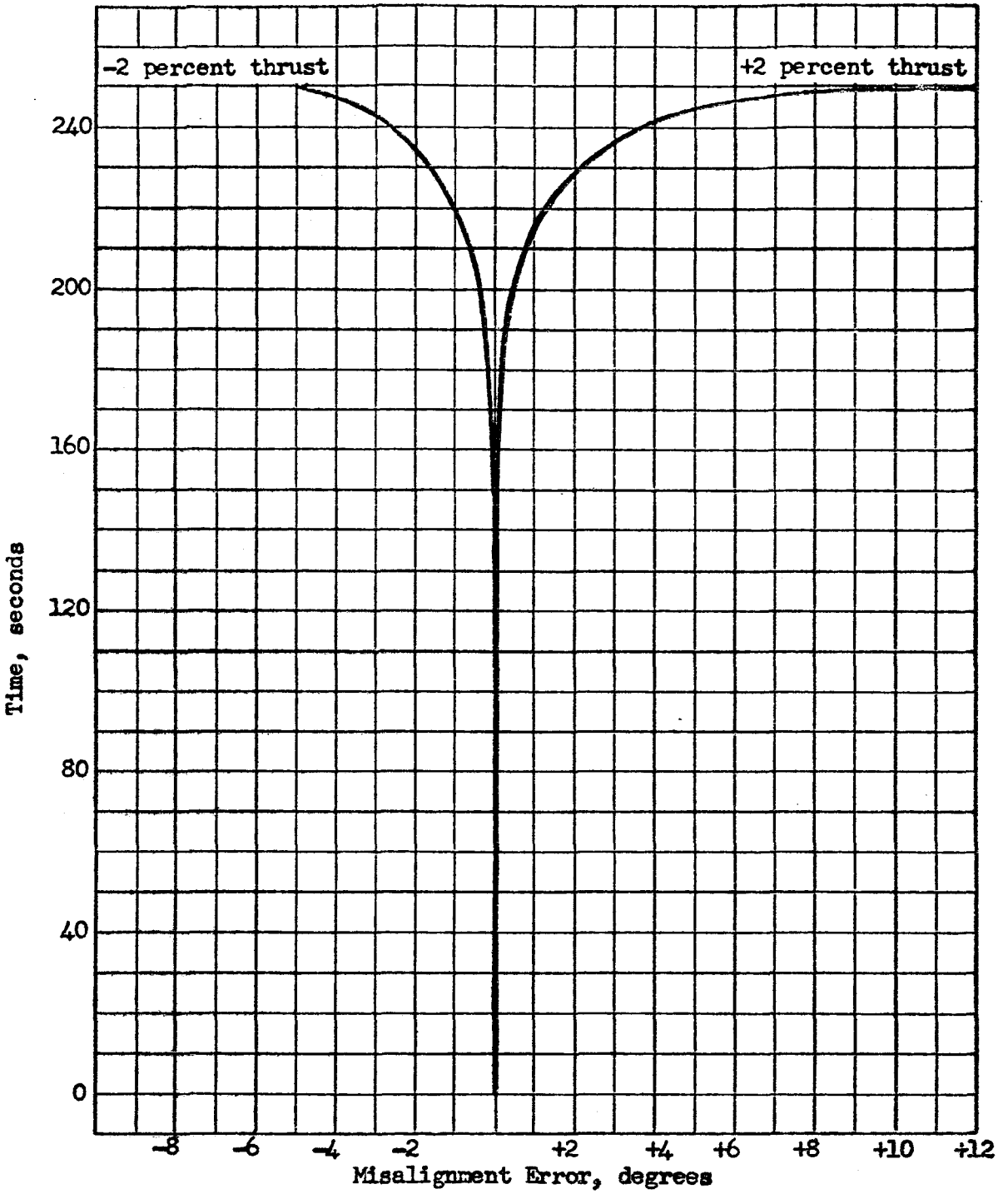

Figure 143 . Thrust Misalignment Error for Mercury Landing Maneuver

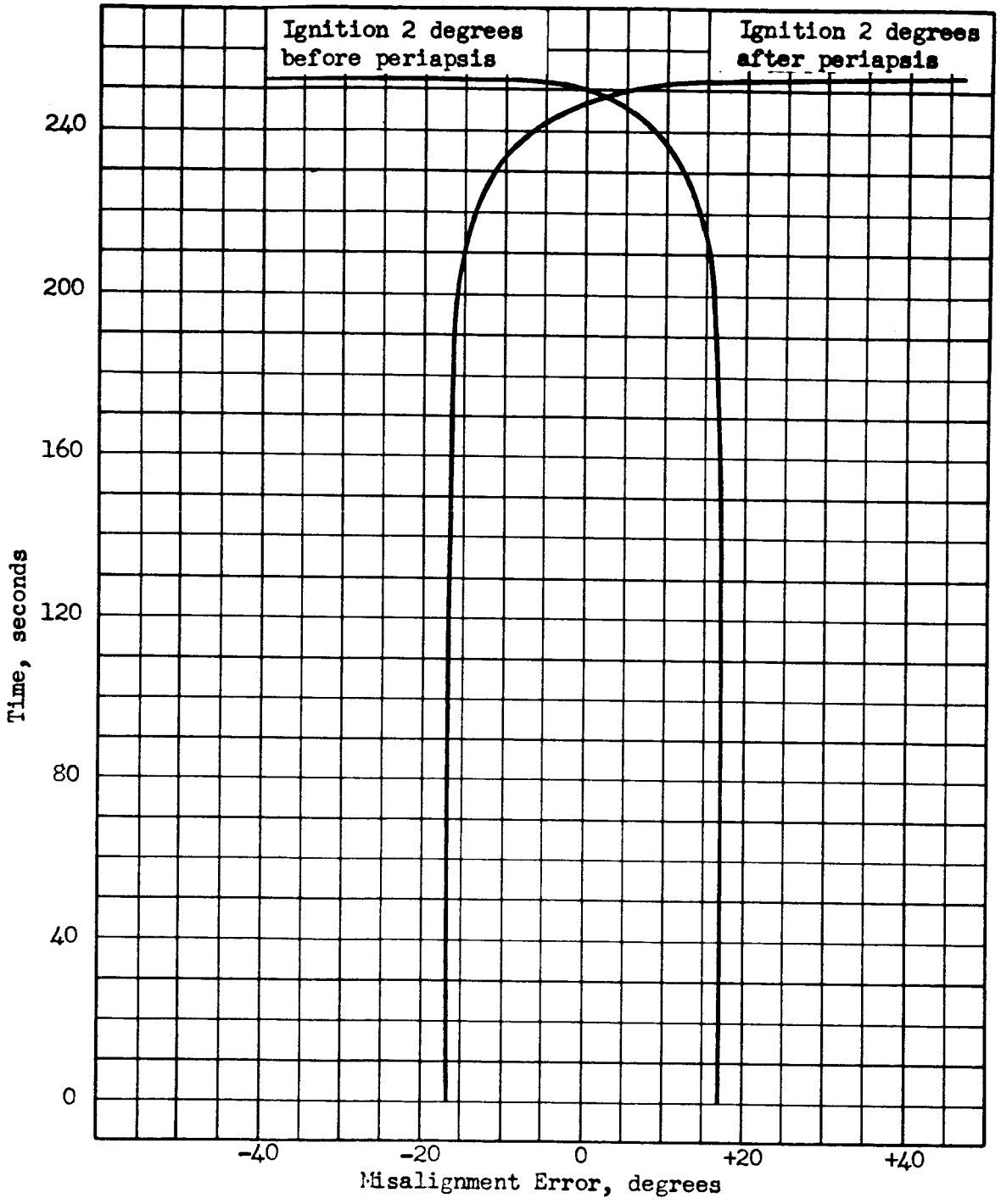

Figure 144 . Effect of Initial Position on Mercury Landing Misalignment Error

Conclusions

Small deviations from nominal performance of Mercury orbit landing maneuvers have little effect on propulsion requirements for achieving zero velocity, but have a significant effect on the position coordinates of the vehicle at the moment it comes to rest. Representative values of displacement from the nominal hover point are presented below.

TABLE 11

HOVER POINT POSITION ERRORS

Error	Altitude, feet	Range, n mi
+2 percent thrust, specific impulse constant	+3130	-4.78
+2 percent thrust, +2 percent specific impulse	+1780	-3.65
Ignition 20 seconds early	-3050	-34.0
+0.5-degree misalignment	-5760	+0.13

The propulsion requirements for translation and descent to the nominal landing site from the positions indicated above are on the order of several thousand ft/sec in most instances, and therefore corrective measures such as engine throttling should be initiated during the main propulsion phase rather than after reaching the hover point.

To account for altitude deviations introduced by one of the propulsion or trajectory errors considered, the nominal hover position should be on the order of 6000 feet above the Mercury surface. Any errors in elliptic orbit periapsis altitude, not evaluated in this study, must also be added to these values.

ENGINE PARAMETER OPTIMIZATION

SELECTION OF PROPULSION SYSTEM CHARACTERISTICS

A propulsion system parameter study was conducted to determine the optimum designs for propulsion systems applicable to extraterrestrial landing missions. The propulsion parameters considered were chamber pressure (P_c), expansion area ratio (ϵ), and thrust chamber mixture ratio (MR).

Because of the numerous applications of propulsion to various landing missions and concepts, it was necessary to formulate and analyze a limited number of propulsion system models that would represent the various landing mission requirements. To determine the representative propulsion systems, ideal velocity and thrust-to-weight ratio requirements, and vehicle gross weight were reviewed. Based on this review, propulsion system thrust levels from 5,000 to 500,000 pounds were selected; the lower value is representative of near-future unmanned landing vehicles, and the larger valves are typical of manned interplanetary missions. These values were utilized in conjunction with the selected thrust-to-weight ratios of 0.3 (typical for an orbit establishment or departure maneuver) and 0.8 (typical landing-from-orbit on Mercury, or Mars takeoff). Mission velocity increments considered were from 6,000 to 22,000 ft/sec, the lower value corresponding to missions such as a lunar landing-from-orbit maneuver and the higher value representative of requirements for injection from an Earth orbit into interplanetary transfer trajectories such as a fast Mars trip. Three propellant combinations representing the most likely candidates for use in chemical bipropellant propulsion systems for extraterrestrial landing missions were selected. Oxygen/hydrogen (O_2/H_2) and nitrogen tetroxide/hydrazine-UDMH (NTO/50-50) were chosen as best suited to near-future applications, and fluorine/hydrogen (F_2/H_2) was selected for somewhat later missions.

A percentage of theoretical shifting equilibrium propellant performance (based on the available performance data) was assumed for thrust chamber performance calculations. For the pump-fed systems, engine performance was based on a bipropellant gas generator, parallel turbine pumping cycle. The engine specific impulse for the pump-fed systems are shown by Figures 145, 146, and 147 for O_2/H_2, F_2/H_2, and NTO/50-50 systems respectively. The O_2/H_2 and F_2/H_2 engine performance is given as a function of thrust chamber mixture ratio for various values of nozzle area ratio and chamber pressure. Engine specific impulse for the NTO/50-50 systems (Figure 147) is presented as a function

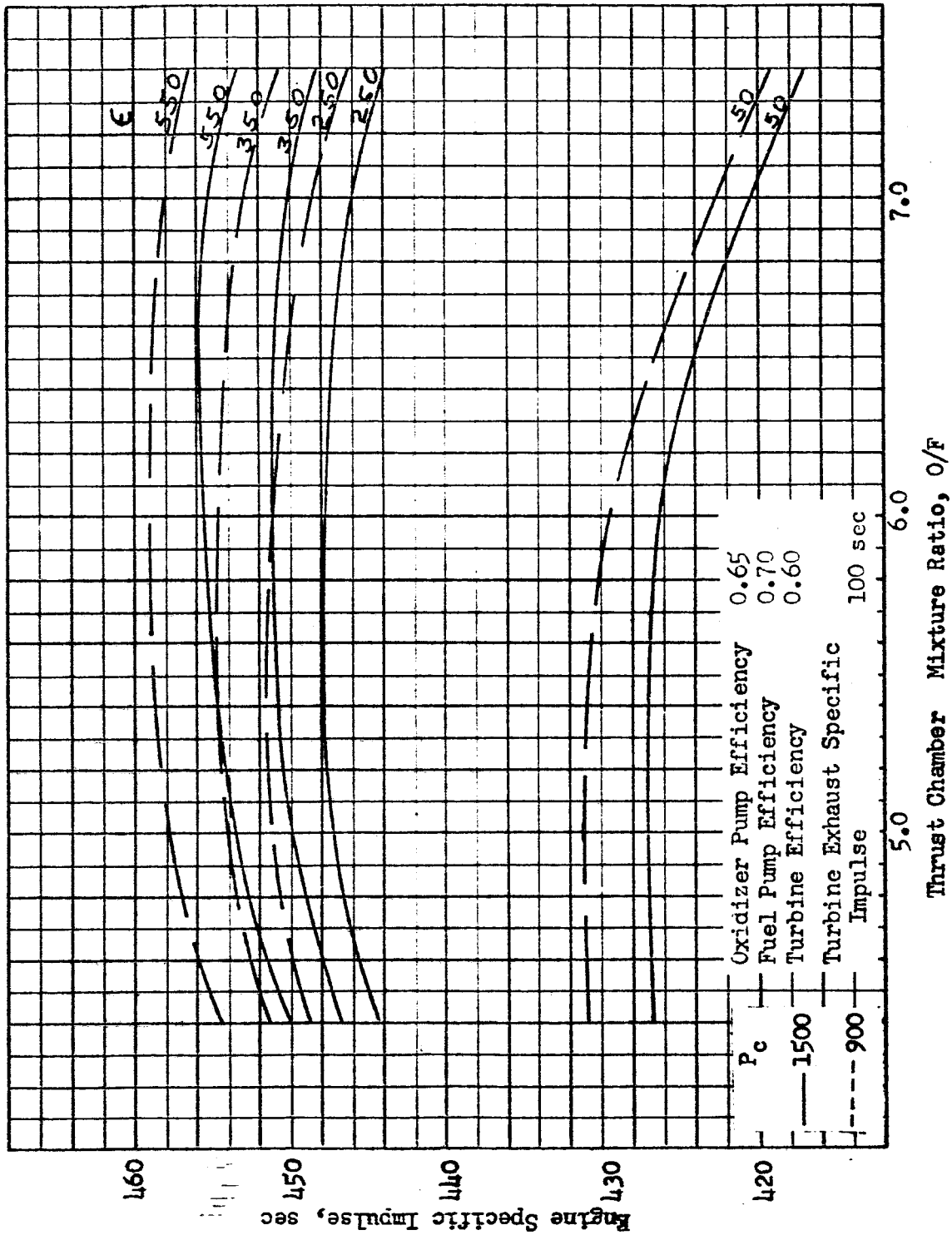

Fig. 145. O_2/H_2 Pump-Fed Engine Performance Data

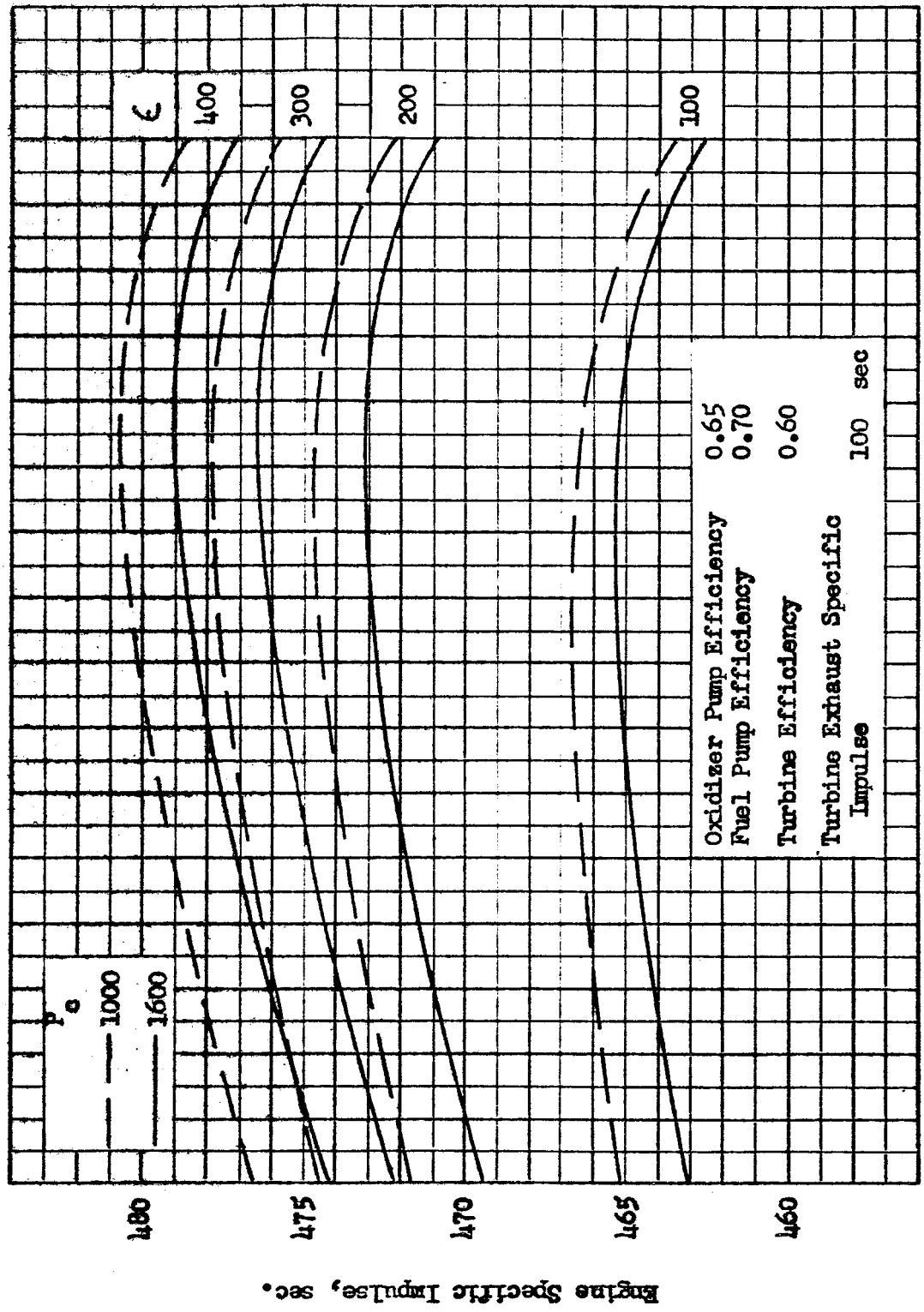

Figure 146. F_2/H_2 Pump-Fed Engine Performance Data

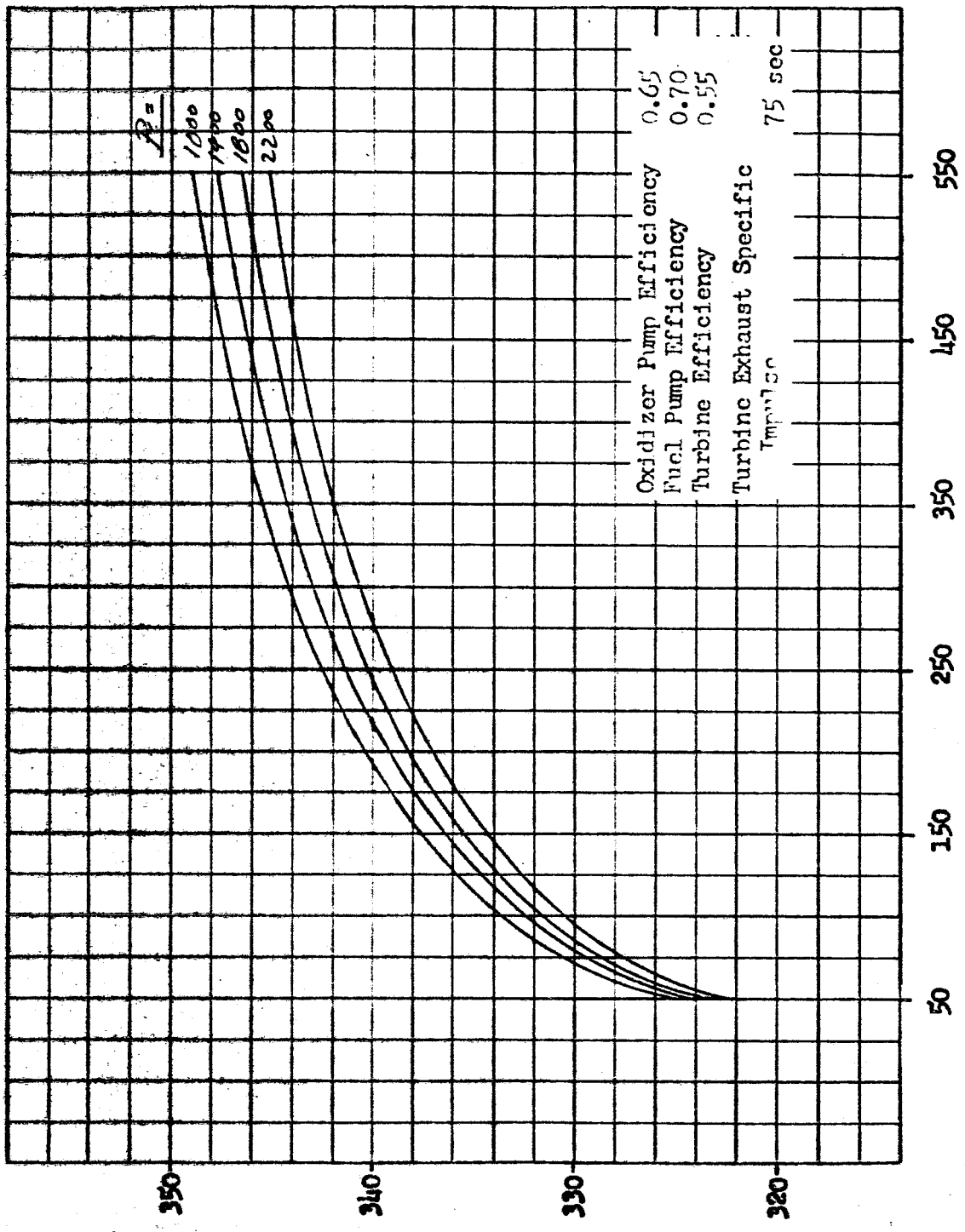

Fig. 147. NTO/50-50 Pump-Fed Engine Performance Data

of area ratio for several values of chamber pressure. All engine systems were assumed to be operating in vacuum conditions. The low thrust systems were assumed to be pressure-fed since the payload gain usually achieved by a pump-fed system is not significant for low thrust, low gross weight vehicle applications. The pressure-fed systems were assumed to use an ablative chamber and nozzle with a radiatively cooled skirt. All pump-fed systems utilized fully regeneratively cooled nozzles.

Propellant dependent weights were separated into tank volume and tank surface-dependent weights. Tank volume-dependent weights consist of tank pressure-shell and pressurization system weights. All tanks were assumed constructed of titanium except those containing oxygen and fluorine, which are aluminum. Tank surface-dependent weight was calculated based on a meteoroid shielding weight of approximately 2.0 lb/ft^2, representative of a consensus of available estimates.

The characteristics of the basic propulsion system models are presented in Table 12. Because the models and missions differ in vehicle gross weight (3 values), thrust-to-(Earth) weight ratio (2 values), mission ideal velocity increment (3 values), and propellant combination (3 selections), there are 54 basic models.

EFFECT OF ASSUMPTIONS

To indicate how several pertinent factors influence the optimum values for nozzle area ratio, chamber pressure, and mixture ratio, a brief examination, based on perturbation from a selected nominal O_2/H_2 case, was made. The resultant trends are shown in Table 13. The assumed nominal factors and the resulting optimum engine parameters are indicated in Case 1. A change in tank weight, Case 2, (with both the fuel and oxidizer tanks heavier) only tends to alter the mixture ratio slightly toward more oxidizer. A higher F/W (Case 3) results mainly in a lower optimum nozzle area ratio, since this results in lower nozzle weight for the heavier, higher-thrust engine. Reduction in the nozzle design weight factor (Case 4) results in a higher optimum area ratio, and a resulting lower optimum chamber pressure. The increased interstage weight for Case 5 reduces the optimum area ratio greatly (and increases P_c) because with a heavy interstage structure, system weight is particularly sensitive to nozzle length. Reducing the mission velocity increment reduces the nozzle area ratio and chamber pressure in the selected case; however, in general, optimum expansion area ratio for a given system is highest at a velocity requirement near gI_s, the effective exhaust velocity of the nozzle.

TABLE 12

SYSTEM DESCRIPTIONS

Thrust (pounds)	5000		50,000		500,000	
Gross Weight, pounds	6,250	16,667	62,500	166,667	625,000	1,666,667
Thrust to Gross Weight Ratio	0.8	0.3	0.8	0.3	0.8	0.3
Propellants	O_2/H_2 F_2/H_2 N_2O_4/50-50		O_2/H_2 F_2/H_2 N_2O_4/50-50			
Propellant Feed System	Pressure		Pump			
Chamber Type (cooling technique)	80-percent Bell (Ablative to ϵ = 20, Radiative to exit)		80-percent Bell (Full Regenerative)			
Interstage Structure, lb/in.	0.2	0.53	2.0	5.34	20.0	53.4
Propellant Dependent Weight Factors, K_1 & K_2	$W_T = C_1 P_T V_T + K_2 V_T^{2/3}$		$W_T = K_1 V_T + K_2 V_T^{2/3}$			

	C_1	K_2
O_2	0.013	8.5
F_2	0.013	8.5
NTO	0.007	8.5
H_2	0.007	5.0
50-50	0.007	8.5

	K_1	K_2
O_2	0.7	17.0
F_2	0.7	17.0
NTO	0.4	12.0
H_2	0.2	12.5
50-50	0.25	15.0

Thrust Chamber Specific Impulse Efficiency		
	O_2/H_2	0.94
	F_2/H_2	0.945
	NTO/50-50	0.94

	O_2/H_2	0.95
	F_2/H_2	0.955
	NTO/50-50	0.95

TABLE 13

INFLUENCE ON OPTIMUM PROPULSION PARAMETERS

Case/Change	Tank Wt	* Thrust/Weight/F/W	K_n, Nozzle Wt Factor, $16/m^2$	Interstage Structure Factor	Ideal Velocity Increment	Nozzle Area Ratio	Chamber Pressure psia	Mixture Ratio
1. (Nominal)/-	A	50/167,000/0.3	0.19	5.34	14,000	460	1360	6.9
2. /Tank Wt	B	50/167,000/0.3	0.19	5.34	14,000	480	1380	7.1
3. /F/W	B	60/150,000/0.4	0.19	5.34	14,000	400	1380	7.0
4. /Nozzle Wt	B	60/150,000/0.4	0.12	5.34	14,000	480	1280	7.1
5. /Interstage	B	60/150,000/0.4	0.12	14.5	14,000	330	1380	6.9
6. /ΔV	B	60/150,000/0.4	0.12	14.5	10,500	200	1170	6.6

Tank Wt Equation:

A) $W_{OT} = 0.7\ V_{OT} + 17\ V_{OT}^{2/3}$

$W_{FT} = 0.2\ V_{FT} + 12.5\ V_{FT}^{2/3}$

B) $W_{OT} = 0.879\ V_{OT} + 23.8\ V_{OT}^{2/3}$

$W_{FT} = 0.364\ V_{FT} + 13\ V_{FT}^{2/3}$

* Thousand Pounds

The influence of several otherassumptions is described briefly in Table 14.

TABLE 14

EFFECT OF SYSTEM ASSUMPTIONS ON OPTIMUM OPERATING PARAMETERS

Assumption	Effect on Optimum Operating Parameters
Shifting Equilibrium Propellant Performance	Results in higher area ratios and mixture ratios relative to those obtained by frozen composition performance
Turbopump Efficiency and Turbine Exhaust Specific Impulse	Higher values will result in higher optimum chamber pressures
Tank Pressure-Dependent Weight Factor, K_1, Pressure-Fed Systems	An increase in K_1 results in a decrease in optimum chamber pressure
Thrust Chamber Specific Impulse Efficiency	The effect is very slight

PROPULSION PARAMETERS

Two types of optimization analysis were conducted: 1) simultaneous optimization of all three propulsion parameters, and 2) optimization of chamber pressure and mixture ratio for a nozzle area ratio of 50:1.

Optimum Values.

The optimum parameters for the different engine/mission/propellant combinations are presented in Tables 15 through 20 . Optimizations assuming the unrestricted nozzle envelope are summarized in Tables 15, 16 and 17 and for the case of ϵ = 50:1, in Tables 18 , 19 and 20 . In addition to the optimum parameters, the tank and engine performance for the optimum designs are tabulated for each case.

A review of the effect of the mission/system parameters on the optimum operating conditions (Tables 15 , 16 , and 17) yields the following:

1. Optimum mixture ratio increases slightly with increasing mission velocity increment.

TABLE 15

LIQUID OXYGEN/LIQUID HYDROGEN SYSTEM OPTIMIZATIONS

UNRESTRICTED AREA RATIO

System Type	Engine Thrust pounds	Gross Weight pounds	Velocity Increment Feet/second	Optimum Parameters: Chamber Pressure, psia	Optimum Parameters: Mixture Ratio	Optimum Parameters: Area Ratio	Propellant Dependent Weight Factors, pound/pound Propellant: Oxygen	Propellant Dependent Weight Factors, pound/pound Propellant: Hydrogen	Propellant Dependent Weight Factors, pound/pound Propellant: Bulk	Engine Weight Factors, pound/pound thrust	Thrust Chamber Specific Impulse, seconds	Engine Specific Impulse, seconds
Pressure-Fed Ablation Cooled to ϵ = 20:1 Then Radiation Cooled To Exit. 80 Percent Bell Nozzle	5,000	6,250	6,000	85	6.1	105	0.070	0.529	0.135	0.0227	439.5	439.5
			14,000	70	6.2	125	0.060	0.460	0.116	0.0270	440.5	440.5
			22,000	62	6.4	105	0.053	0.406	0.101	0.0357	437.4	437.4
		16,666	6,000	75	6.2	200	0.055	0.427	0.107	0.0424	447.9	447.9
			14,000	55	6.2	200	0.044	0.340	0.085	0.0628	447.3	447.3
			22,000	55	6.4	190	0.042	0.329	0.081	0.0637	445.7	445.7
Pump-Fed Fully Regeneratively Cooled 80 Percent Bell Nozzle	50,000	62,500	6,000	1100	6.6	150	0.049	0.381	0.092	0.0210	450.4	443.8
			14,000	1150	6.8	200	0.042	0.321	0.080	0.0235	453.2	446.3
			22,000	1180	6.9	200	0.040	0.303	0.075	0.0235	453.0	446.0
		166,666	6,000	1360	6.8	360	0.038	0.289	0.073	0.0314	460.6	452.3
			14,000	1360	6.9	450	0.033	0.246	0.062	0.0352	462.8	454.6
			22,000	1370	7.0	450	0.031	0.232	0.058	0.0360	462.7	454.5
	500,000	625,000	6,000	1180	6.2	100	0.028	0.199	0.053	0.0187	446.4	439.1
			14,000	1230	6.4	150	0.025	0.173	0.046	0.0213	451.4	443.8
			22,000	1230	6.6	140	0.024	0.164	0.044	0.0206	450.0	442.6
		1,666,666	6,000	1390	6.4	190	0.023	0.157	0.043	0.0233	454.7	446.1
			14,000	1290	6.4	205	0.021	0.138	0.038	0.0242	455.3	447.4
			22,000	1290	6.5	200	0.020	0.131	0.036	0.0235	454.6	446.5

FORM R 18-6-18

TABLE 16

LIQUID FLUORINE/LIQUID HYDROGEN SYSTEM OPTIMIZATIONS

UNRESTRICTED AREA RATIO

System Type	Engine Thrust pounds	Gross Weight pounds	Velocity Increment Feet/second	Optimum Parameters: Chamber Pressure, psia	Optimum Parameters: Mixture Ratio	Optimum Parameters: Area Ratio	Propellant Dependent Weight Factors, pound/pound Propellant: Fluorine	Propellant Dependent Weight Factors, pound/pound Propellant: Hydrogen	Propellant Dependent Weight Factors, pound/pound Propellant: Bulk	Engine Weight Factors, pound/pound thrust	Thrust Chamber Specific Impulse, seconds	Engine Specific Impulse, seconds
Pressure-Fed Ablation Cooled to ϵ = 20:1 Then Radiation Cooled To Exit. 80 Percent Bell Nozzle	5,000	6,250	6,000	140	17.0	150	0.068	0.775	0.108	0.0176	467.1	467.1
			14,000	105	17.0	150	0.054	0.615	0.085	0.0249	465.5	465.5
			22,000	95	17.1	145	0.050	0.566	0.078	0.0279	464.5	464.5
		16,666	6,000	105	16.9	200	0.051	0.578	0.080	0.0310	469.1	469.1
			14,000	80	16.9	200	0.041	0.464	0.064	0.0442	468.4	468.4
			22,000	70	17.1	200	0.037	0.422	0.058	0.0524	467.8	467.8
Pump-Fed Fully Regeneratively Cooled 80 Percent Bell Nozzle	50,000	62,500	6,000	1550	17.3	155	0.040	0.488	0.068	0.0168	476.5	471.0
			14,000	1580	17.4	200	0.034	0.407	0.057	0.0190	479.2	473.7
			22,000	1580	17.6	200	0.032	0.379	0.054	0.0190	479.0	473.6
		166,666	6,000	1750	17.3	295	0.031	0.364	0.052	0.0225	483.0	476.7
			14,000	1770	17.4	410	0.027	0.306	0.044	0.0272	485.9	479.6
			22,000	1750	17.5	390	0.025	0.286	0.042	0.0262	485.4	479.2
	500,000	625,000	6,000	1800	17.1	127	0.023	0.251	0.037	0.0159	474.5	468.2
			14,000	1780	17.2	153	0.020	0.213	0.032	0.0167	476.7	470.5
			22,000	1790	17.3	150	0.019	0.201	0.031	0.0167	476.4	470.2
		1,666,666	6,000	2065	17.1	195	0.018	0.193	0.030	0.0179	479.9	472.6
			14,000	1835	17.1	203	0.017	0.167	0.026	0.0185	479.7	473.3
			22,000	1885	17.2	203	0.016	0.158	0.025	0.0187	479.8	473.1

FORM R 16-8-18

TABLE 17

N_2O_4/N_2H_4 - UDMH (50-50) SYSTEM OPTIMIZATIONS

UNRESTRICTED AREA RATIO

System Type	Engine Thrust pounds	Gross Weight pounds	Velocity Increment Feet/second	Optimum Parameters: Chamber Pressure, psia	Optimum Parameters: Mixture Ratio	Optimum Parameters: Area Ratio	Propellant Dependent Weight Factors, pound/pound Propellant: N_2O_4	Propellant Dependent Weight Factors, pound/pound Propellant: N_2H_4-UDMH	Propellant Dependent Weight Factors, pound/pound Propellant: BULK	Engine Weight Factors, pound/pound thrust	Thrust Chamber Specific Impulse, seconds	Engine Specific Impulse, seconds
Pressure-Fed Ablation Cooled to ϵ = 20:1 Then Radiation Cooled To Exit, 80 Percent Bell Nozzle	5,000	6,250	6,000	230	2.2	200	0.063	0.107	0.077	0.0134	339.6	339.6
			14,000	170		200	0.050	0.086	0.061	0.0185	339.4	339.4
			22,000	130		100	0.044	0.075	0.054	0.0172	331.8	331.8
		16,666	6,000	160		320	0.045	0.077	0.055	0.0280	343.7	343.7
			14,000	130		310	0.037	0.064	0.045	0.0353	343.3	343.3
			22,000	100		200	0.033	0.056	0.040	0.0358	339.0	339.0
Pump-Fed Fully Regeneratively Cooled 80 Percent Bell Nozzle	50,000	62,500	6,000	1670		202	0.028	0.056	0.037	0.0183	345.3	339.2
			14,000	1670		220	0.024	0.048	0.032	0.0190	346.0	340.0
			22,000	1730		202	0.023	0.045	0.030	0.0182	345.4	339.1
		166,666	6,000	1830		432	0.022	0.042	0.028	0.0267	351.6	344.8
			14,000	1800		471	0.019	0.036	0.024	0.0284	352.2	345.5
			22,000	1830		376	0.018	0.034	0.023	0.0245	350.5	343.7
	500,000	625,000	6,000	1950		195	0.016	0.028	0.020	0.0175	345.2	338.1
			14,000	1910		202	0.014	0.025	0.017	0.0178	345.5	338.6
			22,000	1880		157	0.013	0.023	0.017	0.0162	342.8	336.1
		1,666,666	6,000	2060		286	0.013	0.022	0.016	0.0205	348.5	341.0
			14,000	1990		300	0.011	0.019	0.014	0.0211	349.0	341.6
			22,000	1970		206	0.011	0.018	0.013	0.0179	345.7	338.5

FORM R 18-6-58

TABLE 18

LIQUID OXYGEN/LIQUID HYDROGEN SYSTEM OPTIMIZATIONS

EXPANSION AREA RATIO = 50:1

System Type	Engine Thrust pounds	Gross Weight pounds	Velocity Increment Feet/second	Optimum Parameters: Chamber Pressure, psia	Optimum Parameters: Mixture Ratio	Area Ratio	Propellant Dependent Weight Factors, pound/pound Propellant: Oxygen	Hydrogen	Bulk	Engine Weight Factors, pound/pound thrust	Thrust Chamber Specific Impulse, seconds	Engine Specific Impulse, seconds
Pressure-Fed Ablation Cooled to ϵ = 20:1 Then Radiation Cooled To Exit, 80 Percent Bell Nozzle	5,000	6,250	6,000	75	5.5	50	0.067	0.495	0.133	0.0200	429.9	429.9
			14,000	60	5.6	50	0.055	0.409	0.109	0.0294	429.0	429.0
			22,000	56	5.9	50	0.051	0.384	0.099	0.0341	427.1	427.1
		16,666	6,000	56	5.3	50	0.050	0.366	0.100	0.0368	430.4	430.4
			14,000	47	5.4	50	0.043	0.320	0.086	0.0499	429.7	429.7
			22,000	44	5.6	50	0.039	0.297	0.078	0.0598	427.9	427.9
Pump-Fed Fully Regeneratively Cooled 80 Percent Bell Nozzle	50,000	62,500	6,000	645	5.7	50	0.049	0.366	0.098	0.0151	436.1	431.9
			14,000	610	5.8	50	0.042	0.310	0.083	0.0152	435.8	431.9
			22,000	630	5.6	50	0.040	0.293	0.077	0.0150	435.0	431.0
		166,666	6,000	550	5.2	50	0.038	0.272	0.077	0.0159	437.7	433.8
			14,000	460	5.2	50	0.033	0.232	0.066	0.0166	437.4	434.2
			22,000	550	5.8	50	0.031	0.223	0.061	0.0155	435.7	432.1
	500,000	625,000	6,000	775	5.4	50	0.028	0.193	0.055	0.0157	437.3	432.2
			14,000	732	5.4	50	0.025	0.167	0.048	0.0158	437.3	432.4
			22,000	765	5.7	50	0.024	0.160	0.045	0.0154	436.0	431.2
		1,666,666	6,000	756	5.0	50	0.023	0.151	0.045	0.016	438.4	433.1
			14,000	685	5.0	50	0.021	0.132	0.040	0.016	438.3	433.5
			22,000	730	5.3	50	0.020	0.127	0.038	0.158	437.4	432.5

TABLE 19

LIQUID FLOURINE/LIQUID HYDROGEN SYSTEM OPTIMIZATIONS

EXPANSION AREA RATIO = 50:1

System Type	Engine Thrust pounds	Gross Weight pounds	Velocity Increment Feet/second	Optimum Parameters: Chamber Pressure, psia	Optimum Parameters: Mixture Ratio	Area Ratio	Propellant Dependent Weight Factors, pound/pound Propellant: Fluorine	Hydrogen	Bulk	Engine Weight Factors, pound/pound thrust	Thrust Chamber Specific Impulse, seconds	Engine Specific Impulse, seconds
Pressure-Fed Ablation Cooled to ϵ = 20:1 Then Radiation Cooled To Exit. 80 Percent Bell Nozzle	5,000	6,250	6,000	110	16.5	50	0.062	0.705	0.099	0.0137	447.5	447.5
			14,000	85	16.5	50	0.050	0.572	0.080	0.0203	446.5	446.5
			22,000	80	16.6	50	0.046	0.525	0.073	0.0243	446.7	446.7
		16,666	6,000	85	16.3	50	0.046	0.521	0.074	0.0243	446.5	446.5
			14,000	65	16.3	50	0.038	0.4333	0.061	0.0361	445.4	445.4
			22,000	75	16.4	50	0.038	0.430	0.061	0.0369	445.7	445.7
Pump-Fed Fully Regeneratively Cooled 80 Percent Bell Nozzle	50,000	62,500	6,000	1060	16.6	50	0.039	0.486	0.067	0.0122	459.6	456.1
			14,000	1015	16.6	50	0.033	0.406	0.057	0.0122	459.5	456.1
			22,000	1005	16.8	50	0.032	0.380	0.053	0.0122	459.3	455.9
		166,666	6,000	1050	16.3	50	0.030	0.363	0.051	0.0122	459.8	456.3
			14,000	1000	16.3	50	0.026	0.305	0.044	0.0122	459.8	456.3
			22,000	1060	16.5	50	0.025	0.286	0.041	0.0122	459.6	456.2
	500,000	625,000	6,000	1350	16.5	50	0.022	0.250	0.037	0.0125	460.3	455.9
			14,000	1285	16.4	50	0.020	0.213	0.032	0.0124	460.3	455.9
			22,000	1285	16.6	50	0.019	0.201	0.030	0.0124	460.2	455.8
		1,666,666	6,000	1485	16.3	50	0.018	0.193	0.029	0.0126	460.8	455.7
			14,000	1380	16.3	50	0.016	0.167	0.026	0.0125	460.6	455.9
			22,000	1385	16.4	50	0.016	0.158	0.025	0.0125	460.6	455.8

TABLE 20

N_2O_4/N_2H_4-UDMH (50-50) SYSTEM OPTIMIZATIONS
EXPANSION AREA RATIO = 50:1

System Type	Engine Thrust pounds	Gross Weight pounds	Velocity Increment Feet/second	Optimum Parameters: Chamber Pressure, psia	Optimum Parameters: Mixture Ratio	Area Ratio	Propellant Dependent Weight Factors, pound/pound Propellant: N_2O_4	Propellant Dependent Weight Factors, pound/pound Propellant: N_2H_4-UDMH	Propellant Dependent Weight Factors, pound/pound Propellant: BULK	Engine Weight Factors, pound/pound thrust	Thrust Chamber Specific Impulse, seconds	Engine Specific Impulse, seconds
Pressure-Fed Ablation Cooled to ϵ = 20:1 Then Radiation Cooled To Exit. 80 Percent Bell Nozzle	5,000	6,250	6,000	150	2.1	50	0.053	0.091	0.065	0.0107	322.8	322.8
			14,000	120	2.1	50	0.044	0.076	0.054	0.0150	322.5	322.5
			22,000	112	2.1	50	0.041	0.071	0.051	0.0170	322.4	322.4
		16,666	6,000	115	2.1	50	0.039	0.067	0.048	0.0180	322.5	322.5
			14,000	95	2.1	50	0.033	0.056	0.041	0.0256	322.2	322.2
			22,000	85	2.1	50	0.031	0.052	0.038	0.0302	322.1	322.1
Pump-Fed Fully Regeneratively Cooled 80 Percent Bell Nozzle	50,000	62,500	6,000	1265	2.2	50	0.028	0.055	0.037	0.0118	329.4	325.0
			14,000	1255	2.2	50	0.024	0.047	0.032	0.0118	329.4	325.0
			22,000	1265	2.2	50	0.023	0.045	0.030	0.0118	329.4	325.0
		166,666	6,000	1325	2.1	50	0.022	0.041	0.028	0.0119	329.7	325.0
			14,000	1325	2.2	50	0.019	0.035	0.024	0.0119	329.7	325.0
			22,000	1340	2.2	50	0.018	0.034	0.023	0.0119	329.6	325.0
	500,000	625,000	6,000	1495	2.2	50	0.016	0.028	0.020	0.0121	330.1	325.0
			14,000	1495	2.2	50	0.014	0.024	0.017	0.0121	330.1	325.0
			22,000	1520	2.2	50	0.013	0.023	0.017	0.0121	330.1	324.9
		1,666,666	6,000	1615	2.2	50	0.013	0.022	0.016	0.0122	330.4	324.9
			14,000	1580	2.2	50	0.011	0.019	0.014	0.0122	330.3	324.9
			22,000	1655	2.2	50	0.011	0.018	0.013	0.0123	330.5	324.8

2. Optimum area ratio increases slightly when the thrust-to-weight ratio is decreased.

3. The optimum chamber pressure of pressure-fed systems decreases as mission velocity increment is increased.

A comparison of the unrestricted nozzle area ratio and the 50:1 area ratio optimizations (for the 50,000 pound thrust model with F/W of 0.3 and ΔV of 14,000 ft/sec) indicates that if chamber pressure and mixture ratio for the unrestricted optimization are held constant and area ratio is reduced to 50:1, a payload loss of 5.5 per cent results. If MR is held constant and P_c is reoptimized when ϵ is reduced, the loss is 4.8 per cent. If chamber pressure is held constant (at the optimum value for unrestricted ϵ) and mixture ratio is reoptimized, the loss is 5.0 per cent. If both chamber pressure and mixture ratio are reoptimized at the lower area ratio, the loss is 3.8 per cent. The major loss is thus caused by the reduction in expansion area ratio. If the reason for restricting area ratio is to reduce exit diameter, a more favorable alternative is to increase chamber pressure and thereby reduce area ratio less. This conclusion is confirmed by work done under NASA contract NAS 7-164, and presented in the second quarterly report of that study.

From the cases analyzed, engine operating parameters may be selected to yield near-maximum payload, independent of mission velocity increment. Experience from previous studies has shown that the selected operating parameters become more critical with increasing mission velocity increment; therefore, if selections are made independent of ΔV, the selected values should be near the optimum values for the higher energy missions. Selected values of engine operating parameters were taken from the tables of optimum parameters (Tables 15 through 20) and are presented in Tables 21, 22 and 23 for O_2/H_2, F_2/H_2 and NTO/50-50 propellant combinations respectively. The parameters selected are average values of the optima for the 14,000 and 22,000 ft/sec missions.

Effect of Off-Optimum Propulsion Parameters

The effect of perturbing one engine operating parameter, while retaining the optimum values of the remaining parameters, is shown in Figures 148 through 153. For the indicated propellant combination, a pump-fed system and a pressure-fed system are illustrated for a mission velocity increment of 14,000 ft/sec.

TABLE 21

OPERATING PARAMETER SUMMARY, O_2/H_2 SYSTEMS

System Type	Thrust, lb	Thrust / Weight Ratio	Chamber Pressure, psia	Mixture Ratio	Area Ratio
Pressure-Fed	5,000	0.8	65 60	6.3 5.7	110 50
		0.3	55 47	6.3 5.5	200 50
Pump-Fed	50,000	0.8	1150 620	6.8 5.8	200 50
		0.3	1360 500	6.9 5.4	450 50
	500,000	0.8	1230 750	6.4 5.5	140 50
		0.3	1300 700	6.4 5.1	200 50

TABLE 22

OPERATING PARAMETER SUMMARY, F_2/H_2 SYSTEMS

System Type	Thrust, lb	Thrust / Weight Ratio	Chamber Pressure, psia	Mixture Ratio	Area Ratio
Pressure-Fed	5,000	0.8	100 85	17.1 16.5	145 50
		0.3	75 70	17.0 16.3	200 50
Pump-Fed	50,000	0.8	1580 1000	17.5 16.7	200 50
		0.3	1750 1000	17.4 16.4	400 50
	500,000	0.8	1790 1280	17.2 16.5	150 50
		0.3	1850 1380	17.1 16.3	200 50

TABLE 23

OPERATING PARAMETER SUMMARY, NTO/50-50, SYSTEMS

System Type	Thrust, lb	Thrust / Weight Ratio	Chamber Pressure, psia	Mixture Ratio	Area Ratio
Pressure-Fed	5,000	0.8	150 115	2.2 2.1	150 50
		0.3	120 90	2.2 2.1	250 50
Pump-Fed	50,000	0.8	1700 1260	2.2 2.2	210 50
		0.3	1800 1330	2.2 2.2	400 50
	500,000	0.8	1900 1500	2.2 2.2	180 50
		0.3	1980 1600	2.2 2.2	250 50

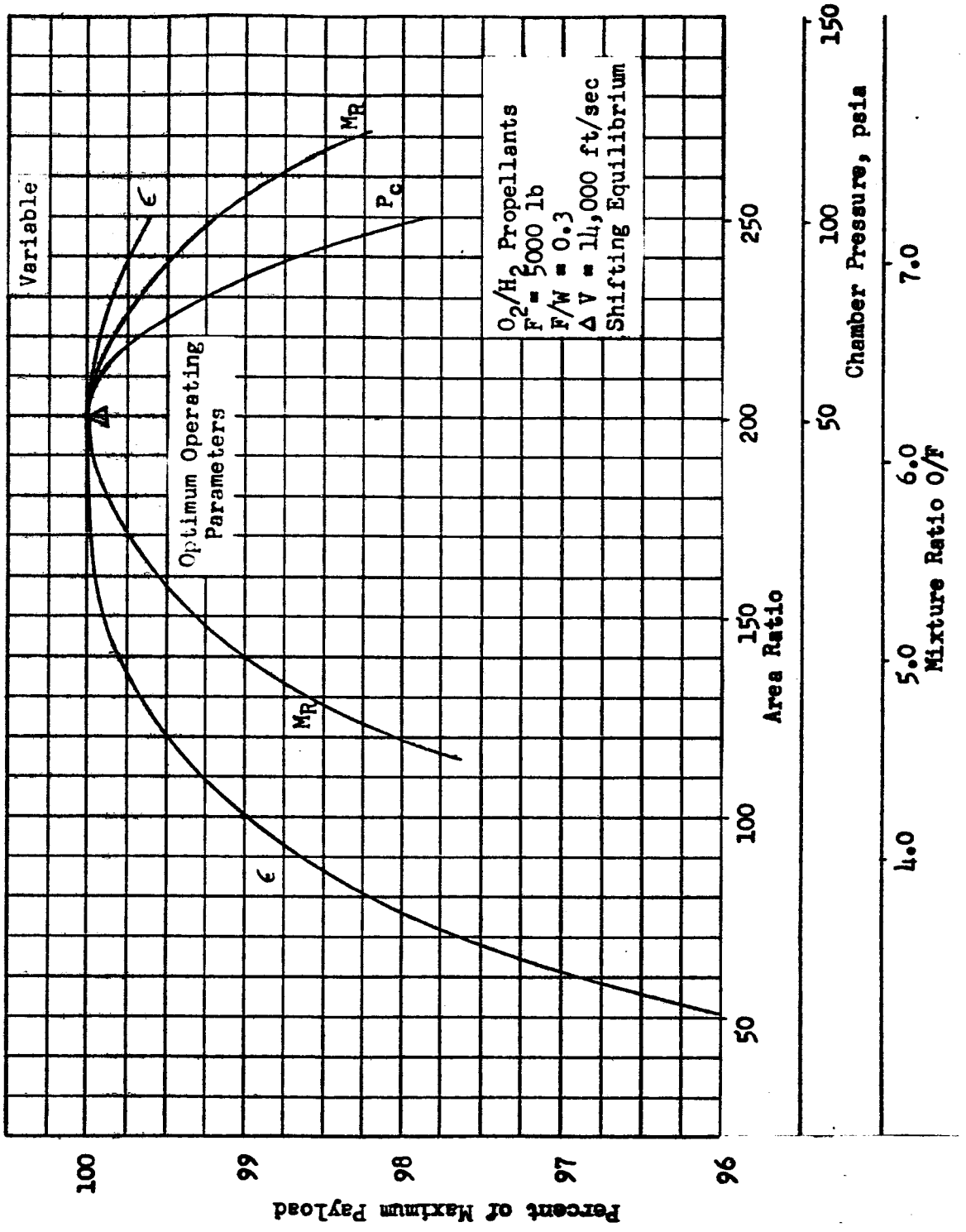

Fig. 148. Effect of Off-Optimum Engine Design, O_2/H_2 Pressure-Fed System

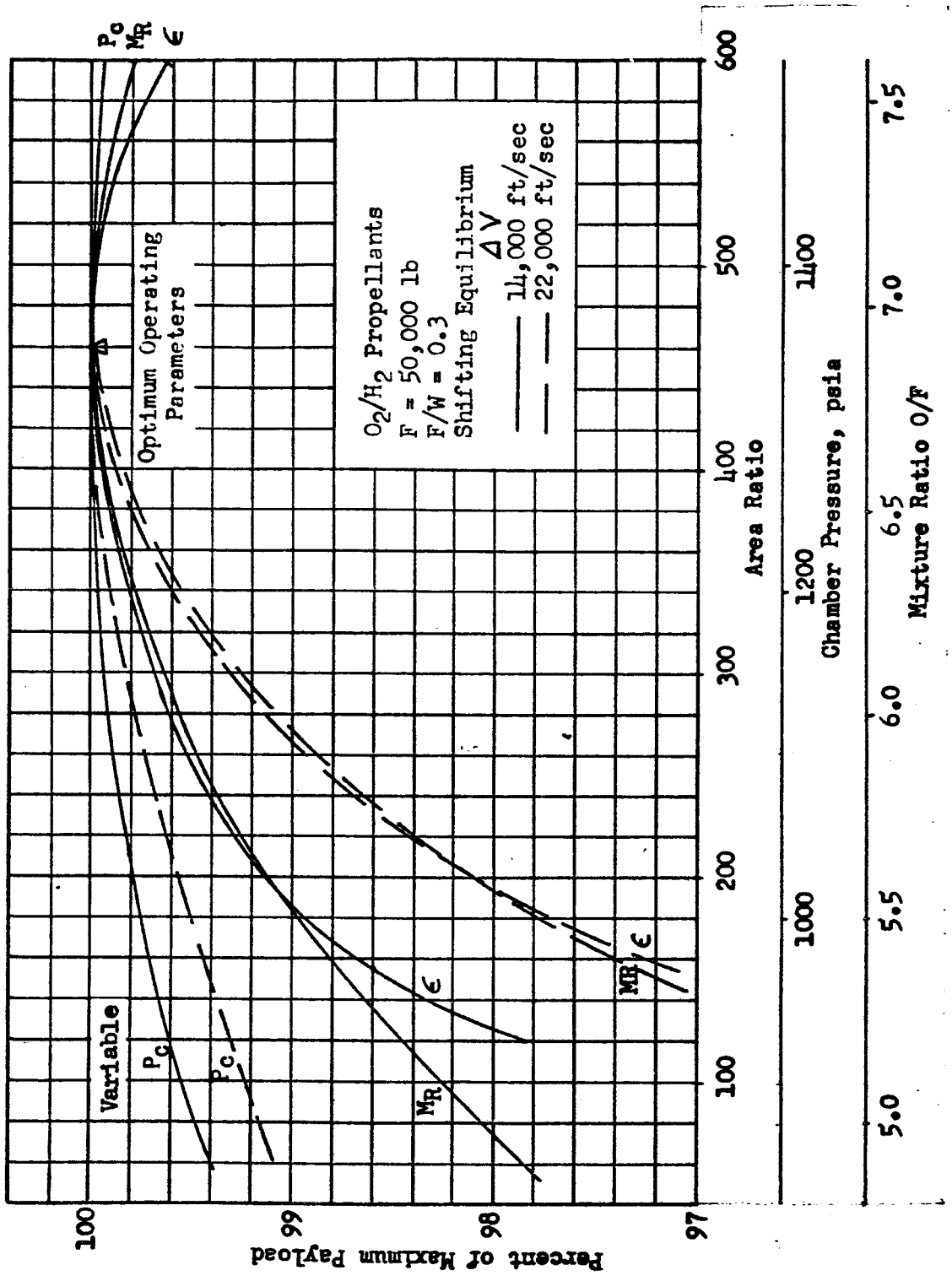

Fig. 149. Effect of Off-Optimum Engine Design, O_2/H_2 Pump-Fed System

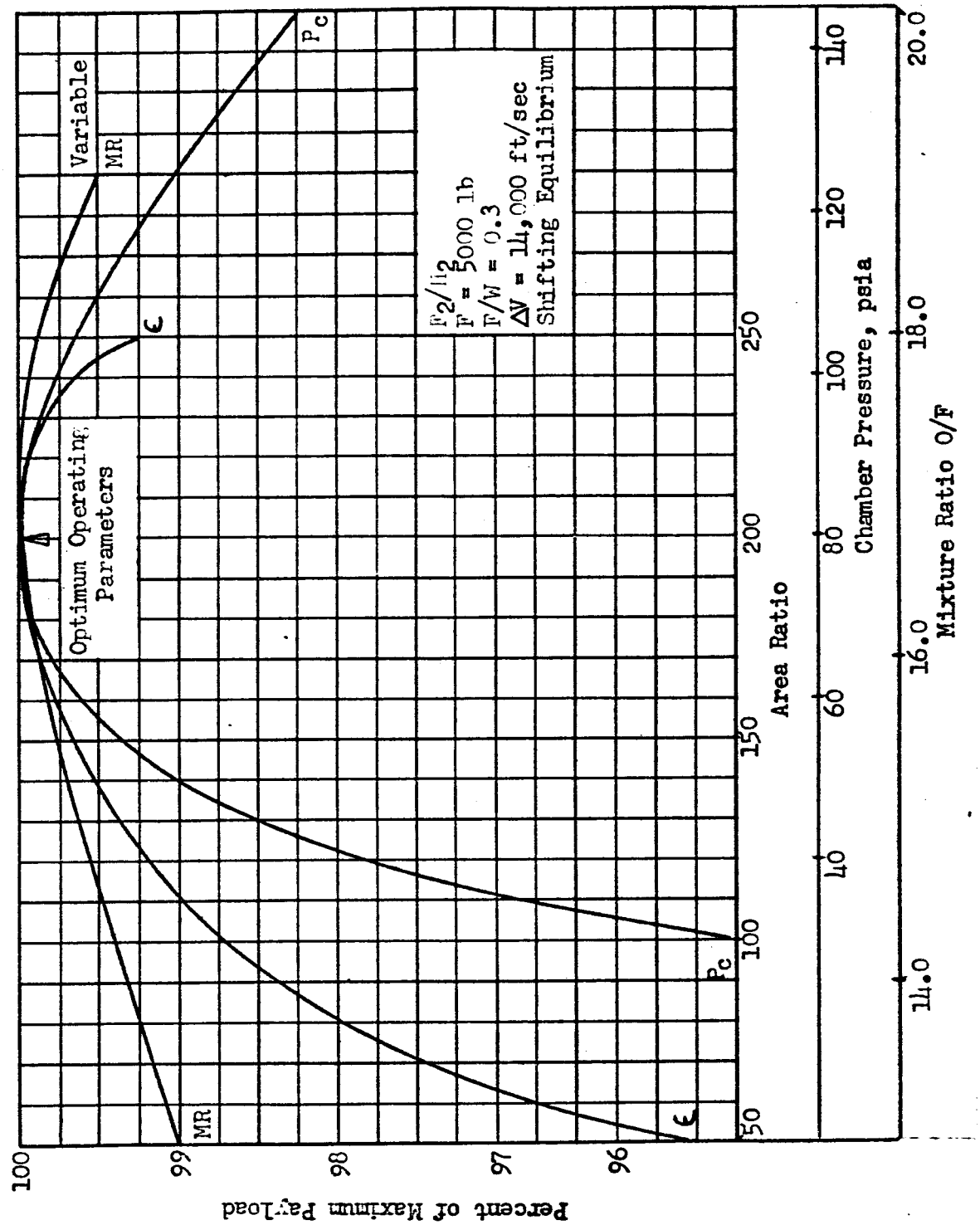

Fig. 150. Effect of Off-Optimum Engine Design, F_2/H_2 Pressure-Fed System

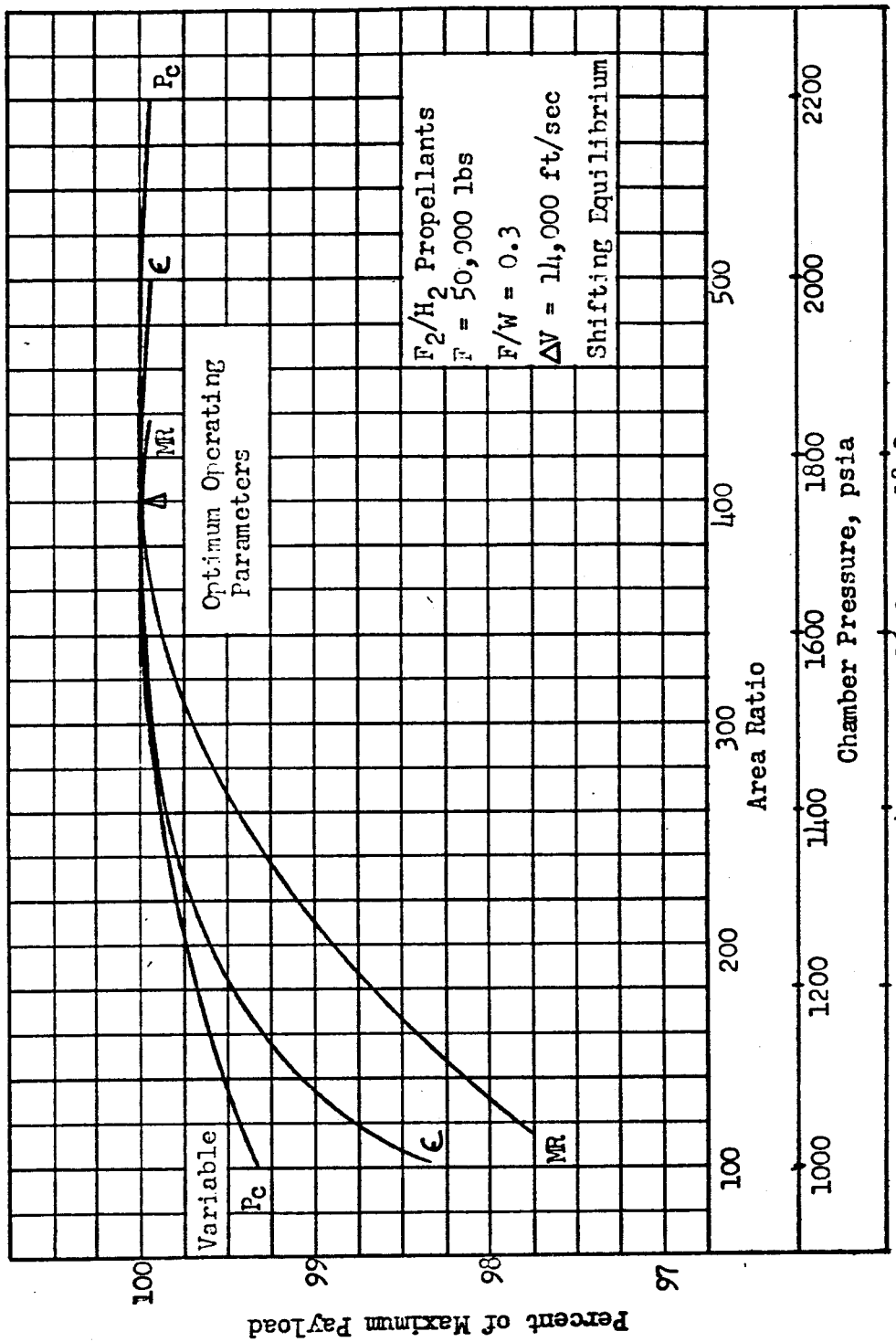

Fig. 51. Effect of Off-Optimum Engine Design F_2/H_2 Pump-Fed System

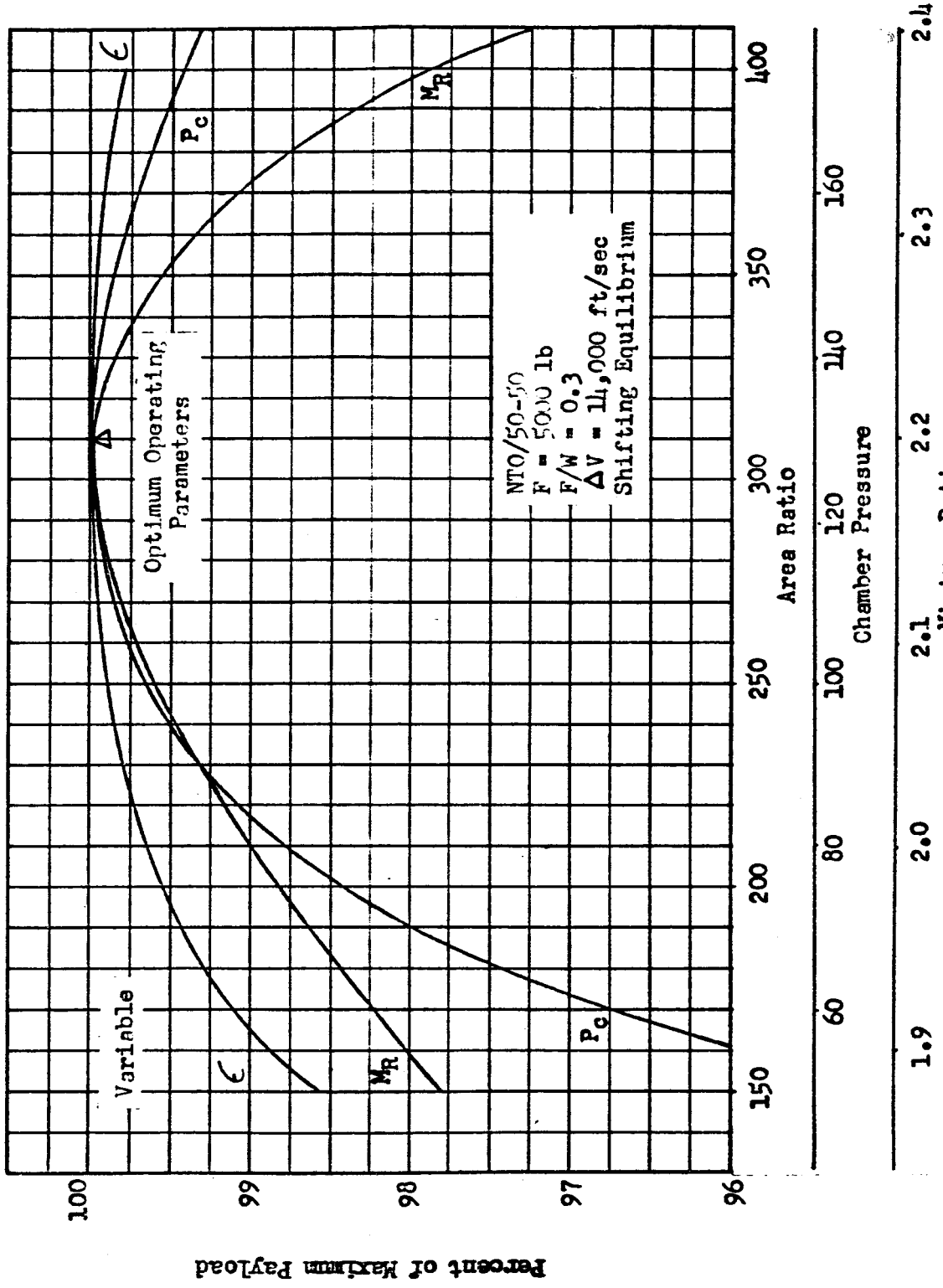

Fig.152.Effect of Off-Optimum Engine Design, NTO/50-50 Pressure-Fed System

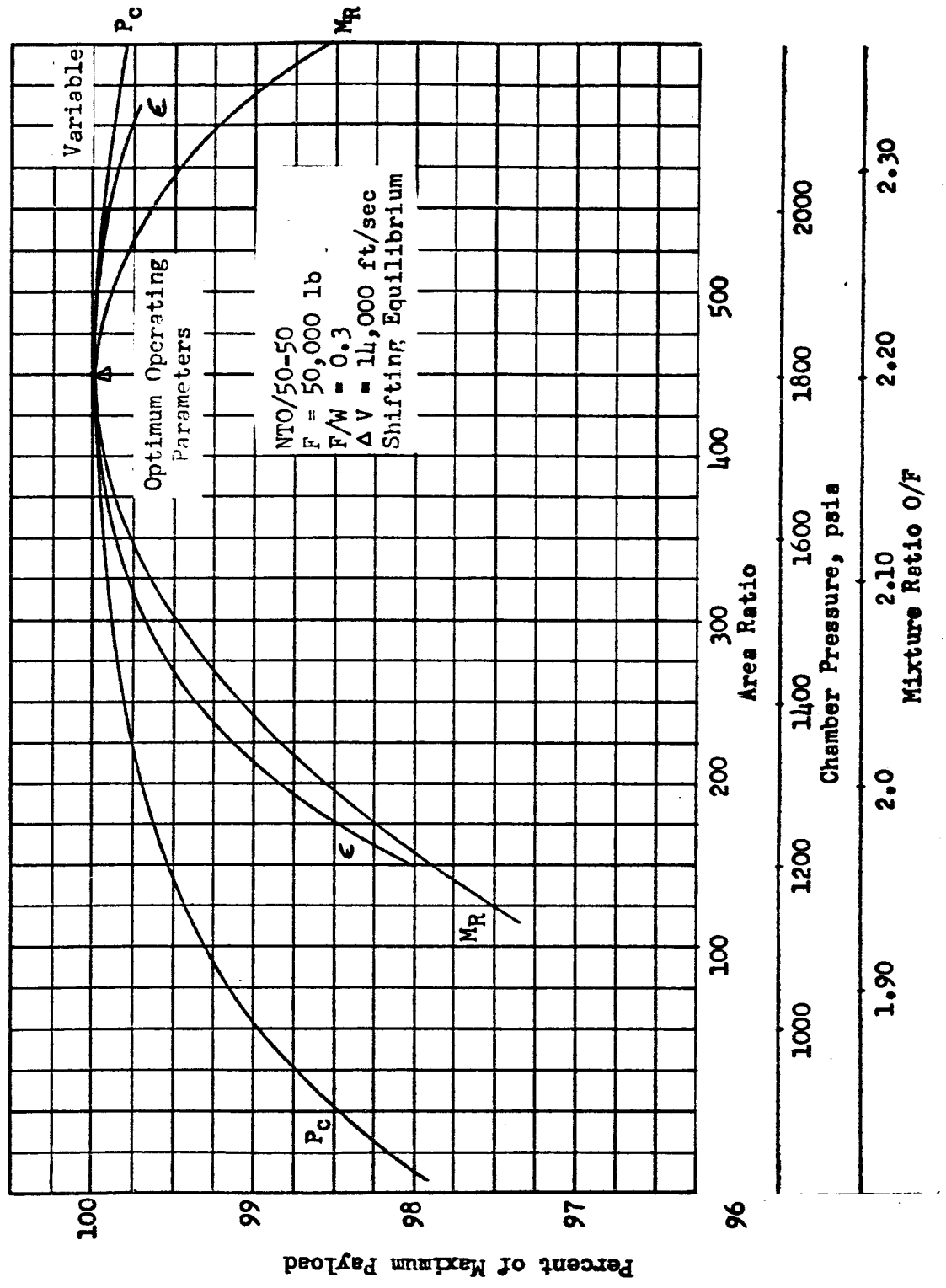

Fig.153.Effect of Off-Optimum Engine Design, NTO/50-50 Pump-Fed System

This information is summarized in Table 24 which presents the allowable parameter variation for a 0.5 and a 1.0 per cent payload loss. The values presented are for a mission $\Delta V = 14{,}000$ ft/sec and $F/W = 0.3$, and based on the condition that the other two parameters are maintainable at their optimum values.

Examination of the data shown in the figures and in Table 24 indicates that design at the exact optimum engine parameters is not a stringent requirement. Deviation can be permitted without seriously penalizing system capability.

Increasing the mission velocity increment increases the payload sensitivity of the engine design parameters. The effect of mission ΔV on the pump-fed O_2/H_2 system is illustrated in Figure 149 ; in addition to the 14,000 ft/sec mission, 22,000 ft/sec velocity increment curves are presented.

For a 0.5 per cent payload loss (from the maximum if optimum parameters are used) chamber pressure can typically vary 30-40 per cent above or below the optimum. Mixture ratio can vary 10-15 per cent for O_2/H_2 or F_2/H_2 and about 5 per cent for N_2O_4/50-50. The nozzle expansion area ratio can vary 30-40 per cent from optimum.

TABLE 24

EFFECT OF OFF-OPTIMUM DESIGN

System Type	Operating Parameter	Allowable Parameter Increment, Percent Payload Loss		Optimum Value
		0.5	1.0	
O_2/H_2 Pressure-Fed	P_c, psia	+25	+35	55
	ϵ	-80	-100	200
F = 5000 pounds	MR	±0.9	±1.2	6.20
F_2/H_2 Pressure-Fed	P_c	±22	±35	80
	ϵ	-60	-90	200
F = 5000 pounds	MR	±2.3	-3.8	16.90
NTO/50-50	P_c	+40	+60	130
Pressure-Fed	ϵ	-110	-145	310
F = 5000 pounds	MR	±0.13	±0.20	2.18
O_2/H_2 Pump-Fed	P_c	-450	-550	1360
	ϵ	-200	-275	450
F = 50,000 pounds	MR	±1.0	±1.4	6.90
F_2/H_2 Pump-Fed	P_c	-650	-900	1770
	ϵ	-230	-270	410
F = 50,000 pounds	MR	-3.2	-4.6	17.35
NTO/50-50	P_c	-600	-800	1800
Pump-Fed	ϵ	-175	-230	471
F = 50,000 pounds	MR	±0.12	±0.18	2.21

Mission ΔV = 14,000 ft/sec, F/W = 0.3, unrestricted area ratio

REFERENCES

1. R-3923: Space Transfer Phase Propulsion System Study, Final Report, Rocketdyne, A Division of North American Aviation, Inc., Canoga Park, California, February 1963.

2. R-3208: Propulsion Requirements for Space Missions, Final Report, Volume II, Rocketdyne, A Division of North American Aviation, Inc., Canoga Park, California, May 1961.

3. Queijo, M. S. and G. K. Miller, Analysis of Two Thrusting Techniques for Soft Lunar Landings Starting from a 50 Mile Altitude Circular Orbit, NASA, TN D-1230.

4. Sivo, J., C. Campbell and V. Hamza, Analysis of Close Lunar Translation Techniques, NASA TR R-126.

5. Duke, W., Lunar Landing Problems, Lunar Flight Symposium, Denver, Colorado, December 1961.